

N68-14576

NASA CR-65811



DETERMINATION OF FLAW GROWTH CHARACTERISTICS OF Ti-6Al-4V SHEET IN THE SOLUTION-TREATED AND AGED CONDITION

83-02-1

by

David W. Hoepfner, Donald E. Pettit,
Charles E. Feddersen, and Walter S. Hyler

prepared for

NATIONAL AERONAUTICS AND SPACE ADMINISTRATION

LIBRARY COPY

Contract NAS 9-6969

LANGLEY RESEARCH CENTER
NASA
CAMP BELL STATION
HAMPTON, VIRGINIA

BATTELLE MEMORIAL INSTITUTE
Columbus Laboratories



FINAL REPORT

on

DETERMINATION OF FLAW GROWTH CHARACTERISTICS OF
Ti-6Al-4V SHEET IN THE SOLUTION-TREATED AND AGED CONDITION

Contract NAS 9-6969

to

NASA, MANNED SPACECRAFT CENTER
STRUCTURE AND MATERIALS BRANCH

January 1, 1968

by

David W. Hoeppepner, Donald E. Pettit,
Charles E. Feddersen, and Walter S. Hyler

BATTELLE MEMORIAL INSTITUTE
Columbus Laboratories
505 King Avenue
Columbus, Ohio 43201

TABLE OF CONTENTS

	<u>Page</u>
INTRODUCTION	1
SUMMARY	3
CONCLUSIONS AND RECOMMENDATIONS	6
Specimen Preparation	10
Material	10
Parent Material	10
Welded Material	12
Specimen Configuration	18
Specimen Fabrication	18
Location and Type of Starter Flaw	21
Introduction of Initial Fatigue Crack	21
Location of EDM Flaw in Welded Material	33
Allocation of Specimens	38
Procedure and Results	38
Fracture Strength	43
Test Apparatus	43
Test Procedure	47
Test Results	47
Data Interpretation	68
Fatigue-Crack Propagation	69
Test Apparatus	69
Test Procedure	72
Test Results	78
Data Interpretation	124
Sustained Load Behavior	126
Apparatus	127
Experimental Procedure	127

TABLE OF CONTENTS (cont.)

	<u>Page</u>
Experimental Results	127
Interpetation	130
CONCLUDING DISCUSSION	130
References	132

INTRODUCTION

During 1966, unexpected failures of Apollo tankage during verification systems testing caused a significant amount of concern about the reliability of pressure vessel tankage. In recognition of the need for more information on the defect tolerance of materials used in pressure vessels, personnel from Grumman Aircraft Engineering Corporation (GAEC) requested that the Manned Spacecraft Center initiate a program at Battelle to study various aspects of the flaw tolerance problem.

Nondestructive inspection and proof testing are important quality assurance procedures for the detection and screening of defects. While the goal of nondestructive testing is the detection of critical defects before service operation, the size of critical defects in high strength materials is frequently below the sensitivity limit of available detection techniques. To circumvent this marginal condition, positive verification of the structural integrity is made by proof testing. When proof testing is conducted at a distinct stress level above the operating condition, not only are defects critical at operating loads screened out, but an additional tolerance for the growth of subcritical flaws is obtained. In principle, the proper integration of fracture and crack propagation data with proof testing procedures will provide a guarantee of tankage reliability.

Currently, proof testing of Apollo tankage is carried out at ambient conditions. In order to screen smaller size defects it has been proposed that proof testing be carried out at cryogenic (liquid nitrogen) temperature. Based on the little information available, the flaw tolerance of Ti-6Al-4V STA at cryogenic temperature should be less than that at room temperature. The program

described herein was aimed at providing a quantitative answer to the question, Should cryogenic proof testing be used to proof test Apollo tankage or more specifically LM tankage?

In addition to the question stated above, there were several secondary questions that this program was to answer. These were:

- (1) What size defect will be eliminated during proof testing?
- (2) In the event a defect goes undetected during proof stressing, will it propagate by fatigue to become a critical size defect during simulated operating cycles and actual operation?
- (3) Will defects that go undetected during proof testing propagate under a sustained load?
- (4) What influence does the environment have on each of the questions posed above? (The specific environments in question are inhibited water, demineralized water, salt spray air, and Aerozine 50.)
- (5) What influence does thickness have on the defect tolerance for sheets up to 0.063 inch thick?

The specific experimental investigation undertaken was designed to answer these questions on Ti-6Al-4V in the solution treated and aged condition. The defect growth and fracture characteristics were studied in parent (unwelded) and welded sheet material.

The results of the study indicate that cryogenic proof testing will screen smaller size defects than proof testing at ambient conditions. However some unusual crack growth behavior during the proof test simulation suggests that some further study be made of stress and time duration effects.

Details of the results and experimental program are presented in succeeding sections.

SUMMARY

The main objective of this program was to determine the feasibility of employing cryogenic proof testing to screen out small defects in LM tankage. The secondary objectives were (1) to establish the size defect that will be eliminated by proof testing, (2) to determine whether undetected flaws will grow to a critical length during simulated operating cycles and in actual operation under a sustained load, (3) to evaluate whether certain specific environments influence any of the above factors, and (4) to assess whether the thickness of LM tankage material affects its tolerance for flaws.

To fulfill the objectives of the program the experimental studies were divided into three specific areas, namely:

- Fracture
- Programmed fatigue crack-propagation
- Sustained load

A brief discussion of the test conditions and variables studied is presented. More detail on these points can be found in Tables 6-8 and in the accompanying text.

In the fracture studies, three conditions were evaluated: (1) fracture strength in air, (2) fracture strength in liquid nitrogen, and (3) fracture strength in characteristic fluid environments.

The studies in air were conducted on flawed samples in three thicknesses of the Ti-6Al-4V STA alloy (0.020-, 0.040-, and 0.063-inch). Normal flaws and elongated flaws were evaluated with defect depths of $t/4$, $t/2$, and $3t/4$ (where t is the sheet thickness). Parent and welded samples were studied.

In liquid nitrogen, only 0.020- and 0.040-inch-thick material was employed with all other variables indicated above included. In the environmental tests, only the 0.040-inch-thick material was employed with a flaw depth of $t/2$. Normal and elongated flaws were studied in parent and welded material. The four environments were (1) inhibited water, (2) demineralized water, (3) salt-spray air, and (4) Aerozine 50.

The three parts of the programmed fatigue-crack propagation studies were as follows:

- (1) Two proof tests in air followed by 400 cycles of stress simulating operating conditions.
- (2) A cryogenic proof cycle followed by an air proof cycle followed by the 400 stress cycles as above.
- (3) Two proof cycles in inhibited water followed by 400 stress cycles in one of the four environments described under the fracture tests.

In Part (1), sheet in the three thicknesses was evaluated in parent and welded material. Normal and elongated surface flaws were studied with nominal depths of $t/4$, $t/2$, and $3t/4$. The two proof cycles in air were applied at 140 ksi gross section stress. The first proof test was held at load for 3 minutes; the second, 30 minutes. Each of the 400 subsequent load cycles was held for 55 seconds at the nominal operating stress of 105 ksi. Flaw growth observations were made.

In Part (2), only parent material in 0.040-inch-thick material was evaluated. Both flaw types and the three flaw depths were studied. In this part of the program, the cryogenic proof cycle was applied at a gross section stress of 186 ksi for three minutes with the samples immersed in liquid nitrogen. The remainder of the stress exposure (proof test in air followed by 400 stress cycles) was carried out under the stress and time conditions noted above.

In Part (3), parent and welded material in each of the three sheet thicknesses and with both flaw types were evaluated. Only the $t/2$ flaw depth was investigated. The proof loading conditions and 400 stress cycles were applied as in Part (1). However, proof testing was accomplished in inhibited water, and the 400 cycles were applied in one of the four environments. Actually, a test series was conducted in each of the four environments.

Finally, the sustained load tests were carried out in air and in each of the four environments. Parent and welded samples of 0.040-inch sheet were used. Both flaw configurations with but one flaw depth were tested. The test consisted of stressing the specimen at 105 ksi for 100 hours or failure, whichever occurred first.

The program results on plane sheet specimens have indicated that cryogenic proof testing offers a real advantage over air proof testing in screening small flaws. Specific flaw sizes that can be screened by both proof test methods are presented. Some undetected flaws, namely those that do not fail in the proof test, were found to grow during simulated operating cycles, but only to the extent that the sheet thickness is breached. The flaws did not grow to a large enough extent to yield a critical through crack that would fracture. Environmental studies suggest that no important differences exist from air behavior in regard to fracture, crack propagation and sustained load. Some thickness effects were observed that suggest some need for caution in the thicker sheet gages in regard to this problem. In this connection, recommendations are made for additional studies of thickness effects, flaw size and shape factors, and biaxial stress effects in order to provide more definite indication of the applicability of these results to the actual stress environment of LM tankage.

CONCLUSIONS AND RECOMMENDATIONS

This program studied the behavior of Ti-6Al-4V STA alloy sheet in regard to flaw tolerance under a variety of loading conditions and environments. The overall objective was to determine the feasibility of employing cryogenic proof testing to screen out small defects in LM tankage. The program of study has involved a detailed examination of axially loaded sheet panels with presized flaws. From this study, the following conclusions can be made:

- (1) Fracture tests of the sheet specimens have shown that cryogenic proof testing can lead to the detection of smaller flaws than can an ambient test condition.
- (2) Fracture tests show that surface flaws of an area ranging from 0.001 square inch to 0.003 square inch (depending upon sheet thickness) can be detected during a cryogenic proof test. The comparable value from an ambient proof test is 0.005 square inch.
- (3) All flaw sizes studied that are not detected during the proof tests can be expected to grow during simulated operating cycles of 105 ksi.
- (4) Some of these flaws will propagate through the thickness of the tank wall during the 400 cycles and result in a leak.
- (5) Based upon small, flat sheet specimens, it appears that the material is tough enough so that at a 105 ksi operating stress, propagating flaws will not reach a critical size to cause rapid fracture before breakthrough occurs.

- (6) Of the four environments studied, it is not expected, for the range of flaws studied, that environment will influence fracture behavior or fatigue-crack propagation. Under a sustained load, simulating the operating stress condition, only the salt-spray air environment may stimulate crack growth, however, only to a slight degree.
- (7) Sheet thickness has a noticeable effect on fracture behavior at cryogenic temperature and on crack propagation at room temperature.
- (8) No consistent trends were observed in the behavior of welded specimens in comparison with parent material with the possible exception of fracture.
- (9) For some flaw sizes, flaw growth appears to occur under the sustained proof test load whether in air or in the cryogenic medium. Whether this growth is only load dependent or time dependent was not determined.

These conclusions generally lead one to the idea that cryogenic proof testing of LM tankage will increase reliability. As noted above, however, certain precautions are raised by the wording of various conclusions. These precautions generally have led to the following recommendations for further work:

- (a) Biaxial Stress Studies

The data obtained to date are on plane sheet specimens and indicate that the cryogenic proof testing can separate out smaller flaws than does the air proof test. It is believed desirable to investigate the effect of stress state on fracture and crack propagation of the Ti-6Al-4V sheet by using small

scale tests on cylindrical specimens. This type specimen introduces three factors into the problem all of which are characteristic of IM tankage: (1) the biaxial stress state, (2) secondary stresses from bending in the vicinity of the flaw, and (3) the curved cylindrical surface. Small scale studies should be followed by full scale tests.

(b) Flaw Growth During Proof Testing

The data have shown for the deeper flaws and thicker material that at 186 ksi in liquid nitrogen and 140 ksi in air sustained load flaw growth may be occurring. The fractographs also show that a tunneling type of flaw growth is occurring that is not manifested by the flaw growth measured at the surface. Thus a potentially more severe flaw may be present after proof testing, particularly, in cryogenic testing. It is, therefore, suggested that some further study be made of the stress and time dependence of flaw growth in air and at cryogenic temperature as well as the effect of the tunneling type flaw growth on fracture strength and crack propagation.

(c) Cryogenic Testing of 63-mil Material

Based on the findings of the program it appears necessary to determine the fracture characteristics of the 63-mil material at cryogenic temperatures. This is in part based on the observation that thickness plays an important role with regard to the defect size that is to be screened by cryogenic proof testing.

(d) Through-the-Thickness Flaws

The present study has shown that certain size cracks will grow through the thickness without reaching a critical size to cause complete failure. It would appear useful to have available some data that shows the effect of small flaw length of through-the-thickness flaws on the fracture, crack propagation, and sustained load behavior of the alloy, since some further growth may occur after the thickness is breached.

(e) Forged Material

On the basis of extremely limited data it appears that further evaluation of forged material is needed.

(f) Additional Needs

In this program design mechanical properties of the STA alloy were needed at cryogenic temperature. Sources such as MIL-HDBK-5 did not have such data on the STA condition. Consequently, estimated values of F_{ty} have been used primarily in the fracture section. It is suggested that some mechanical testing be done at cryogenic temperatures to establish the statistical distribution of mechanical properties as is done for MIL-HDBK-5 values.

Also, fracture characteristics are known to have quite a bit of scatter with normal variations in chemical composition and heat treatment. It is suggested that additional fracture testing be done to explore heat-to-heat characteristics in regard to fracture strength and inspectable flaw size.

Specimen Preparation

Details of the specimen preparation are presented in this section. Six subsections are included for a complete discussion of all aspects.

Material

The material used in this investigation was Ti-6Al-4V in the solution treated, and aged condition. All material was in the form of sheet except for four tests on forged material that were conducted for comparison. All sheet material was supplied by Grumman Aircraft Engineering Corporation (GAEC). Three thicknesses of material were employed in the investigation; viz, 0.020-, 0.040-, and 0.063-inch. These thicknesses cover the range of thicknesses used on propellant storage pressure vessels for the ascent and descent stages of LM.

Parent Material. Two forms of material were basic to the program; these were unwelded and welded material. The unwelded material is referred to as parent material throughout the report. The parent material was sheared into the form of blanks with dimensions of 5-1/4 x 16-1/2 inches by GAEC. The 16-1/2 inch dimension was parallel to the longitudinal axis of the original sheet. These blanks then were forwarded to Battelle for processing into specimens.

Each blank of parent material was numbered prior to processing at Battelle. The numbering system consisted of a code number designating thickness followed by a number designating the specimen. The thicknesses were designated by the following code:

2 = 0.020-inch gage

4 = 0.040-inch gage

6 = 0.063-inch gage

For example, a specimen designated 4-21 was the 21st specimen 0.040 inch thick.

Mechanical property tests were conducted on the parent material in the Mechanical Test Laboratory at Battelle. The results are listed in Table 1.

TABLE 1. MECHANICAL PROPERTIES OF
Ti-6Al-4V STA PARENT MATERIAL-
LONGITUDINAL DIRECTION

Specimen Number	Thickness, inch	Ultimate Tensile Strength, ksi	Yield Strength, 0-2 percent offset, ksi	Elongation, percent in 2 inches
2-1	.0218	170.8	161.5	8.0
2-2	.0218	171.8	163.7	--
2-3	.022	<u>171.2</u>	<u>160.9</u>	<u>9.0</u>
Average values		171.3	162.0	8.5
4-1	.039	170.7	162.6	9.5
4-2	.0415	170.0	160.8	11.0
4-3	.0405	171.4	162.6	11.0
4-4	.042	170.1	--	9.5
4-5	.0402	<u>169.2</u>	<u>161.0</u>	<u>11.0</u>
Average values		170.3	161.8	10.4
6-1	.0605	159.2	154.3	14.0
6-2	.0652	171.1	162.7	9.0
6-3	.066	170.6	161.8	11.0
6-4	.066	171.4	161.8	10.0
6-5	.0658	<u>170.3</u>	<u>161.4</u>	<u>11.5</u>
Average values		168.5 170.8	160.4 161.9	11.1
		<i>Avg (all)</i> 171	162	

Below each group of values for a given thickness the average value of the property is indicated. Comparing the average values of ultimate tensile strength for the thicknesses a decrease in value is observed for an increase in thickness. Likewise, the 0.2 percent offset yield strength decreases slightly as the thickness is increased. Elongation, on the other hand, increases with increasing thickness. If data for specimen 6-1 is not included in the averaging the average values of UTS and TYS become 170.8 ksi and 162.9 ksi and one would conclude no difference exists in tensile strength of material from the three sheet thicknesses. Examination of the specimen shows no reason for discarding the data, consequently it has been included and one therefore observes the slight decreases in strength with thickness shown in the table.

Welded Material. The welded material was blanked from sheets taken from the same heats of material as the parent material. In this case, GAEC blanked the original 30 x 96-inch sheets into panels 30 x 16-1/2 inches. These panels were, in turn, sectioned into two pieces 30 x 8-1/4 inches. The two pieces then were welded using tungsten inert gas welding. All panels then were radiographed. The radiographs were examined to assure conformance to LM tankage Weldment Specifications. The data on the welding operation are provided in Tables 2, 3, and 4.

In all cases, the welded specimens were designated by a letter (A, B, or C) followed by a number. The letter designates that the specimen is welded with a thickness of 0.020-, 0.040-, or 0.063-inch for the A, B, and C designations, respectively. Thus, the parent material is identified by a number-number sequence and the welded material by a letter-number sequence.

Tensile blanks were sectioned from the welded sheets at random and tested to determine the mechanical properties. The tensile tests on the welded specimens were conducted so that the welded properties could be compared with those of the parent material. It also was desired to locate the position of

TABLE 2. WELD PARAMETER DATA FOR
Ti-6Al-4V SHEET MATERIAL .020" THICKNESS

Base Material	-	.020", 6Al-4V Titanium alloy, solution heat treated and aged
Filler Metal	-	.030" diameter commercially pure Titanium
Process	-	Tungsten Inert Gas
Electrode	-	1/16" diameter, 2% Thoriated Tungsten
Back-up	-	Copper, groove width .125" by .040" deep
Hold Down	-	Copper, 3/16" spacing
Torch Nozzle	-	Copper, 1/2" ID orifice
Welding Position	-	Flat
Pre-Weld Prep.	-	Machine edges, acid clean, draw file edges, polish with 320 grit emery, clean with stainless steel wire brush and wash with alcohol.
Amperage	-	40, DCSP
Voltage	-	7.5
Travel Speed	-	18 IPM
Wire Speed	-	18 IPM
Torch Gas	-	Argon, 25 cfh.
Back-up Gas	-	Argon, 3 cfh.
Trailing Shield Gas	-	Argon, 7 cfh.

TABLE 3. WELD PARAMETER DATA FOR
FOR Ti-6Al-4V SHEET MATERIAL .040" THICKNESS

Base Material	-	.040", 6Al-4V Titanium alloy*
Filler Metal	-	.030", diameter commercially pure Titanium
Process	-	Tungsten Inert Gas
Electrode	-	1/16" diameter, 2% Thoriated Tungsten
Back-up	-	Copper, groove width .250" by .040" deep
Hold Down	-	Copper, 5/16" spacing
Torch Nozzle	-	Copper, 1/2" ID orifice
Welding Position	-	Flat
Pre-Weld Prep.	-	Machine edges, acid clean, draw file edges, polish with 320 grit emery, clean with stainless steel wire brush and wash with alcohol.
Amperage	-	85, DCSP
Voltage	-	7.5
Travel Speed	-	18 IPM
Wire Speed	-	34 IPM
Torch Gas	-	Argon, 25 cfh.
Back-up Gas	-	Argon, 3 cfh.
Trailing Shield Gas	-	Argon, 7 cfh.

* Solution heat treated and aged

TABLE 4. WELD PARAMETER DATA FOR
FOR Ti-6Al-4V SHEET MATERIAL .063" THICKNESS

Base Material	-	.063", 6Al-4V Titanium alloy*
Filler Metal	-	.030", diameter commercially pure Titanium
Process	-	Tungsten Inert Gas
Electrode	-	3/32" diameter, 2% Thoriated Tungsten
Back-up	-	Copper, groove width .312" by .040" deep
Hold Down	-	Copper, 13/32" spacing
Torch Nozzle	-	Copper, 1/2" ID orifice
Welding Position	-	Flat
Pre-Weld Prep.	-	Machine edges, acid clean, draw file edges, polish with 320 grit emery, clean with stainless steel wire brush and wash with alcohol
Amperage	-	140, DCSP
Voltage	-	8
Travel Speed	-	18 IPM
Wire Speed	-	50 IPM
Torch Gas	-	Argon, 30 cfh.
Back-up Gas	-	Argon, 3 cfh.
Trailing shield Gas	-	Argon, 12 cfh.

* Solution heat treated and aged

failure with respect to the weld bead in the welded specimens. The results of the tensile tests on the welded specimens are listed in Table 5. In Table 5, those specimens where failure occurred on the weld fusion line are denoted by an asterisk; all other specimens failed some distance from the weld.

In studying Table 5, it is noted that there is a tendency for tensile strength and yield strength to decrease with thickness, primarily on the basis of the 0.063 inch sheet data. There also appear to be considerable differences in the percent elongation, however.

The average value of UTS for the 63-mil welded specimens is considerably below the average value of UTS for the 20 and 40-mil welded specimens. However, the average value of 162.9 ksi for the 63-mil specimens falls within the range of values that were observed for the parent material. Thus, on the basis of UTS, the weld efficiency seems to be 100 percent for all three thicknesses. This statement is verified by a comparison of average values of UTS for parent and welded specimens for each of the three thicknesses tested.

Lower values of elongation were generally observed for the welded material when compared with the parent material. For the 20-mil welded specimens, where 4 out of 5 specimens failed on the weld fusion line, the average value of elongation is quite a bit lower than that for the other two thicknesses. The elongation could be expected to be lower in the welded material for two reasons. First, the weld bead is in the center of the gage section and if failure occurs near the weld, the material in the vicinity of the weld is constrained more than if the weld were not present, and the resultant elongation is less. Second, where failures occurred a considerable distance from the weld bead, and thus a considerable distance from the center of the gage section, the value of elongation observed in the initial 2-inch gage section would be

TABLE 5. MECHANICAL PROPERTIES OF
Ti-6Al-4V STA WELDED MATERIAL -
LONGITUDINAL DIRECTION

Specimen Number	Thickness, inch	Ultimate Strength, ksi	Yield Strength, 0.2 percent offset, ksi	Elongation Percent in 2 inches
A-1*	.0202	167.4	158.4	6.0
A-2*	.0220	172.5	182.0	4.0
A-3*	.0195	172.9	165.5	3.0
A-4*	.0218	172.1	163.6	7.5
A-5*	.0203	<u>170.6</u>	<u>166.0</u>	<u>6.0</u>
Average values		171.1	163.1	5.3
B-1	.0413	170.3	164.4	9.0
B-2	.0393	173.5	164.0	9.0
B-3*	.0408	170.3	164.6	7.5
B-4	.0421	172.9	163.0	10.5
B-5	.0421	<u>172.7</u>	<u>162.8</u>	<u>10.0</u>
Average values		171.9	163.8	9.2
C-1	.0600	164.6	157.2	10.0
C-2	.0625	163.1	155.2	9.5
C-3	.0608	160.3	155.1	8.5
C-4	.0625	164.8	157.2	10.0
C-5	.0595	<u>161.7</u>	<u>155.6</u>	<u>11.0</u>
Average values		162.9	156.1	9.8

* Specimens designated with an asterisk failed on the weld fusion line; all others failed a considerable distance from the weld.

lower than the value expected. This is because a significant amount of deformation is occurring outside the original gage section.

Specimen Configuration

The specimen used in the experimental program is shown in Figure 1. The section width of 3 inches was selected for the critical section to accommodate the elongated flaw configuration. It is sufficiently wide to avoid deleterious width effects and, yet, maintained material economy.

Specimen Fabrication

The first step in the fabrication of specimens was a blanking operation to provide the specimen dimensions shown in Figure 1. Subsequent to blanking, the specimen preparation procedure was as follows (the specimens were always handled using clean white gloves):

- (1) Polish the specimen edges with successively finer grades of emery paper using 600-grit paper last.
- (2) Wash the specimen in a dilute Alconox solution and rinse with Acetone.
- (3) Stress relieve the specimen at 1000 F for 4 hours-air cool.
- (4) Introduce the EDM (electric discharge machined) notch at the desired location.
- (5) Grit blast both ends of the specimen including the radius between the critical section and grip end.

A colored picture of the specimen is shown in Figure 2. The blue oxide film which resulted from the stress relieving treatment was desired to be certain the specimens had the same surface condition that Apollo tankage material has. In a portion of the experimental program, as explained in the defect location section, it was found that this stress relief has an effect on the crack-propagation characteristics of the Ti-6Al-4V alloy.

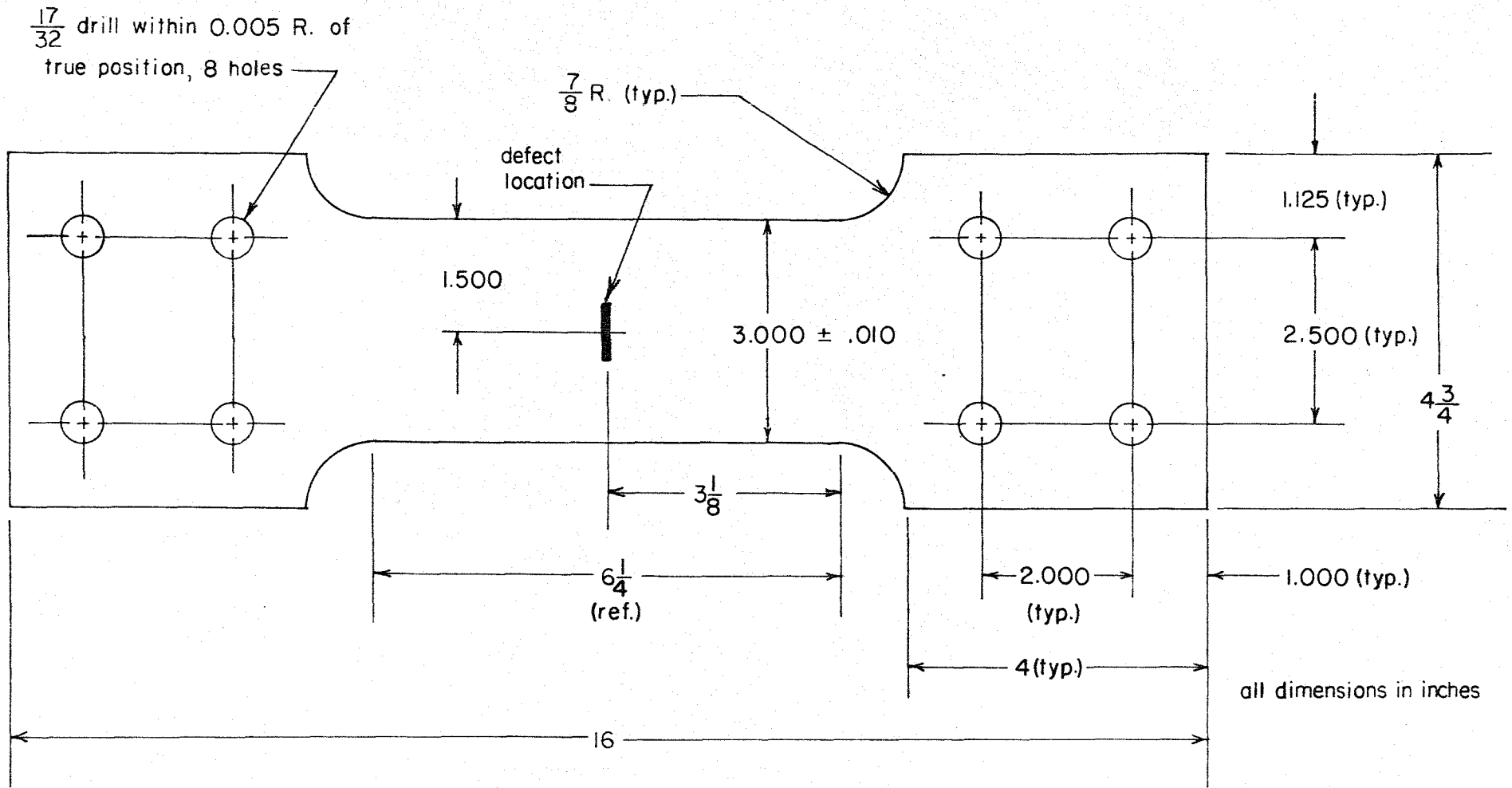
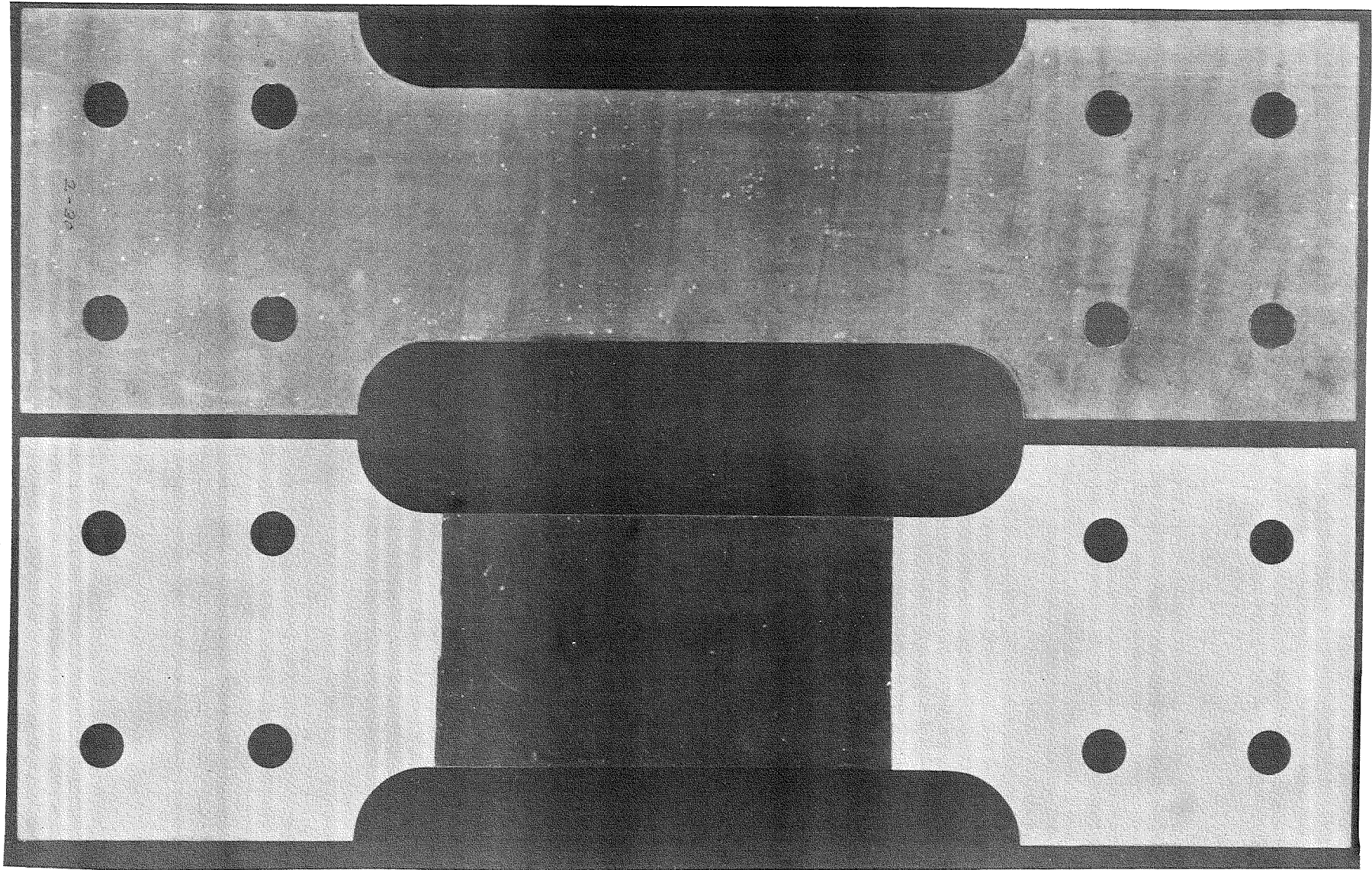


FIGURE 1. SPECIMEN USED THROUGHOUT THE EXPERIMENTAL PROGRAM



C-4896

FIGURE 2. STRESS RELIEVED SPECIMEN, REDUCED TO SLIGHTLY OVER 1/2 SIZE.
TOP - SPECIMEN AFTER STRESS RELIEF.
BOTTOM - SPECIMEN AFTER GRIT BLASTING.

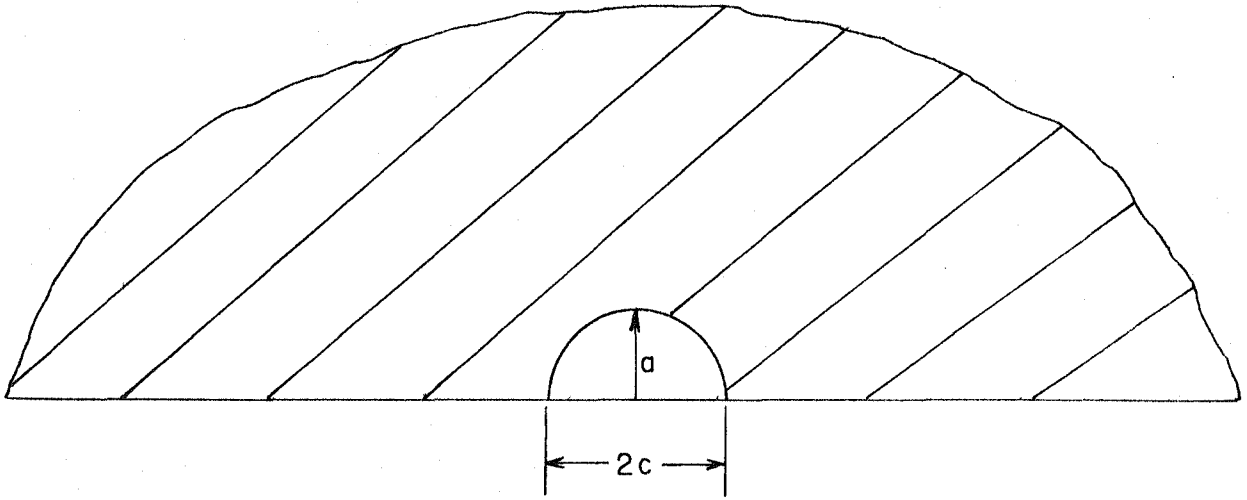
Location and Type of Starter Flaw

In all cases, the starting flaw was an EDM surface flaw approximately hemispherical in shape. This flaw was located in the center of the critical section of the specimen, and the initial fatigue crack was grown from it as described subsequently. In the case of the welded specimen, the location of the EDM notch varied somewhat; this will also be described.

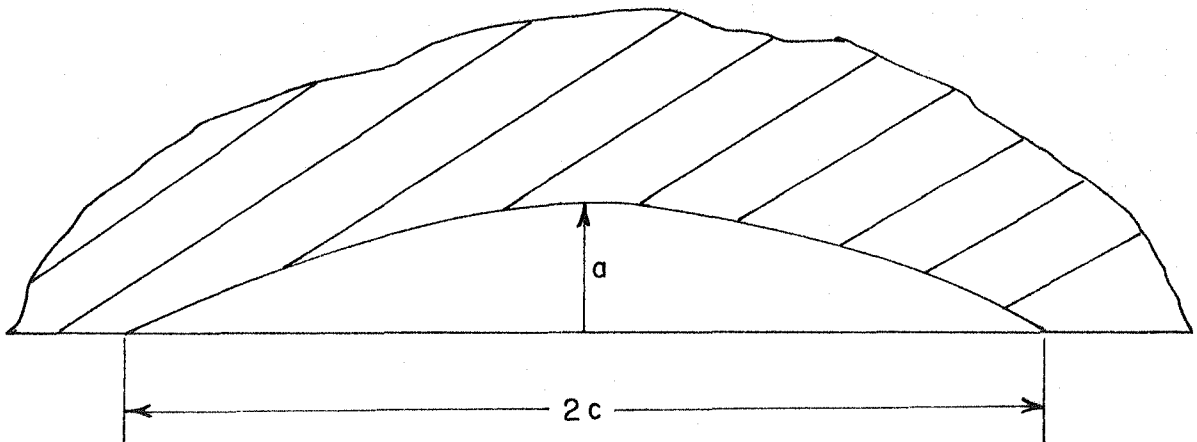
Flaws may occur in structures as a design discontinuity or may be embedded flaws, through-the-thickness flaws, or surface flaws which extend part-way through the thickness. The surface flaw was selected for this study since it was believed that it represents the real flaw that might be encountered in service most frequently. An embedded flaw was not selected since the study of its behavior is quite complex and research tools are still being developed to study its characteristics. The through-the-thickness flaw was not selected for this initial program, since it was considered likely that flaws of this nature will leak and be located.

Initially, two types of starting flaws were desired, a normal flaw and an elongated flaw. These flaws are depicted in Figure 3. It was initially believed that the normal and elongated flaws could be introduced by an EDM operation and that the normal fatigue crack and elongated fatigue crack (with $2c/a > 10/1$) then could be grown from the starting EDM flaw.

Introduction of Initial Fatigue Crack. The initial flaws studied in this investigation consisted of fatigue cracks grown to the desired depth and configuration. In order to determine the most satisfactory method of producing fatigue cracks of the desired configuration, a preliminary study was conducted on small blanks of parent material which had not been heat treated. In addition, this portion of the study was undertaken to develop curves relating crack depth to crack length. This was necessary because the crack depth was specified as the significant variable rather than crack length. Furthermore, in the actual



A. A typical normal flow, $\frac{2c}{a} = \frac{2}{1}$



B. A typical elongated flow, $\frac{2c}{a} > \frac{10}{1}$

FIGURE 3. TYPICAL FLAW CONFIGURATIONS DESIRED

experiments, the quantity to be measured was crack length, not crack depth, and it was thus necessary to be able to predict the flaw depth from knowledge of the flaw surface length.

The first half of the preliminary tests showed that the normal flaws could be developed under axial loading from a small hemispherical surface notch (≈ 0.004 inch diameter, 0.003 inch deep) produced by Electric Discharge Machining. The load ratio, R, used for the cracking process was 0.1, the maximum stress employed varying from 50,000 psi to 75,000 psi depending on specimen thickness. This procedure developed the desirable cracks with a nearly semicircular crack front in less than 100,000 cycles. In order to calibrate the surface crack length with the crack depth, the preliminary specimens for each thickness were fractured and the surface crack length and crack depth were measured with a traversing microscope. The resulting plots relating surface crack length and crack depth for the normal flaws developed in the preliminary study are shown in Figure 4. These curves were used to determine the surface crack length necessary to produce a given depth normal flaw for the full size specimens. The typical crack configurations for the normal flaws are shown in Figure 5.

Preliminary attempts to develop an elongated fatigue crack under axial fatigue from variously shaped EDM surface notches proved unsuccessful. Instead of developing an elongated crack front, several normal flaws would initiate at random locations along the notch and propagate until they linked together. The result was an unreproducible crack shape. The next approach was to change the type of loading from axial fatigue to bending fatigue. It was found that the combination of EDM hemispherical surface notch used for developing the normal flaws and three-point bending fatigue could be used successfully to develop the elongated flaws. The correlation between the surface crack length and the crack depth for the elongated flaws was determined in the same manner as for the normal flaws. The resulting curve for each thickness is shown in Figure 6. In Figure 7 typical elongated cracks are shown.

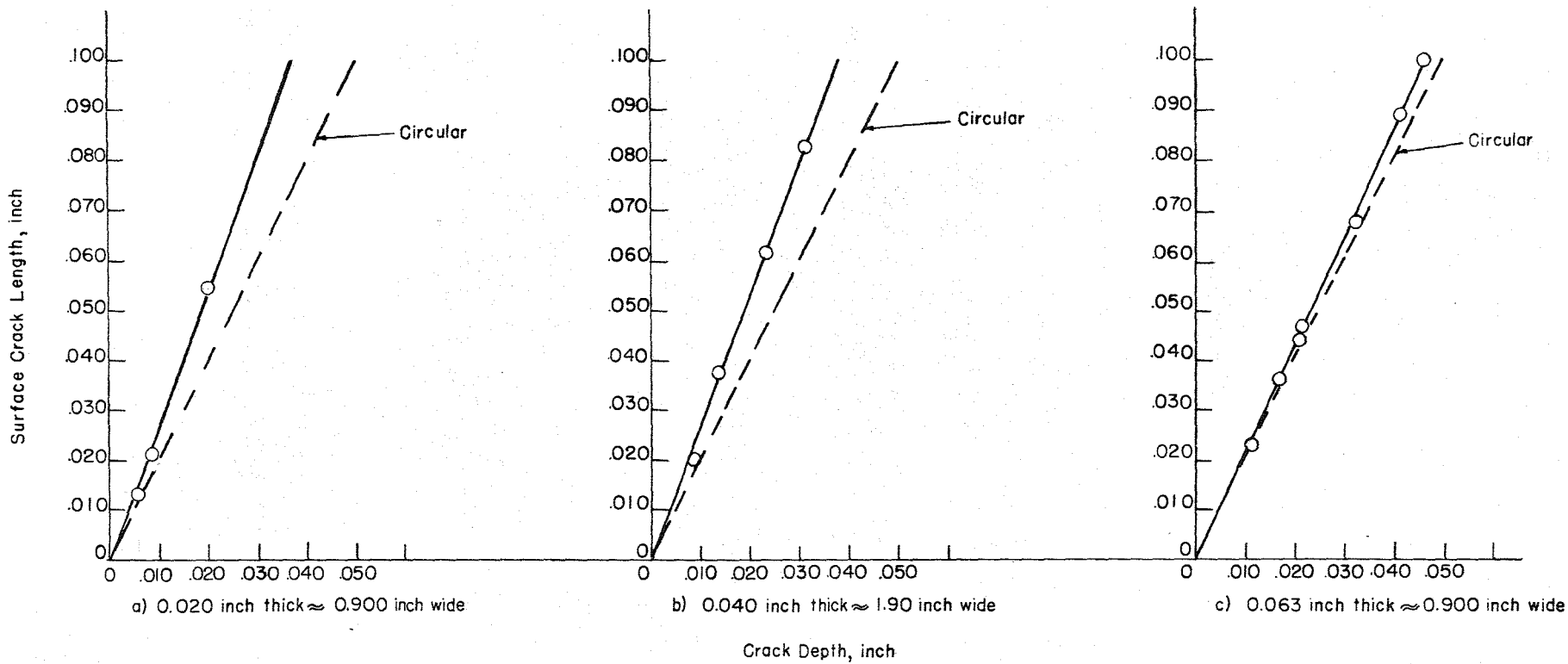
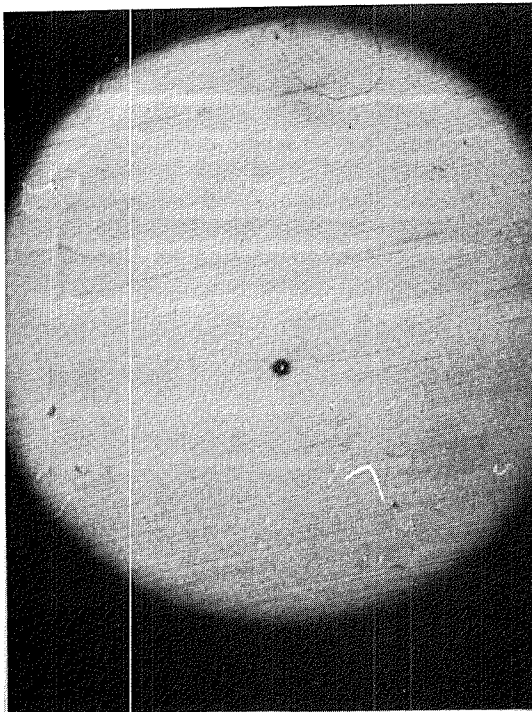
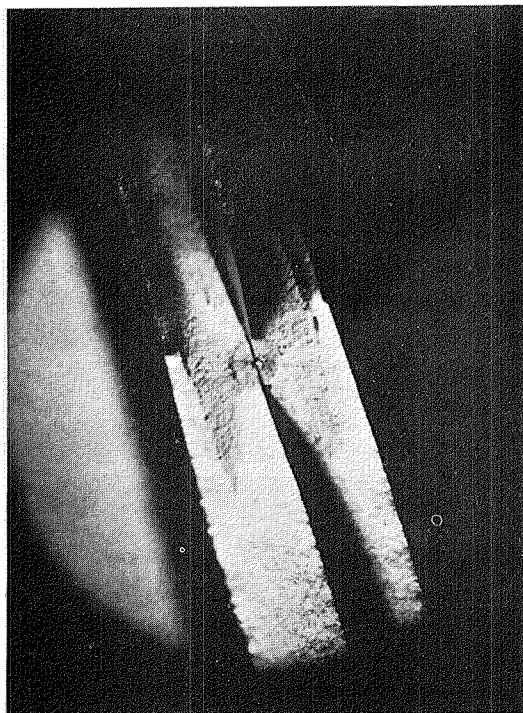


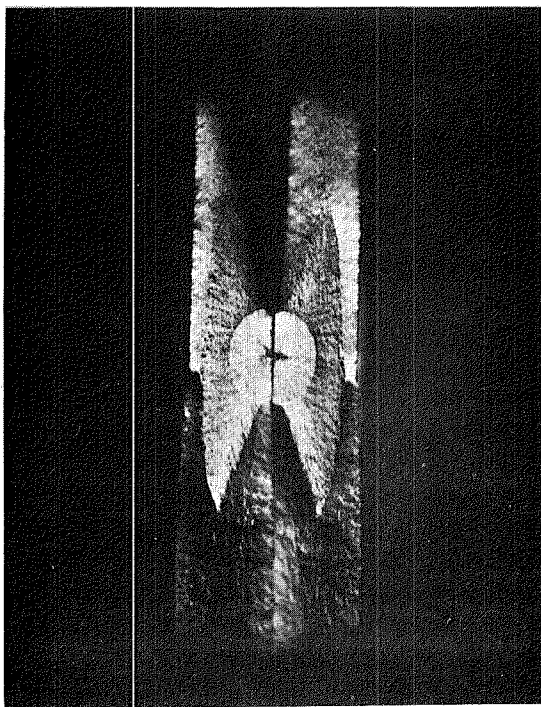
FIGURE 4. CURVES OF SURFACE CRACK LENGTH VERSUS CRACK DEPTH FOR Ti-6Al-4V STA IN THE INDICATED THICKNESSES



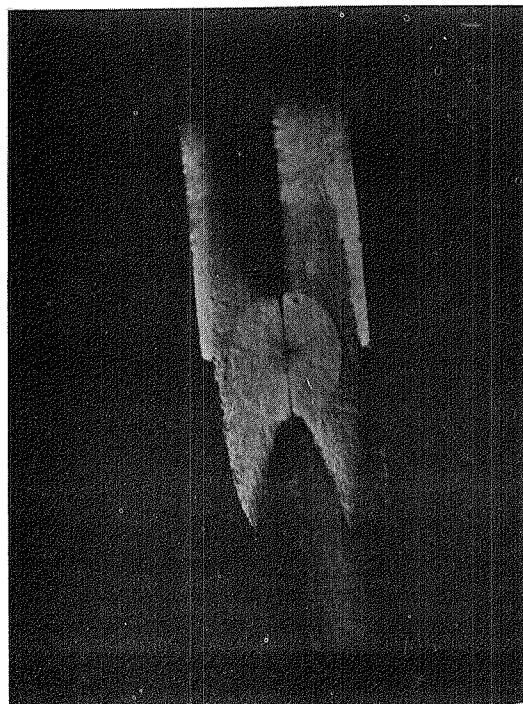
a) EDM Notch - 0.004 inch diam.



b) Fatigue Crack (7X),
 $2c=0.0359$ inch, $a=0.017$ inch



c) Fatigue Crack (7X)
 $2c=0.0678$ inch, $a=0.0321$ inch



d) Fatigue Crack (7X)
 $2c=0.0996$ inch, $a=0.0460$ inch

FIGURE 5. DETAILS OF THE NORMAL FLAW

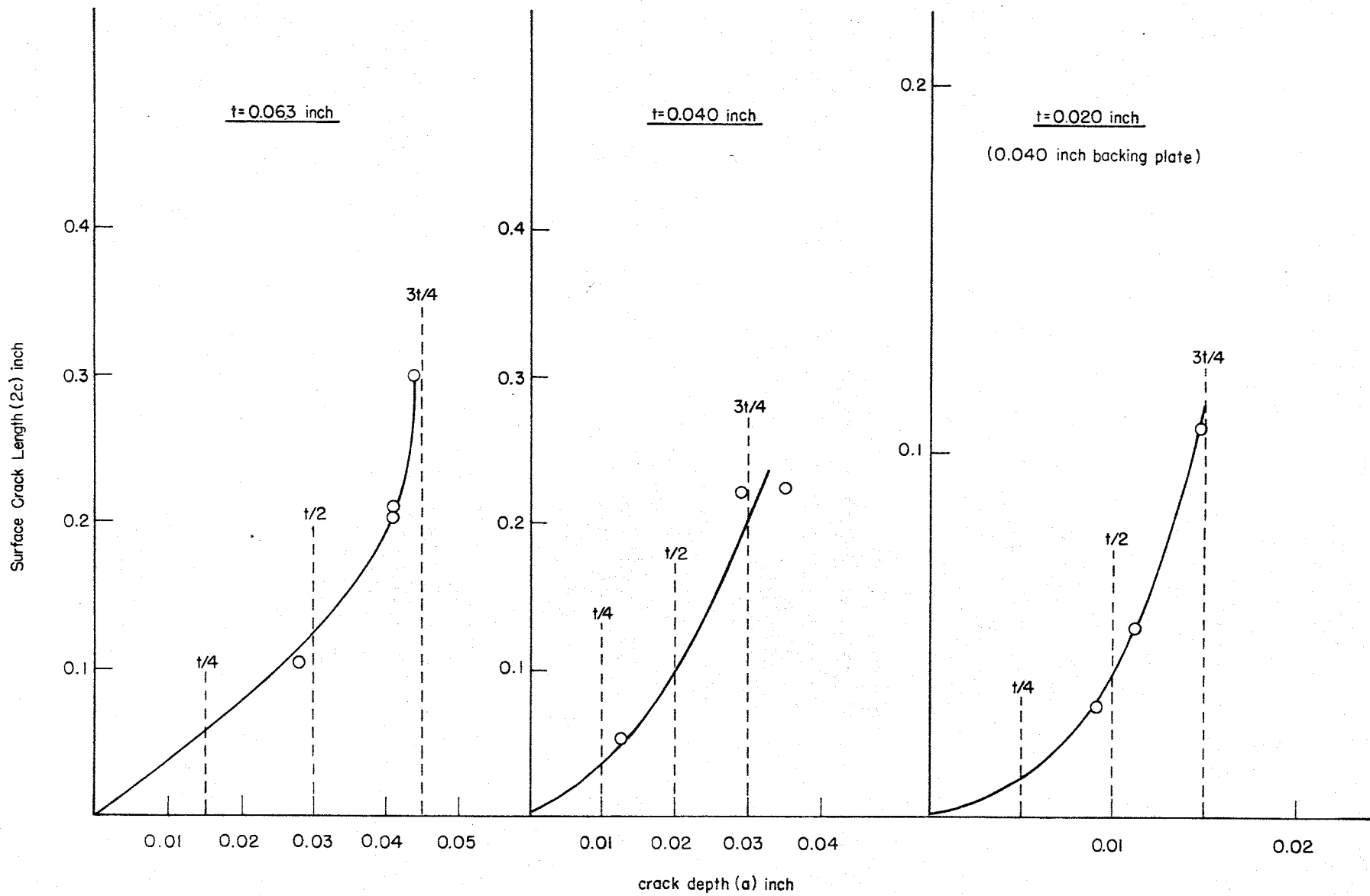
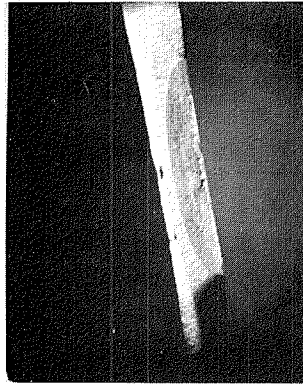
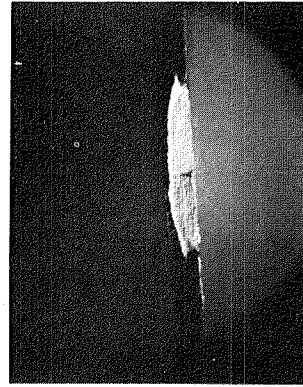


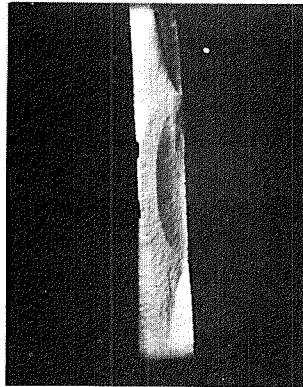
FIGURE 6. SURFACE CRACK LENGTH VERSUS CRACK DEPTH for Ti-6Al-4V SPECIMENS PRECRACKED in BENDING



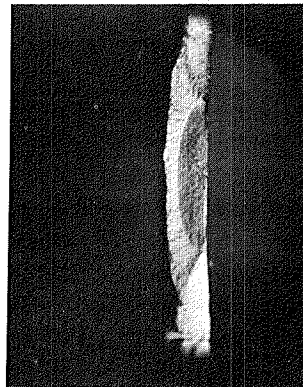
(a) Fatigue crack
 $2c = 0.301$ inch
 $a = 0.0444$ inch
 $2c/a = 6.78:1$
 $t = 0.0655$ inch



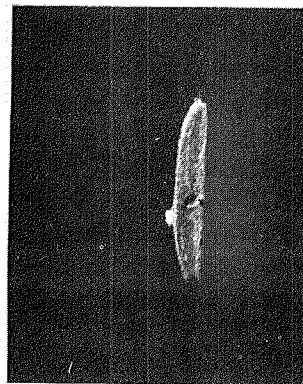
(b) Fatigue crack
 $2c = 0.2236$ inch
 $a = 0.0346$ inch
 $2c/a = 6.46:1$
 $t = 0.0435$ inch



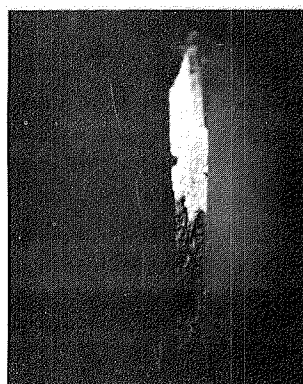
(c) Fatigue crack
 $2c_{\text{bending}} = 0.2029$ inch
 $a_{\text{bending}} = 0.041$ inch
 $2c_{\text{total}} = 0.2341$ inch
 $a_{\text{total}} = 0.0654$ inch
 $(2c/a)_{\text{bending}} = 4.95:1$
 $t = 0.066$ inch



(d) Fatigue crack
 $2c = 0.2011$ inch
 $a = 0.0406$ inch
 $2c/a = 4.95:1$
 $t = 0.0662$ inch



(e) Fatigue crack
 $2c = 0.1064$ inch
 $a = 0.016$ inch
 $2c/a = 6.7:1$
 $t = 0.022$ inch



(f) Fatigue crack
 $2c = 0.051$ inch
 $a = 0.0115$ inch
 $2c/a = 4.45:1$
 $t = 0.022$ inch

FIGURE 7. DETAILS OF ELONGATED FLAW INTRODUCED BY BENDING

Upon the completion of the preliminary tests, the cracking of the full-size specimens was initiated. The normal flaw specimens were then cracked under axial fatigue, $R = 0.1$ and a maximum stress of 70,000 psi for all thicknesses, parent and welded material, to the desired crack depth. Since the surface crack length was the crack dimension that could be directly measured, the surface crack length corresponding to the desired crack depth was obtained for each thickness from Figure 4. This use of Figure 4 for the full size specimen cracking assumed that the normal flaw growth characteristics were the same for the small blanks that were not stress-relieved as for the full-size specimens. To verify this assumption, the surface crack lengths and corresponding crack depths were measured for several of the full size specimens after fracture. These results are shown in Figures 8 and 9 for parent and welded material, respectively. Comparison of Figures 4 and 8 show that there is no appreciable difference between the flaws in the full-size specimens and those of the small preliminary specimens. Figures 8 and 9 also show that there is little difference between the normal flaw shapes for the parent and the welded material. The data in Figures 8 and 9 were used to determine the initial flaw depth for the fatigue crack propagation computations and analyses.

The elongated flaws were introduced into the full size specimens by three-point bending fatigue with $R = 0.1$ and a maximum stress of 130,000 psi for all thicknesses, parent and welded material. Although the stress of 130,000 psi appears high in relation to the yield stress, no evidence of plastic yielding was observed at the crack tip. The preliminary curves of surface crack length versus crack depth shown in Figure 6 were used to determine crack depth for the initial cracking. Flaw dimension measurements from full size specimens also were plotted for comparison with the preliminary data. The data for the full size specimens are shown in Figures 10 and 11 for the parent and welded material, respectively. Comparison of Figures 10 and 11 and Figure 6 again show good agreement between the preliminary specimen data and the full-size specimen data.

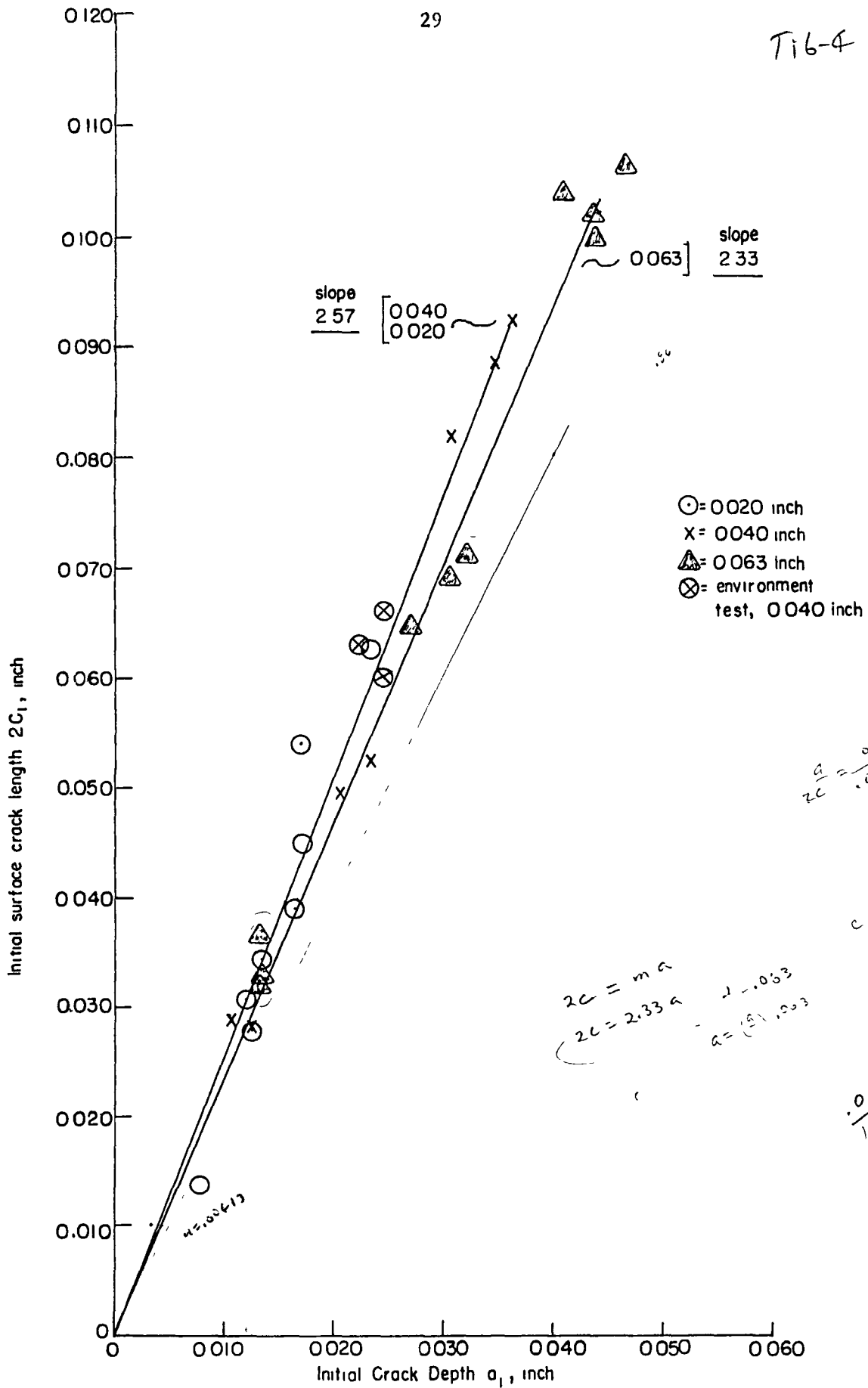


FIGURE 8. INITIAL SURFACE CRACK LENGTH VERSUS INITIAL CRACK DEPTH FOR NORMAL FLAWS IN PARENT MATERIAL

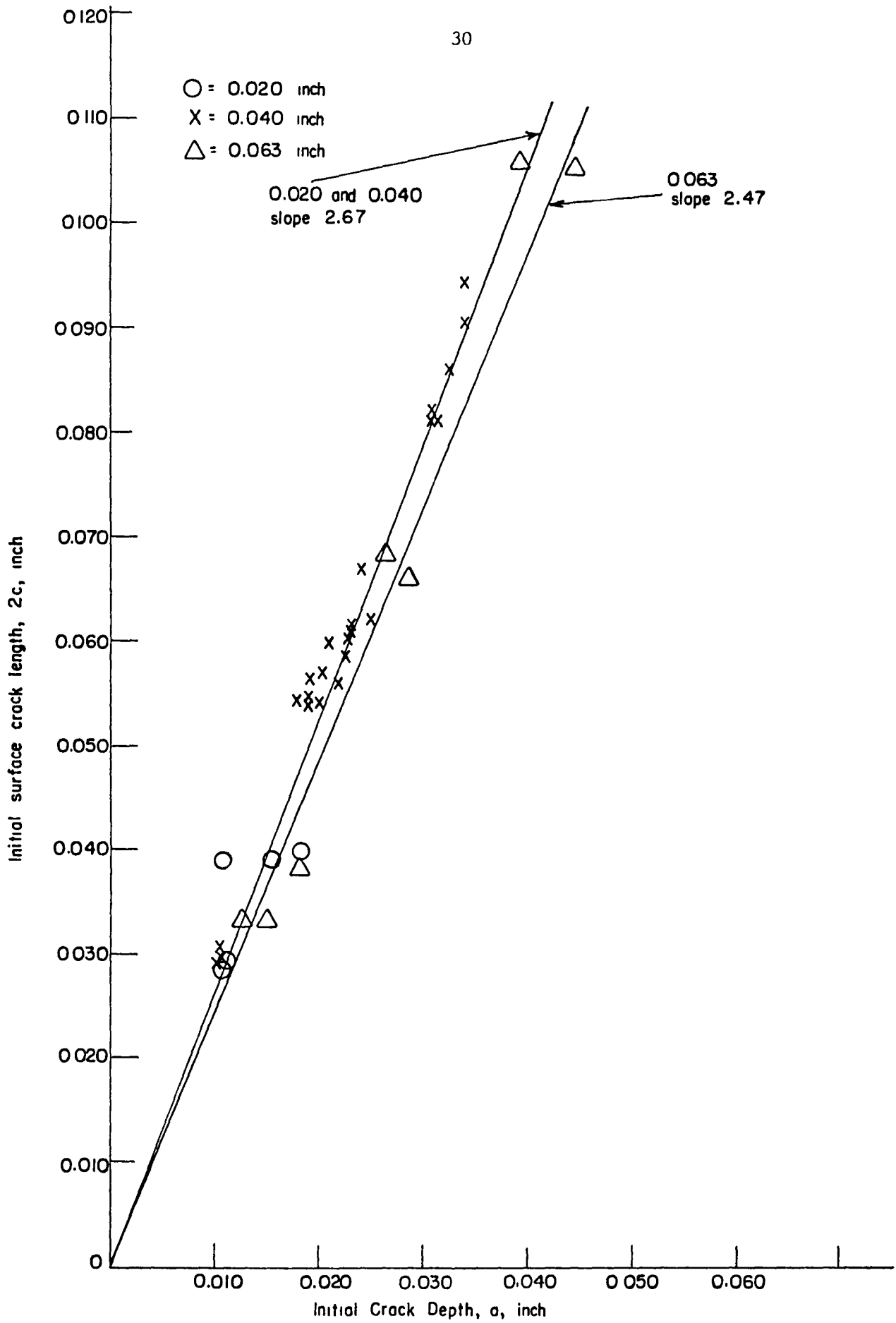


FIGURE 9. INITIAL SURFACE CRACK LENGTH VERSUS INITIAL CRACK DEPTH FOR NORMAL FLAWS IN WELDED MATERIALS

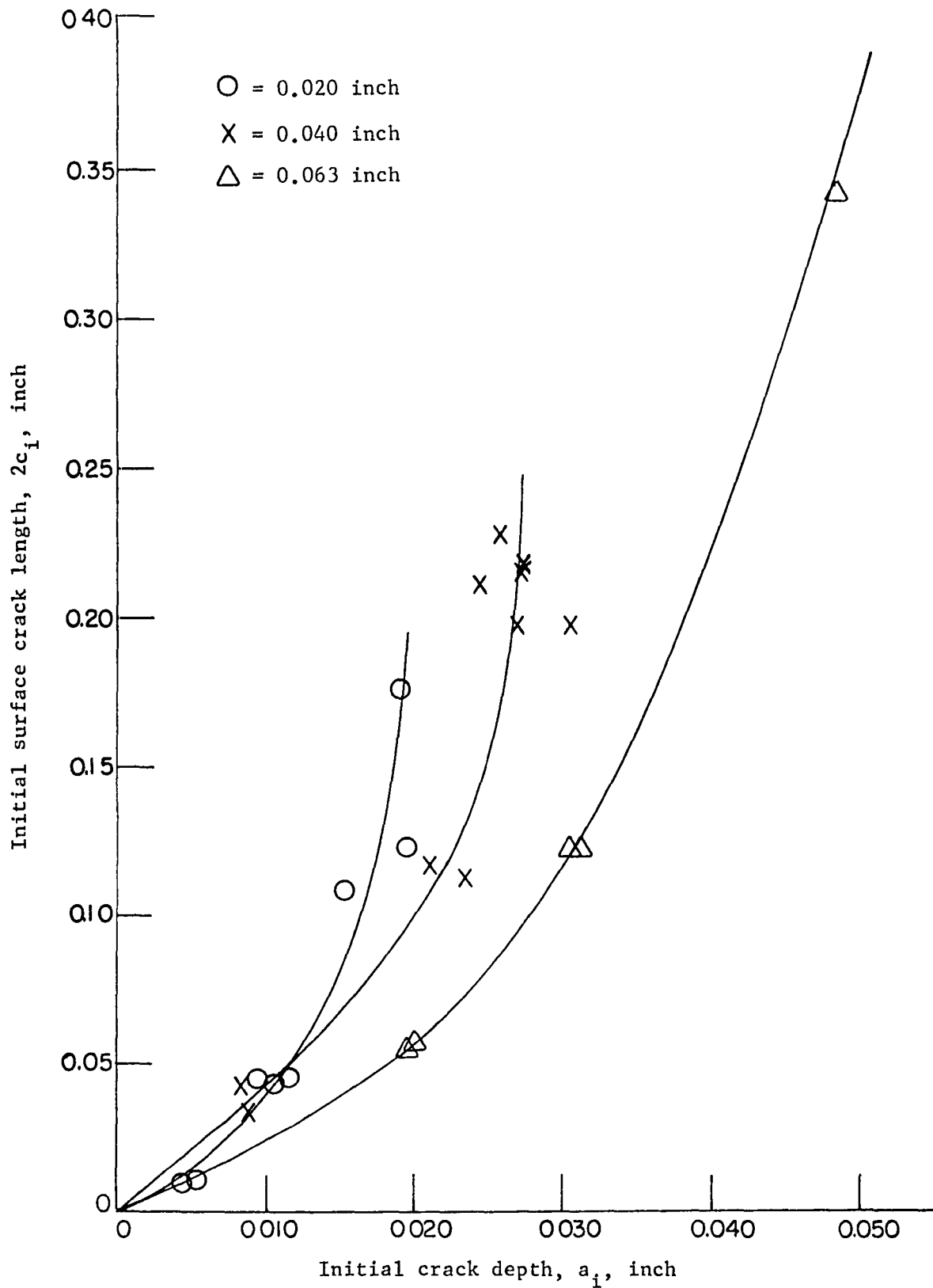


FIGURE 10. INITIAL SURFACE CRACK LENGTH VERSUS CRACK DEPTH FOR ELONGATED FLAWS IN PARENT MATERIAL

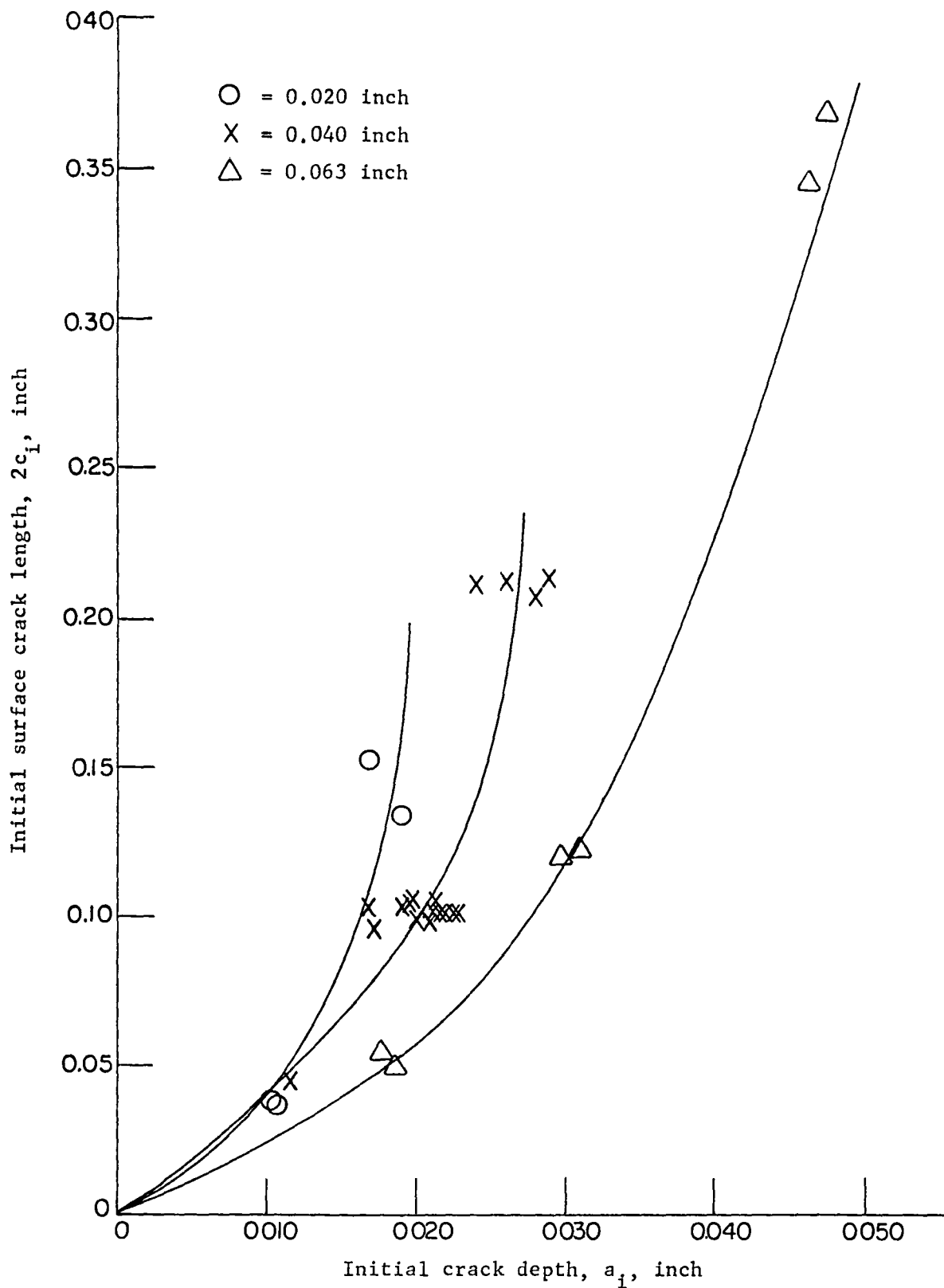


FIGURE 11. INITIAL SURFACE CRACK LENGTH VERSUS INITIAL CRACK DEPTH FOR ELONGATED FLAWS IN WELDED MATERIAL.

The data shown in Figures 10 and 11 were used in the fatigue-crack propagation computations and analyses.

Initially it was hoped that a surface crack length to depth ratio ($2c/a$) of 10 to 1 could be obtained for the elongated flaws. However, the flaws actually obtained had a $2c/a$ ratio of less than 10 and the ratio varied with the flaw depth as can be seen in Figures 10 and 11.

Location of EDM Flaw in Welded Material

In conversation between Battelle and NASA personnel, it was agreed that the possibility existed that the crack propagation characteristics and fracture toughness of the welded specimens might be dependent on the location of the EDM starting flaw. (Since the weld fusion line was difficult to locate, the center of the weld was selected as the reference point.) In fatigue crack propagation tests conducted in a methanol environment on specimens 0.058 inch thick, Tiffany (1)* found the most critical location for the starting flaw to be 0.030 to 0.050 inch from the weld fusion line. In all cases the specimens Tiffany used were machined flat in the gage area to provide a uniform cross-section. Results indicated that crack initiation most readily occurred at the weld centerline. However, the defect was located 0.030 to 0.050 inch from the weld fusion line since its propagation characteristics were next highest. Also, in the as-weld condition, the weld bead acts as reinforcing material for the weld and the applied stresses are lower at this location.

In this program tests to decide where to locate the flaw were conducted on full-size heat-treated specimens. The tests were conducted in axial loading in either a 20-kip or 50-kip electro-hydraulic servo-controlled fatigue testing system. (More detail on the equipment used is provided in the next section.) During the course of a test, the machine would be stopped and a record of crack length made at the indicated number of cycles. In this manner, tests were conducted

* Numbers in parentheses refer to the references.

on several specimens of each material thickness with the EDM starting flaws located at various distances from the weld centerline. All tests were conducted at a maximum stress of 70,000 psi and an R ratio of 0.1.

The results, plotted as surface crack length versus number of cycles of propagation, are shown in Figures 12, 13, and 14 for the 0.020-, 0.040-, and 0.063-inch thick material, respectively. In these tests, the weld bead was not machined off the specimens; thus, the crack propagation at the center of the weld bead does not appear critical for any of the specimens.

In Figure 12, for the 0.020 inch thick material, the curves indicate a large amount of scatter. The curve for the 0.124-inch location is the boundary on the left and the curve for the 0.147-inch location is the boundary on the right. The 1.60-inch location (for the EDM flaw located well within parent material) curve falls in the midst of the data. All curves to the left of this curve indicate more rapid propagation near the weld. However, some curves fall to the right of the parent material curve indicating that the scatter in the data may override the influence of the weld. Nonetheless, it was decided to position the flaw at a location yielding propagation similar to the curve on the left boundary. This decision held for all three thicknesses. Thus, for the 0.020-inch thick material the flaw was located 0.120 inch from the weld bead centerline.

In the case of the 0.040- and 0.063-inch-thick material, curves such as those shown in Figures 13 and 14 result. For the 0.040-inch-thick material, the critical location appears to be between 0.175 and 0.210 inch. Again, however, a large amount of scatter is exhibited. The EDM flaw actually was located 0.175 inch from the center of the weld. In Figure 14, a large range of results will be noted. The starting flaw was located 0.140 inch from the weld centerline in the 0.063-inch-thick material, as this was determined to be the critical location.

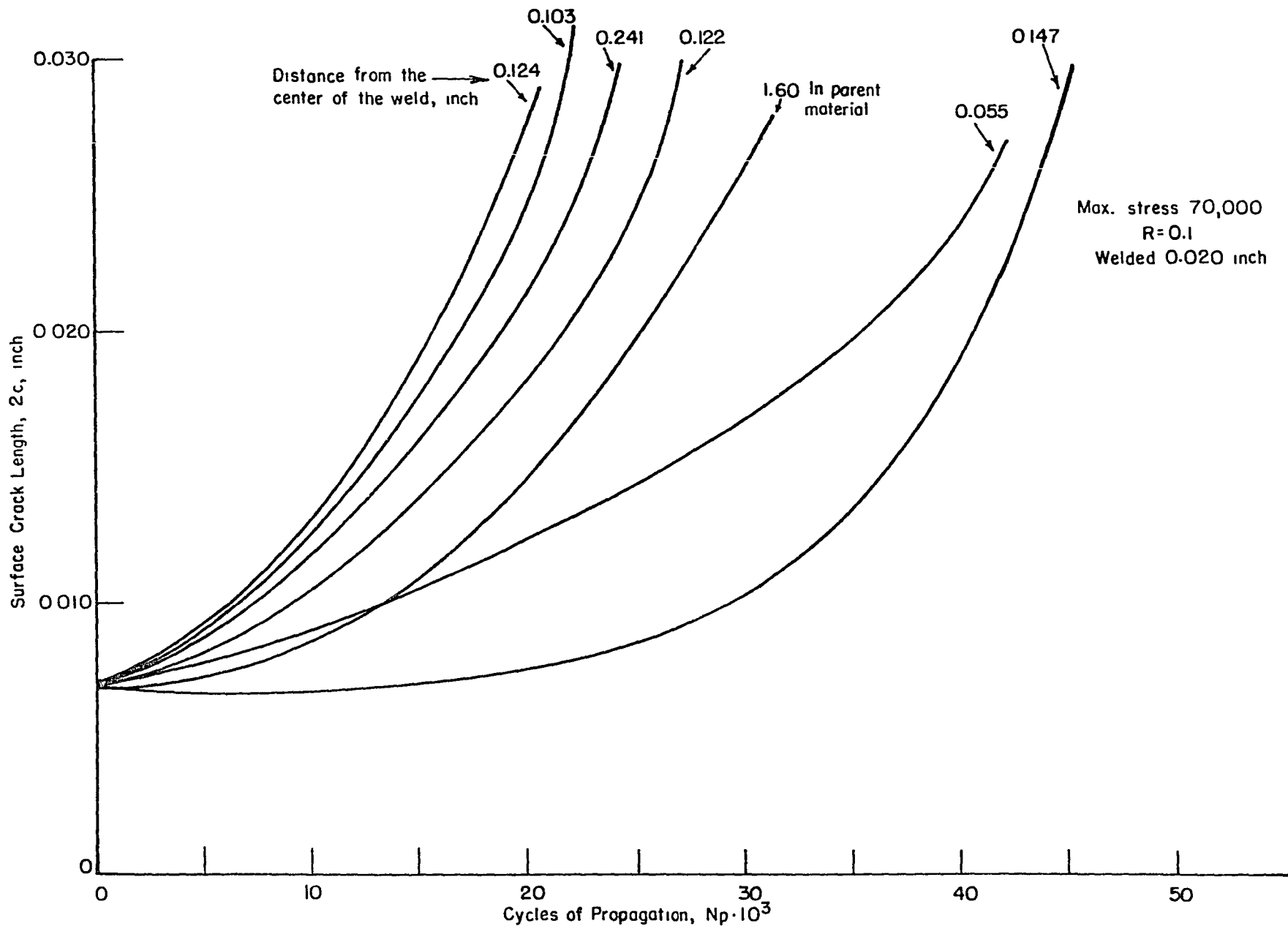


FIGURE 12. SURFACE CRACK LENGTH VERSUS CYCLES OF PROPAGATION FOR 0.020-INCH-THICK WELDED FULL-SIZE SPECIMENS OF Ti-6Al-4V STA WITH STARTER FLAWS LOCATED AT VARIOUS DISTANCES FROM THE CENTER OF THE WELD

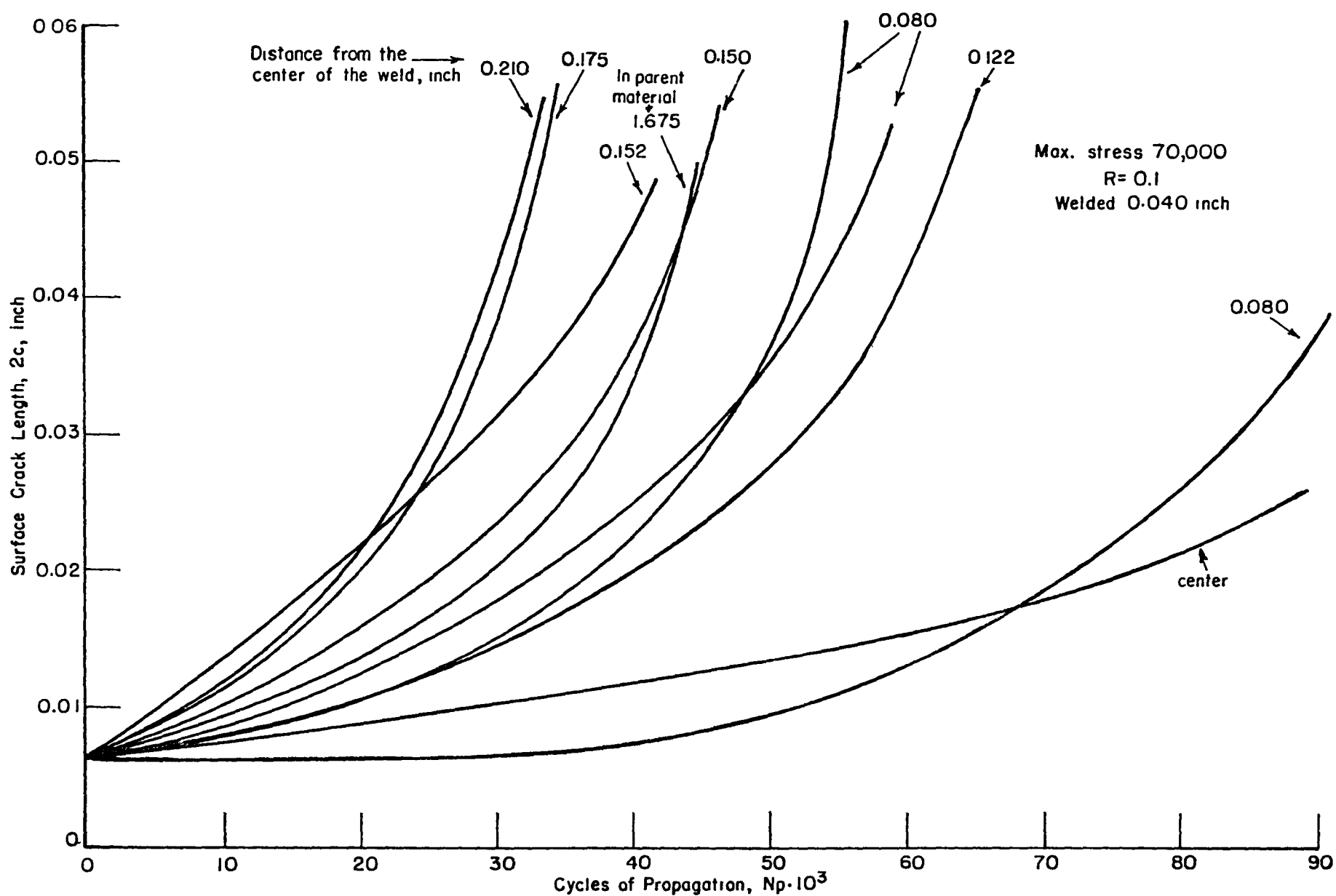


FIGURE 13. SURFACE CRACK LENGTH VERSUS CYCLES OF PROPAGATION FOR 0.040-INCH-THICK WELDED FULL-SIZE SPECIMENS OF Ti-6Al-4V STA WITH STARTER FLAWS LOCATED AT VARIOUS DISTANCES FROM THE CENTER OF THE WELD

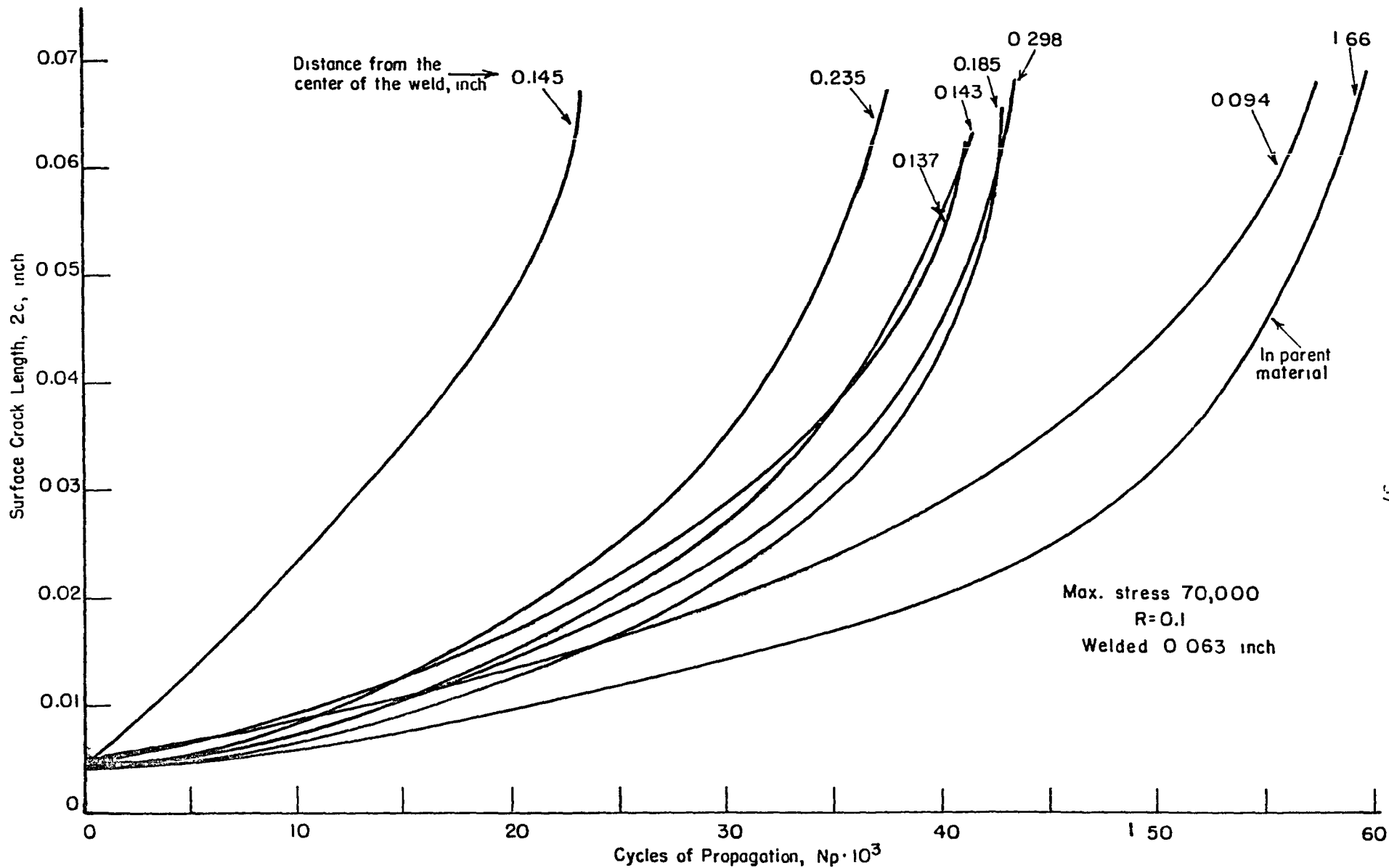


FIGURE 14. SURFACE CRACK LENGTH VERSUS CYCLES OF PROPAGATION FOR 0.063-INCH THICK WELDED FULL-SIZE SPECIMENS OF T1-6Al-4V STA WITH STARTER FLAWS LOCATED AT VARIOUS DISTANCES FROM THE CENTER OF THE WELD

In these two cases the flaw locations were within the weld heat-affected zone.

Figure 15 summarizes the location of the EDM notches in the welded specimens. Subsequent to the EDM operation, the fatigue cracks were introduced into the welded specimen using the same procedures as used for parent material. Some difficulties were encountered in the introduction of elongated flaws in the welded specimens. The problem was that several flaws would develop in a scratch resulting from a polishing operation prior to welding. However, using special experimental techniques, the difficulty was, in most cases, eliminated.

Allocation of Specimens

There were three principal aspects of the study as previously indicated. The specimens were allocated to the three areas; fracture, programmed fatigue-crack propagation and sustained load, as indicated in Tables 6, 7, and 8. The flaw size is indicated in these tables by $t/4$, $t/2$, and $3t/4$. In all cases this refers to the initial fatigue crack depth (a , inch) and is used throughout the report. Table 6 gives the allocation of specimens for the room temperature tests. The variables environment, flaw depth, flaw location were studied for each of the three areas. Table 7 denotes the specimens allocated to a study of the influence of cryogenic temperature on the fracture toughness test results. Table 8 denotes the specimen allocation for the specimens used to study the influence of the initial cryogenic proof tests.

Procedures and Results

In the following subsections the fracture, crack propagation, and sustained load testing procedures and results are presented. Each subsection is divided into four parts, namely; equipment, procedure, results, and interpretation.

Thickness, inch	Distance of EDM flaw from center of weld, X, inch
0.020	0.120
0.040	0.175
0.063	0.140

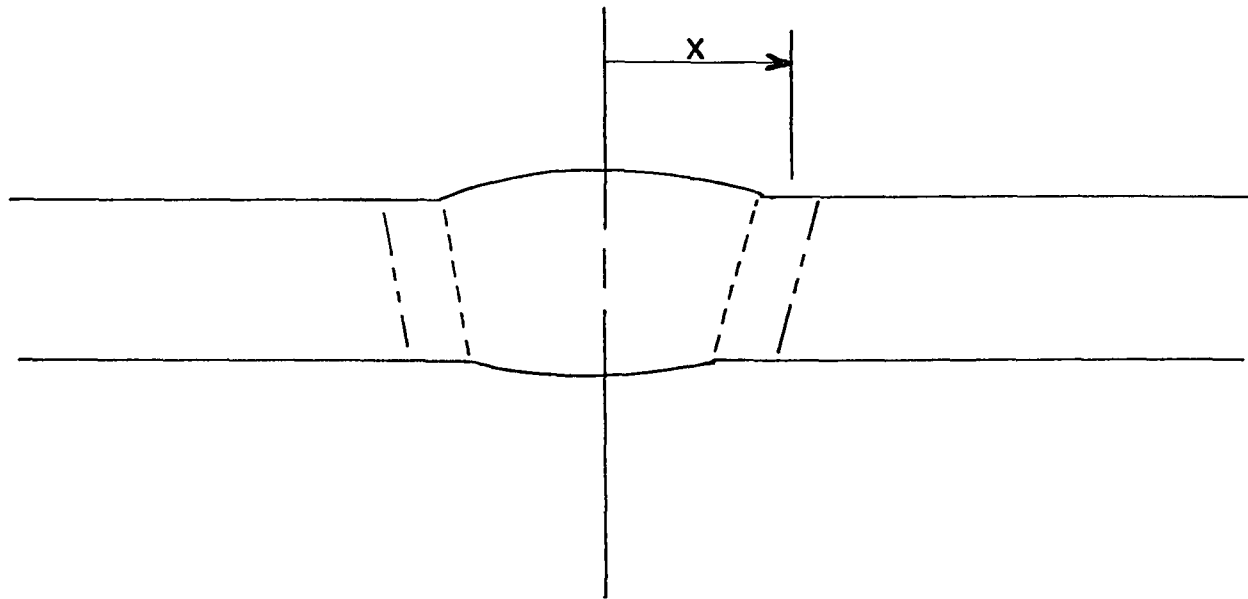


FIGURE 15. FLAW PLACEMENT DETAIL IN THE WELDED SPECIMENS

TABLE 6. SPECIMEN ALLOCATION ROOM TEMPERATURE TESTS

Thickness, inch	Environment	Material	Test Type			
			(Duplicate Specimens at t/4, t/2, 3t/4) ⁽¹⁾			
			Fract. ⁽²⁾	Prog. ⁽³⁾	Sust. ⁽⁴⁾	
Forging	Air	Parent	5			
0.020	Air	Parent	12	12		
		Weld	12	12		
0.040	Air	Parent	12	12	4	
		Weld	12	12	4	
		P&W ⁽⁵⁾	8 ⁽⁶⁾	8	8	
		Demineralized Water	P&W	8	8	8
		Aerozine 50	P&W	8	8	8
		Inhibited Water	P&W	8	8	8
0.063	Air	Parent	12	12		
		Weld	<u>12</u>	<u>12</u>	—	
Totals			109	104	40	

(1) Two flaw types--normal and elongated, see Note (6).

(2) Fract.--fracture toughness test.

(3) Prog.--programmed load test.

(4) Sust.--sustained load test.

(5) P--parent, W--weld.

(6) For the environmental tests--one flaw size, t/2.

TABLE 7. SPECIMEN ALLOCATION CRYOGENIC TESTING

Thickness	Material	Fracture Toughness Tests Only ⁽¹⁾
.020	Parent	12
	Weld	12
.040	Parent	12
	Weld	<u>12</u>
Total		48

(1) See Table 6 for nomenclature.

TABLE 8. SPECIMEN ALLOCATION INFLUENCE OF
INITIAL CRYOGENIC PROOF STRESS

Thickness	Material	No. of Specimens for a Programmed Load Test(1)
0.040	Parent	12

(1) Two flaw types, normal and elongated; three flaw depths; and two specimens per condition.

Fracture Strength

The primary objective of this portion of the study was to ascertain whether cryogenic proof testing will reveal smaller defects than proof testing in air. Two corollary questions were:

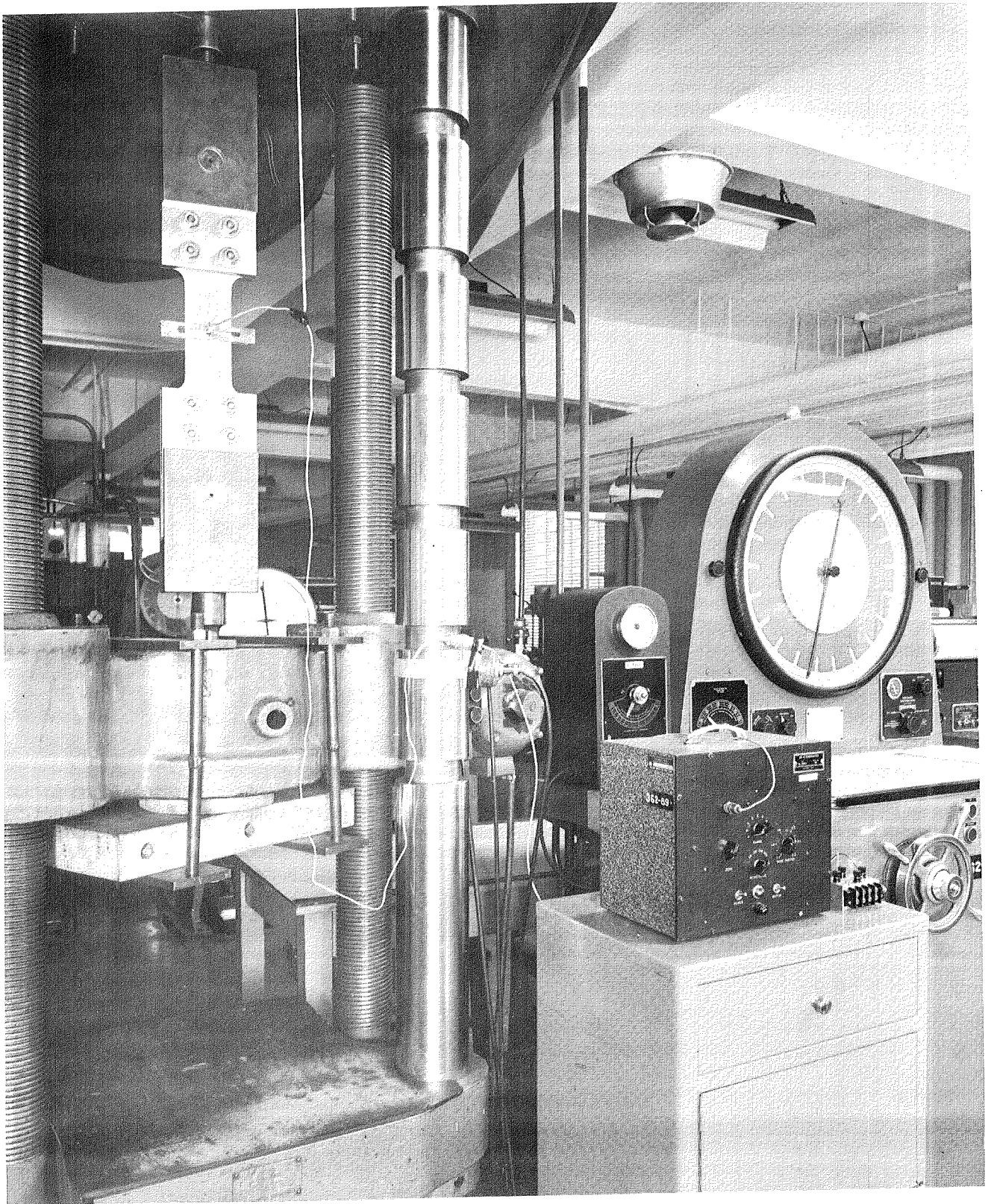
- (1) What is the fracture strength of specimens of each material thickness with natural defects in them?
- (2) What is the influence of environment on the fracture strength?

Answers to these questions were found using the equipment and procedures described in the four following subsections. Results are presented and several new aspects of the thin sheet fracture problem were observed in the data analysis. These suggest future research that is discussed subsequently.

Test Apparatus. The fracture tests were performed in a 200,000-lb capacity Baldwin Universal Testing Machine in the Battelle Mechanical Testing Laboratory. The basic test and equipment arrangement is illustrated in Figure 46.

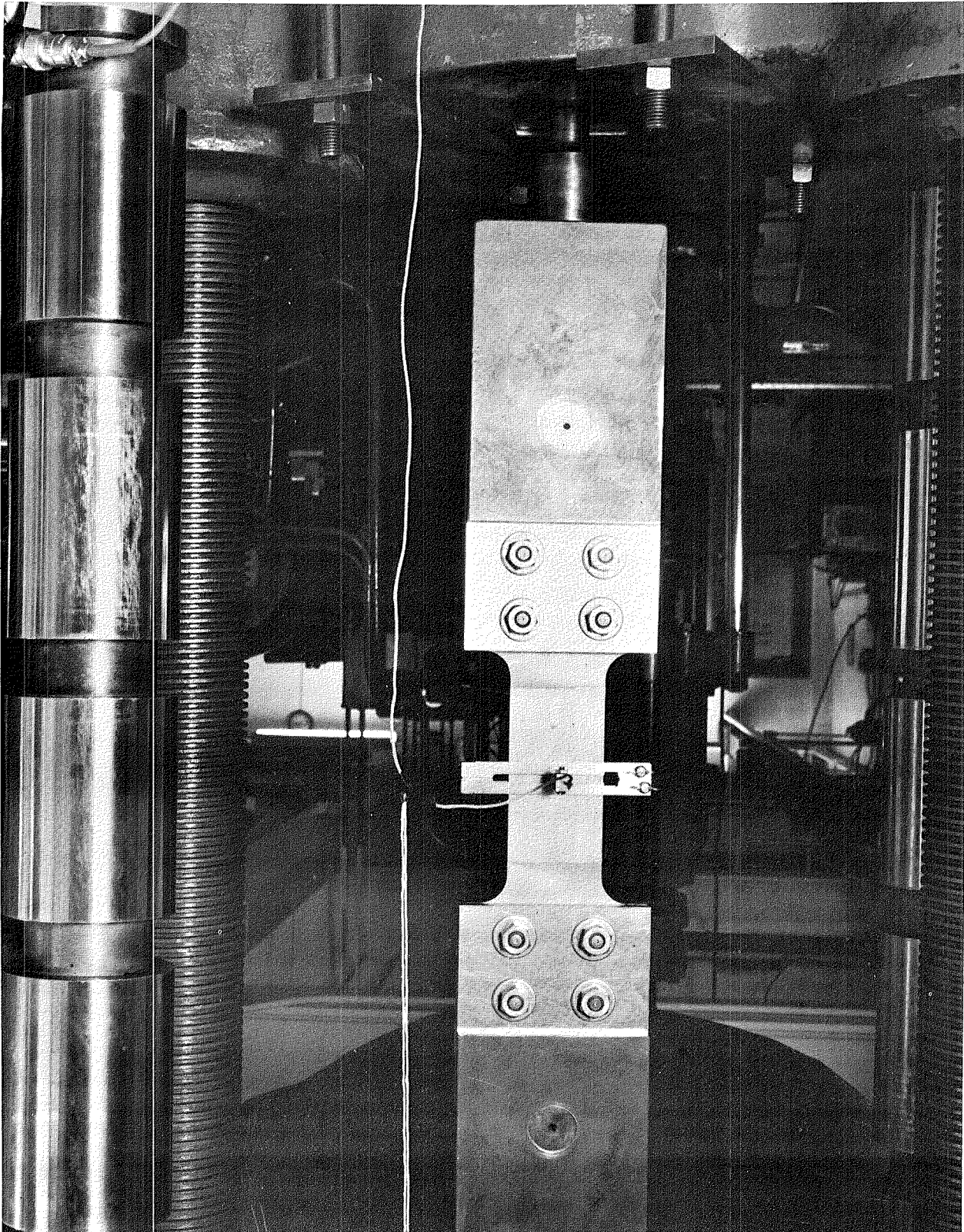
Test Set-up. The fracture test specimen was mounted between the loading heads of the testing machine as shown in Figure 17. The thin sheet specimen was bolted between grit-blasted load plates to assure a uniform development of load in the critical section. The load plate sandwich then was joined to the loading clevis by a hardened steel pin that permits axial alignment of the load.

Compliance Gage. The double cantilever compliance gage and support bracket shown in Figure 18 were mounted on the specimen prior to loading. The gage was centrally located over the flaw with a nominal gage length of one-half inch. Four 350-ohm foil strain gages, one mounted at the root of each side of the cantilevers, formed the active bridge for an SR-4 strain converter.



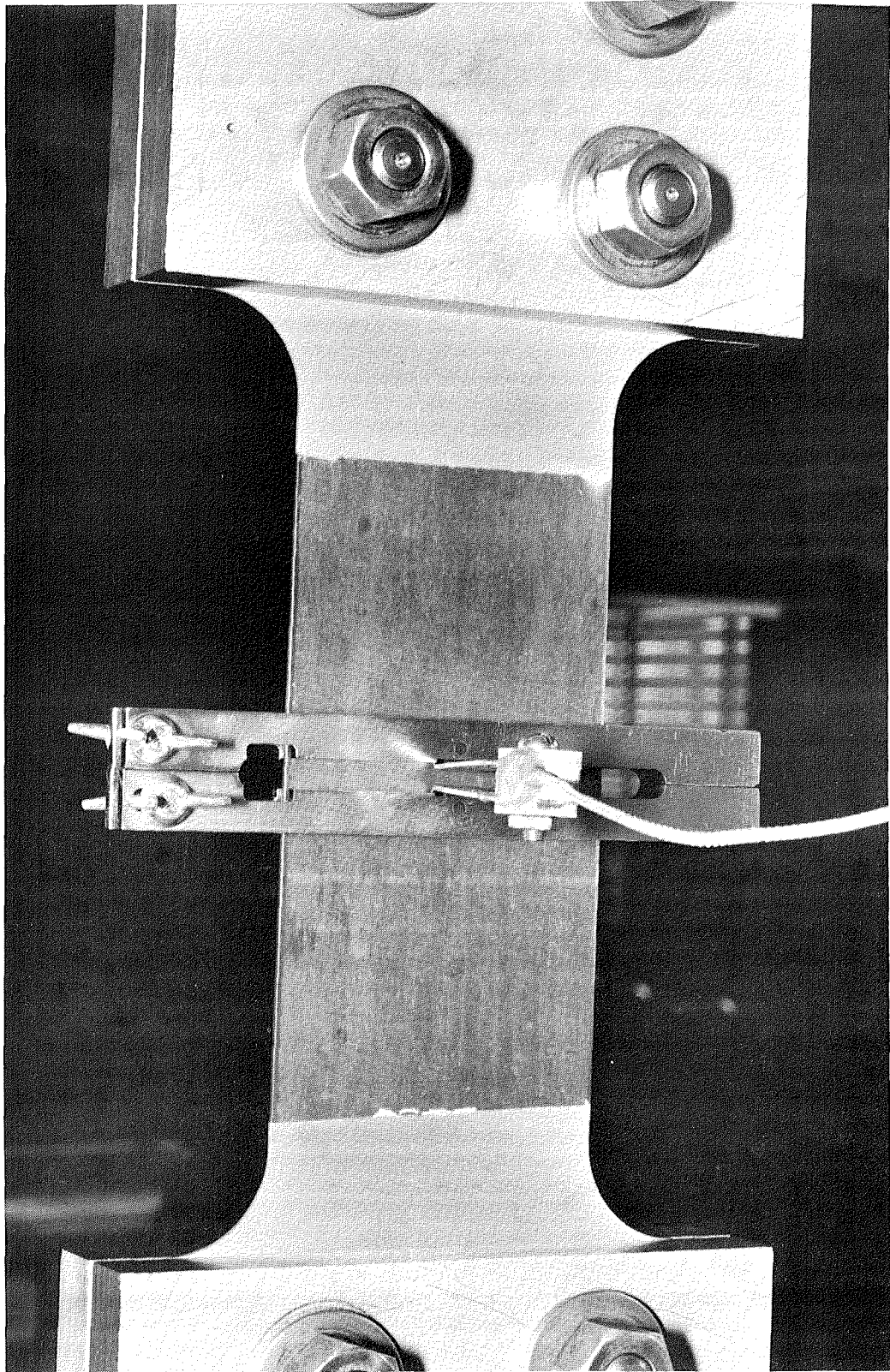
39190

FIGURE 16. THE BASIC TEST AND EQUIPMENT USED IN THE FRACTURE STUDIES.



39187

FIGURE 17. THE TEST SPECIMEN MOUNTED IN THE TEST MACHINE FOR A FRACTURE TEST.



39189

FIGURE 18. THE DOUBLE CANTILEVER COMPLIANCE GAGE MOUNTED IN POSITION ON THE SUPPORT BRACKET.

The converter output drove the deformation axis of a microformer recorder on the testing machine. The load axis was driven by the system hydraulic pressure.

Environmental Chambers. Aqueous, salt-spray, and Aerozine 50 environmental chambers similar to those described in the fatigue-crack propagation studies were used in the fracture studies. For the cryogenic environment, a large stainless steel dewar with a pull rod adapter was used to surround the entire specimen and compliance gage. The test specimen and grips were immersed and thoroughly stabilized in liquid nitrogen to assure an ambient temperature of -320 F.

Test Procedure. The fracture tests were conducted with a slowly increasing tensile load. A nominal strain rate of 0.003 in/in per minute was used. A load-deformation record was made for each specimen utilizing the compliance gage previously described.

Specimens were loaded to fracture and maximum load was recorded. Whenever a "pop-in" was noted either by a distinct horizontal offset on the recorder or by an audible "ping", the load was recorded. In almost all cases, such "pop-in" occurred when the specimen was deformed into the plastic range.

The same basic procedure was used in all fracture tests. Test in aqueous, saline, and Aerozine 50 environments were conducted with chambers enclosing the critical sections. The fluids were introduced shortly before loading; in no case was exposure in excess of 30 minutes. Cryogenic fracture tests were run after temperature stabilization, which usually required from 5 to 10 minutes.

Test Results. Presentation and analysis of fracture strength data are included in this section. Emphasis of fracture testing was placed on obtaining engineering data directly meaningful to the design function. Accordingly,

the display of this information is made as direct and meaningful as possible.

Basic Data. The tabulations of basic fracture data presented in Tables 9 through 30 are computer-derived print-outs. For each nominal gage of titanium tested in the indicated environment, the data tables contain the following information. After the specimen number, the specimen dimensions of thickness, T, and width, W, in inches are printed. The product area (T x W) is then computed and printed. The input load data are displayed as P1, the ultimate load, P2, the pop-in load (if it was detected), and P3, the 5 percent secant offset load, all in 1000-lb units. The respective stresses, S1, S2, and S3, are computed as the quotient of load to gross area and printed in ksi units. Following this are presented flaw size dimensions. The crack depth, A*, and surface crack length, 2C* are dimensions of the fatigue crack measured after fracture. The flaw area is computed as

$$\text{Area} = \pi AC/2$$

which is representative of the semi-elliptical or semi-circular flaw shapes. The remaining information is a first analytical presentation of data.

Stress Intensity Factors. The fracture data were first analyzed in terms of the stress intensity factor concepts of fracture mechanics^(2,3).

Using the formulation

$$K = 1.1 \sqrt{\sigma} \sqrt{\pi A} / \bar{\Phi}$$

where

σ = gross stress, ksi

A = flaw depth, inches

$$\bar{\Phi} = \text{elliptic integral of the second kind} \\ = \int_0^{\pi/2} \left[1 - \left(1 - \frac{A^2}{C^2} \right) \sin^2 \theta \right]^{1/2} d\theta$$

* Because the print out letters for a and c are A and C, use of the upper case letters is made at this point. In the remainder of the report a and c are used according to convention.

act in prop-in 500sec after

TABLE 9. 20 MIL TI-6AL-4V PARENT MATERIAL TESTED IN AIR

SPEC NO	SPEC. DIM., INCH			LOADS, KIPS			STRESSES, KSI			FLAW SIZE, INCH			STRESS INTENSITY FACTORS, KSI-SQRT(INCH)					
	T	W	AREA	P1	P2	P3	S1	S2	S3	A	2C	AREA	K1	K2	K3	K1	K2	K3
2001N	.021	2.990	.0643	10.60	0.00	9.45	164.9	0.0	147.0	.0050	.0135	.00009	16.5	0.0	14.7	0.0	0.0	15.0
2041N	.020	2.992	.0604	9.90	0.00	8.90	163.8	0.0	147.3	.0050	.0125	.00005	15.9	0.0	14.3	0.0	0.0	15.0
2023N	.020	2.987	.0597	9.45	0.00	8.55	158.2	0.0	143.1	.0131	.0346	.00036	25.0	0.0	23.0	20.4	0.0	24.1
2045N	.020	2.991	.0607	10.00	0.00	9.50	164.7	0.0	150.5	.0123	.0279	.00027	24.1	0.0	22.9	0.0	0.0	24.1
2025N	.020	2.994	.0599	9.30	0.00	8.05	155.3	0.0	134.4	.0169	.0540	.00072	30.4	0.0	28.3	32.2	0.0	27.0
2044N	.020	2.990	.0613	9.90	0.00	8.95	161.5	0.0	146.0	.0162	.0390	.00050	27.8	0.0	25.1	0.0	0.0	27.0
2028E	.021	2.990	.0626	9.95	0.00	8.75	158.5	0.0	139.4	.0051	.0111	.00004	14.6	0.0	12.0	15.4	0.0	13.3
2031E	.021	2.993	.0623	9.90	0.00	8.80	159.0	0.0	141.4	.0050	.0108	.00004	14.5	0.0	12.0	15.2	0.0	15.4
2003E	.021	2.987	.0642	10.40	0.00	9.05	161.9	0.0	140.9	.0106	.0428	.00035	26.7	0.0	23.4	0.0	0.0	24.4
2029E	.020	2.988	.0613	9.65	0.00	8.40	157.5	0.0	137.1	.0102	.0394	.00032	23.4	0.0	22.1	27.7	0.0	23.3
2043E	.021	2.988	.0627	9.60	8.57	0.00	153.0	136.7	0.0	.0151	.1134	.00134	33.9	30.3	0.0	37.2	32.6	0.0
2008E	.021	2.992	.0643	9.55	4.90	4.90	148.5	76.2	76.2	.0190	.1753	.00242	37.7	19.4	14.4	41.2	17.0	14.0

TABLE 10. 40 MIL TI-6AL-4V PARENT MATERIAL TESTED IN AIR

SPEC NO	SPEC. DIM., INCH			LOADS, KIPS			STRESSES, KSI			FLAW SIZE, INCH			STRESS INTENSITY FACTORS, KSI-SQRT(INCH)					
	T	W	AREA	P1	P2	P3	S1	S2	S3	A	2C	AREA	K1	K2	K3	K1	K2	K3
4003N	.044	2.990	.1331	22.20	0.00	18.75	166.8	0.0	140.9	.0115	.0300	.00027	25.0	0.0	21.1	0.0	0.0	22.1
4108N	.044	2.993	.1325	21.85	0.00	20.10	164.8	0.0	151.6	.0124	.0288	.00028	24.4	0.0	22.5	0.0	0.0	27.5
4032N	.042	2.991	.1256	20.25	0.00	18.75	161.2	0.0	149.3	.0229	.0525	.00047	32.3	0.0	29.9	0.0	0.0	31.0
4088N	.044	2.992	.1316	20.75	0.00	16.75	157.6	0.0	127.2	.0230	.0605	.00112	33.6	0.0	27.2	33.7	0.0	24.1
4095N	.042	2.990	.1256	19.30	0.00	16.90	153.7	0.0	134.6	.0304	.0820	.00196	38.0	0.0	33.3	40.1	0.0	34.7
4104N	.045	2.992	.1346	20.75	20.50	17.00	154.1	152.3	126.3	.0355	.0917	.00256	40.5	40.0	33.2	42.7	42.1	34.3
4073E	.041	2.992	.1233	20.60	0.00	18.00	167.1	0.0	146.0	.0088	.0348	.00024	25.2	0.0	22.0	0.0	0.0	23.4
4081E	.042	2.990	.1262	21.15	0.00	19.10	167.6	0.0	151.4	.0106	.0346	.00029	26.2	0.0	23.6	0.0	0.0	25.1
4037E	.043	2.992	.1293	19.90	0.00	16.75	154.0	0.0	129.6	.0207	.1086	.00177	37.9	0.0	31.9	41.1	0.0	33.7
4077E	.044	2.990	.1316	20.25	0.00	18.65	153.9	0.0	141.8	.0240	.1006	.00207	39.6	0.0	35.0	42.5	0.0	35.5
4102E	.045	2.992	.1346	18.50	17.25	13.20	137.4	128.1	98.4	.0340	.2377	.00044	45.5	42.5	32.6	48.2	45.2	33.0

TABLE 11. 60 MIL TI-6AL-4V PARENT MATERIAL TESTED IN AIR

SPEC NO	SPEC. DIM., INCH			LOADS, KIPS			STRESSES, KSI			FLAW SIZE, INCH			STRESS INTENSITY FACTORS, KSI-SQRT(INCH)					
	T	W	AREA	P1	P2	P3	S1	S2	S3	A	2C	AREA	K1	K2	K3	K1	K2	K3
6002N	.064	2.991	.1920	29.55	0.00	27.60	153.9	0.0	143.7	.0131	.0371	.00033	24.0	0.0	22.4	25.3	0.0	23.4
6004N	.064	2.990	.1929	29.90	0.00	27.70	155.0	0.0	143.6	.0134	.0343	.00036	24.9	0.0	23.1	26.5	0.0	24.2
6001N	.062	2.991	.1863	27.75	0.00	27.10	148.9	0.0	145.4	.0269	.0648	.00137	33.1	0.0	32.3	34.3	0.0	33.7
6010N	.064	2.993	.1910	28.65	0.00	27.50	150.0	0.0	144.0	.0296	.0690	.00161	34.5	0.0	33.1	40.1	0.0	34.5
6005N	.064	2.993	.1916	27.80	0.00	24.10	145.1	0.0	125.8	.0431	.1071	.00346	40.5	0.0	35.1	42.0	0.0	35.2
6025N	.063	2.994	.1880	27.50	0.00	25.10	146.3	0.0	133.5	.0435	.1001	.00342	40.5	0.0	30.9	42.0	0.0	35.3
6035E	.063	2.994	.1871	28.65	0.00	27.60	153.1	0.0	147.5	.0165	.0509	.00065	24.3	0.0	22.2	31.1	0.0	24.8
6037E	.063	2.993	.1901	28.85	0.00	27.90	151.8	0.0	146.9	.0187	.0549	.00060	30.4	0.0	29.4	32.3	0.0	31.0
6036E	.064	2.992	.1909	28.40	0.00	26.30	148.8	0.0	137.8	.0312	.1253	.00307	42.4	0.0	34.2	45.3	0.0	41.5
6045E	.063	2.991	.1869	27.40	0.00	25.30	146.6	0.0	135.3	.0309	.1335	.00324	42.3	0.0	39.0	45.2	0.0	41.3
6033E	.064	2.993	.1916	23.20	21.40	13.90	121.1	111.7	72.6	.0460	.3470	.01254	46.9	43.3	28.1	47.0	43.3	28.7
6034E	.063	2.994	.1901	22.55	20.50	15.80	118.6	107.8	83.1	.0477	.3544	.01328	46.7	42.5	32.7	49.2	44.3	33.6

TABLE 12. 40 MIL TI-6AL-4V PARENT MATERIAL TESTED IN DEMINERALIZED WATER

SPEC NO	SPEC. DIM., INCH			LOADS, KIPS			STRESSES, KSI			FLAW SIZE, INCH			STRESS INTENSITY FACTORS, KSI-SQRT(INCH)					
	T	W	AREA	P1	P2	P3	S1	S2	S3	A	2C	AREA	K1	K2	K3	K1	K2	K3
4014N	.044	2.992	.1322	20.80	0.00	19.75	157.3	0.0	149.3	.0236	.0593	.00110	33.3	0.0	31.6	35.1	0.0	33.2
4101N	.042	2.989	.1261	20.15	0.00	19.00	159.7	0.0	150.6	.0194	.0541	.00082	31.9	0.0	30.1	0.0	0.0	31.8
4076E	.044	2.991	.1304	20.25	0.00	19.25	155.3	0.0	147.6	.0210	.1108	.00183	38.5	0.0	36.6	41.0	0.0	34.5
4114E	.044	2.989	.1321	20.45	0.00	19.00	154.8	0.0	143.8	.0216	.1140	.00193	39.0	0.0	36.2	42.1	0.0	35.5

TABLE 13. 40 MIL TI-6AL-4V PARENT MATERIAL TESTED IN INHIBITED WATER

SPEC NO	SPEC. DIM., INCH			LOADS, KIPS			STRESSES, KSI			FLAW SIZE, INCH			STRESS INTENSITY FACTORS, KSI-SQRT(INCH)					
	T	W	AREA	P1	P2	P3	S1	S2	S3	A	2C	AREA	K1	K2	K3	K1	K2	K3
4027N	.042	2.991	.1241	20.00	0.00	18.85	161.1	0.0	151.9	.0188	.0547	.00081	32.2	0.0	30.4	0.0	0.0	30.1
4092N	.045	2.991	.1340	21.30	0.00	20.10	159.0	0.0	150.0	.0230	.0575	.00104	33.1	0.0	31.3	0.0	0.0	32.8
4008E	.044	2.991	.1325	20.55	0.00	19.00	155.1	0.0	143.4	.0242	.1141	.00217	40.4	0.0	37.5	43.7	0.0	39.4
4113E	.044	2.992	.1331	20.40	0.00	18.25	153.2	0.0	137.1	.0226	.1170	.00208	39.3	0.0	35.2	42.5	0.0	37.5

TABLE 14. 40 MIL TI-6AL-4V PARENT MATERIAL TESTED IN SALT SPAY AIR

SPEC NO	SPEC. DIM., INCH			LOADS, KIPS			STRESSES, KSI			FLAW SIZE, INCH			STRESS INTENSITY FACTORS, KSI-SQRT(INCH)					
	T	W	AREA	P1	P2	P3	S1	S2	S3	A	2C	AREA	K1	K2	K3	K1	K2	K3
4026N	.041	2.991	.1226	19.40	0.00	18.90	158.2	0.0	154.1	.0191	.0571	.00086	32.2	0.0	31.4	34.5	0.0	33.3
4028N	.041	2.992	.1233	19.60	0.00	19.00	159.0	0.0	154.1	.0214	.0560	.00094	32.6	0.0	31.6	0.0	0.0	33.3
4005E	.045	2.992	.1346	20.90	0.00	19.50	155.2	0.0	144.8	.0240	.1157	.00218	40.4	0.0	37.7	43.7	0.0	40.4
4093E	.042	2.993	.1272	19.85	0.00	19.00	156.1	0.0	149.4	.0190	.1040	.00155	37.1	0.0	35.5	40.5	0.0	34.4

TABLE 15. 40 MIL TI-6AL-4V PARENT MATERIAL TESTED IN AEROZINE 50

SPEC NO	SPEC. DIM., INCH			LOADS, KIPS			STRESSES, KSI			FLAW SIZE, INCH			STRESS INTENSITY FACTORS, KSI-SQRT(INCH)					
	T	W	AREA	P1	P2	P3	S1	S2	S3	A	2C	AREA	K1	K2	K3	K1	K2	K3
4030N	.041	2.994	.1228	19.45	0.00	0.00	158.4	0.0	0.0	.0239	.0617	.00116	34.1	0.0	0.0	36.1	0.0	0.0
4091N	.041	2.994	.1228	19.85	0.00	0.00	161.7	0.0	0.0	.0198	.0575	.00083	32.3	0.0	0.0	0.1	0.0	0.0
4047E	.044	2.994	.1317	20.60	0.00	0.00	156.4	0.0	0.0	.0239	.1205	.00220	41.0	0.0	0.0	44.0	0.0	0.0
4116E	.044	2.994	.1287	20.10	0.00	0.00	156.1	0.0	0.0	.0205	.1107	.00178	38.4	0.0	0.0	41.0	0.0	0.0

TABLE 16. 20 MIL TI-6AL-4V WELDED MATERIAL TESTED IN AIR

SPEC NO	SPEC. DIM., INCH			LOADS, KIPS			STRESSES, KSI			FLAW SIZE, INCH			STRESS INTENSITY FACTORS, KSI-SQRT(INCH)						
	T	W	AREA	P1	P2	P3	S1	S2	S3	A	2C	AREA	K1	K2	K3	K1	K2	K3	
A033N	.020	2.978	.0596	9.65	0.00	8.50	162.0	0.0	142.7	.0050	.0121	.00005	15.5	0.0	14.7	0.0	0.0	14.3	
A084N	.020	2.987	.0657	11.05	0.00	9.80	168.2	0.0	149.1	.0050	.0159	.00006	17.9	0.0	15.9	0.0	0.0	16.0	Failed outside flaw.
A023N	.020	2.986	.0612	10.10	0.00	9.00	165.0	0.0	147.0	.0121	.0316	.00030	25.4	0.0	22.6	0.0	0.0	23.8	
A091N	.020	2.980	.0606	9.65	0.00	8.15	159.2	0.0	134.5	.0108	.0254	.00022	22.5	0.0	19.0	23.7	0.0	19.5	
A025N	.020	2.982	.0602	10.00	0.00	8.75	166.0	0.0	145.3	.0143	.0381	.00043	28.0	0.0	24.5	0.0	0.0	25.7	
A095N	.021	2.987	.0615	9.30	0.00	8.00	151.1	0.0	130.0	.0202	.0540	.00089	30.8	0.0	26.5	32.7	0.0	27.5	
A083E	.022	2.983	.0656	11.00	0.00	9.75	167.6	0.0	148.6	.0050	.0123	.00005	16.2	0.0	14.3	0.0	0.0	15.0	
A014E	.021	2.986	.0597	10.00	0.00	9.00	167.4	0.0	150.7	.0050	.0119	.00005	15.9	0.0	14.3	0.0	0.0	15.0	Failed outside flaw.
A054E	.021	2.984	.0639	6.05	6.05	6.05	94.7	94.7	94.7	.0100	.0440	.00035	15.6	15.6	15.6	16.0	16.0	16.0	Multiple flaws.
A115E	.020	2.974	.0583	8.50	0.00	8.25	145.8	0.0	141.5	.0097	.0400	.00030	23.3	0.0	22.6	24.7	0.0	24.0	
A103E	.020	2.988	.0586	9.00	7.70	7.55	153.7	131.5	128.9	.0157	.1110	.00137	34.5	29.5	28.9	37.7	31.5	31.8	

TABLE 17. 40 MIL TI-6AL-4V WELDED MATERIAL TESTED IN AIR

SPEC NO	SPEC. DIM., INCH			LOADS, KIPS			STRESSES, KSI			FLAW SIZE, INCH			STRESS INTENSITY FACTORS, KSI-SQRT(INCH)						
	T	W	AREA	P1	P2	P3	S1	S2	S3	A	2C	AREA	K1	K2	K3	K1	K2	K3	
B233N	.041	2.978	.1230	20.75	0.00	19.00	168.7	0.0	154.5	.0100	.0279	.00022	24.2	0.0	22.2	0.0	0.0	23.5	
B245N	.042	2.975	.1249	20.80	0.00	18.75	166.5	0.0	150.1	.0100	.0277	.00022	23.8	0.0	21.5	0.0	0.0	22.7	Failed outside flaw.
B051N	.041	2.973	.1213	19.70	0.00	18.25	162.4	0.0	150.5	.0189	.0544	.00081	32.4	0.0	30.1	0.0	0.0	31.7	
B201N	.043	2.988	.1279	20.25	0.00	19.10	158.3	0.0	149.4	.0231	.0612	.00111	33.9	0.0	32.0	35.0	0.0	33.6	
B031N	.042	2.959	.1237	18.70	0.00	17.30	151.2	0.0	139.9	.0338	.0948	.00252	40.0	0.0	37.0	42.7	0.0	38.8	
B075N	.041	2.972	.1224	18.90	0.00	17.00	154.4	0.0	138.8	.0307	.0809	.00195	38.0	0.0	34.2	40.1	0.0	35.7	
B161E	.042	2.974	.1258	21.05	0.00	18.90	167.3	0.0	150.2	.0115	.0434	.00039	28.4	0.0	25.5	0.0	0.0	27.3	
B194E	.041	2.960	.1277	17.00	17.00	17.00	133.2	133.2	133.2	.0245	.1326	.00255	35.9	35.9	35.9	38.1	38.1	38.1	Multiple flaws.
B204E	.044	2.976	.1309	20.15	0.00	18.75	153.9	0.0	143.2	.0194	.1054	.00161	30.9	0.0	34.3	40.1	0.0	34.9	
B215E	.041	2.964	.1215	19.10	0.00	17.50	157.2	0.0	144.0	.0168	.0967	.00128	35.4	0.0	32.5	38.1	0.0	34.9	
B125E	.040	2.953	.1255	10.75	10.75	10.75	85.7	85.7	85.7	.0264	.2183	.00487	26.1	26.1	26.1	26.4	26.4	26.6	Multiple flaws.

TABLE 18. 60 MIL TI-6AL-4V WELDED MATERIAL TESTED IN AIR

SPEC NO	SPEC. DIM., INCH			LOADS, KIPS			STRESSES, KSI			FLAW SIZE, INCH			STRESS INTENSITY FACTORS, KSI-SQRT(INCH)						
	T	W	AREA	P1	P2	P3	S1	S2	S3	A	2C	AREA	K1	K2	K3	K1	K2	K3	
C111N	.062	2.969	.1832	29.10	0.00	26.40	158.9	0.0	144.1	.0150	.0325	.00038	25.1	0.0	22.8	25.3	0.0	23.7	Failed outside flaw.
C053N	.064	2.961	.1898	30.35	0.00	27.30	159.9	0.0	143.8	.0138	.0343	.00037	25.8	0.0	23.2	0.0	0.0	24.2	
C003N	.063	2.973	.1873	28.95	0.00	27.60	154.6	0.0	147.4	.0255	.0637	.00128	33.0	0.0	32.3	35.7	0.0	33.9	
C062N	.063	2.963	.1858	28.05	0.00	27.00	151.0	0.0	145.3	.0278	.0653	.00143	33.7	0.0	32.4	35.3	0.0	33.4	
C121N	.062	2.959	.1835	27.00	0.00	15.00	119.9	0.0	81.8	.0450	.1000	.00353	33.2	0.0	22.6	34.1	0.0	22.9	Multiple flaws.
C034N	.062	2.954	.1820	24.80	0.00	23.40	136.3	0.0	128.6	.0455	.1176	.00421	40.5	0.0	34.2	42.2	0.0	34.7	
C071E	.062	2.959	.1849	28.90	0.00	26.50	156.3	0.0	143.3	.0188	.0518	.00076	30.6	0.0	28.1	32.4	0.0	28.5	Multiple flaws.
C043E	.065	2.973	.1932	27.45	0.00	26.20	142.0	0.0	135.6	.0299	.1266	.00297	40.1	0.0	34.3	42.7	0.0	40.5	
C072E	.064	2.958	.1893	23.80	23.80		125.7	125.7	125.7	.0301	.1165	.00275	34.8	34.8	34.8	36.1	36.1	36.4	Multiple flaws.

TABLE 19. 40 MIL TI-6AL-4V WELDED MATERIAL TESTED IN DEMINERALIZED WATER

SPEC NO	SPEC. DIM., INCH			LOADS, KIPS			STRESSES, KSI			FLAW SIZE, INCH			STRESS INTENSITY FACTORS, KSI-SQRT(INCH)						
	T	W	AREA	P1	P2	P3	S1	S2	S3	A	2C	AREA	K1	K2	K3	K1	K2	K3	
B124N	.043	2.957	.1266	20.00	0.00	18.60	158.0	0.0	147.0	.0249	.0624	.00122	34.3	0.0	31.9	36.2	0.0	33.4	
B164N	.042	2.969	.1232	20.55	0.00	19.10	166.8	0.0	155.0	.0179	.0541	.00076	33.0	0.0	30.7	0.0	0.0	32.6	
B093E	.042	2.960	.1237	19.40	0.00	17.00	156.9	0.0	137.5	.0198	.0994	.00155	37.4	0.0	32.8	40.2	0.0	34.4	
B241E	.042	2.975	.1255	19.75	0.00	18.30	157.3	0.0	145.8	.0166	.1000	.00130	35.5	0.0	32.4	36.1	0.0	35.5	

TABLE 20. 40 MIL TI-6AL-4V WELDED MATERIAL TESTED IN INHIBITED WATER

SPEC NO	SPEC. DIM., INCH			LOADS, KIPS			STRESSES, KSI			FLAW SIZE, INCH			STRESS INTENSITY FACTORS, KSI-SQRT(INCH)						
	T	W	AREA	P1	P2	P3	S1	S2	S3	A	2C	AREA	K1	K2	K3	K1	K2	K3	
B043N	.044	2.970	.1310	20.95	0.00	18.85	160.0	0.0	143.9	.0224	.0581	.00102	33.4	0.0	30.1	0.0	0.0	31.5	
B044N	.044	2.981	.1318	20.75	0.00	19.10	157.5	0.0	145.0	.0237	.0671	.00125	35.0	0.0	32.2	37.2	0.0	33.9	
B094E	.042	2.977	.1235	19.40	0.00	17.80	157.0	0.0	144.1	.0207	.1022	.00166	38.2	0.0	37.0	41.5	0.0	37.5	
B111E	.042	2.957	.1251	19.55	0.00	17.60	156.3	0.0	140.7	.0189	.1073	.00152	37.0	0.0	33.3	40.2	0.0	35.6	

TABLE 21. 40 MIL TI-6AL-4V WELDED MATERIAL TESTED IN SALT SPRAY AIP

SPEC NO	SPEC. DIM., INCH			LOADS, KIPS			STRESSES, KSI			FLAW SIZE, INCH			STRESS INTENSITY FACTORS, KSI-SQRT(INCH)					
	T	W	AREA	P1	P2	P3	S1	S2	S3	A	2C	AREA	PHI CORRECTION			Y CORRECTION		
													K1	K2	K3	K1	K2	K3
B205N	.044	2.983	.1313	20.50	0.00	19.20	156.2	0.0	146.3	.0205	.0548	.00091	32.0	0.0	30.0	33.4	0.0	31.5
B242N	.042	2.976	.1255	20.30	0.00	18.90	160.5	0.0	149.4	.0198	.0578	.00090	33.0	0.0	30.7	0.0	0.0	32.4
B172E	.043	2.968	.1267	19.95	0.00	16.50	157.4	0.0	130.2	.0206	.1030	.00167	38.3	0.0	31.7	41.7	0.0	33.5
B212E	.041	2.975	.1226	11.35	11.35	11.35	92.6	92.6	92.6	.0194	.1035	.00158	22.1	22.1	22.1	22.0	22.0	22.0

TABLE 22. 40 MIL TI-6AL-4V WELDED MATERIAL TESTED IN AEROZINE 50

SPEC NO	SPEC. DIM., INCH			LOADS, KIPS			STRESSES, KSI			FLAW SIZE, INCH			STRESS INTENSITY FACTORS, KSI-SQRT(INCH)					
	T	W	AREA	P1	P2	P3	S1	S2	S3	A	2C	AREA	PHI CORRECTION			Y CORRECTION		
													K1	K2	K3	K1	K2	K3
B073N	.041	2.978	.1221	19.75	0.00	0.00	161.8	0.0	0.0	.0220	.0543	.00094	32.8	0.0	0.0	0.0	0.0	0.0
B214N	.041	2.972	.1219	20.10	0.00	0.00	165.0	0.0	0.0	.0207	.0531	.00086	33.0	0.0	0.0	0.0	0.0	0.0
B181E	.042	2.976	.1250	19.75	0.00	0.00	158.0	0.0	0.0	.0213	.0989	.00165	38.5	0.0	0.0	0.0	0.0	0.0
B234E	.041	2.971	.1218	19.60	0.00	0.00	160.9	0.0	0.0	.0200	.1108	.00174	39.3	0.0	0.0	0.0	0.0	0.0

TABLE 23. 20 MIL TI-6AL-4V PARENT MATERIAL TESTED IN LIQUID NITROGEN

SPEC NO	SPEC. DIM.,		INCH AREA	LOADS, KIPS			STRESSES, KSI			FLAW SIZE, INCH			STRESS INTENSITY FACTORS, KSI-SQRT(INCH)			REMARKS			
	T	W		P1	P2	P3	S1	S2	S3	A	2C	AREA	K1	K2	K3				
2016N	.022	2.991	.0658	15.85	0.00	14.75	240.9	0.0	224.2	.0050	.0141	.00006	24.6	0.0	22.9	26.0	0.0	24.0	Failed at grip.
2052N	.025	2.990	.0747	14.70	0.00	0.00	196.7	0.0	0.0	.0063	.0124	.00006	19.2	0.0	0.0	19.7	0.0	0.0	
2005N	.021	2.984	.0633	14.75	0.00	0.00	233.2	0.0	0.0	.0099	.0271	.00021	33.1	0.0	0.0	34.2	0.0	0.0	
2040N	.020	2.989	.0613	14.00	0.00	0.00	228.5	0.0	0.0	.0100	.0272	.00021	32.5	0.0	0.0	34.1	0.0	0.0	Failed at grip
2010N	.021	2.990	.0637	13.60	0.00	0.00	213.5	0.0	0.0	.0189	.0467	.00068	40.1	0.0	0.0	41.1	0.0	0.0	
2048N	.021	2.993	.0529	13.75	0.00	13.60	218.3	0.0	216.4	.0169	.0429	.00057	39.3	0.0	38.9	41.1	0.0	40.5	
2042E	.021	2.990	.0504	13.60	0.00	0.00	225.2	0.0	0.0	.0054	.0142	.00004	20.9	0.0	0.0	21.7	0.0	0.0	Failed at grip
2054E	.021	2.992	.0637	15.30	0.00	0.00	240.1	0.0	0.0	.0050	.0120	.00005	22.9	0.0	0.0	24.1	0.0	0.0	
2030E	.021	2.992	.0622	14.10	0.00	0.00	226.6	0.0	0.0	.0090	.0406	.00021	35.2	0.0	0.0	38.7	0.0	0.0	
2020E	.020	2.990	.0613	13.95	0.00	0.00	227.6	0.0	0.0	.0106	.0476	.00040	36.8	0.0	0.0	41.1	0.0	0.0	
2013E	.022	2.990	.0652	10.50	0.00	0.00	161.1	0.0	0.0	.0163	.1243	.00159	37.2	0.0	0.0	34.7	0.0	0.0	
2038E	.021	2.992	.0619	4.55	4.55	4.55	73.5	73.5	73.5	.0151	.1092	.00130	16.2	16.2	15.2	15.4	15.4	16.4	Multiple flaws

TABLE 24. 40 MIL TI-6AL-4V PARENT MATERIAL TESTED IN LIQUID NITROGEN

SPEC NO	SPEC. DIM.,		INCH AREA	LOADS, KIPS			STRESSES, KSI			FLAW SIZE, INCH			STRESS INTENSITY FACTORS, KSI-SQRT(INCH)			REMARKS			
	T	W		P1	P2	P3	S1	S2	S3	A	2C	AREA	K1	K2	K3				
4001N	.045	2.989	.1345	33.65	0.00	32.55	250.2	0.0	242.0	.0103	.0249	.00023	36.5	0.0	35.3	0.0	0.0	37.4	
4002N	.045	2.990	.1345	33.60	0.00	32.40	249.7	0.0	240.8	.0107	.0304	.00026	37.4	0.0	36.0	0.0	0.0	38.1	
4016N	.044	2.992	.1316	30.50	0.00	0.00	231.7	0.0	0.0	.0225	.0592	.00105	48.8	0.0	0.0	51.3	0.0	0.0	
4070N	.041	2.992	.1233	29.10	0.00	28.50	236.1	0.0	231.2	.0200	.0551	.00087	47.7	0.0	46.7	50.3	0.0	44.2	
4052N	.045	2.988	.1336	26.50	0.00	0.00	198.4	0.0	0.0	.0341	.0934	.00242	51.6	0.0	0.0	53.5	0.0	0.0	
4053N	.044	2.994	.1332	27.75	27.75	27.75	208.3	208.3	208.3	.0313	.0811	.00199	51.4	51.4	51.4	53.5	53.5	53.5	
4009E	.043	2.993	.1287	32.50	0.00	0.00	252.5	0.0	0.0	.0104	.0363	.00030	39.9	0.0	0.0	0.0	0.0	0.0	
4060E	.041	2.991	.1226	30.45	23.00	23.90	248.3	187.6	194.9	.0110	.0368	.00032	39.8	30.1	31.3	42.7	32.3	32.6	
4040E	.042	2.994	.1263	27.85	0.00	0.00	220.4	0.0	0.0	.0183	.1074	.00154	52.0	0.0	0.0	55.2	0.0	0.0	
4056E	.042	2.992	.1251	28.10	28.10	28.10	224.7	224.7	224.7	.0180	.1005	.00142	52.1	52.1	52.1	56.1	56.1	56.1	
4035E	.042	2.991	.1256	20.20	0.00	18.00	160.8	0.0	143.3	.0256	.2151	.00432	47.0	0.0	41.9	48.4	0.0	43.2	
4074E	.041	2.992	.1227	19.75	0.00	0.00	161.0	0.0	0.0	.0255	.1976	.00396	46.6	0.0	0.0	48.5	0.0	0.0	

TABLE 25. 20 MIL TI-6AL-4V WELDED MATERIAL TESTED IN LIQUID NITROGEN

SPEC NO	SPEC. DIM.,		INCH AREA	LOADS, KIPS			STRESSES, KSI			FLAW SIZE, INCH			STRESS INTENSITY FACTORS, KSI-SQRT(INCH)			REMARKS			
	T	W		P1	P2	P3	S1	S2	S3	A	2C	AREA	K1	K2	K3				
A031N	.020	2.980	.0596	14.40	0.00	0.00	241.6	0.0	0.0	.0048	.0120	.00005	23.0	0.0	0.0	24.2	0.0	0.0	
A043N	.022	2.988	.0660	16.25	0.00	0.00	246.1	0.0	0.0	.0081	.0142	.00009	25.7	0.0	0.0	26.5	0.0	0.0	
A042N	.022	2.983	.0663	15.10	0.00	0.00	227.6	0.0	0.0	.0151	.0346	.00041	37.0	0.0	0.0	38.2	0.0	0.0	
A073N	.021	2.983	.0620	14.90	0.00	0.00	240.1	0.0	0.0	.0115	.0277	.00025	34.9	0.0	0.0	35.2	0.0	0.0	
A034N	.020	2.979	.0602	13.35	0.00	0.00	221.8	0.0	0.0	.0157	.0385	.00047	37.9	0.0	0.0	39.4	0.0	0.0	
A123N	.022	2.990	.0658	14.35	0.00	0.00	218.2	0.0	0.0	.0173	.0454	.00062	40.2	0.0	0.0	42.0	0.0	0.0	
A042E	.020	2.983	.0603	14.05	0.00	0.00	233.2	0.0	0.0	.0050	.0117	.00005	22.0	0.0	0.0	23.1	0.0	0.0	
A044E	.020	2.985	.0603	14.05	0.00	0.00	233.0	0.0	0.0	.0050	.0117	.00004	21.4	0.0	0.0	22.3	0.0	0.0	Failed outside flaw
A064E	.020	2.987	.0606	13.90	0.00	0.00	229.2	0.0	0.0	.0079	.0423	.00026	35.0	0.0	0.0	37.7	0.0	0.0	
A072L	.021	2.985	.0636	14.35	0.00	0.00	225.7	0.0	0.0	.0088	.0395	.00027	35.1	0.0	0.0	37.2	0.0	0.0	
A052E	.021	2.969	.0618	10.65	0.00	0.00	172.5	0.0	0.0	.0156	.1154	.00141	38.8	0.0	0.0	40.5	0.0	0.0	
A153L	.021	2.985	.0627	10.65	0.00	0.00	169.9	0.0	0.0	.0174	.1318	.00180	40.5	0.0	0.0	42.5	0.0	0.0	

TABLE 26. 40 MIL TI-6AL-4V WELDED MATERIAL TESTED IN LIQUID NITROGEN

SPEC NO	SPEC. DIM., INCH		LOADS, KIPS	STRESSES, KSI			FLAW SIZE, INCH			STRESS INTENSITY FACTORS, $K\sqrt{S}$ (INCH)			PHI CORRECTION			W CORRECTION		
	T	W		P1	P2	P3	S1	S2	S3	A	2C	APEA	K1	K2	K3	K1	K2	K3
B224N	.042	2.959	.1237	31.40	0.00	0.00	253.9	0.0	0.0	.0107	.0291	.00024	37.3	0.0	0.0	0.0	0.0	0.0
B224N	.042	2.964	.1242	31.65	23.60	23.60	254.8	190.0	190.0	.0111	.0289	.00025	37.5	28.0	26.0	0.0	24.0	1.9
B041N	.044	2.975	.1315	31.85	0.00	0.00	242.2	0.0	0.0	.0185	.0523	.00076	47.5	0.0	0.0	50.4	0.0	0.0
B111N	.042	2.948	.1229	29.25	0.00	0.00	237.9	0.0	0.0	.0220	.0596	.00106	50.3	0.0	0.0	53.0	0.0	0.0
B213N	.042	2.970	.1233	24.75	0.00	0.00	200.8	0.0	0.0	.0314	.0828	.00204	50.0	0.0	0.0	51.0	0.0	0.0
B013N	.042	2.963	.1283	25.60	0.00	0.00	199.5	0.0	0.0	.0300	.0827	.00195	49.4	0.0	0.0	51.0	0.0	0.0
B115E	.042	2.969	.1256	30.75	0.00	0.00	244.8	0.0	0.0	.0104	.0379	.00030	38.9	0.0	0.0	41.0	0.0	0.0
B025E	.042	2.977	.1265	22.30	22.30	22.30	176.3	176.3	176.3	.0348	.2165	.00502	57.9	57.9	57.9	60.5	60.5	60.5
B102E	.041	2.975	.1220	26.10	0.00	23.20	214.0	0.0	190.2	.0179	.1073	.00151	50.1	0.0	44.5	53.0	0.0	46.9
B172E	.043	2.973	.1269	20.60	0.00	0.00	162.3	0.0	0.0	.0267	.2041	.00438	48.1	0.0	0.0	50.1	0.0	0.0

Flaw section shattered
Multiple flaws

TABLE 27. 60 MIL TI-6AL-4V FORGED MATERIAL TESTED IN AIR

SPEC NO	SPEC. DIM., INCH			LOADS, KIPS			STRESSES, KSI			FLAW SIZE, INCH			STRESS INTENSITY FACTORS, KSI-SQRT(INCH)						
	T	W	AREA	P1	P2	P3	S1	S2	S3	A	2C	AREA	PHI CORRECTION			J CORRECTION			
													K1	K2	K3	K1	K2	K3	
60F5N	.060	2.994	.1781	12.90	12.90	12.90	72.4	72.4	72.4	.0150	.0311	.00037	11.2	11.2	11.2	11.3	11.3	11.3	Multiple flaws
60F4N	.059	2.992	.1765	27.05	0.00	26.10	153.2	0.0	147.9	.0247	.0610	.00118	32.9	0.0	31.8	34.8	0.0	33.3	
60F2N	.059	2.992	.1765	20.40	0.00	20.00	115.6	0.0	113.3	.0392	.1006	.00310	31.8	0.0	31.2	32.7	0.0	32.1	
60F3N	.060	2.990	.1779	19.85	0.00	19.00	111.6	0.0	106.8	.0431	.0976	.00330	30.5	0.0	29.2	31.2	0.0	29.8	

TABLE 28. 20 MIL TI-6AL-4V PARENT MATERIAL CONTROL TESTS

SPEC NO	SPEC. DIM., INCH			LOADS, KIPS			STRESSES, KSI			FLAW SIZE, INCH			STRESS INTENSITY FACTORS, KSI-SQRT(INCH)					
	T	W	AREA	P1	P2	P3	S1	S2	S3	A	2C	AREA	PHI CORRECTION			CORRECTION		
													K1	K2	K3	K1	K2	K3
2015N	.022	2.991	.0652	10.60	0.00	9.40	162.6	0.0	144.2	.0077	.0138	.00008	16.7	0.0	14.8	0.0	0.0	15.3
2037N	.021	2.987	.0627	10.20	0.00	9.15	162.6	0.0	145.9	.0120	.0307	.00029	24.7	0.0	22.2	0.0	0.0	23.2
2004N	.021	2.990	.0634	10.20	0.00	9.05	160.9	0.0	142.8	.0169	.0451	.00060	29.5	0.0	26.2	0.0	0.0	27.4
2035E	.021	2.988	.0619	9.85	0.00	8.90	159.3	0.0	143.9	.0045	.0114	.00004	14.8	0.0	13.2	17.0	0.0	14.0
2021E	.022	2.989	.0658	8.30	0.00	8.30	126.2	0.0	126.2	.0094	.0456	.00034	20.6	0.0	20.6	21.7	0.0	21.7
2018E	.022	2.989	.0649	9.80	7.95	7.95	151.1	122.0	122.6	.0195	.1234	.00189	37.2	30.2	30.2	40.5	31.0	31.0

Multiple flaws.

TABLE 29. 40 MIL TI-6AL-4V PARENT MATERIAL CONTROL TESTS

SPEC NO	SPEC. DIM., INCH			LOADS, KIPS			STRESSES, KSI			FLAW SIZE, INCH			STRESS INTENSITY FACTORS, KSI-SQRT(INCH)					
	T	W	AREA	P1	P2	P3	S1	S2	S3	A	2C	AREA	PHI CORRECTION			CORRECTION		
													K1	K2	K3	K1	K2	K3
4005N	.045	2.994	.1347	22.25	0.00	20.40	165.1	0.0	151.4	.0103	.0294	.00024	24.3	0.0	22.3	0.0	0.0	23.5
4068N	.044	2.990	.1301	20.45	0.00	19.25	157.2	0.0	148.0	.0205	.0597	.00096	32.8	0.0	30.9	34.4	0.0	32.5
4051N	.045	2.993	.1341	20.50	0.00	19.85	152.9	0.0	148.0	.0343	.0889	.00239	39.5	0.0	35.3	41.5	0.0	40.2
4063E	.042	2.990	.1250	20.55	0.00	19.05	164.4	0.0	152.4	.0085	.0365	.00024	24.8	0.0	23.0	0.0	0.0	24.8
4120E	.044	2.992	.1331	20.40	0.00	18.85	153.2	0.0	141.0	.0234	.1225	.00225	40.1	0.0	37.0	43.4	0.0	39.5
4075E	.040	2.990	.1199	17.30	17.12	15.30	144.3	142.8	127.6	.0307	.1976	.00476	44.7	44.3	39.6	44.5	47.7	47.0
4094E	.042	2.992	.1266	17.65	17.65	14.95	139.5	139.5	118.1	.0273	.2190	.00470	41.9	41.9	35.5	45.7	45.7	37.4

TABLE 30. 50 MIL TI-6AL-4V PARENT MATERIAL CONTROL TESTS

SPEC NO	SPEC. DIM., INCH			LOADS, KIPS			STRESSES, KSI			FLAW SIZE, INCH			STRESS INTENSITY FACTORS, KSI-SQRT(INCH)					
	T	W	AREA	P1	P2	P3	S1	S2	S3	A	2C	AREA	PHI CORRECTION			CORRECTION		
													K1	K2	K3	K1	K2	K3
6011N	.064	2.992	.1915	29.55	0.00	0.00	154.3	0.0	0.0	.0138	.0317	.00034	24.0	0.0	0.0	25.7	0.0	0.0
6016N	.064	2.991	.1905	29.80	0.00	27.80	156.4	0.0	145.9	.0131	.0365	.00038	25.7	0.0	24.0	25.7	0.0	25.7
6017N	.065	2.994	.1946	29.20	0.00	27.90	150.0	0.0	143.4	.0304	.0694	.00166	34.6	0.0	33.0	36.7	0.0	34.6
6018N	.065	2.994	.1976	29.45	0.00	28.30	149.0	0.0	143.2	.0317	.0713	.00178	34.8	0.0	33.5	36.4	0.0	34.8
6003V	.065	2.994	.1945	28.50	0.00	26.00	146.4	0.0	133.6	.0460	.1062	.00384	41.7	0.0	35.1	43.6	0.0	41.7
6013N	.065	2.987	.1942	27.80	0.00	25.00	143.2	0.0	128.8	.0453	.1042	.00371	40.4	0.0	35.3	42.1	0.0	40.4
6009E	.063	2.994	.1886	28.85	0.00	27.50	153.0	0.0	145.3	.0200	.0573	.00090	31.4	0.0	29.9	33.7	0.0	31.4
6006E	.062	2.994	.1856	27.90	0.00	27.00	150.3	0.0	145.5	.0198	.0561	.00087	30.5	0.0	29.6	32.7	0.0	30.5
6000E	.062	2.994	.1856	27.30	0.00	25.60	147.1	0.0	137.9	.0315	.1216	.00301	41.6	0.0	39.0	44.7	0.0	41.6
6042E	.064	2.994	.1916	27.90	0.00	26.00	145.6	0.0	135.7	.0305	.1226	.00294	41.0	0.0	38.2	43.7	0.0	41.0
6022E	.063	2.994	.1886	22.90	14.70	16.00	121.4	104.4	84.8	.0486	.3429	.01309	48.0	41.3	33.5	50.4	42.1	34.4
6041E	.062	2.994	.1856	22.25	20.40	16.80	119.9	109.9	90.5	.0470	.3470	.01281	46.8	42.9	33.4	49.1	41.1	33.7

C = half of surface crack length, inches,

stress intensity factors without the plasticity correction were computed. These are printed as K1, K2, and K3 for the respective stresses; S1, S2, and S3 under the heading "Phi Correction" in Tables 9 through 30. A similar formulation,

$$K = 1.1 \sqrt{\pi A/Q}$$

where

$$Q = \sigma^2 - 0.212 \left(\frac{\sigma}{S_Y}\right)^2$$

S_Y = tensile yield stress, ksi,

was used to determine the stress intensity factors with the plasticity correction. The respective values are listed in Tables 9 through 30 under heading "Q Correction". A discussion of these results is contained in the section on "Data Interpretations".

Graphical Presentations. The fundamental results of this portion of the program can be vividly illustrated by direct graphical displays of the raw data. These are presented and discussed in the following paragraphs.

The critical flaw sizes for partial-through cracks in thin sheet titanium in room temperature air and liquid nitrogen are shown in Figures 19 and 20 for parent and welded material respectively. As would be expected, gross fracture stress decreases with increasing flaw area. Over this narrow range of flaw areas, the relationship between stress and flaw area is basically linear. (Note: This is not contradictory to the general hyperbolic relationship between stress and flaw size; rather, it represents only a small segment of the general expression; hence is nearly linear.) In general, the cryogenic data have a steeper slope than the room temperature data both for parent and welded material. This indicates that the material is more sensitive to the presence of flaws in a cryogenic environment. The fracture data for room temperature do not exhibit a clear-cut thickness effect for these gages or flaw sizes. However,

$w = 3''$

2.2

Plot Symbols

$\sigma_u = 171$ (ult ts)	Nominal Gage	R.T. Air	Cryogenic
	20 mil	○	●
	40 mil	□	■
	63 mil	△	
	63 mil Forged	X	

Longit.

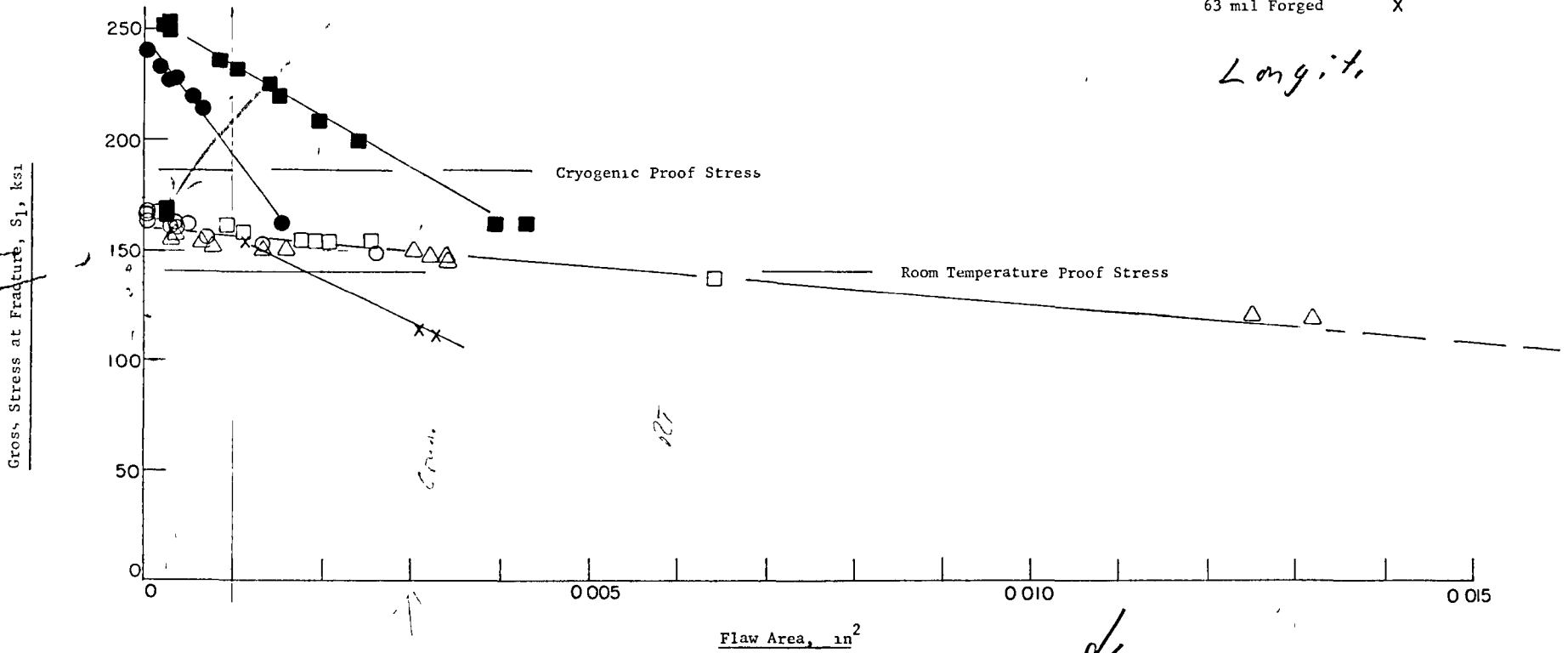


FIGURE 19. VARIATION OF GROSS FRACTURE STRESS WITH FLAW AREA FOR PARENT MATERIAL SPECIMENS TESTED IN ROOM TEMPERATURE AIR AND LIQUID NITROGEN ENVIRONMENTS

$\sigma_u = 260 + 265$ @ -320 for annealed 6-9
for a part sheet (L) *Fig 3.03153*

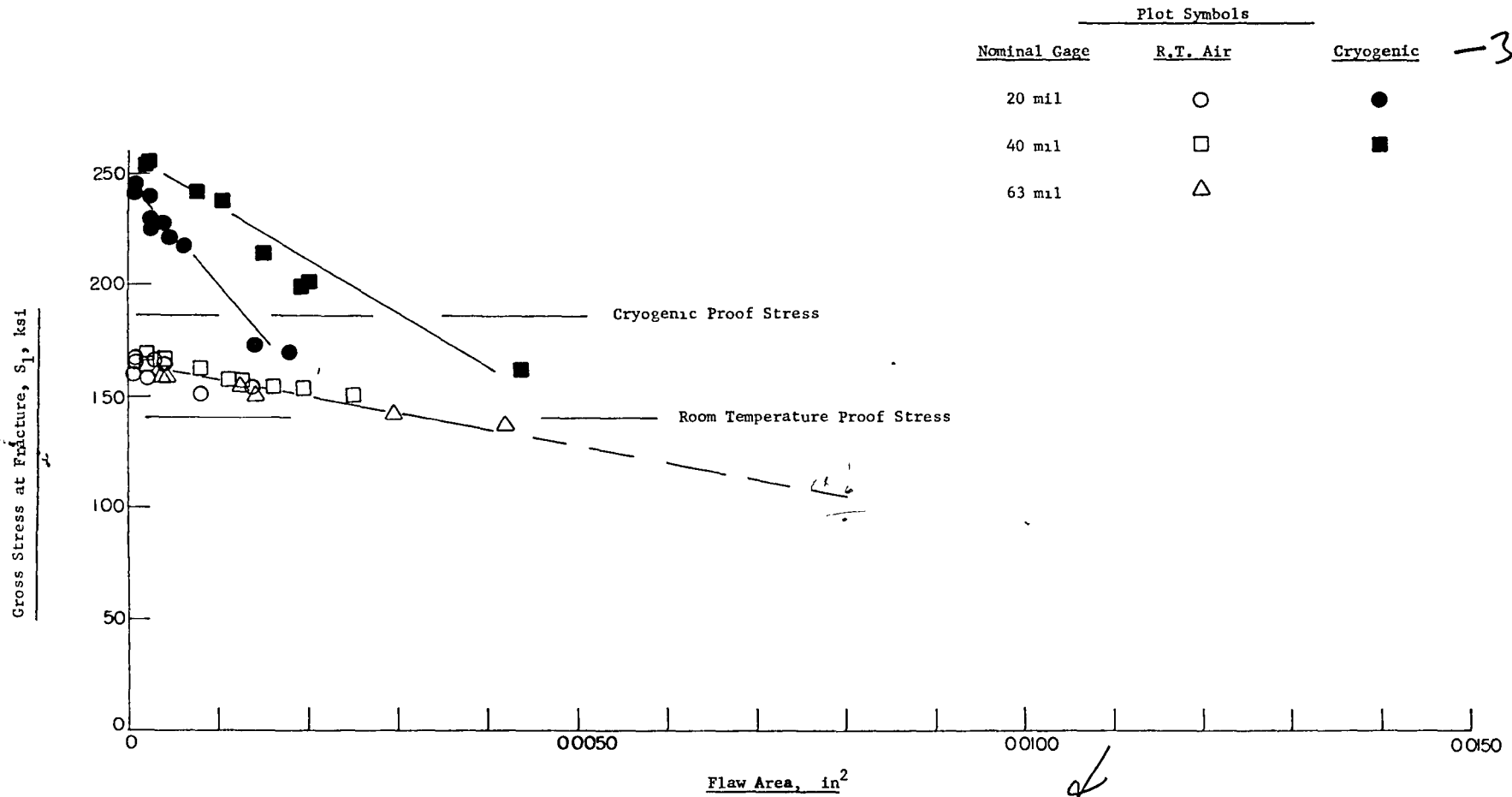


FIGURE 20. VARIATION OF GROSS FRACTURE STRESS WITH FLAW AREA FOR WELDED MATERIAL SPECIMENS TESTED IN ROOM TEMPERATURE AIR AND LIQUID NITROGEN ENVIRONMENTS

the cryogenic data display very distinct thickness effects for the 20- and 40-mil material. This observation brings forth two questions: "What is the fracture behavior of 63-mil material?" and "Is this effect due to thickness or metallurgical behavior at low temperatures?" It is also to be noted that the welded material appears to be 20 to 30 percent more sensitive to a given flaw size.

The data of the figures just presented may be used to evaluate the influence of the proof test on screening flaw sizes. Table 31 gives a listing of the approximate minimum flaw sizes screened out by room temperature and cryogenic proof tests.

The fracture data for aqueous, saline, and propellant environments are shown in Figure 21. No radical degradation is noted.

The relative merits of room temperature and cryogenic proof testing are most dramatically illustrated in Figures 22 and 23 for parent and welded material, respectively. These plots present the ratio of gross fracture stress to tensile yield stress versus flaw area. For a given flaw size in both the 20- and 40-mil material, the cryogenic environment was a more severe test of the useful load capacity of the specimen. In terms of a screening procedure, the cryogenic environment offers a finer grid for screening flaws. While the room temperature data for parent material fractured in air, as presented in Figures 19 and 20, do not exhibit a "clear cut" thickness effect, there does appear to be a secondary influence of thickness. This is best illustrated by the non-dimensional plot of these data in Figure 24. The ratio of gross fracture stress to yield stress is plotted versus the ratio of flaw depth to sheet thickness. Fracture data for both normal and elongated flaws in the three sheet thicknesses of parent material are presented. In addition to the decrease in fracture strength with increasing flaw size (i.e., the downward slope to the right), there is also a vertical stacking of data by sheet thickness. Thus, with the normalization to thickness, the gross fracture stress decreases with increasing sheet thickness.

TABLE 31. APPROXIMATE MINIMUM FLAW SIZE SCREENED
OUT BY PROOF TESTING

Proof Test	Flaw Size, in ²	
	Parent Material	Welded Material
Room Temperature-140 ksi (20-, 40-, 63-mil)	0.005	0.0035
Cryogenic-186 ksi		
20-mil	0.001	0.0013
40-mil	0.003	0.003

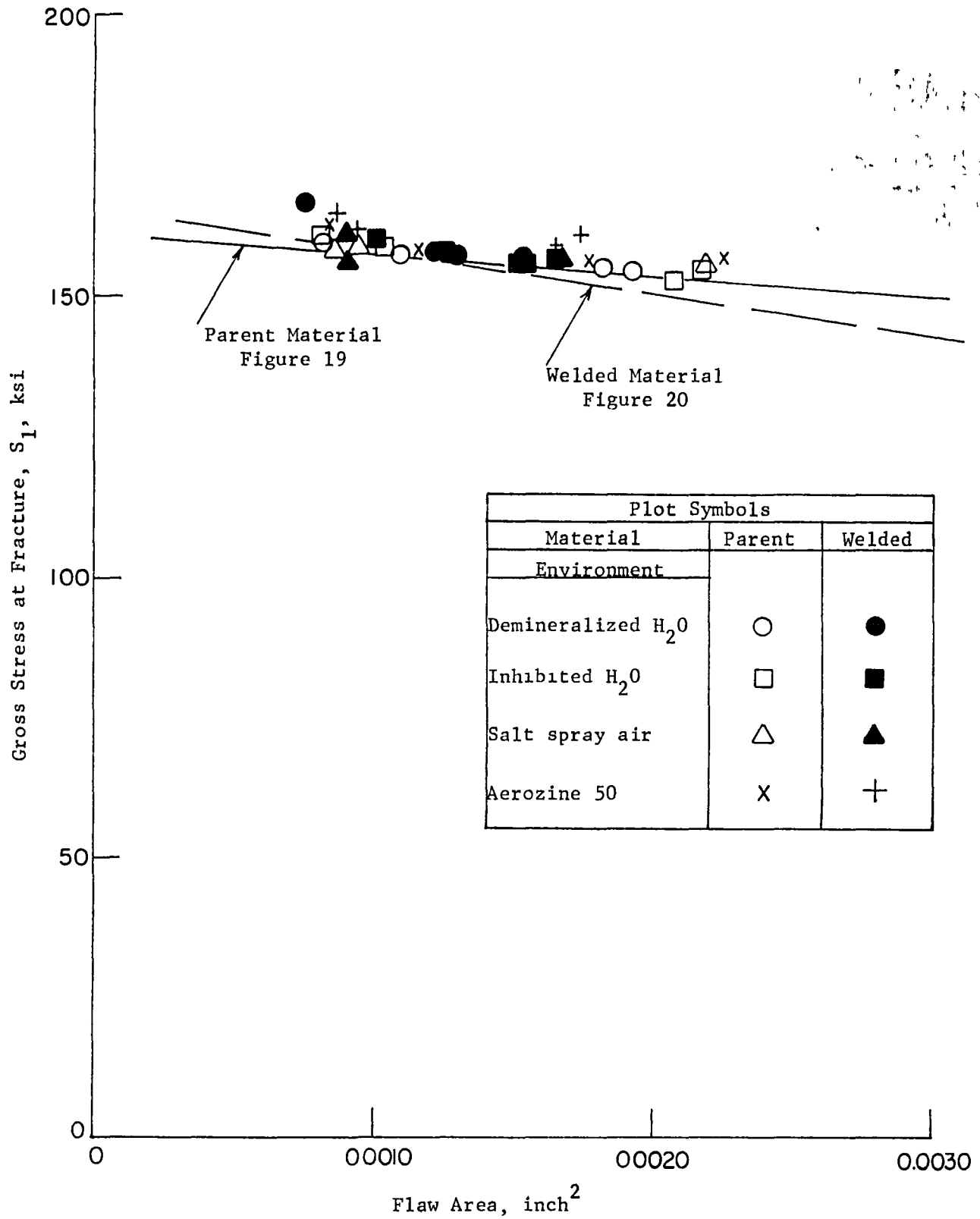


FIGURE 21. VARIATION OF GROSS FRACTURE STRESS WITH FLAW AREA FOR PARENT AND WELDED MATERIAL TESTED IN ROOM TEMPERATURE ENVIRONMENTS

Parent Material

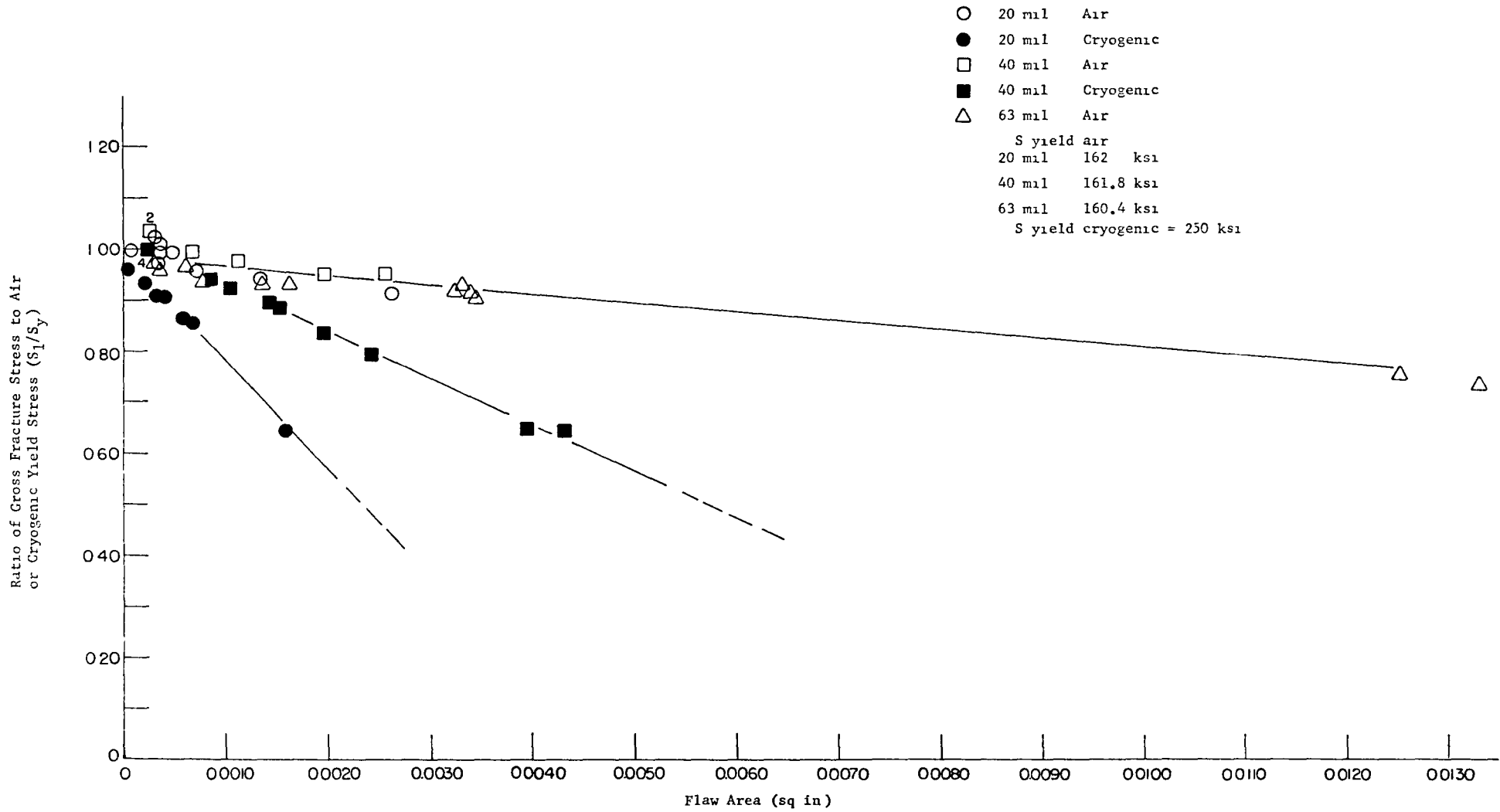


FIGURE 22. RATIO OF GROSS FRACTURE STRESS TO YIELD STRESS (AIR OR CRYOGENIC) VERSUS FLAW AREA FOR PARENT MATERIAL OF ALL THREE THICKNESSES

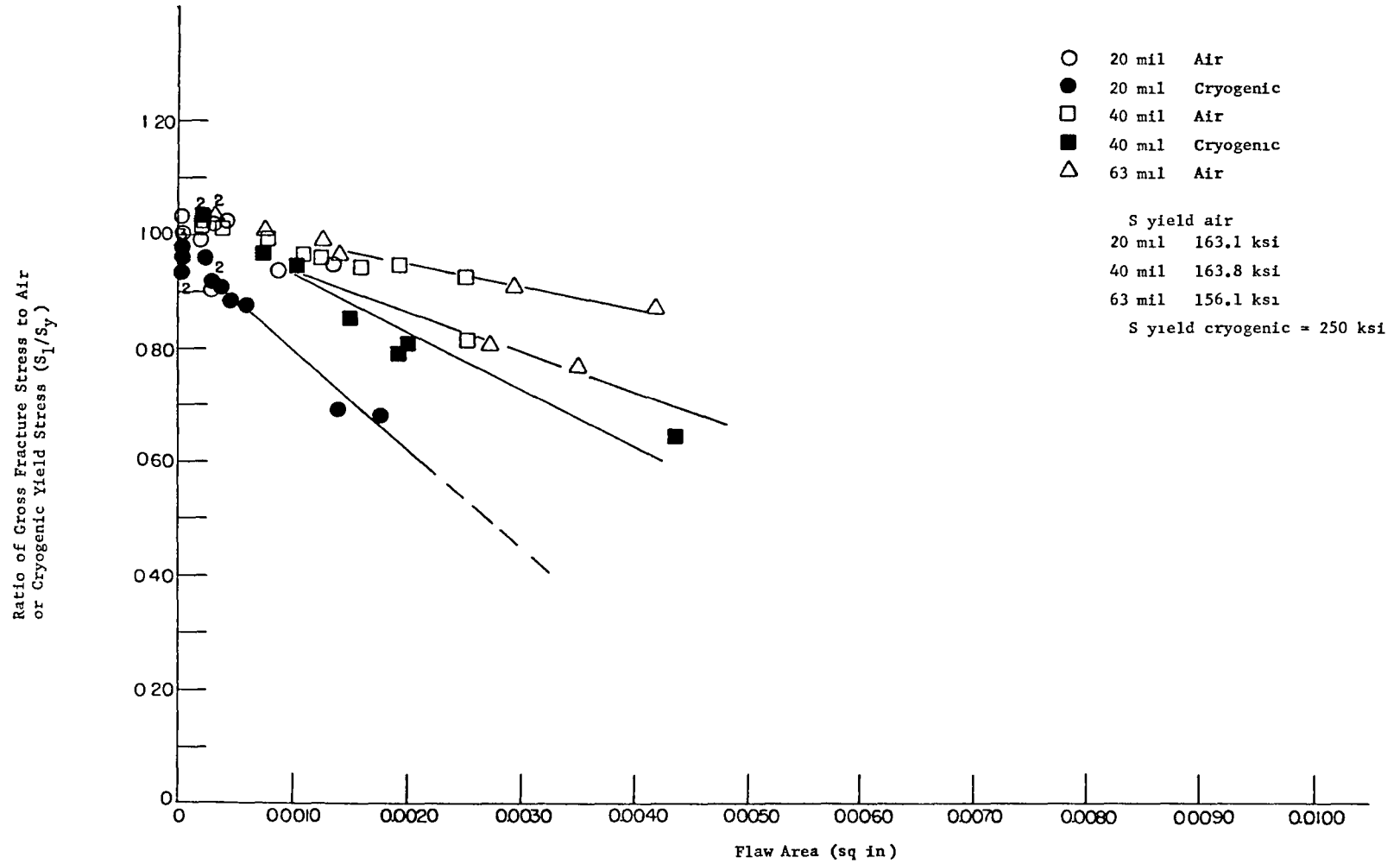


FIGURE 23. RATIO OF GROSS FRACTURE STRESS TO YIELD STRESS (AIR OR CRYOGENIC) VERSUS FLAW AREA FOR WELDED MATERIAL OF ALL THREE THICKNESSES

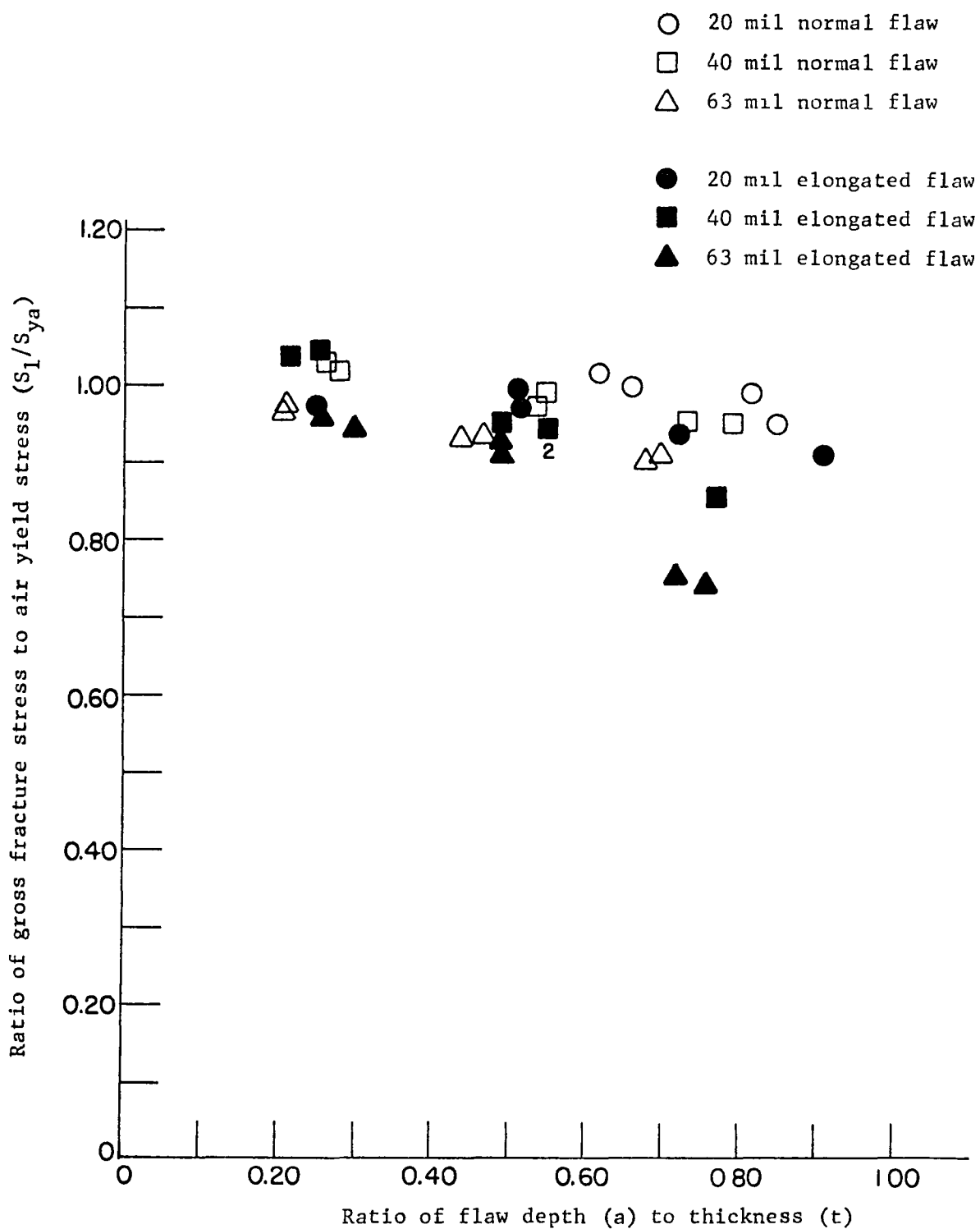


FIGURE 24. RATIO OF GROSS FRACTURE STRESS TO AIR YIELD STRESS VERSUS RATIO OF FLAW DEPTH TO THICKNESS FOR PARENT MATERIAL

Furthermore, the elongated flaw shape emphasizes this effect even more. Undoubtedly this effect is complex in its interaction; however, it correlates well with the qualitative concepts of fracture mechanics. This particular aspect should be appraised more thoroughly in future research.

The results of the four fracture tests on forged material are tabulated in Table 27 and plotted in Figure 19 with the parent fracture data. From the extremely limited data obtained it appears that there are substantial differences in the fracture behavior of the sheet and forged product, as might be expected. Even though this appears to be the case, the conclusions regarding the usefulness of cryogenic proof testing would still be valid.

Data Interpretation. The observations and conjectures which can be made from the data presented in the "Test Results" section are discussed in the following sections.

Critical Flaw Size. The relatively shallow slopes of the room temperature data shown in Figures 19, 20, 22, and 23 can be viewed from two perspectives. On one hand, modest variations in room temperature proof load cause considerable variation of the screening grid size (i.e., minimum size flaw rejected). On the other hand, increasing the difference between operating and proof load levels is a powerful lever for extending the tolerable growth of subcritical flaws. The steepness of the cryogenic data indicate a more precise screening procedure. When the fracture stress is expressed as percent of tensile yield stress, the cryogenic fracture occurs below room temperature fracture for a given size flaw.

Thickness Effect. The steep and distinctly different slopes of cryogenic fracture data for the two thicknesses in the graphical displays indicates some form of thickness effect contrary to what might be expected. This does

raise a question about the behavior of 63-mil material. A further study of this effect is recommended.

Cryogenic Proof Test. Without exception, the fracture data derived in this program indicate that a cryogenic proof is more severe and preferable for the purpose of screening flaw sizes. Dependent on the design condition some variation in the proof level may be advisable.

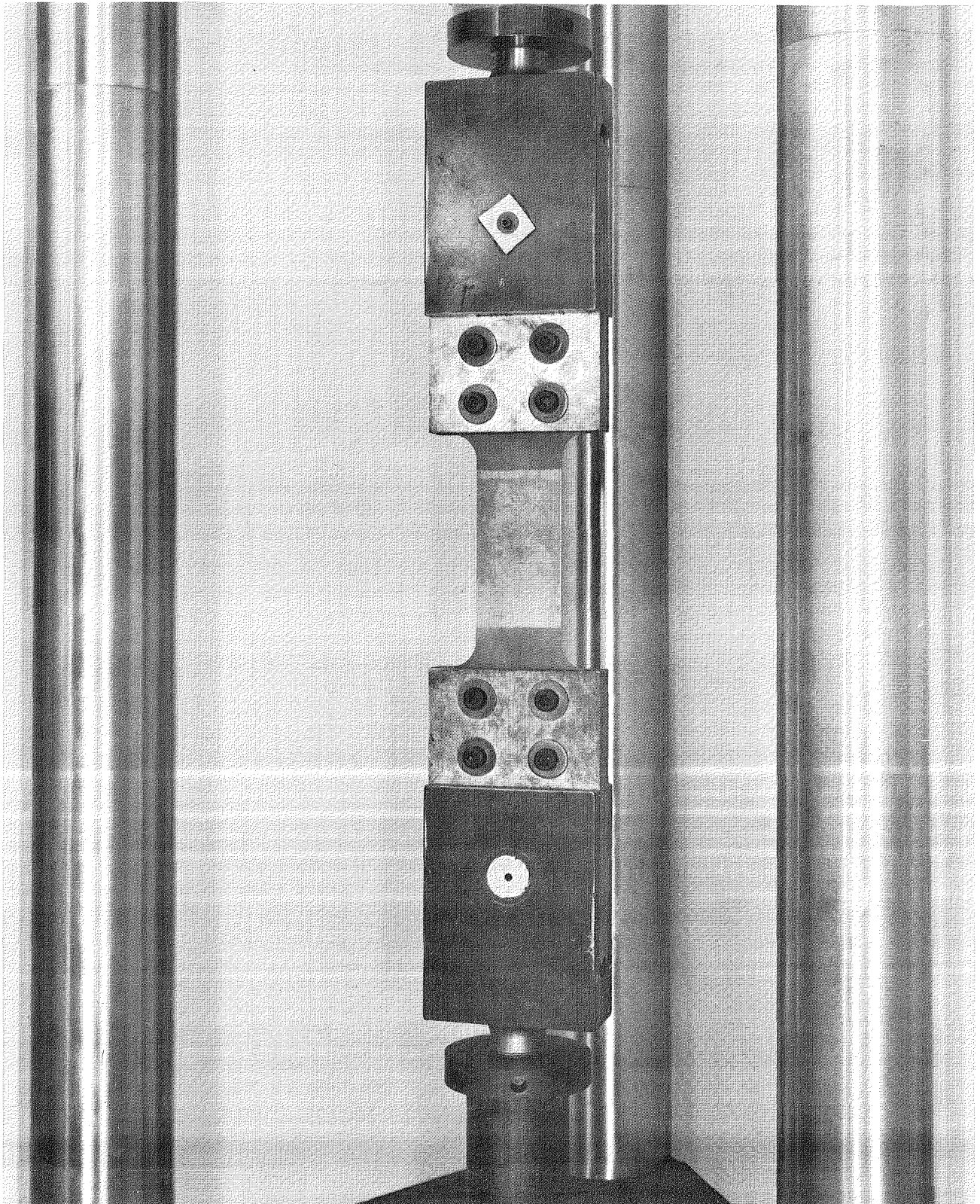
Fatigue Crack Propagation

One of the more important ways in which a flaw can grow to critical size during testing and operating cycles is by fatigue. In the case at hand, the fatigue behavior of the Ti-6Al-4V alloy was studied to ascertain if cracks which passed the nondestructive tests and were not screened in the proof test would propagate through the wall thickness or become critical during 400 operating cycles. A corollary question that was studied was what influence the initial proof cycle, whether air or cryogenic, would have on the subsequent crack growth during fatigue. Finally, the influence of environment on the fatigue crack growth was studied.

Test Apparatus. The basic equipment used in the fatigue crack propagation studies was either a 20 kip or 50 kip electro-hydraulic servo-controlled fatigue test system. These units were used because the cyclic load-time relationship was not a simple sine function but rather a trapezoidal function.

Accuracy of loading was $\pm 1/2$ percent. This extremely good accuracy was due to the use of a digital voltmeter to monitor the loads. A view of the specimen mounted in the 50 kip loading frame is shown in Figure 25.

Environmental Tests. The environments used for the three areas of study were demineralized water, inhibited water, salt spray air, and Aerozine 50. The composition of these environments is given in Table 32.



39177

FIGURE 25. THE SPECIMEN MOUNTED IN THE 50 KIP LOADING FRAME FOR THE FATIGUE CRACK PROPAGATION STUDY.

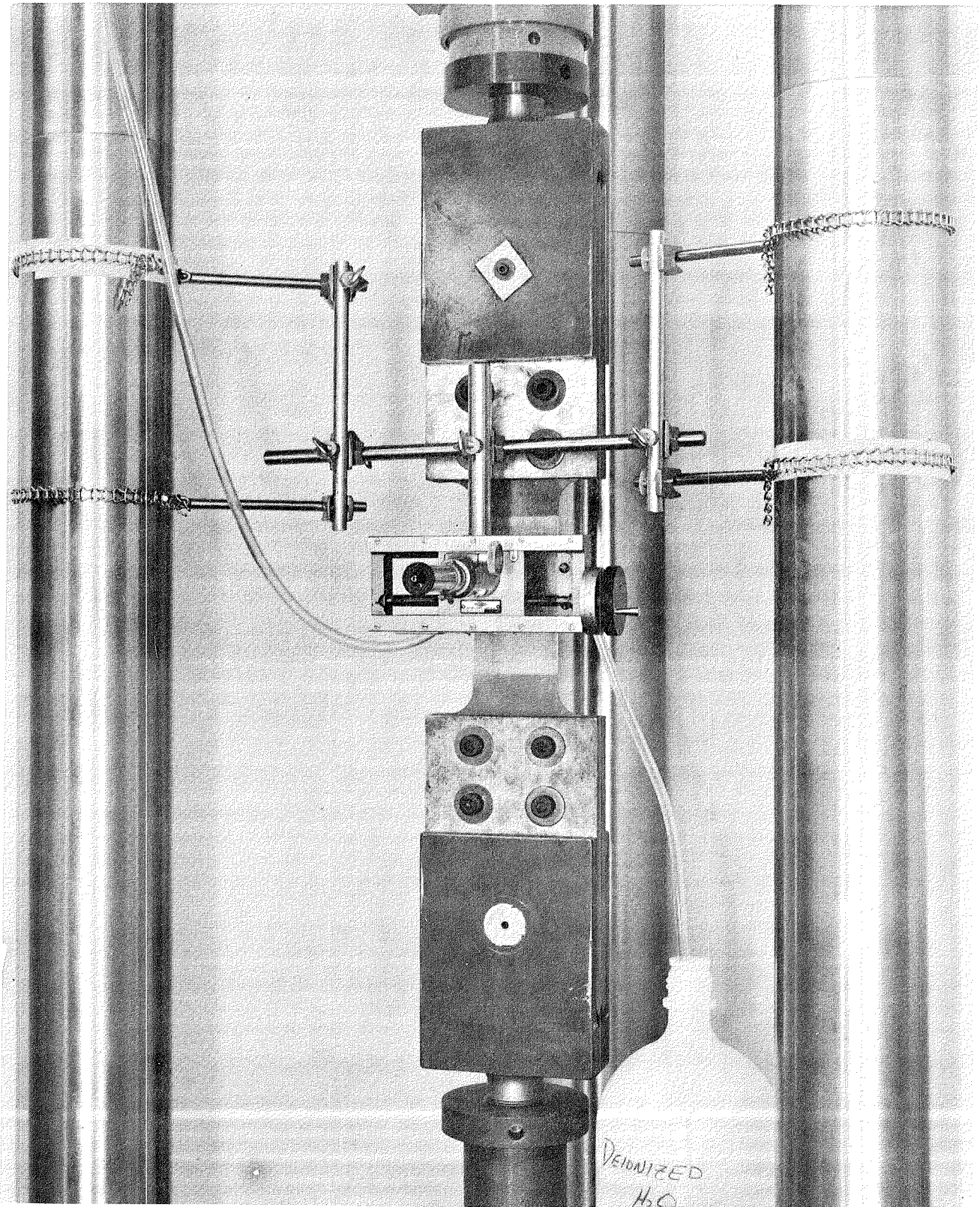
TABLE 32. COMPOSITION OF THE CHEMICAL ENVIRONMENTS

Demineralized water	- Standard deionized water from a still run through an ion exchange column. ph 5.5-5.75
Inhibited water	- Distilled water inhibited with sodium dichromate. - 500 ppm of sodium dichromate ph 4.45-4.55
Salt spray air	- Distilled water used. 3.5 percent NaCl ph 6.75-6.85
Aerozine 50	- (Gas Chromatograph Analysis) 51.2 percent N_2H_4 42.7 percent UDMH 6.1 percent impurity

The environmental chamber for the demineralized and inhibited water consisted of a plexiglas container surrounding the specimen. The fluid was fed into the container by gravity feed. A view of the experimental setup for these tests is shown in Figure 26. The salt spray air chamber, shown in Figure 27, provided a fine spray of the 3.5 percent NaCl solution into the plexiglas container. An air hose was connected to the inlet and the solution was sucked up the column and injected into a nozzle which provided the spray. The experimental setup for the Aerozine 50 tests is shown in Figure 28. The small teflon cylinder shown in the center of the figure contained the Aerozine 50. There was a sufficient amount of Aerozine 50 to submerge the initial crack and material in the vicinity of the crack. The teflon cylinder was encased in a stainless steel container and surrounded by water to prevent ignition of the Aerozine 50 upon fracture of the specimen. The Aerozine was pumped into the container using a negative pressure effect.

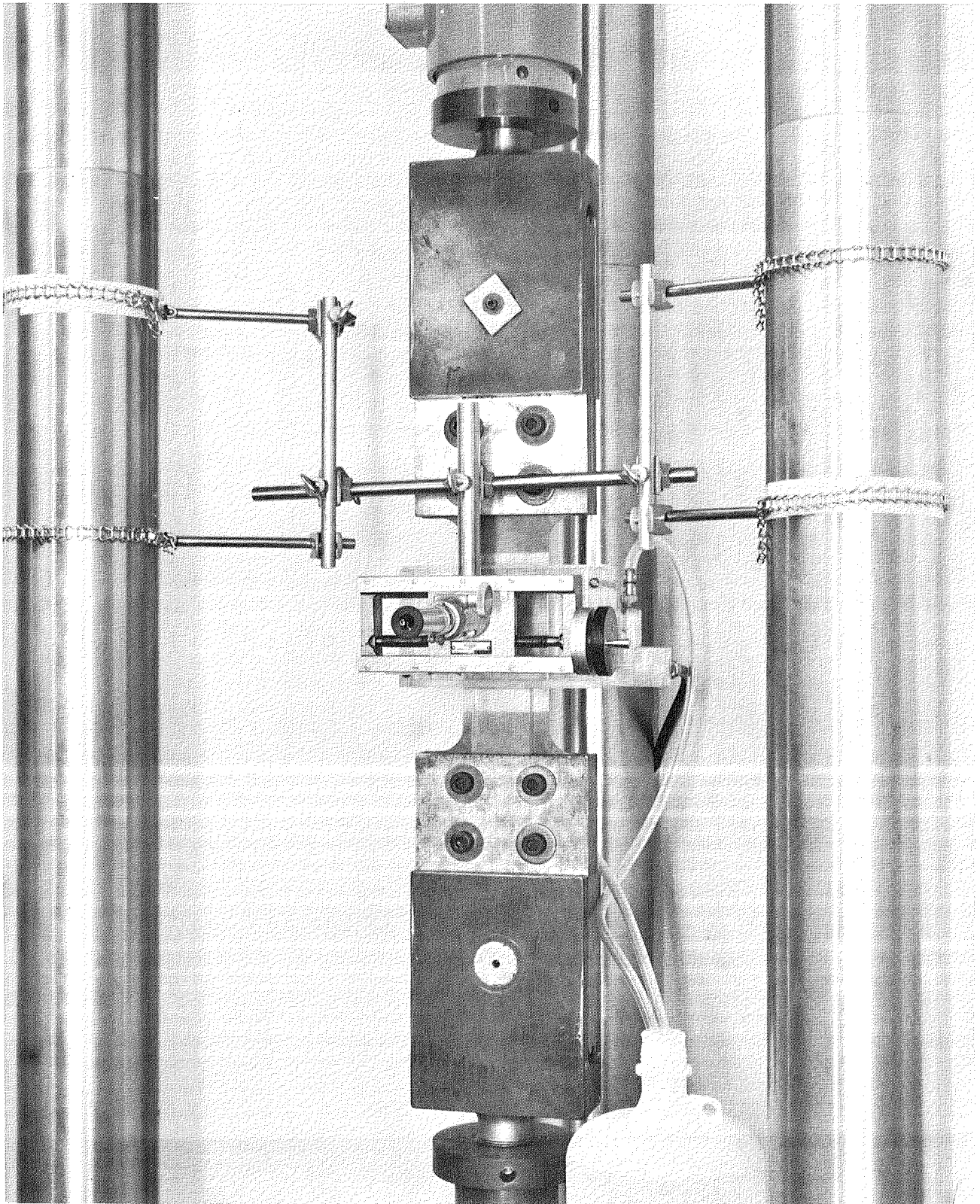
These environmental chambers were used throughout the experimental program on the fatigue crack propagation, fracture, and sustained load studies.

Test Procedure. The loading sequences used for the fatigue crack propagation studies are shown in Figure 29. In Figure 29a, the loading sequence for all specimens receiving air proof cycles is shown. The first proof cycle was applied to the specimen using the Data-Trak unit in the electronic console of the fatigue units. The loading rate was set at 30 ksi per minute and the load necessary to reach a proof stress of 140 ksi applied. After the 140 ksi level was reached, the load was held at that level for 3 minutes. During this hold period a measurement of crack length was taken. After this period expired the load was gradually released. The second proof cycle was applied using a loading rate of 30 ksi per minute, and the maximum load was held for 30 minutes after which the load was released. A measurement of crack length was always taken at the beginning of



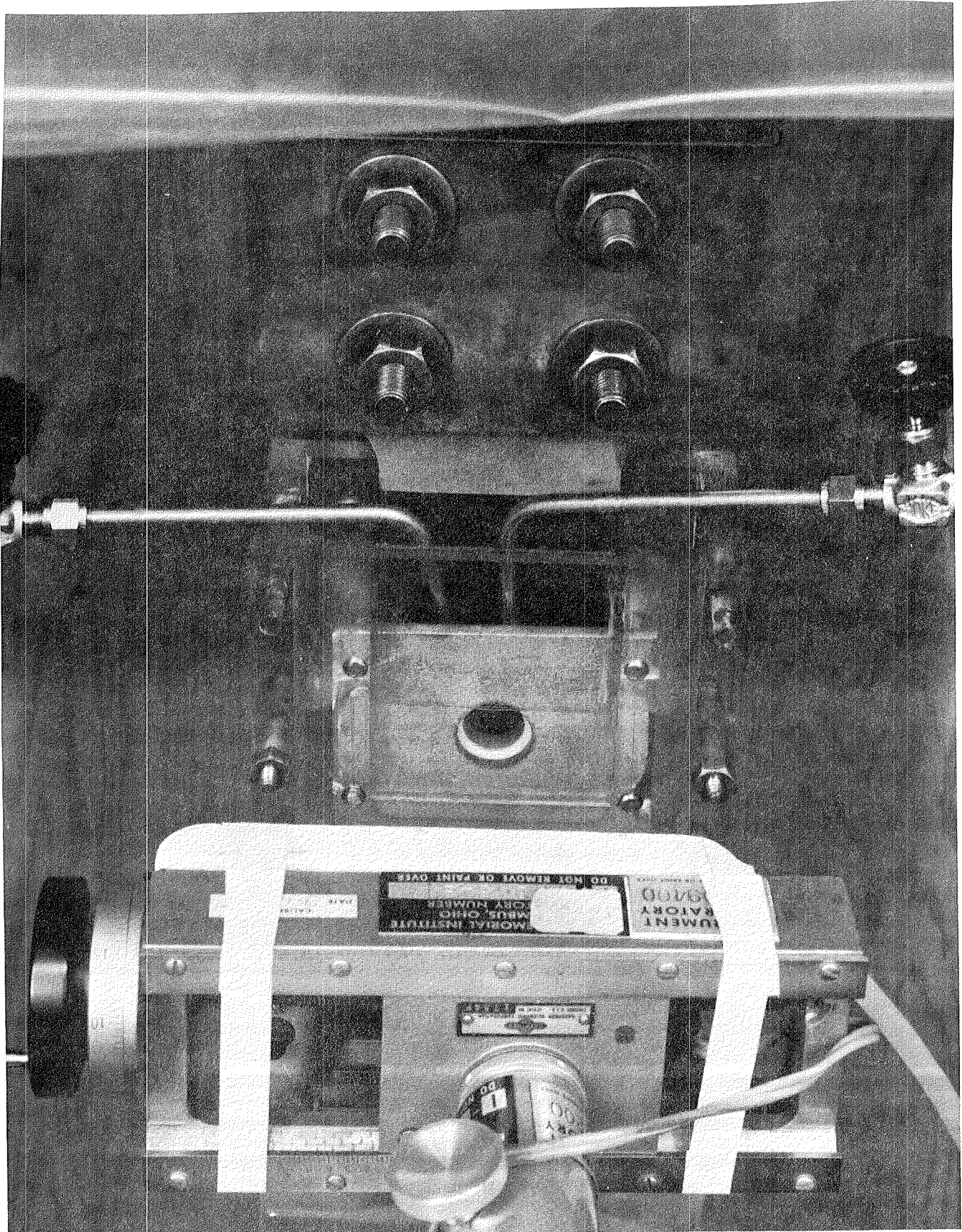
39176

FIGURE 26. THE EXPERIMENTAL SETUP FOR THE DEMINERALIZED WATER AND INHIBITED WATER STUDIES.



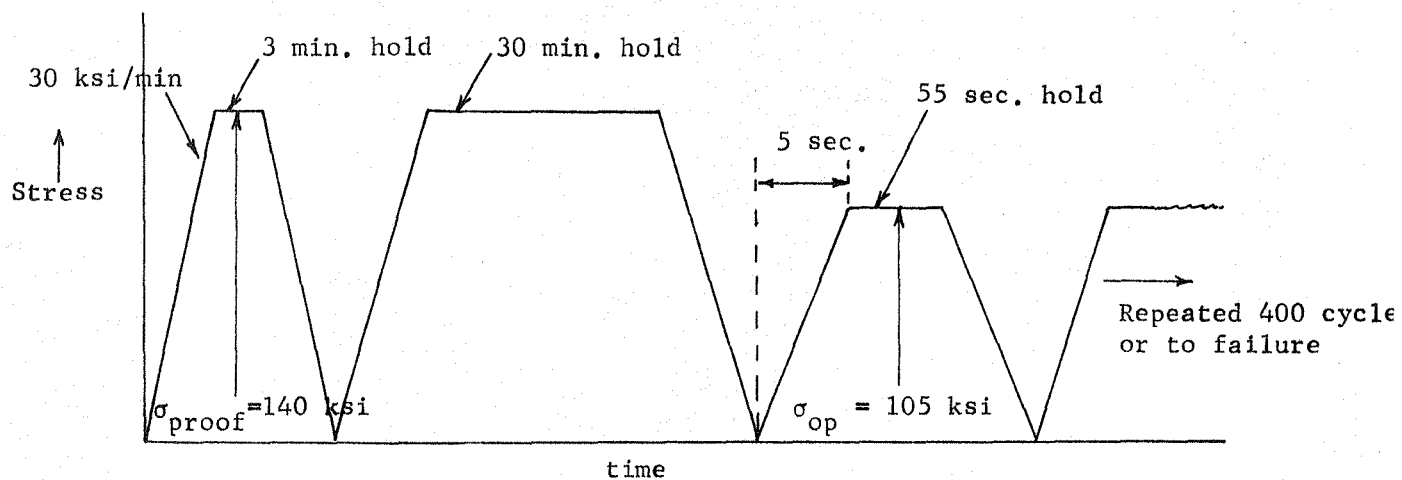
39175

FIGURE 27. THE EXPERIMENTAL SETUP FOR THE SALT SPRAY AIR TESTS.

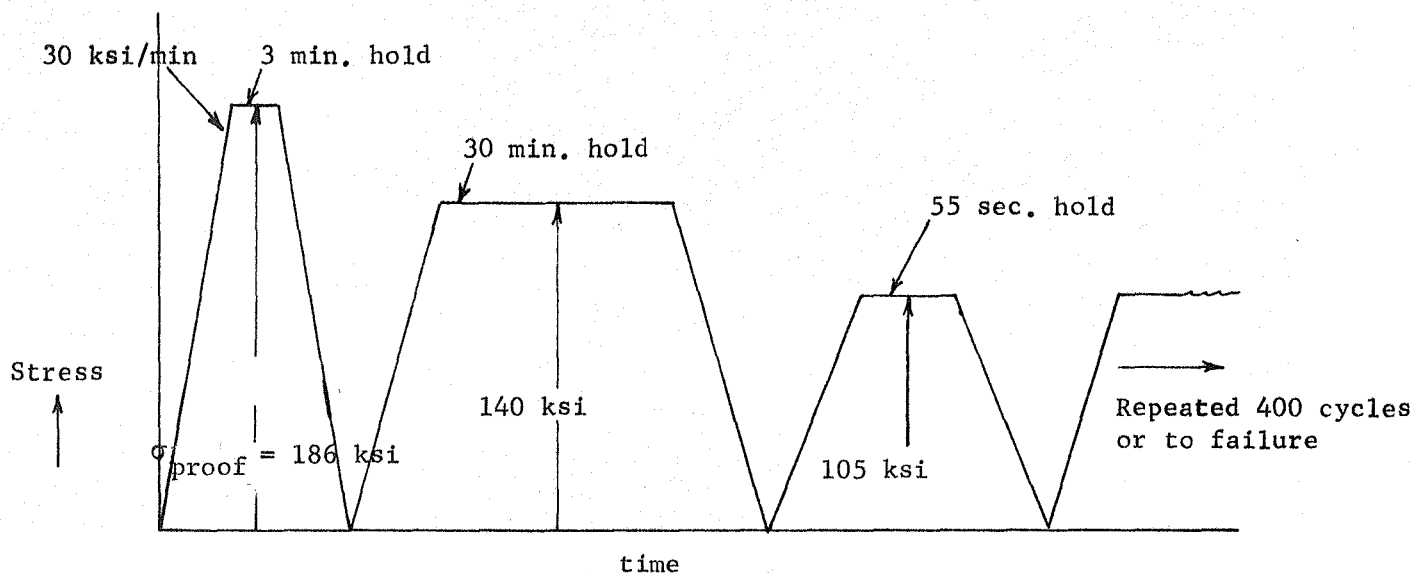


39613

FIGURE 28. EXPERIMENTAL SETUP FOR THE AEROZINE 50 TESTS.



(a) Loading Sequence for All Tests Except Those Where a Cryogenic Proof Cycle was Applied



(b) Loading Sequence Used for Those Specimens Which Received a Cryogenic Proof Cycle

FIGURE 29. LOADING SEQUENCES USED FOR THE PROGRAMMED-FATIGUE-CRACK PROPAGATION TESTS

the 30-minute hold and another measurement near the end of the 30-minute hold. After the two proof cycles were applied in air, the Data-Trak unit was changed to one that provided the repeating pattern of the loading cycle shown in Figure 29a. As can be seen, the load was applied over a 5-second period to a level that provided a stress of 105 ksi. The maximum load was held for 55 seconds and then released. This cycle was repeated 400 times or to failure, whichever occurred first. The stress values employed are those specified for LEM tankage. Likewise, the 400 operating cycles is the maximum specified number of cycles expected of the spacecraft tankage from fabrication to end use.

For those specimens that were tested in the environments, the two proof cycles were always applied using inhibited water.

Figure 29b shows the loading sequence used when the initial proof cycle was put on in the liquid nitrogen cryogenic environment. In testing, the specimen temperature was lowered to -320 F prior to the application of load. The loading rate used to apply the first proof cycle was 30 ksi per minute. The maximum stress achieved was 186 ksi. This value is approximately 0.8 times the cryogenic ultimate strength indicated by NASA personnel as the design value. The first proof cycle in liquid nitrogen was held at maximum load for 3 minutes. A crack length measurement was taken before and after the cryogenic proof cycle to ascertain if flaw growth occurred during the proof cycle. The second proof cycle was applied in air using the Data-Trak and the fatigue testing unit. It was held for 30 minutes. After the first proof cycle, the loading sequence was the same as for the air proof tests.

A brief description of the techniques used to measure the crack lengths is in order. For the air tests, a replication procedure was always employed. This technique involved the application of acetone to the area of the crack and pressing a sheet of cellulose acetate on the specimen surface. In this manner, a replica of the crack was made. In all cases the replicas were made with the

maximum load applied to the specimen. This allowed more accurate determination of the crack length. The replicas then were measured to an accuracy of a thousandth of an inch using an optical comparator. For the environmental tests the optical comparator was mounted on the machine as shown in Figures 26, 27, and 28. Viewing ports were always provided on the environmental chambers to permit viewing of the crack.

Test Results. Presentation and analysis of the programmed fatigue-crack propagation data are included in this section. Since the proof tests tend to screen flaws of a given size, a restatement of the interpretation of the fracture tests is made at this time. The results of the proof tests and the cyclic load tests will be measured and judged in terms of these statements.

- (1) The cryogenic proof stress of 186 ksi is a more severe test than is the air proof test at 140 ksi. Thus smaller flaws should be detected with the cryogenic test.
- (2) At room temperature, no gross thickness effect was observed in the fracture data and it appeared as though the fracture strength of HAZ material was less than that of the parent material.
- (3) At cryogenic temperature, a distinct thickness effect between 20- and 40-mil sheet was observed and there was little significant difference in fracture strength of HAZ material and that of the parent material.
- (4) Approximate flaw sizes estimated to be screened out by proof tests are as follows:

<u>Proof Test</u>	<u>Flaw Size, in²</u>	
	<u>Parent Material</u>	<u>Welded Material</u>
RT - 140 ksi		
20-, 40-, 63-mil	0.005	0.0035
Cryogenic - 186 ksi		
20-mil	0.001	0.0013
40-mil	0.003	0.003

Data Presentation. All of the data obtained during this portion of the program are summarized in Tables 33 through 37. Tables 33, 34, and 35 summarize the major events that occurred during the crack propagation test for the 0.020-, 0.040-, and 0.063-inch-thick material, respectively. The major occurrences included no flaw growth, flaw growth, failed in proof cycle, and breakthrough during cycling. Table 36 presents data on the crack growth that was observed during the two proof cycles. Table 37 presents the flaw size and the amount of growth that occurred during the fatigue cycling after the proof tests. These data will be amplified further in subsequent sections.

Proof Test Results. The failure or non-failure of the flawed samples during the first or second proof test depends upon the size of the actual flaw under test. For the two flaw types and the three flaw depths in the three sheet thicknesses, the following nominal flaw sizes were tested:

<u>Flaw type</u>	<u>t, inch</u>	<u>Flaw area, inch²</u>		
		<u>t/4</u>	<u>t/2</u>	<u>3t/4</u>
Normal	0.020	.0001	.0002	.0005
	0.040	.0003	.0008	.0018
	0.063	.0005	.001	.0042
Elongated	0.020	.0001	.0003	.0010
	0.040	.0003	.001	.0052
	0.063	.0005	.0032	.0129

TABLE 33. PROGRAMMED-FATIGUE-CRACK PROPAGATION TEST RESULTS FOR 0.020-INCH-THICK PARENT AND WELDED Ti-6Al-4V STA MATERIAL, AIR TESTS

Specimen Number	Flaw Depth, inch, f (thickness)	Flaw Type, Normal (N) or Elongated (E)	Material, Parent (P) Welded (W)	Cycles to Breakthrough	Fracture Occurrence	Comments (a)
2-20	t/4	N	P	--	--	NG
2-55	"	N	P	--	--	NG
A8-5	"	N	W	--	--	SG
A1-3	"	N	W	--	--	G
2-46	t/2	N	P	--	--	G
2-X	"	N	P	--	--	G
A7-1	"	N	W	--	--	G
A5-1	"	N	W	--	--	G
2-53	3t/4	N	P	300	--	BDC
2-9	"	N	P	--	--	G
A2-1	"	N	W	--	--	G
A3-5	"	N	W	--	--	G
2-11	t/4	E	P	--	--	NG
2-7	"	E	P	--	--	NG
A7-5	"	E	W	--	--	NG
A6-1	"	E	W	--	--	NG
2-17	t/2	E	P	--	--	G
2-14	"	E	P	--	--	G
A7-4	"	E	W	--	--	G
A10-2	"	E	W	--	--	G
2-26	3t/4	E	P	Proof 1	--	G
2-27	"	E	P	"	--	G
A1-2	"	E	W	"	326 cycles	FDC(b)
A11-3	"	E	W	See Next Column	13-3/4 min. into Proof 2	--

- (a) NG = no growth
 SG = slight growth
 G = growth
 BDC = breakthrough during cycling
 FDC = failed during cycling.

- (b) Secondary flaw present.

TABLE 34. PROGRAMMED-FATIGUE-CRACK PROPAGATION TEST RESULTS FOR
0.040-INCH-THICK PARENT AND WELDED Ti-6Al-4V STA MATERIAL

Specimen Number	Flaw Depth, inch, f (thickness)	Flaw Type, Normal (N) or Elongated (E)	Environment	Material, Parent (P) Welded (W)	Cycles to Breakthrough	Fracture Occurrence	Comments (a)
4-4	t/4	N	Air	P	--	--	NG
4-66	"	N	"	P	--	--	NG
4-X	"	N	Cryogenic	P	--	--	G
4-29	"	N	"	P	--	--	NG
B-12-1	"	N	Air	W	--	--	G
B8-2	"	N	"	W	--	--	G
4-64	t/2	N	"	P	--	--	G
4-62	"	N	"	P	--	--	G
4-20	"	N	Cryogenic	P	--	--	G
4-17	"	N	"	P	--	--	G
4-33	"	N	Salt spray	P	--	--	G
4-39	"	N	"	P	--	--	G
4-24	"	N	Demineralized water	P	--	--	G
4-21	"	N	"	P	--	--	G
4-78	"	N	Inhibited water	P	--	--	G
4-71	"	N	"	P	--	--	G
4-23	"	N	Aerozine 50	P	--	--	NG
B23-1	"	N	Air	W	--	--	G
B24-4	"	N	"	W	--	--	G
B22-2	"	N	Salt spray	W	--	--	G
B14-3	"	N	"	W	--	--	G
B4-2	"	N	Demineralized water	W	--	--	G
B25-2	"	N	"	W	--	--	G
B9-1	"	N	Inhibited water	W	--	--	G
B14-1	"	N	"	W	--	--	G
B6-5	"	N	Aerozine 50	W	--	--	G
B18-5	"	N	"	W	--	--	G
4-100	3t/4	N	Air	P	--	--	G
4-115	"	N	"	P	--	--	G
4-12	"	N	Cryogenic	P	210	--	BDC

TABLE 34. (Continued)

Specimen Number	Flaw Depth, inch, f (thickness)	Flaw Type, Normal (N) or Elongated (E)	Environment	Material, Parent (P) Welded (W)	Cycles to Breakthrough	Fracture Occurrence	Comments (a)
4-90	3t/4	N	Cryogenic	P	390	--	BDC
B22-5	"	N	Air	W	--	--	G
B8-3	"	N	"	W	--	--	G
4-87	t/4	E	"	P	--	--	NG
4-89	"	E	"	P	--	--	G
4-117	"	E	Cryogenic	P	--	--	NG
4-112	"	E	"	P	--	--	G
B15-3	"	E	Air	W	--	--	NG
B15-2	"	E	"	W	--	--	G
4-46	t/2	E	"	P	--	--	G
4-48	"	E	"	P	--	--	G
4-42	"	E	Cryogenic	P	--	--	G
4-86	"	E	"	P	--	--	G
4-105	"	E	Salt spray	P	--	--	G
4-106	"	E	"	P	--	--	G
4-55	"	E	Deminerlized water	P	--	--	G
4-110	"	E	"	P	--	--	G
4-7	"	E	Inhibited water	P	--	--	G
4-10	"	E	"	P	--	--	G
4-97	"	E	Aerozine 50	P	--	--	G
4-102	"	E	"	P	--	--	G
B18-3	"	E	Air	W	--	--	G
B15-5	"	E	"	W	--	--	G
B23-2	"	E	Salt spray	W	--	--	G
B11-2	"	E	"	W	--	--	G
B10-4	"	E	Deminerlized water	W	--	--	G
B10-3	"	E	"	W	--	--	G
B16-2	"	E	Inhibited water	W	--	--	G
B8-5	"	E	"	W	See next column	Proof 1 ^(b)	--
B11-4	"	E	Aerozine 50	W	--	--	G
B16-3	"	E	"	W	--	--	G

TABLE 34. (Continued)

Specimen Number	Flaw Depth, inch, f (thickness)	Flaw Type, Normal (N) or Elongated (E)	Environment	Material, Parent (P) Welded (W)	Cycles to Breakthrough	Fracture Occurrence	Comments (a)
B-72	3t/4	E	Air	P	See next column	45 sec. into Proof 1	--
4-79	"	E	"	P	"	Proof 1 on loading	--
B18-4	"	E	"	W	"	Proof 1 on loading	--
B17-1	"	E	"	W	"	Proof 1 on loading	--
4-15	"	E	Cryogenic	P	"	Cryo proof on loading	--
4-98	"	E	"	P	"	Cryo proof on loading	--

(a) NG = no growth
 G = growth
 BDC = breakthrough during cycling

(b) Secondary flaw present.

TABLE 35. PROGRAMMED-FATIGUE-CRACK PROPAGATION TEST RESULTS FOR 0.063-INCH-THICK PARENT AND WELDED Ti-6Al-4V STA MATERIAL, AIR TESTS

Specimen Number	Flaw Depth, inch, f (thickness)	Flaw Type, Normal (N) or Elongated (E)	Material, Parent (P) Welded (W)	Cycles to Breakthrough	Fracture Occurrence	Comments (a)
6-7	t/4	N	P	--	--	G
6-6	"	N	P	--	--	NG
C5-2	"	N	W	--	--	G
C6-4	"	N	W	--	--	G
6-9	t/2	N	P	--	--	G
6-8	"	N	P	--	--	G
C5-1	"	N	W	--	--	G
C1-5	"	N	W	--	--	G
6-19	3t/4	N	P	--	--	G
6-15	"	N	P	290	--	BDC
C11-3	"	N	W	See next column	6 min. into Proof 2	--
C10-5	"	N	W	See next column	1-1/2 min. into Proof 2	--
6-40	t/4	E	P	--	--	G
6-31	"	E	P	--	--	G
C11-5	"	E	W	--	--	G
C3-3	"	E	W	--	--	G
6-26	t/2	E	P	See next column	20 sec. into Proof 2	--
6-42	"	E	P	--	--	G
C3-1	"	E	W	See next column	Proof 2 on loading	--
C4-1	"	E	W	"	2-1/4 min. into Proof 1	--
6-24	3t/4	E	P	"	Proof 1 on loading	--
6-23	"	E	P	"	Proof 1 on loading	--
C4-5	"	E	W	"	Proof 1 on loading	--
C4-2	"	E	W	"	Proof 1 on loading	--

(a) G = growth
 NG = no growth
 BDC = breakthrough during cycling.

TABLE 36. MEASURED SURFACE CRACK LENGTH GROWTH DURING THE PROOF TESTS

Specimen Number	Material, Parent(P) Welded(W)	Initial Flaw Depth, a ₁ , inch	Thickness, t, inch	Initial Surface Crack Length, 2 c ₁ , inch	Surface Crack Length, Proof 1, inch	Surface Crack Length, Start of Proof 2, inch	Surface Crack Length, End of Proof 2, inch	Surface Crack Growth, Proof 1, inch	Surface Crack Growth, Proof 2, inch	Tests Environment (Proof Cycle 1)
<u>0.020 Inch Thick Material</u>										
2-20	P	t/4 N	.021	.0137	.0143	.0144	.0142	.0005	0	Air
2-55	P	"	.021	.0135	.0138	.0135	.0134	0	0	"
A8-5	W	"	.022	.0130	.0130	.0130	.0130	0	0	"
A1-3	W	"	.021	.0130	.0135	.0135	.0132	≈ 0	0	"
2-46	P	t/2 N	.020	.0265	.0265	.0267	.0263	0	0	"
2-X	P	"	.020	.0266	.0267	.0267	.0267	0	0	"
A7-1	W	"	.020	.0290	.0302	.0305	.0303	.0012	≈ 0	"
A5-1	W	"	.020	.0265	.0284	.0285	.0287	.0019	≈ 0	"
2-9	P	3t/4 N	.021	.0435	.0440	.0441	.0446	.0005	.0005	"
2-11	P	"	.021	.0435	.0442	.0441	.0442	.0006	≈ 0	"
A2-1	W	"	.021	.0401	-	.0410	.0407	-	0	"
A3-5	W	"	.020	.0393	.0403	.0400	.0405	.0008	.0004	"
2-11	P	t/4 E	.021	.0115	.0121	.0114	.0116	0	0	"
2-7	P	"	.021	.0113	.0114	.0111	.0116	0	≈ 0	"
A7-5	W	"	.021	.0113	.0114	.0119	.0115	0	0	"
A6-1	W	"	.020	.0101	.0108	.0108	.0108	.0007	0	"
2-17	P	t/2 E	.022	.0447	.0449	.0450	.0454	.0002	.0004	"
2-11	P	"	.020	.0433	.0435	.0434	.0434	0	0	"
A7-4	W	"	.020	.0384	.0386	.0386	.0386	0	0	"
A10-2	W	"	.020	.0401	.0402	.0402	.0404	0	0	"
2-26	P	3t/4 E	.020	.0974	.0970 B.T.	.0981	.0988	B.T.	.0007	"
2-27	P	"	.021	.1240	- B.T.	.1298	≈ .1400	B.T.	.0102	"
A1-2	W	"	.020	.1516	.1523 B.T.	.1520	.1526	B.T.	.0006	"
A11-3	W	"	.021	.1350	.1387 B.T.	(Fractured 13-3/4 minutes into hold)	-	B.T.	Fractured	"
<u>0.040 Inch Thick Material</u>										
4-4	P	t/4 N	.043	.0291	.0298	.0297	.0297	0	0	"
4-6a	P	"	.041	.0277	.0287	.0287	.0287	.0010	0	"
4-29	P	"	.039	-	.0269	.0265	.0270	0	0	Cryo Proof
B12-1	W	"	.042	.0284	.0281	.0285	.0287	0	≈ 0	Air
B8-2	W	"	.042	.0274	.0276	.0281	.0277	≈ 0	0	"
4-42	P	"	.044	.0587	.0592	.0602	.0595	.0005	0	"
4-20	P	"	.043	.0558	.0574	.0575	.0576	.0016	0	Cryo Proof
4-17	P	"	.044	.0613	.0623	.0621	.0626	.0010	0	"
4-33	P	"	.043	.0566	.0570	.0575	.0577	.0004	0	I.H. *

TABLE 14 (CONTINUED)

Specimen Number	Material Parent (P) Welded (W)	Initial Flaw Depth, a_1 , inch	Thickness, t , inch	Initial Surface Crack Length, $2c_1$, inch	Surface Crack Length, Proof 1, inch	Surface Crack Length, Start of Proof 2, inch	Surface Crack Length, End of Proof 2, inch	Surface Crack Growth, Proof 1, inch	Surface Crack Growth, Proof 2, inch	Tests Environment (Proof Cycle 1)
4-39	P	t/2 N	.043	.0578	.0582	.0577	.0577	0	0	I.W.
4-24	P	"	.044	.0567	.0572	.0572	.0572	.0005	0	I.W.
4-21	P	"	.044	.0574	.0579	.0579	.0579	.0005	0	"
4-70	P	"	.042	.0537	-	.0541	.0542	-	.0005	"
4-71	P	"	.042	.0544	.0544	.0541	.0545	0	0	"
4-23	P	"	.042	.0505	.0505	.0504	.0504	0	0	"
B23-1	W	"	.040	.0531	.0547	.0545	.0549	.0016	0	Air
B24-4	W	"	.042	.0560	.0560	.0576	.0581	.0005	.0005	"
B22-2	W	"	.042	.0549	.0548	.0547	.0551	0	0	I.W.
B14-3	W	"	.042	.0545	.0548	.0550	.0550	.0003	0	"
B4-2	W	"	.043	.0555	.0558	.0557	.0557	0	0	"
B75-2	W	"	.042	.0568	.0575	.0578	.0577	.0007	0	"
B7-1	W	"	.041	.0550	.0551	.0550	.0550	0	0	"
B14-1	W	"	.042	.0588	.0615	.0618	.0620	.0027	.0005	"
B0-5	W	"	.041	-	.0599	.0597	.0601	-	0	"
B18-5	W	"	.042	.0552	.0566	.0569	.0562	.0010	0	"
4-100	P	3t/4 N	.041	.0800	.0792	.0798	.0797	0	0	Air
4-115	P	"	.043	.0847	.0833	.0838	.0831	0	0	"
4-12	P	"	.044	.0857	.1011	.1057	.1066	.0154	.0046	Cryo Proof
4-90	P	"	.041	.0807	.0884	.0932	.0946	.0077	.0048	"
B22-5	W	"	.042	.0818	.0826	.0826	.0854	.0008	.0028	Air
B8-3	W	"	.042	.0840	.0856	.0858	.0864	.0016	.0006	"
4-87	P	t/4 E	.041	.0368	.0365	.0365	.0365	0	0	"
4-89	P	"	.042	.0405	.0407	.0411	.0406	0	0	"
4-117	P	"	.044	.0391	.0396	.0400	.0395	.0005	0	Cryo Proof
4-112	P	"	.044	.0392	.0398	.0398	.0396	.0004	0	"
B15-3	W	"	.042	.0382	.0390	.0387	.0390	.0005	0	Air
B15-2	W	"	.043	.0380	.0379	.0379	.0380	0	0	"
4-46	P	t/2 E	.044	.1160	.1167	.1167	.1174	.0007	.0007	"
4-8	P	"	.044	.1147	.1148	.1150	.1148	0	0	"
4-42	P	"	.043	.1073	.1076	.1076	.1077	.0003	0	Cryo Proof
4-86	P	"	.041	.0994	.1001	.0997	.1001	.0007	0	"
4-105	P	"	.044	.1120	.1128	.1121	.1131	.0005	.0005	I.W.
4-106	P	"	.044	.1225	.1234	.1234	.1234	.0009	0	"
4-55	P	"	.044	.1135	.1137	.1135	.1135	0	0	"
4-110	P	"	.044	.1094	.1105	.1105	.1105	.0009	0	"
4-7	P	"	.044	.1137	.1137	.1137	.1137	0	0	"
4-10	P	"	.044	.1169	.1164	.1164	.1166	0	0	"
4-97	P	"	.042	.1027	.1029	.1027	.1030	0	0	"
4-102	P	"	.044	.1127	.1154	.1156	.1158	.0027	0	"
B13-3	W	"	.042	.1028	.1019	.1023	.1017	0	0	Air
B15-5	W	"	.042	.1020	.1018	.1018	.1022	0	0	"
B23-2	W	"	.041	.0992	.0991	.0992	.0990	0	0	I.W.
B11-2	W	"	.042	.1023	.1024	.1024	.1026	0	0	"

TABLE 36. (Continued)

Specimen Number	Material Parent(P) Welded(W)	Initial Flaw Depth, a_1 , inch	Thickness, t , inch	Initial Surface Crack Length, $2c_1$, inch	Surface Crack Length, Proof 1, inch	Surface Crack Length, Start of Proof 2, inch	Surface Crack Length, End of Proof 2, inch	Surface Crack Growth, Proof 1, inch	Surface Crack Growth, Proof 2, inch	Tests Environment (Proof Cycle 1)
B10-4	W	t/2 E	.041	.0998	.0998	.1015	.1010	0	0	I.W.
B10-3	W	"	.041	.1000	.1000	.1000	.0998	0	0	"
B10-2	W	"	.042	.1034	.1026	.1026	.1026	0	0	"
B3-5	W	"	.042	.1011	void	-	-	-	-	"
B11-4	W	"	.042	.1014	-	.1015	.1012	0	0	"
B16-3	W	"	.042	.1020	.1018	.1012	.1012	0	0	"
4-72	P	3t/4 E	.041	.2115	Fracture	-	-	Fracture	-	Air
4-79	P	"	.043	.2330	Fracture	-	-	Fracture	-	"
4-15	P	"	.042	.2185	"	-	-	"	-	Cryo Proof
4-98	P	"	.043	.2287	"	-	-	"	-	"
B18-4	W	"	.042	.2156	"	-	-	"	-	Air
<u>0.063 Inch Thick Material</u>										
6-7	P	t/4 N	.064	.0326	.0323	.0328	.0326	0	0	"
6-6	P	"	.063	.0328	.0327	.0321	.0322	0	0	"
G5-2	W	"	.064	.0338	.0334	.0334	.0331	0	0	"
G6-4	W	"	.062	.0333	.0318	.0315	.0315	0	0	"
6-9	P	t/2 N	.064	.0664	.0673	.0680	.0679	.0009	0	"
6-8	P	"	.062							
C5-1	W	"	.062	.0662	.0675	.0672	.0670	.0010	0	"
C1-5	W	"	.062	.0663	.0663	.0661	.0661	0	0	"
6-19	P	3t/4 N	.065	.1000	.0987	.1001	.48	0	.0137	"
6-15	P	"	.064	.1020	.1042	.1068	.1113	.0022	.0045	"
C11-3	W	"	.063	.1012	-	Fracture	-	-	Fracture	"
C10-5	W	"	.063	.1020	Fracture	-	-	Fracture	6 min.	"
								1 min 20 sec	-	
6-40	P	t/4 E	.062	-	.0516	.0518	.0520	-	0	"
6-31	P	"	.061	.0508	.0507	.0505	.0510	0	0	"
C11-5	W	"	.061	.0504	.0501	.0503	.0502	0	0	"
C3-3	W	"	.062	.0510	.0508	.0504	.0512	0	0	"
6-26	P	t/2 E	.063	.1265	.1297	Fracture	-	.0028	Fracture	"
6-42	P	"	.063	.1237	.1230	.1238	.1248	0	.0010	"
C3-1	W	"	.062	.1193	Fracture	-	-	Fracture	-	"
C4-4	W	"	.064	.1234	Fracture	-	-	Fracture	-	"
								2 min 15 sec	-	
6-24	P	3t/4 E	.063	.3476	Fracture	-	-	Fracture	-	"
6-23	P	"	.063	.3495	Fracture	-	-	Fracture	-	"
C4-5	W	"	.063	.3669	Fracture	-	-	Fracture	-	"
C4-2	W	"	.063	.3466	Fracture	-	-	Fracture	-	"

* I. W. - Inhibited Water

TABLE 37. PROGRAMMED FATIGUE CRACK PROPAGATION TEST RESULTS

Specimen No. Ser	Initial Flaw Depth, inch	Material (P) Parent (W) Welded	Environment	Thickness, t, inch	Initial Surface Crack Length After Proof Cycles 2 c _i , inch	Final Surface Crack Length 2 c _f , inch	Computed Initial Crack Depth After Proof Cycles a _i , inch	Computed Change in Crack Depth Δ a, inch	Comments
<u>0.020 inch Material</u>									
2-20	t/4 N	P	Air	.021	.0142	--	.0057	0	
2-55	"	P	"	.021	.0138	--	.0056	0	
A3-5	"	W	"	.022	.0132	--	.0052	0	
A1-3	"	W	"	.021	.0134	--	.0052	0	
2-49	t/2 N	P	Air	.020	.0263	.0300	.0102	.0015	
2-5	"	P	"	.020	.0266	.0288	.0104	.0008	
A7-1	"	W	"	.020	.0294	.0315	.0110	.0008	
A5-1	"	W	"	.020	.0286	.0310	.0107	.0009	
2-53	3t/4 N	P	"	.022	.0446	.0528	.0174	-	B. T.** 300 cycles
2-9	"	P	"	.021	.0442	.0500	.0172	.0023	
A2-1	"	W	"	.021	.0411	.0458	.0154	.0018	
A3-5	"	W	"	.020	.0404	.0468	.0151	.0024	
2-11	t/4 E	P	"	.021	.0118	.0118	.0049	0	
2-7	"	P	"	.021	.0116	.0116	.0048	0	
A7-5	"	W	"	.021	.0117	.0117	.0048	0	
A6-1	"	W	"	.020	.0108	.0108	.0045	0	
2-17	t/2 E	P	"	.022	.0454	.0487	.0105	.0016	
2-14	"	P	"	.020	.0434	.0464	.0103	.0015	
A7-	"	W	"	.020	.0386	.0392	.0100	.0003	
A10-2	"	W	"	.020	.0385	.0425	.0100	.0020	
2-25	3t/4 E	P	"	.020	.0988	.1283	.0160*	--	B. T. Proof 1, Did not fail
2-27	"	P	"	.021	.1550	.2204	.0185*	--	B. T. Proof 1, Did not fail
A1-2	"	W	"	.020	.1539	--	.0185*	--	--- Void-Secondary Flaw
A11-3	"	W	"	.021	.1342	--	.0172*	--	B. T. Proof 1, Fractured Proof 2
<u>0.040 inch Material</u>									
4-	t/4 N	P	Air	.043	.0300	.0300	.0121	0	
4-03	"	P	"	.041	.0288	.0288	.0117	0	
--	"	P	Cryo Proof	--	--	--	--	--	Void
4-29	"	P	Cryo Proof	.039	.0270	.0270	.0109	0	
312-1	"	W	Air	.042	.0285	.0292	.0106	.0003	
38-2	"	W	"	.042	.0279	.0298	.0105	.0007	

* Flaw size at start of Proof Cycles.

** B. T.- Broke through thickness

TABLE 37. (Continued)

Specimen Number	Initial Flaw Depth, inch	Material (P) Parent (W) Welded	Environment**	Thickness, t, inch	Initial Surface Crack Length After Proof Cycles $2c_i$, inch	Final Surface Crack Length $2c_f$, inch	Computed Initial Crack Depth After Proof Cycles a_i , inch	Computed Change in Crack Depth Δa , inch	Comments
<u>0.040 inch Material (Continued)</u>									
4-64	t/2 N	P	Air	.042	.0587	.0632	.0228	.0018	
4-62	"	P	"	.044	.0589	.0636	.0228	.0020	
4-20	"	P	Cryo Proof	.043	.0576	.0628	.0224	.0020	
4-17	"	P	"	.044	.0621	.0697	.0242	.0030	
4-33	"	P	SSA	.043	.0577	.0630	.0225	.0020	
4-30	"	P	"	.043	.0580	.0648	.0226	.0026	
4-24	"	P	D.W.	.044	.0574	.0615	.0223	.0016	
4-21	"	P	"	.044	.0579	.0614	.0225	.0013	
4-78	"	P	I W.	.042	.0543	.0573	.0211	.0012	
4-71	"	P	"	.042	.0545	.0575	.0211	.0012	
4-23	"	P	Aero. 50	.042	.0530	.0582	.0203	.0020	
B23-1	t/2 N	W	Air	.040	.0547	.0588	.0203	.0017	
P24-4	"	W	"	.042	.0578	.0630	.0219	.0020	
B22-2	"	W	SSA	.042	.0551	.0601	.0206	.0019	
B14-3	"	W	"	.042	.0550	.0593	.0206	.0016	
B7-7	"	W	D W.	.043	.0557	.0601	.0209	.0016	
B25-2	"	W	"	.042	.0581	.0693	.0218	.0042	
B9-1	"	W	I W.	.041	.0550	.0608	.0206	.0022	
B14-1	"	W	"	.042	.0620	.0662	.0232	.0016	
B6-5	"	W	Aero. 50	.041	.0542	.0605	.0202	.0025	
B18-5	"	W	"	.042	.0547	.0619	.0220	.0017	
4-100	3t/4 N	P	Air	.041	.0816	.0923	.0318	.0041	
4-115	"	P	"	.043	.0841	.0981	.0327	.0055	
4-12	"	P	Cryo Proof	.044	.1066	.1445	≈.0410	--	B. T., 210 cycles
4-90	"	P	"	.041	.0946	.1207	≈.0368	--	B. T., 390 cycles
B22-5	"	W	Air	.042	.0857	.1084	.0321	.0082	
B3-3	"	W	"	.042	.0864	.1041	.0324	.0068	
4-87	t/4 E	P	Air	.041	.0366	.0366	.0090	0	
4-89	"	P	"	.042	.0406	.0427	.0100	.0009	
4-117	"	P	Cryo Proof	.044	.0400	.0400	.0096	0	
4-112	"	P	"	.044	.0396	.0406	.0095	.0005	
B15-3	"	W	Air	.042	.0388	.0388	.0093	0	
B15-2	"	W	"	.043	.0377	.0390	.0092	.0006	

TABLE 37. (Continued)

Specimen Number	Initial Flaw Depth, inch	Material (P) Parent (W) Welded	Environment	** Thickness, t, inch	Initial Surface Crack Length After Proof Cycles $2c_1$, inch	Final Surface Crack Length $2c_f$, inch	Computed Initial Crack Depth After Proof Cycles a_1 , inch	Computed Change in Crack Depth Δa , inch	Comments
<u>0.040 inch Material (Continued)</u>									
4-46	t/2 E	P	Air	.044	.1174	.1269	.0222	.0048	
4-48	"	P	"	.044	.1148	.1233	.0218	.0038	
4-42	"	P	Cryo Proof	.043	.1076	.1191	.0212	.0057	
4-46	"	P	"	.041	.1001	.1058	.0201	.0029	
4-105	"	P	SSA	.044	.1144	.1228	.0216	.0042	
4-106	"	P	"	.045	.1234	.1355	.0228	.0060	
4-55	"	P	D.W.	.044	.1135	.1207	.0217	.0036	
4-110	"	P	"	.044	.1106	.1140	.0215	.0017	
4-7	"	P	I.W.	.045	.1131	.1212	.0219	.0041	
4-10	"	P	"	.044	.1173	.1300	.0222	.0063	
4-97	"	P	Aero. 50	.042	.1041	.1097	.0190	.0034	
4-102	"	P	"	.044	.1140	.1223	.0240	.0039	
D10-3	t/2 E	W	Air	.042	.1024	.1090	.0211	.0032	
F15-5	"	W	"	.042	.1022	.1084	.0210	.0032	
U23-2	"	W	SSA	.041	.0995	.1045	.0207	.0025	
D11-2	"	W	"	.042	.1026	.1106	.0211	.0040	
D10-4	"	W	D.W.	.041	.0992	.1037	.0207	.0023	
D10-3	"	W	"	.041	.0997	.1114	.0208	.0058	
D10-2	"	W	I.W.	.042	.1026	.1088	.0212	.0031	
D10-5	"	W	"	.042	--	--	--	--	Void - Secondary Crack
D11-4	"	W	Aero. 50	.042	.1015	.1104	.0212	.0042	
D10-3	"	W	"	.042	.1000	.1050	.0201	.0024	
4-72	3t/4 E	P	Air	.041	.2115*	--	.0270*	--	Fractured, Proof 1 on loading;
4-79	"	P	"	.043	.2330*	--	.0273*	--	Fractured, Proof 1 on loading
4-15	"	P	Cryo. Proof	.042	.2186*	--	.0271*	--	Fractured, Cryo - Proof on loading
4-98	"	P	"	.042	.2286*	--	.0273*	--	Fractured, Cryo - Proof on loading
D10-4	"	W	Air	.042	.2136*	--	.0261*	--	Fractured, Proof 1 on loading
D17-1	"	W	"	.043	.2102*	--	.0242*	--	Fractured, Proof 1 on loading
<u>0.063 inch Material</u>									
6-7	t/4 N	P	Air	.064	.0326	.0352	.0140	.0012	
6-6	"	P	"	.063	.0320	.0320	.0137	0	
CS-2	"	W	"	.064	.0330	.0370	.0134	.0016	
CS-4	"	W	"	.062	.0317	.0358	.0128	.0016	
6-9	t/2 N	P	"	.064	.0679	.0768	.0291	.0039	
6-4	"	P	"	.062	.0760	.1108	.0326	.0149	
CS-1	"	W	"	.062	.0674	.0776	.0273	.0041	

* Flaw size at start of Proof Cycles.

** I.W. = Inhibited water.
D.W. = Deionized water.
SSA = Salt-spray-air.
Aero. 50 = Aerozine 50.

TABLE 37. (Continued)

Specimen Number	Initial Flaw Depth, inch	Material (P) Parent (W) Welded	Environment	Thickness, t, inch	Initial Surface Crack Length After Proof Cycles $2 c_i$, inch	Final Surface Crack Length $2 c_f$, inch	Computed Initial Crack Depth After Proof Cycles a_i , inch	Computed Change in Crack Depth Δa , inch	Comments
<u>0.063 inch Material (Continued)</u>									
C1-5	t/2 N	W	Air	.062	.0664	.0749	.0268	.0035	
6-9	3t/4 N	P	"	.065	.1148	.1787	.0496	.015	Large Dimplr, No Breakthrough
u-5	"	P	"	.064	.1265	.2052	.0544	--	Broke through, 290 cycles
C1-3	"	W	"	.063	.1012*	Fractured	.0472*	--	Fractured, 6 min. of Proof 2
C10-5	"	W	"	.063	.1020*	Fractured	.0472	--	Fractured, 1 min. 20 sec. of Proof 1
u-10	t/4 E	P	Air	.062	.0520	.0551	.0182	.0016	
u-31	"	P	"	.061	.0510	.0537	.0180	.0013	
C11-5	"	W	"	.061	.0501	.0516	.0179	.0008	
C3-3	"	W	"	.062	.0505	.0532	.0179	.0013	
u-20	t/2 E	P	"	.063	.1265	--	.0310	--	Fractured, Proof 2, 20 sec.
u-42	"	P	"	.063	.1243	.1500	.0308	.0125	
C3-1	"	W	"	.062	.1193*	--	.0303*	--	Fractured, Proof 1 on Loading
C4-4	"	W	"	.064	.1234*	--	.0305*	--	Fractured, Proof 1, 2 min 15 sec.
u-21	3t/4 E	P	"	.063	.3476*	--	.0480*	--	Fractured, Proof 1, on Loading
u-23	"	P	"	.063	.3495*	--	.0485*	--	Fractured, Proof 1, on Loading
C4-5	"	W	"	.063	.3669*	--	.0490*	--	Fractured, Proof 1, on Loading
C4-2	"	W	"	.063	.3466*	--	.0476*	--	Fractured, Proof 1 on Loading

* Flaw size at start of Proof Cycles.

On the basis of these values and those in the previous tabulation showing inspectable crack sizes (area) from the fracture tests, one can (after the fact) point toward certain flaws in the three sheets that would be expected to fail in the first proof test. These include the following: (1) normal shaped flaws, 0.063, 3t/4*; (2) elongated flaws, 0.020, 3t/4*; 0.040, 3t/4; 0.063, t/2*; 0.063, 3t/4. The three sheet thickness/flaw depth combinations with the asterisk (*) are those where the indicated flaw area in the tabulation above are slightly less than the area required for fracture in the air or cryogenic test. In regard to the 0.063, t/2 combination, the indicated flaw area may exceed the cryogenic flaw size for the 0.063 inch sheet. No value was available for comparison since it had been agreed not to test that particular thickness in the fracture program.

Although Tables 33-35 provide the detailed events and Table 36 the surface flaw lengths after the various proof tests, Table 38 has been prepared that specifically lists the comparative information on flaw area before testing, and fracture occurrence (or not) on the first proof cycle for the five groups of specimens. From this table, it is seen that in each case where the flaw area at the start of Proof 1 was greater than the area from the fracture test, that failure actually occurred on the proof test for parent and welded material at air temperature and at cryogenic temperature.

In two cases, flaws less than the area from the fracture test failed in the proof test, often after some time lapse at proof stress. In both cases only welded samples failed. So affected were 3t/4 N flaws and t/2 E flaws in 0.063-inch sheet. This suggests that the initial flaws grew slowly under stress to a critical size causing fracture or that the approximations used in computing flaw area were not entirely valid.**

** Flaw areas were computed assuming an elliptical crack front and that the relations between 2c and a were as shown in Figures 8-11.

TABLE 38. SUMMARY OF INITIAL FLAW SIZES AND FRACTURE BEHAVIOR OF SELECTED SAMPLES GIVEN PROOF CYCLE ONE.

Specimen Number	Flaw	Predicted Area for Fracture at Proof Load, inch ²	Environment Proof 1	Flaw Area at Start of Proof 1, inch ²	Fracture on Proof 1
<u>0.063-inch-thick material</u>					
6-19 (P)	3t/4 N	.005	Air	.00337	No
6-15 (P)	"	.005	"	.00351	No
C11-3 (W)	"	.0035	"	.00326	No
C10-5 (W)	"	.0035	"	.00328	Yes, 1 min. 20 sec.
<u>0.020-inch-thick material</u>					
2-26 (P)	3t/4 E	.005	Air	.00124	No, broke through thickness
2-27 (P)	"	.005	"	.00170	No, broke through thickness
A1-2 (W)	"	.0035	"	.00221	No, broke through thickness
A11-3 (W)	"	.0035	"	.00191	No, broke through thickness
<u>0.040-inch-thick material</u>					
4-72 (P)	3t/4 E	.005	Air	.00649	Yes
4-79 (P)	"	.005	"	.00745	Yes
B18-4 (W)	"	.0035	"	.00686	Yes
B17-1 (W)	"	.0035	"	Void	-
4-15 (P)	"	.0030	Cryogenic	.00680	Yes
4-98 (P)	"	.0030	"	.00726	Yes

TABLE 38. (Continued)

Specimen Number	Flaw	Predicted Area for Fracture at Proof Load, inch ²	Environment Proof 1	Flaw Area at Start of Proof 1, inch ²	Fracture on Proof 1
<u>0.063-inch-thick material</u>					
6-26 (P)	t/2 E	.005	Air	.00310	No
6-42 (P)	"	.005	"	.00301	No
C3-1 (W)	"	.0035	"	.00278	Yes
C4-4 (W)	"	.0035	"	.00302	Yes, 2 min. 15 sec.
6-24 (P)	3t/4 E	.005	Air	.0131	Yes
6-23 (P)	"	.005	"	.0132	Yes
C4-5 (W)	"	.0035	"	.0134	Yes
C4-2 (W)	"	.0035	"	.0131	Yes

In the case of the $3t/4$ E flaws in the 0.020-inch sheet, the flaws grew and broke through the thickness under proof stress without causing fracture. This behavior is characteristic of a more ductile type, thin sheet failure.

In a similar manner, the behavior of the various specimens during the second proof cycle can be assessed. In this case, Table 39 summarizes the flaw area at the start of the second cycle and the occurrence of fracture for those flaws that approached the critical size estimated from the fracture tests. Also shown in the table are the flaw areas after the second proof cycle. Included in this tabulation are all those specimens from Table 38 that did not fail in the first proof cycle.

It is seen from the 0.063, $3t/4$ N group, that neither parent material specimen failed, although flaw growth occurred to some size less than the critical size. The remaining welded specimen did fracture after some time at stress, even though the starting flaw size was slightly less than critical.

The 0.020-inch-thick group with $3t/4$ E flaws that had broken through during the first cycle, showed little growth on the second cycle except for one welded sample. This one broke as a through-the-thickness flaw after 13 minutes, 45 seconds at proof load. Both of these examples suggest the welded material to be somewhat inferior to the parent material and further that the flaws close to the critical flaw size, may grow to critical size during the proof test.

The $t/2$ E flaws in 0.063-inch sheet again initially were less than the critical area. One failed on the proof cycle, 20 seconds, after attaining load, the other showed essentially little flaw growth.

Finally all 0.040-inch sheet specimens with $3t/4$ N flaws had initial flaws at the start of the second proof cycle that were substantially less than critical. Slight flaw growth occurred during the second cycle, but no failures occurred.

TABLE 39. SUMMARY OF FLAW SIZES FOR
SPECIMENS THAT RECEIVED THE SECOND PROOF CYCLE

Specimen Number	Flaw	Predicted Area to Fracture at Proof Load, inch ²	Environment Proof 2	Flaw Area at Start of Proof 2, inch ²	Flaw Area at End of Proof 2, inch ²	Fracture on Proof 2
<u>0.063-inch-thick material</u>						
6-19 (P)	3t/4 N	.005	Air	.00333	.00440	No
6-15 (P)	"	.005	"	.00384	.00420	No
C11-3 (W)	"	.0035	"	.00324	--	Yes, 6 min.
<u>0.020-inch-thick material</u>						
2-26 (P)	3t/4 E	.005	Air	.00196*	.00198*	No
2-27 (P)	"	.005	"	.00272*	.00294*	No
A1-2 (W)	"	.0035	"	.00305*	.00306*	No
A11-3 (W)	"	.0035	"	.00292*	--	Yes, 13 min. 45 sec.
<u>0.063-inch-thick material</u>						
6-26 (P)	t/2 E	.005	Air	.00325	--	Yes, 20 sec.
6-42 (P)	"	.005	"	.00302	.00306	No
<u>0.040-inch-thick material</u>						
4-100 (P)	3t/4 N	.005	Air	.00194	.00194	No
4-115 (P)	"	.005	"	.00219	.00219	No
B22-5 (W)	"	.0035	"	.00201	.00214	No
B8-3 (W)	"	.0035	"	.00218	.00220	No
4-12 (P)	"	.005	Air	.00340	.00348	No
4-90 (P)	"	.005	(Cryo. on Proof 1) Air	.00270	.00274	No
			(Cryo. on Proof 1)			

* Based on through-the-thickness flaws.

Thus from these tests it again appears that when flaws approach the critical size, slow growth may occur at the proof loads and cause failure. However, flaws substantially below the critical size as estimated by the fracture tests, either did not grow under the second air proof cycle or grew only slightly.

Incidentally all other specimens listed in Tables 33, 34, 35, and 36 showed essentially no growth during the proof cycles. This includes all specimens proof tested in inhibited water.

Fatigue Crack Propagation Results. Failure or non-failure of flawed samples during the 400 simulated cycles depends upon (1) the crack growth that occurred during both proof test cycles, (2) the crack growth that occurred during the simulated operating cycles, and (3) the flaw size that would cause failure at a gross stress level of 105 ksi. It is of interest to examine Item (3) first.

From Figures 19 and 20 for parent and weld material respectively the flaw areas of 0.0160 inch² and 0.0080 inch² are obtained by extrapolating the straight lines to 105 ksi. It is recognized that this extrapolation may lead to some error; however, the above values represent approximate critical flaw sizes at 105 ksi gross stress. It is of interest also in this connection to show a listing of flaw areas that can be obtained when a flaw has grown to just intersect the opposite side of the sheet. This computed area would be the flaw area at breakthrough. The following tabulation shows these areas:

Flaw Type	Depth	Flaw area at breakthrough, sq. in.		
		0.020-inch	0.040-inch	0.063-inch
Normal	t/4	0.0008	0.0031	0.0078
	t/2	0.0008	0.0031	0.0078
	3t/4	0.0008	0.0031	0.0078
Elongated	t/4	0.0007	0.0033	0.0066
	t/2	0.0010	0.0044	0.0090
	3t/4	--	--	--

With the exception of the two values followed by P, all values in the tabulation could apply to either welded or parent material. The two values (with P) are for parent material only since all welded samples failed during Proof 1 or 2. No values are listed for 3t/4 E flaws for any thickness since they would be detected in the proof tests. The remaining areas then can be compared with the parent material flaw size (0.0160 inch) and weld material flaw size (0.0080 inch) judged to be critical for fracture at 105 ksi.

This comparison suggests that certain combinations of flaw depth, flaw type, and sheet thickness could result in a flaw becoming a through crack before catastrophic fracture occurred. Whether this actually occurs or not depends upon the flaw size after proof testing and the rate of crack propagation. Examination of Tables 33, 34, and 35 will show how well the experimental results fit within this simple picture. It is seen in these tables that sometimes no growth occurred during the 400 simulated operating cycles, sometimes crack growth occurred but no failure or breakthrough, and sometimes the crack grew and became a through crack but did not cause failure. With the exception of Specimen A1-2 (Table 32) no specimen failed during cycling with the crack becoming a critical length or area. Actually Specimen A1-2 had two flaws in it, lowering its strength considerably.

Thus these experiments suggest that the proof tests essentially screen out intolerably large flaws and that the simulated operating cycles may cause the formation of through cracks by crack propagation. This suggests a leak before break philosophy.

It also suggests that the critical flaw sizes for through cracks be investigated as well as crack propagation of the through cracks.

Table 40 lists pertinent data on the four samples that propagated through the thickness. It is seen that all but one had flaw areas less than the breakthrough areas previously listed. Yet all areas grew by fatigue to a through crack. The fourth specimen area suggests that it already was a through crack. It is suspected that its crack form was not elliptical.

TABLE 40. FLAW AREA OF SPECIMENS THAT
 PROPAGATED THROUGH THE THICKNESS IN 400 CYCLES
 AT A STRESS OF 105 KSI.

Specimen Number	Material	Flaw	Proof Cycle Environment	Test Environment	Initial Flaw Area After Proof Cycle inch ²	Cycles to Breakthrough
2-53	.020" P	3t/4 N	Air	Air	.00061	300
4-12	.040" P	3t/4 N	Cryogenic	Air	.00383	210
4-90	.040" P	3t/4 N	Cryogenic	Air	.00302	390
6-15	.063" P	3t/4 N	Air	Air	.0054*	290

* Note: The measured crack length at the end of proof 2 was 0.1113 inch (Area .0042 inch²), length measured during the initial fatigue cycles was 0.1265 inch. Thus the flaw area was not of critical size during the proof cycles.

Table 41 presents the fatigue-crack propagation data and flaw length after the two proof cycles (initial flaw length) for all tests. The crack propagation data was considered to have a linear relationship between crack length and cycles over the 400 cycle lifetime. This is a gross simplification since it had been shown that a fourth degree curve could be made to fit the data. The simplification did permit one to roughly examine how crack propagation rate was influenced by a number of test variables.

Values of average crack propagation rate and initial flaw size were taken from Table 41 and plotted on Figures 30, 31, and 32 for 0.020-inch-sheet, 0.040-inch sheet and 0.063-inch sheet, respectively. Through the plotted points it was found on each graph that two curves could be drawn. One curve was for normal flaws, the other for elongated flaws. Examination of all 3 figures shows the following:

- (1) For equal initial surface crack length, the rate of crack propagation of normal flaws always was greater than that of elongated flaws.
- (2) There was no real difference in propagation rates for welded and parent material.
- (3) As the initial surface crack length increased, the rate of crack propagation also increased.
- (4) For initial crack sizes that were about equal, the crack propagation rate was greater in the 0.063-inch material than it was in the 0.040-inch material.

Also plotted on Figure 31 are the data for tests in cryogenic fluid, inhibited water, deionized water, salt spray and Aerozine 50. There is quite a scattering of data from these tests. The general result seems to be that the observed behavior is about that in air.

TABLE 41. CRACK GROWTH RATE DATA FROM PROGRAMMED FATIGUE-CRACK PROPAGATION TESTS

Thickness, t, inch	Flaw Type, Normal (N) or Elongated (E)	Material, Parent (P) Welded (W)	Environment*	Initial Flaw Length, 2 c _i , inch	Initial Flaw Depth, a _i , inch	Average Crack Growth Rate, μin/cycle
.020	N	P	A	.014	t/4	3.5
.020	E	P	A	.0125	"	-
.020	N	W	A	.0132	"	2.5
.020	E	W	A	.0110	"	-
.020	N	P	A	.0260	t/2	5.0
.020	E	P	A	.044	"	8.37
.020	N	W	A	.029	"	5.5
.020	E	W	A	.0392	"	5.0
.020	N	P	A	.044	3t/4	19.5
.020	E	P	A	--	"	-
.020	N	W	A	.0408	"	14.0
.020	E	W	A	.1342	"	-
.040	N	P	A	--	t/4	-
.040	E	P	A	.0386	"	3.25
.040	N	W	A	.0282	"	3.25
.040	E	W	A	.0377	"	3.25
.040	N	P	Cryo	--	"	-
.040	E	P	Cryo	.0396	"	2.5
.040	N	P	A	.059	t/2	10.0
.040	E	P	A	.1161	"	22.5
.040	N	W	A	.0562	"	11.5
.040	E	W	A	.1023	"	15.2
.040	N	P	Cryo	.0598	"	16.0
.040	E	P	Cryo	.1039	"	9.0
.040	N	P	I.W.	.0542	"	8.25
.040	N	W	I.W.	.0585	"	12.5
.040	E	P	I.W.	.1151	"	27.0
.040	E	W	I.W.	.1026	"	15.5
.040	N	P	D.W.	.0577	"	9.5
.040	N	W	D.W.	.0569	"	19.5
.040	E	P	D.W.	.1121	"	13.25
.040	E	W	D.W.	.0995	"	20.25

TABLE 41. (Continued)

Thickness, t, inch	Flaw Type, Normal (N) or Elongated (E)	Material, Parent (P) Welded (W)	Environment*	Initial Flaw Length, 2 c _i , inch	Initial Flaw Depth, a _i , inch	Average Crack Growth Rate, μ in/cycle
.040	N	P	S.S.	.0577	t/2	15.5
.040	N	W	S.S.	.0555	"	11.75
.040	E	P	S.S.	.1189	"	13.25
.040	E	W	S.S.	.1010	"	16.25
.040	N	P	Aero	.0530	"	13.0
.040	N	W	Aero	.0545	"	16.75
.040	E	P	Aero	.1095	"	17.25
.040	E	W	Aero	.1007	"	17.5
.040	N	P	A	.0825	3t/4	32.4
.040	E	P	A	--	"	-
.040	N	W	A	.0866	"	50.5
.040	E	W	A	.2110	"	-
.040	N	P	Cryo	.1066	"	94.8
.040	E	P	Cryo	--	"	-
.063	N	P	A	.033	t/4	7.5
.063	E	P	A	.0515	"	7.25
.063	N	W	A	.0323	"	10.0
.063	E	W	A	.0503	"	4.5
.063	N	P	A	.075	t/2	37.5
.063	E	P	A	.1248	"	63.5
.063	N	W	A	.0669	"	22.3
.063	E	W	A	.1220	"	-
.063	N	P	A	.120	3t/4	176.3
.063	E	P	A	--	"	-
.063	N	W	A	--	"	-
.063	E	W	A	--	"	-

* A = air
 Cryo = cryogenic proof
 I.W. = inhibited water
 D.W. = demineralized water
 S.S. = salt-spray air
 Aero = Aerozine 50

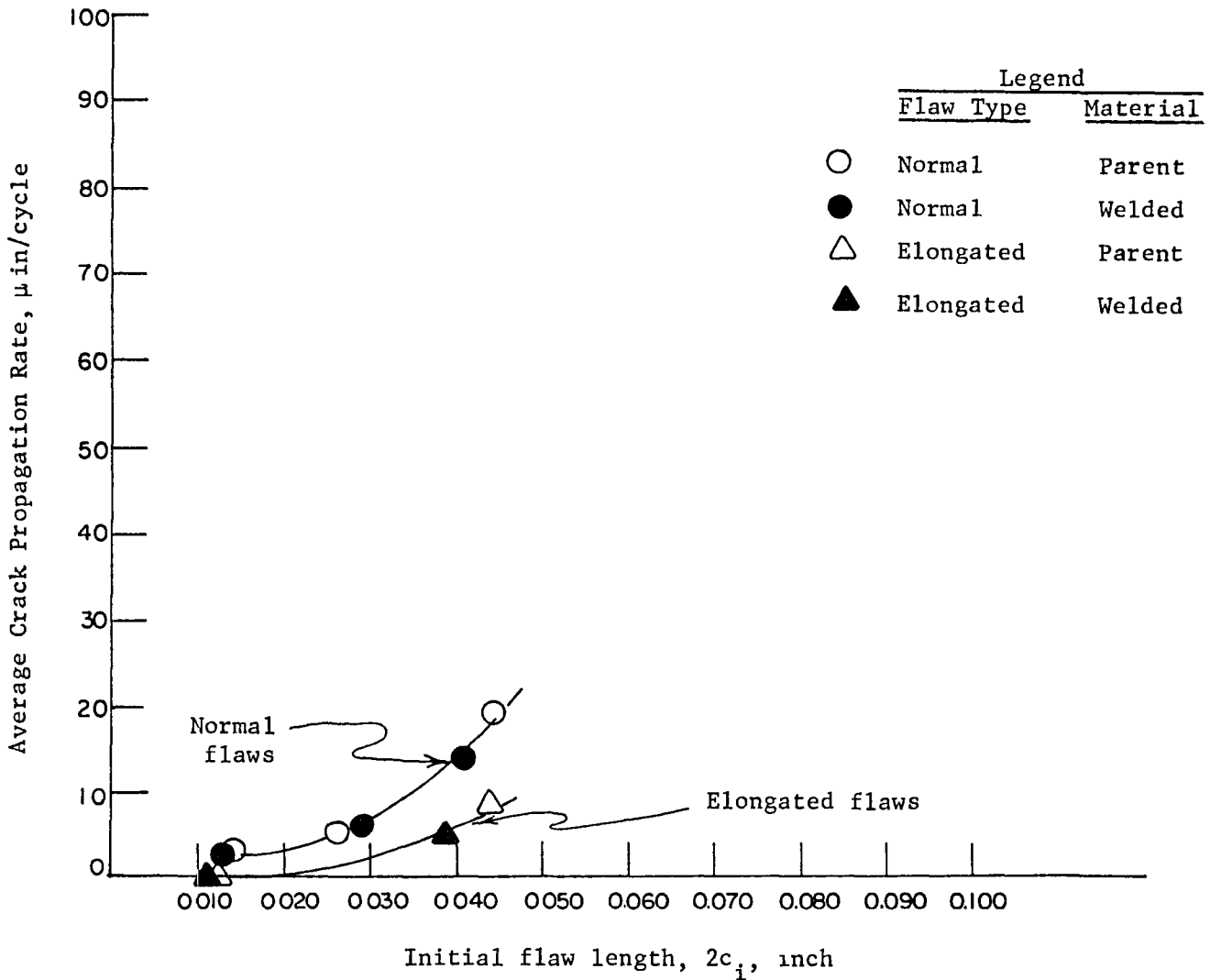


FIGURE 30. AVERAGE CRACK PROPAGATION RATE DATA FOR 0.020-INCH MATERIAL

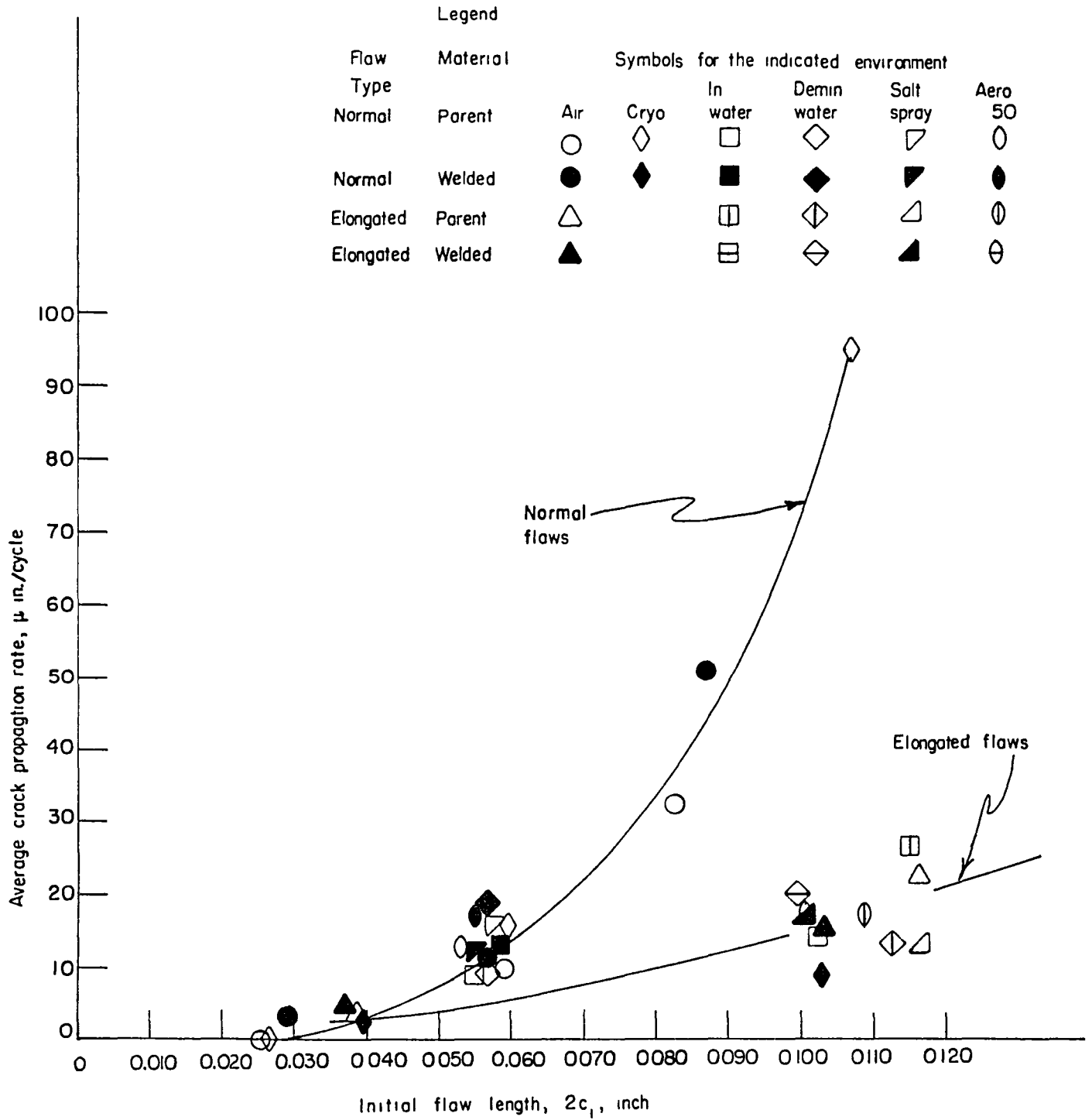


FIGURE 31. AVERAGE CRACK PROPAGATION RATE DATA FOR 0.040 INCH MATERIAL

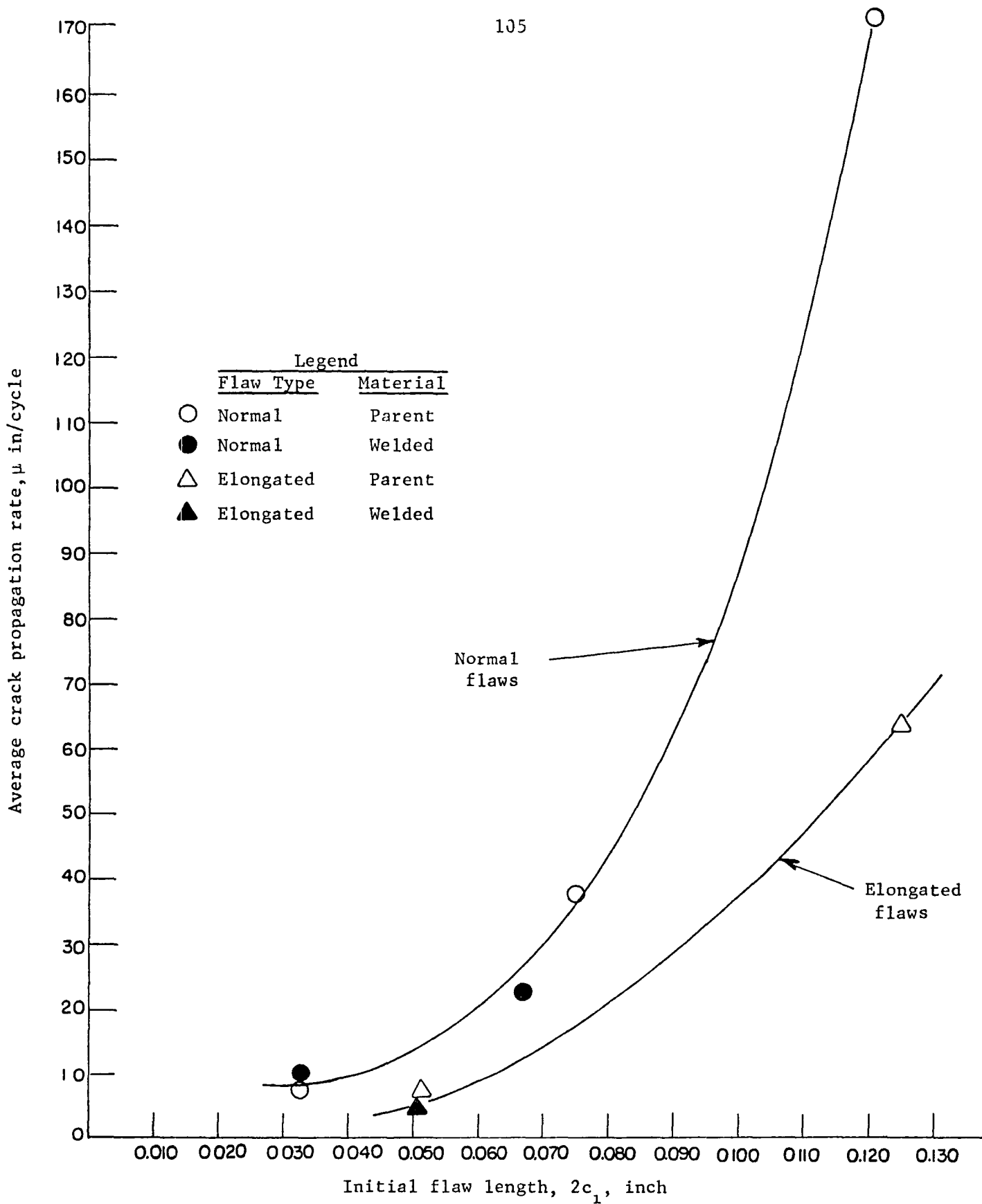


FIGURE 32. AVERAGE CRACK PROPAGATION RATE DATA FOR 0.063-INCH MATERIAL.

Analytical Study of Crack Propagation. In an effort to determine if the crack propagation data could be described in terms of a general crack-propagation equation, a computer program was developed to examine the data in terms of the following equation forms:

$$d\ell/dN = C_1 \ell \quad (\text{Liu})^{(4)}$$

$$d\ell/dN = C_2 \ell^M \quad (\text{Hoeppner, et al})^{(5)}$$

$$d\ell/dN = C_3 K^V \quad (\text{Paris})^{(6)}$$

where

ℓ = surface crack length

$K = 1.1 \sigma \sqrt{\pi a} / \phi$

ϕ = elliptic integral

σ = operating stress

a = crack depth

M, V, C_1, C_2, C_3 = constants

The paired values of surface crack length and number of cycles of propagation at the operating stress, i.e., the number of cycles following the proof cycles, were used as input data for the computer program. This computer program is presented in Appendix A for both the normal and elongated flaws.

Basically, the following computations were conducted by the computer program:

- (1) Paired values of surface crack length and number of cycles of propagation were input.
- (2) The surface crack length versus number of cycles of propagation was plotted for each specimen.
- (3) The log of the surface crack length versus number of cycles of propagation was plotted.
- (4) The input data were used to compute the best fit fourth-order polynomial equation to describe the data.

- (5) The equation determined in Step 2 was differentiated and the crack-propagation rate at 8 referenced surface crack lengths determined. The reference crack lengths corresponded to 50 cycle increments during the test.
- (6) The log of the crack-propagation rate versus log of the surface crack length was plotted.
- (7) The crack depth was computed for the specific type of flaw at the 8 values of the referenced surface crack length.
- (8) The value of K_{\max} , the maximum stress-intensity factor, was computed for each of the reference crack lengths.
- (9) $\log K_{\max}$ versus log of the crack-propagation rate was plotted.
- (10) The values of reference number of cycles, referenced surface crack length, K_{\max} , and the crack-propagation rate were output in table form for all specimens. In addition, the value of crack depth at the referenced surface crack length was output for the elongated flaws only.

Typical computer plots are shown in Figures 33 and 34 of some of the results. The tabulated input and output data for all specimens which exhibited flaw growth during the fatigue cycling are given in Appendix B.

Examination of the resulting curves revealed the following:

- (1) The fourth-order polynomial equation provided a very good fit for the experimental data points. (See Figure 33)
- (2) The log surface crack length versus cycles of propagation was not a linear plot for any of the data. Therefore, the equation of the form, $d\ell/dN = C\ell$, is not applicable.
- (3) The plots of the log surface crack-propagation rate versus log surface crack length also were not linear for any of the data. This indicates that the equation of the form $d\ell/dN = C\ell^M$ is not applicable.

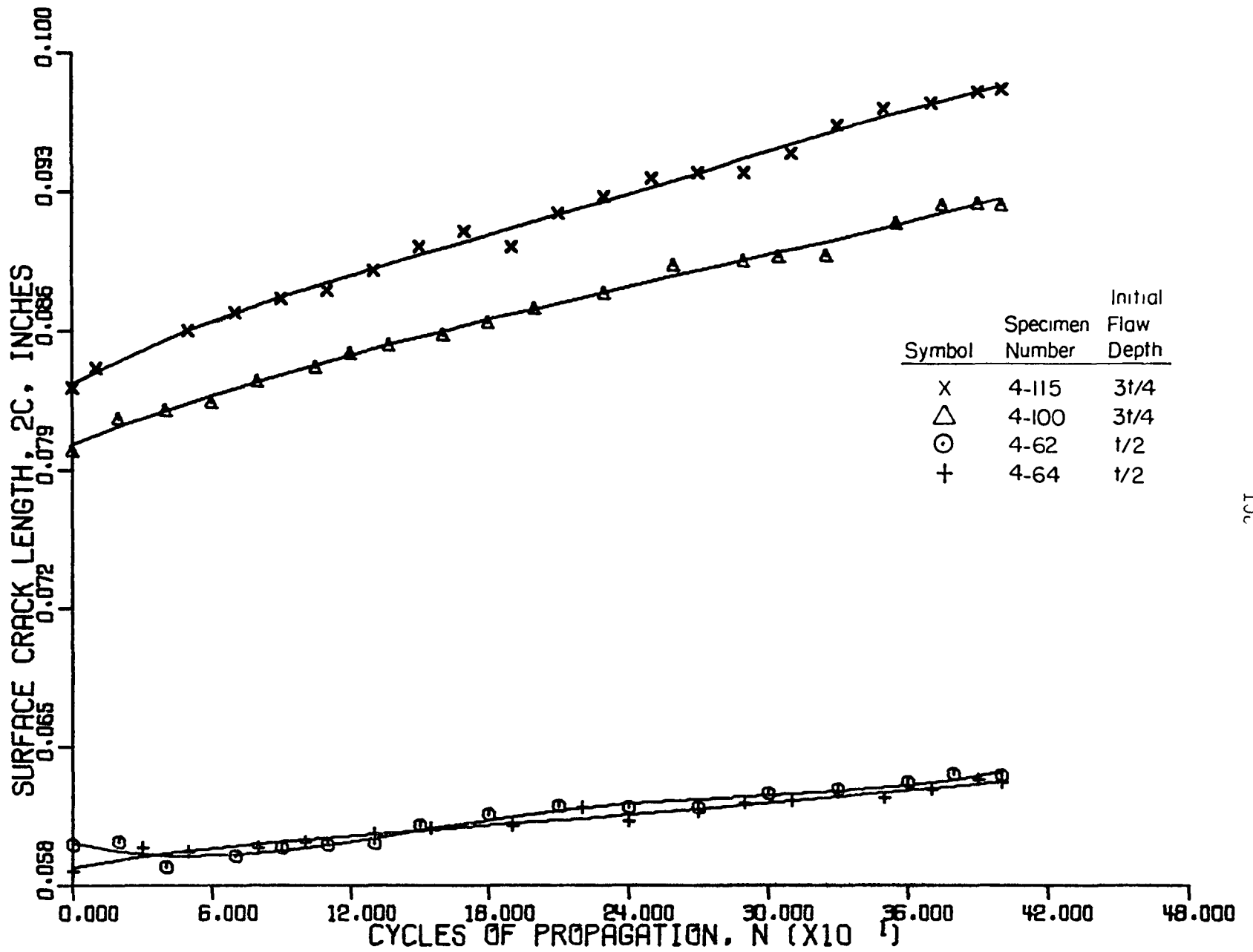


FIGURE 33. TYPICAL COMPUTER PLOT OF SURFACE CRACK LENGTH VERSUS CYCLES OF PROPAGATION. (40 MIL NORMAL FLAW, AIR TEST).

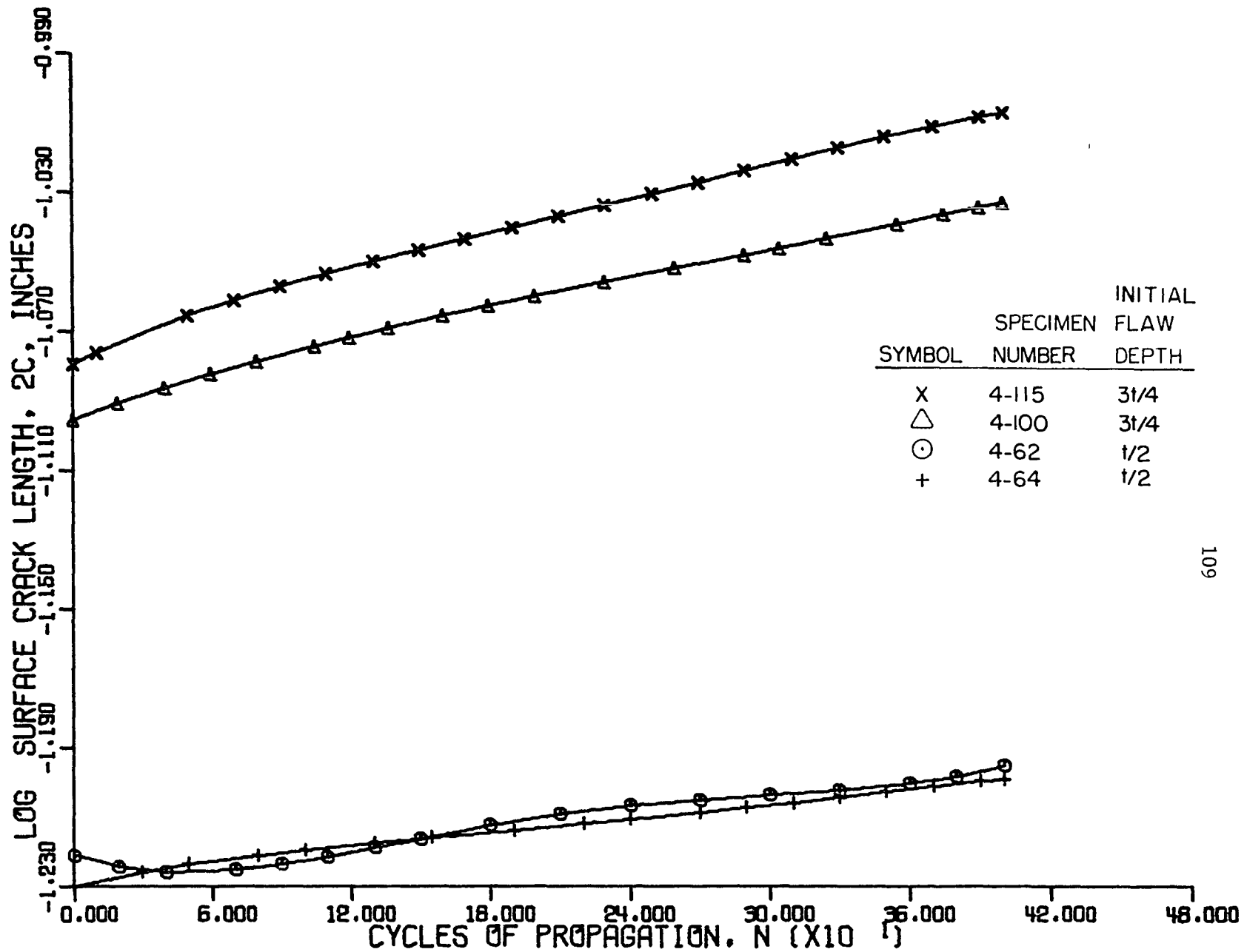


FIGURE 34. TYPICAL COMPUTER PLOT OF LOG SURFACE CRACK LENGTH VERSUS CYCLES OF PROPAGATION. (40 MIL NORMAL FLAW, AIR TEST).

- (4) The log stress-intensity factor versus log surface crack propagation rate were not linear plots. This indicates that an equation of the form $d\ell/dN = CK^V$ is not applicable.

Since only the fourth-order polynomial equation provided a good fit to the data, it was decided to treat the crack propagation curves as linear functions as described in the previous section.

Growth in Flaw Depth Diagrams. To provide some better idea of the flaw severity after proof testing that can lead to failure by breakthrough through cycling, Figures 35-37 have been prepared. Plotted on each of these figures (one for each sheet thickness) are the change in flaw depth from 400 cycles of simulated operating stress as a function of the flaw depth after proof testing--both coordinates expressed as a percentage of sheet thickness.

The points on the graph are taken from the data listed in Table 36. The slanted line at the right is the boundary representing when the initial flaw has changed in depth to cause breakthrough. The dashed curves on each figure represent the approximate scatter of the data.

The interpretation of these figures is as follows. If a given flaw after proof testing has a depth equal to 60 percent of sheet thickness (see Figure 36 for the 0.040 inch sheet) it will be expected to grow during the 400 simulated operating cycles by about 5 to 10 percent t (the intersection of a vertical line with the two dashed curves) to a depth of 65 to 70 percent of thickness. With such a curve then it should be possible to estimate the size flaw depth that will cause breakthrough during the simulated cycling. These approximate minimum flaw depths when breakthrough may occur are indicated on each graph by the dotted vertical line on the right of the graph. These values are as follows:

0.020-inch sheet	--	80 percent
0.040-inch sheet	--	75 percent
0.063-inch sheet	--	65 percent

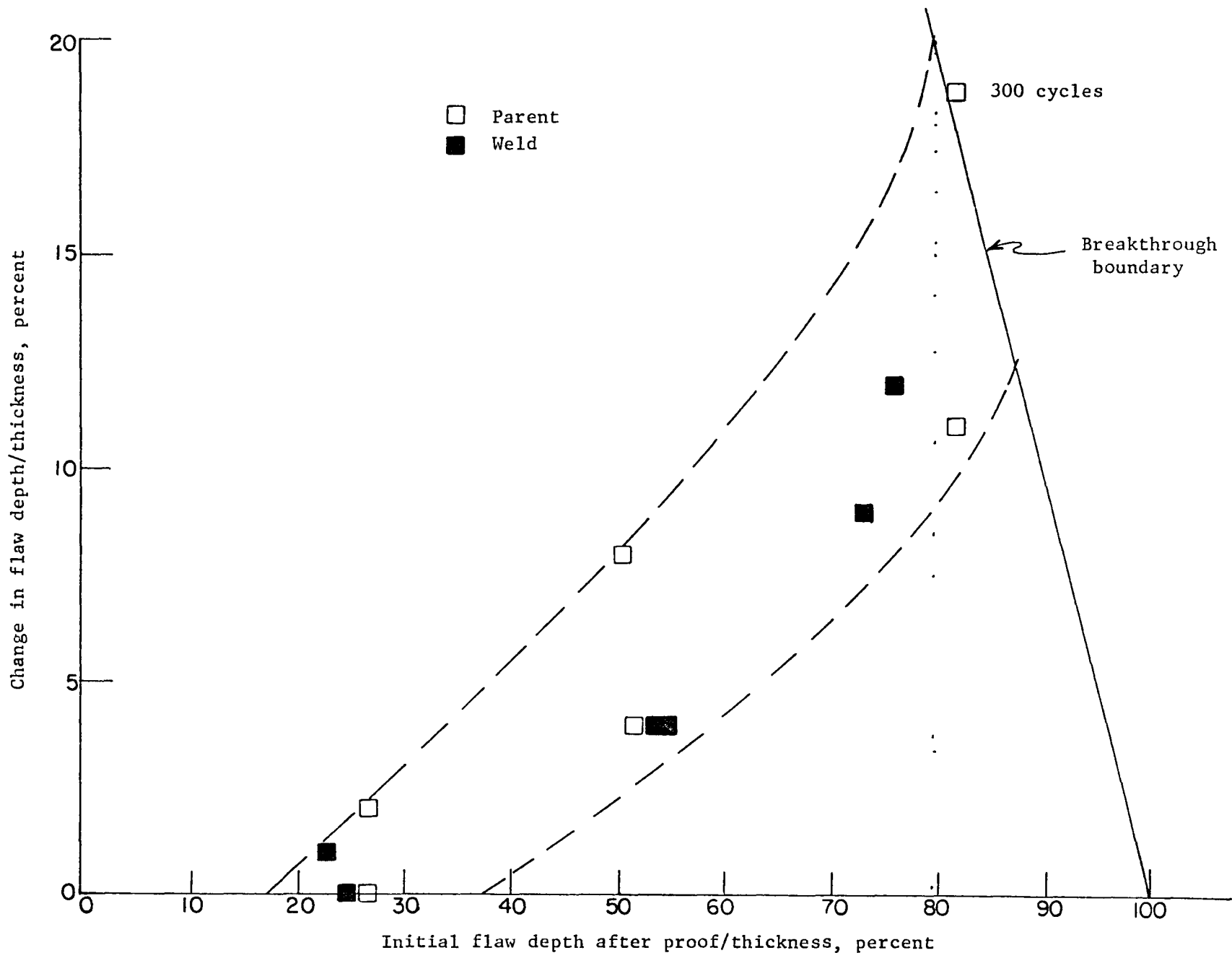


FIGURE 35. FLAW DEPTH GROWTH FOR NORMAL FLAWS IN 20-MIL MATERIAL

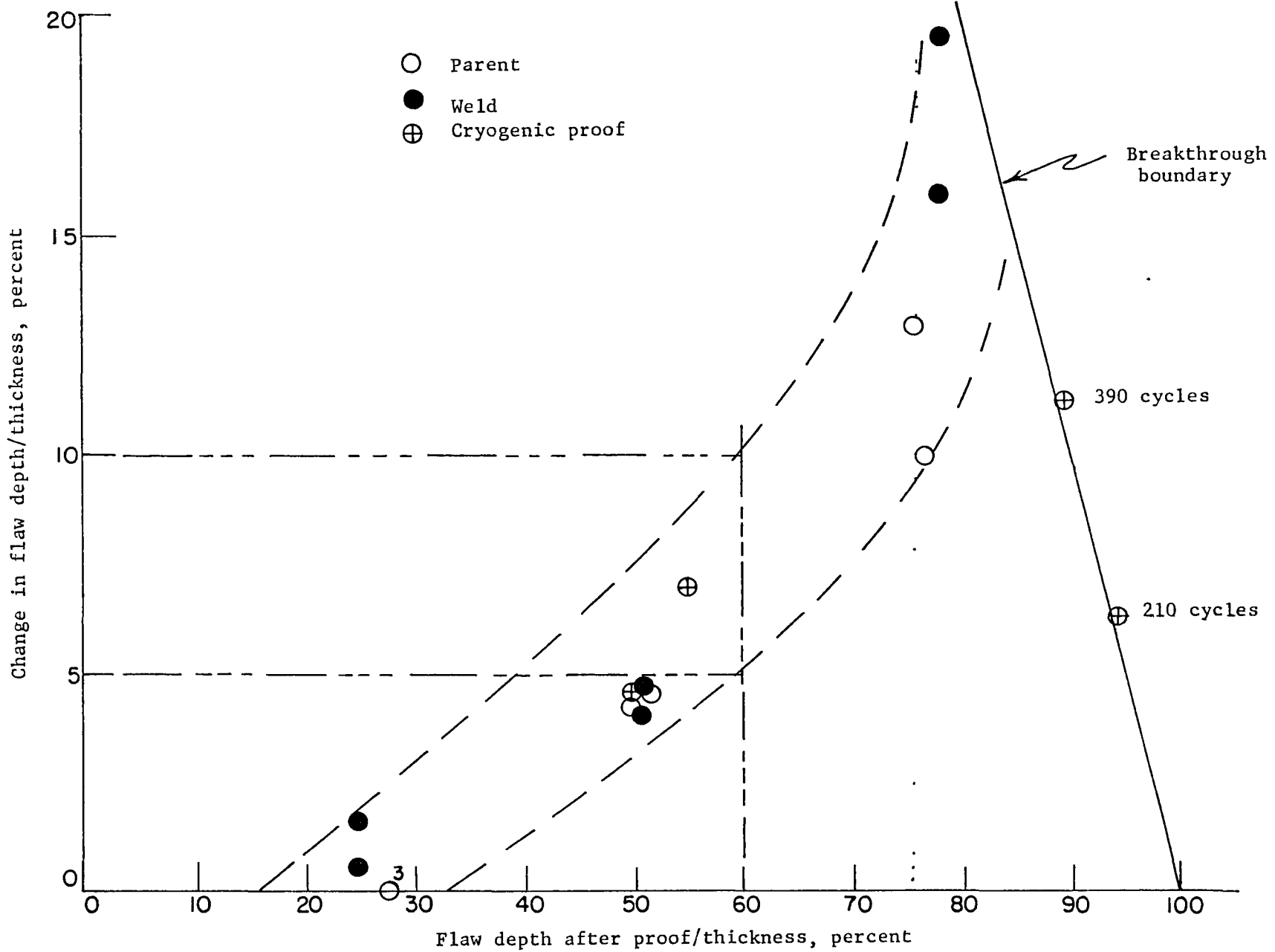


FIGURE 36. FLAW DEPTH GROWTH FOR NORMAL FLAWS IN 40-MIL MATERIAL

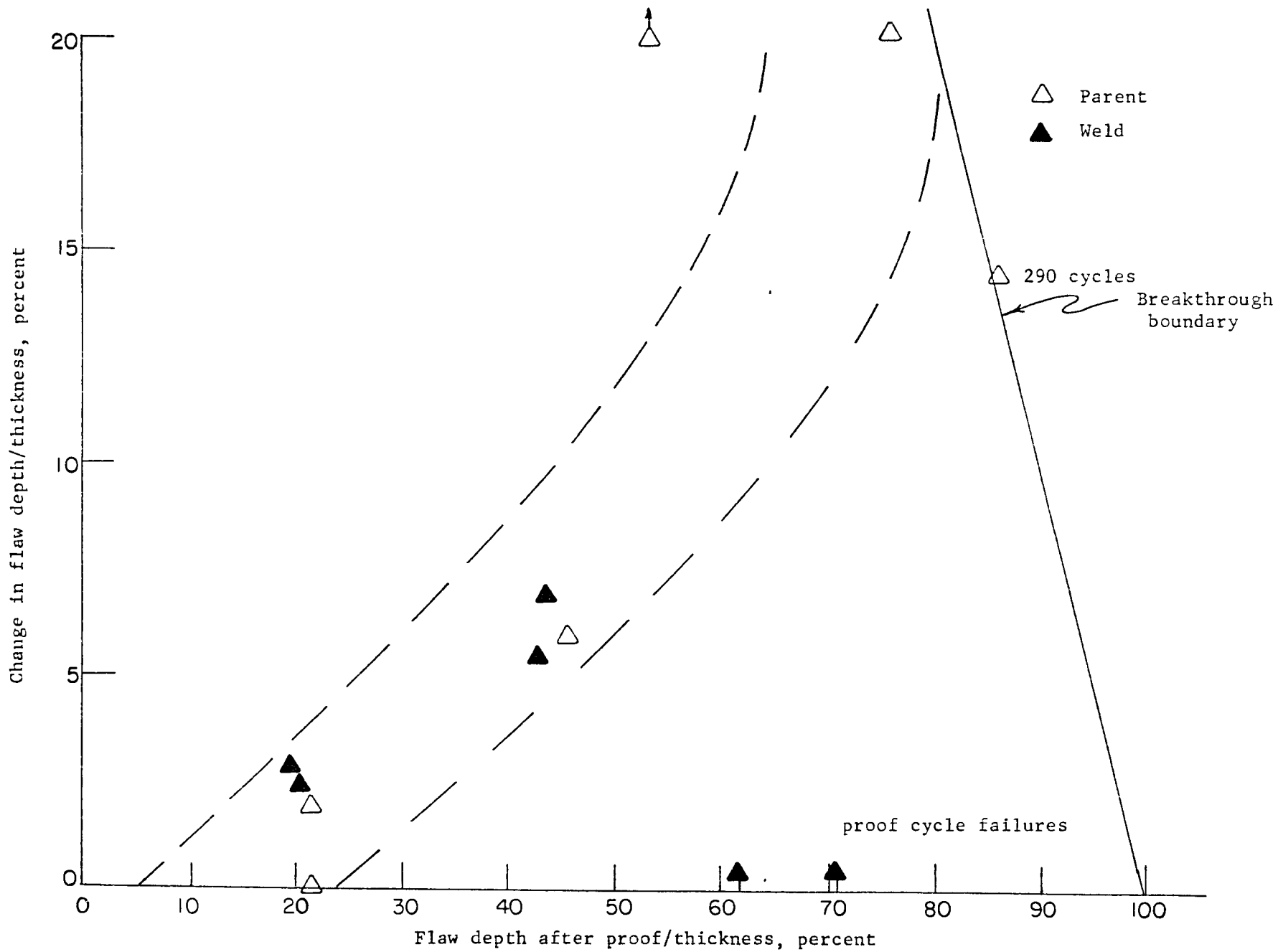


FIGURE 37. FLAW DEPTH GROWTH FOR NORMAL FLAWS IN 63-MIL MATERIAL.

The amount of flaw growth that might be expected for elongated flaws is presented in Figure 38. As for the normal flaw data, the flaw depth and change in flaw depth were divided by the specimen thickness to normalize the data. Also a box at the lower right identifies the flaw depths for which proof test failures are expected. It will be noted on Figure 38 that data for all three thicknesses are presented and that no curves are drawn through the data. This was done because the $2c/a$ ratio for the elongated flaws varies from 3 to 9 for the flaw depth variations. This means that the $t/4$, $t/2$, and $3t/4$ elongated flaws all have a slightly different shape, thus preventing the combination of the points to form a meaningful curve. For this reason only a qualitative discussion of Figure 38 is permitted.

The effect of the weld does not seem to be a detriment to the crack growth characteristics as shown before. The behavior of the $t/2$ elongated flaw (50 percent) in the 63-mil material is quite interesting in that one flaw failed at the proof load while the second (very slightly smaller) survived the proof tests and 400 cycles of propagation without fracture or breakthrough. This might be viewed as a very tentative indication that elongated flaws ($2c/a = 5$) of a size necessary to grow through the thickness in 400 cycles may not survive the proof cycles. However, before any definite statement can be made, more elongated flaws must be examined in this size range for each thickness. In addition, more work is necessary to adequately evaluate the effect of the $2c/a$ ratio on flaw behavior.

Fracture Studies. On the basis of early fractographic studies of the fatigue-crack propagation specimens, it was observed that crack propagation was reasonably uniform around the periphery of the crack. This is illustrated in Figure 39. On this basis area computations were made assuming a uniformly propagating elliptical crack front. The fractographically measured change in surface crack length versus the change in crack depth is shown in Figure 40 for both the normal and the elongated flaws.

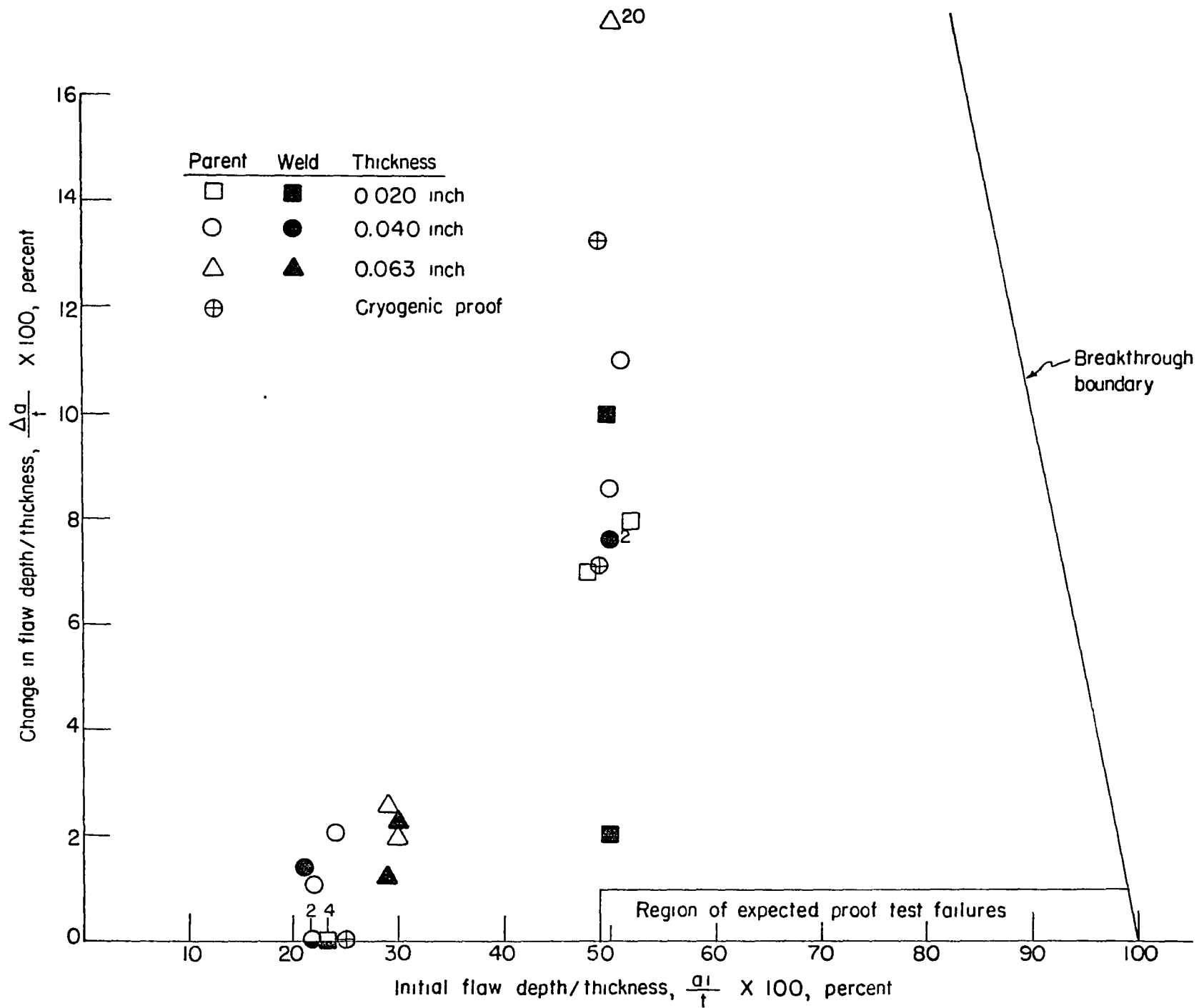
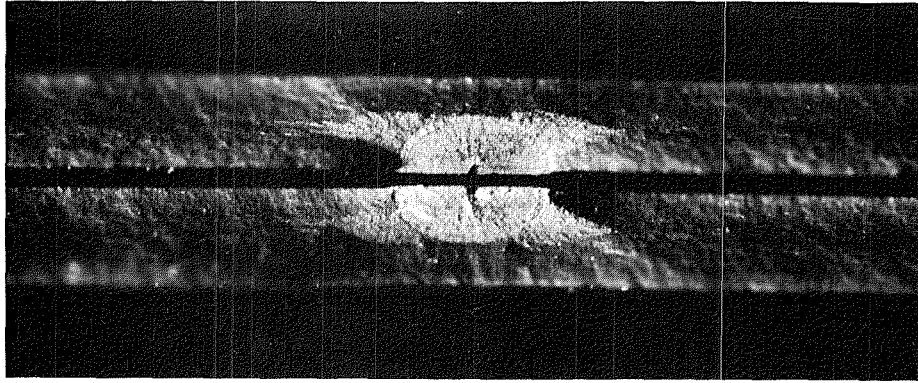


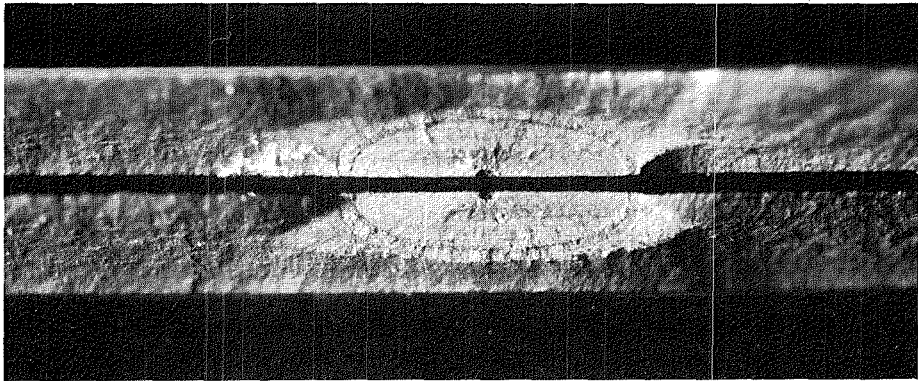
FIGURE 38 FLAW DEPTH GROWTH FOR ELONGATED FLAWS



12X

2C100

(a) Normal flaw



12X

2C098

(b) Elongated flaw

FIGURE 39. TYPICAL FLAW GROWTH MARKINGS FOR NORMAL AND ELONGATED FLAWS.

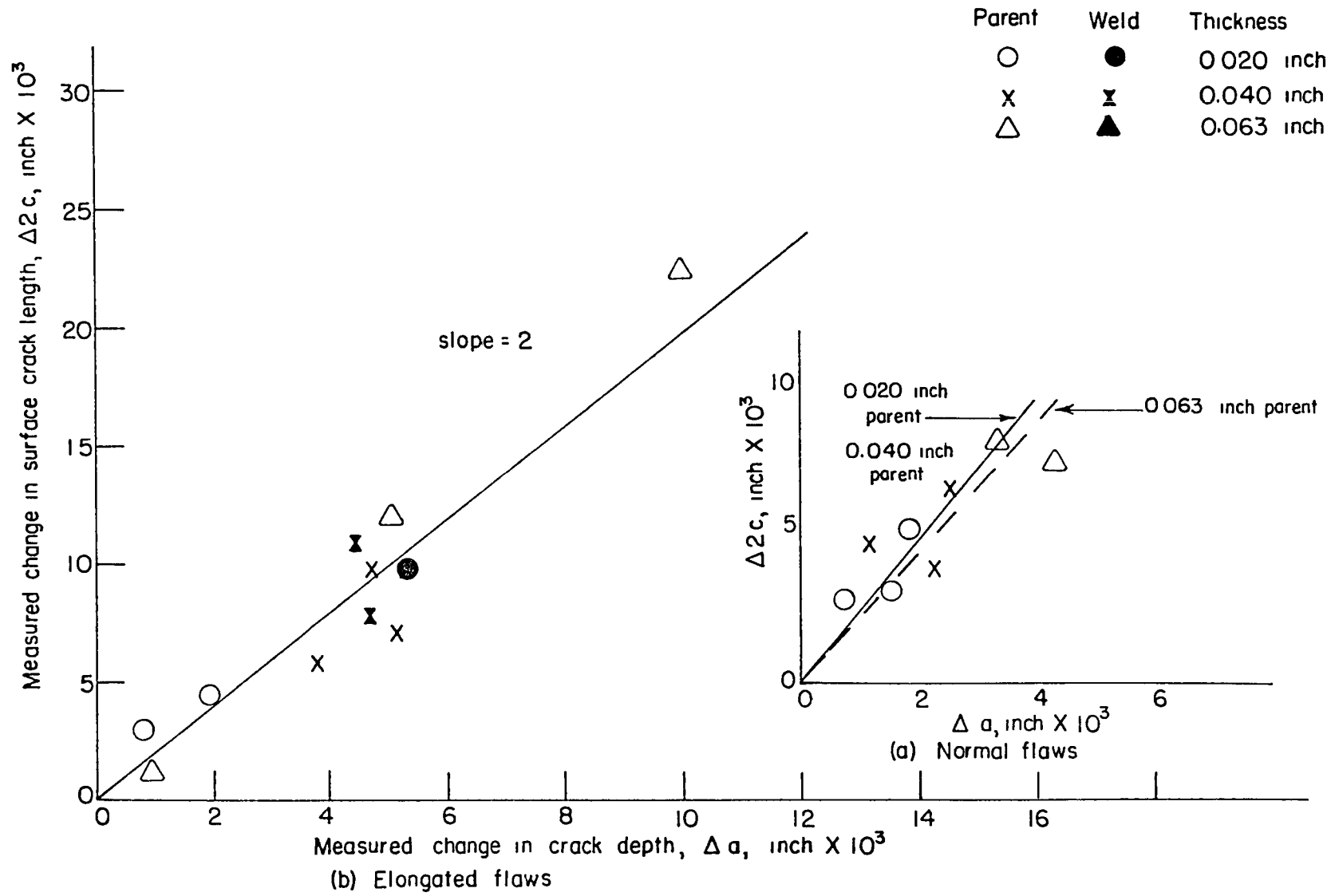


FIGURE 40. MEASURED FLAW GROWTH PARAMETERS DURING PROGRAMMED FATIGUE-CRACK PROPAGATION TESTS

Figure 40 shows the measured values and link denoting the $2c/a$ ratio found during the initial cracking of the normal flaws. These lines were shown in Figures 8 to 11. Examination of Figure 40 indicates that there is no appreciable change in the $2c/a$ ratio for the normal flaws during fatigue crack growth. The relationships between $\Delta 2c$ and Δa used to compute crack growth through the thickness for the fatigue specimens with normal flaws is tabulated below:

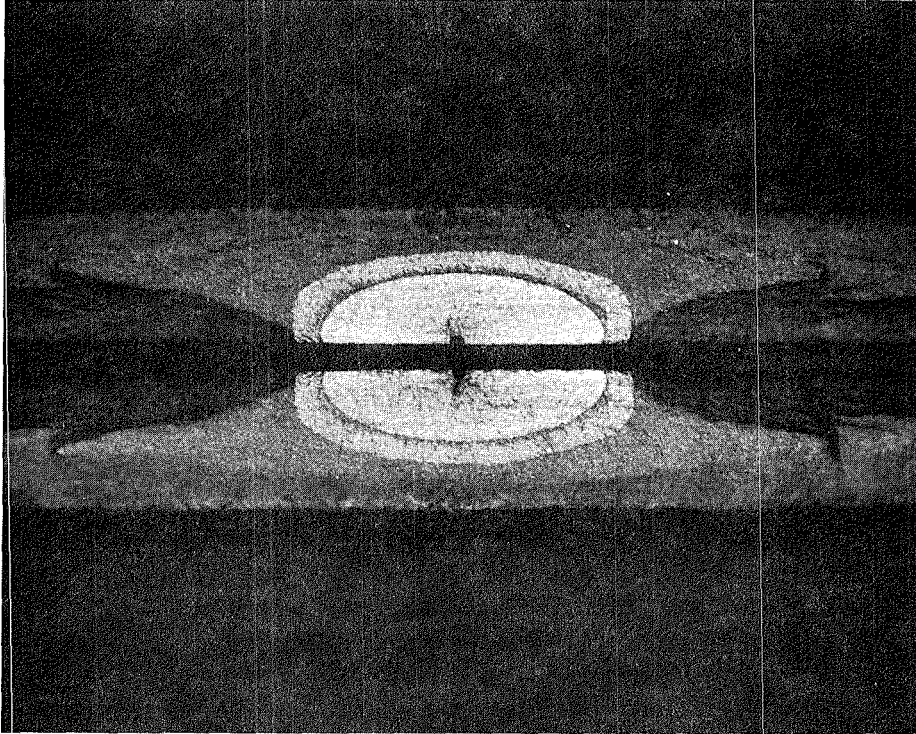
Material	$\frac{\Delta 2c}{\Delta a}$
0.020 Parent	2.57
0.040 Parent	2.57
0.063 Parent	2.33
0.020 Weld	2.67
0.040 Weld	2.67
0.063 Weld	2.47

The fractographically increased change in surface crack length is plotted as the measured change in crack depth in Figure 40 for the elongated flaws.

From Figure 40 it was found that the line $\frac{2c}{\Delta a} = 2$ shown provides a good fit of the data for all three thicknesses, parent and weld material. The relationship $\Delta a = \frac{\Delta 2c}{2}$ was used to compute the crack growth through the thickness for all fatigue specimens containing elongated flaws.

The assumption that the cracks maintained an elliptical crack front during the proof cycles and the following 400 cycles of fatigue is valid for the majority of flaws studied. The few exceptions will now be discussed.

The $t/2$ E flaw in the 0.063 inch thick parent material tested in air was found to have a rather "squared off" crack front at the end of the fatigue crack propagation test. This is shown in Figure 41. Examination of Figure 41 reveals several distinct regions of crack growth. The elliptical light colored region is the initial fatigue crack area. The dark bond around the initial crack area represents the crack growth which occurred during the proof cycles. The outer light



12X

1C969

FIGURE 41. VIEW OF A 63-MIL $t/2$ ELONGATED FLAW WHICH EXHIBITED A TENDENCY TO "SQUARE OFF".

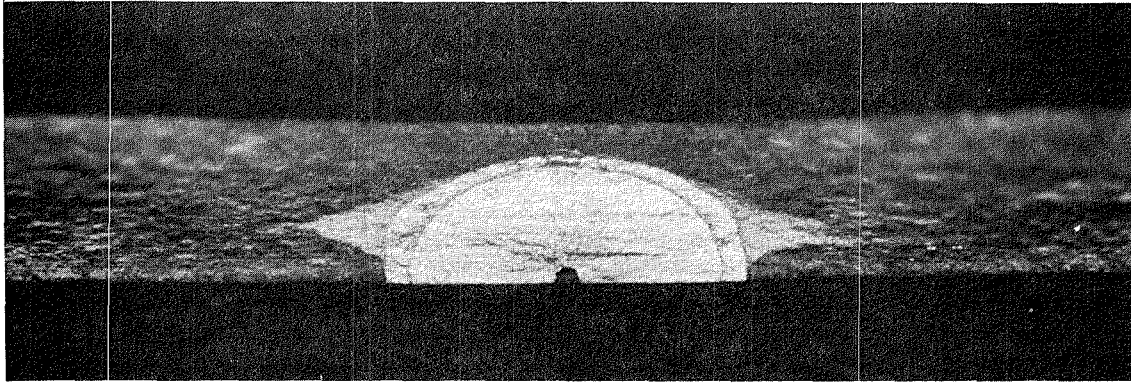
colored bond represents the growth of the crack during 400 cycles of fatigue crack propagation and the large dark region is that of final fracture.

A second deviation from the elliptical flaw shape was that of the 3t/4 N flaw in the 0.040 inch thick parent material tested in air. This is shown in Figure 42a. Again the crack front tended to "square off" slightly, thus resulting in a flaw area slightly larger than the calculated value. The same crack growth regions discussed in the previous paragraph were observed in Figure 42a.

The 3t/4 N flaw in the 0.040 inch parent material given a cryogenic proof cycle is shown in Figure 42b. This flaw shows a drastically different growth pattern than was observed for the same flaw size proof cycled in air. The difference in appearance between the air proof specimen shown in Figure 42a and the cryogenic proof specimen shown in Figure 42b results from the large amount of flaw growth that occurred during the cryogenic proof cycle but which did not occur during the air proof cycle. The regions of crack growth are shown schematically in Figure 43.

The path of the crack growth during the cryogenic proof cycle is quite interesting in that the flaw was found to tunnel, i.e., to grow parallel to the width of the sheet rather than to grow through the thickness. This pattern of growth results in a sizable increase in the crack area without fracture or breakthrough occurring. The enlarged flaw can then propagate through the thickness during cycling at the operating stress. Breakthrough during cycling did not occur for the air proofed specimens. Thus it appears that the cryogenic proof cycle produced a flaw that was much more likely to break through the thickness during fatigue cycling.

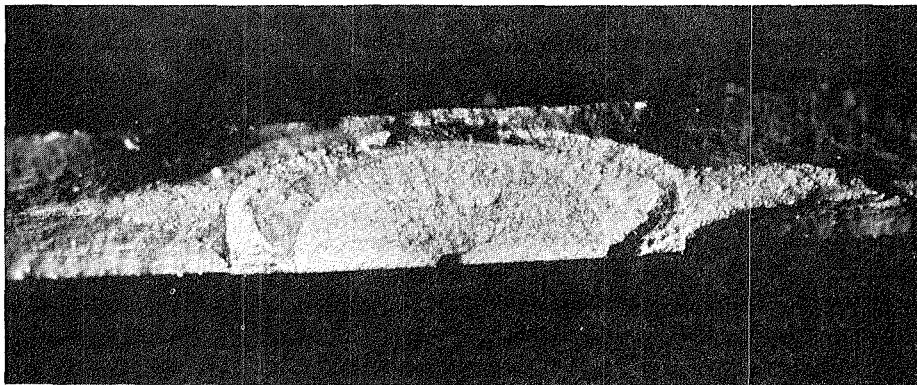
The final case of deviation from the elliptical flaw shape was that of the 3t/4 N flaw in the 0.063 inch thick parent material tested in air. The similarity of the 63-mil air proof specimen (3t/4 N flaw) shown in Figure 44 and



20X

20965

(a) Air proof

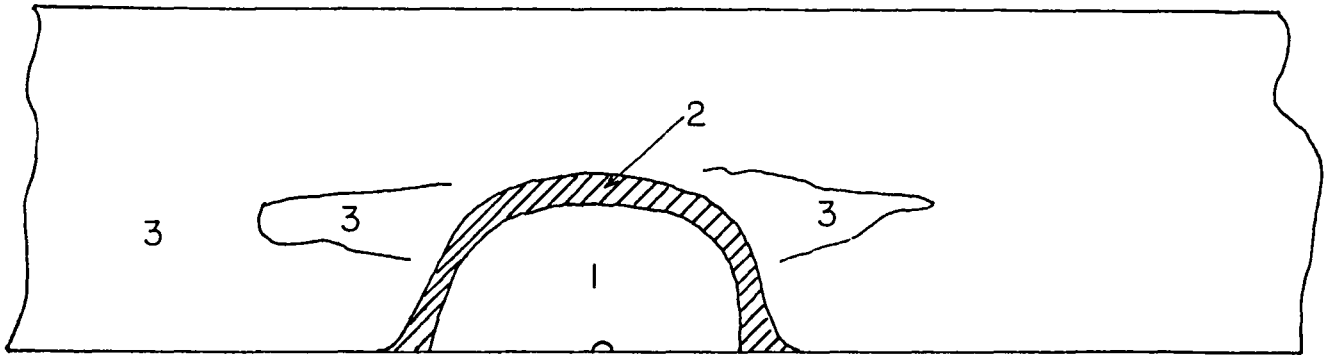


20X

26767

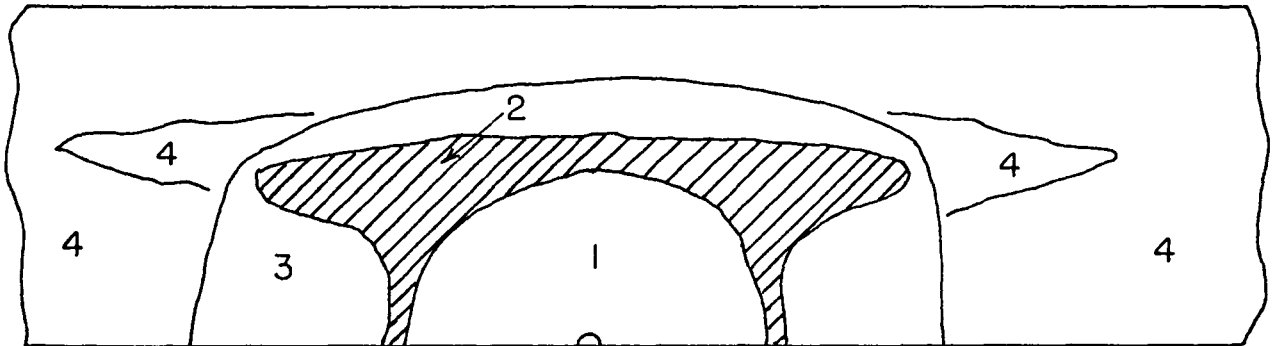
(b) Cryo proof

FIGURE 42. FLAW APPEARANCE OF 40-MIL SPECIMENS, 3t/4 NORMAL FLAWS, WHICH WERE GIVEN AN AIR PROOF TEST OR A CRYOGENIC PROOF TEST.



A. Normal programmed-fatigue-crack propagation specimen fracture surface after testing.

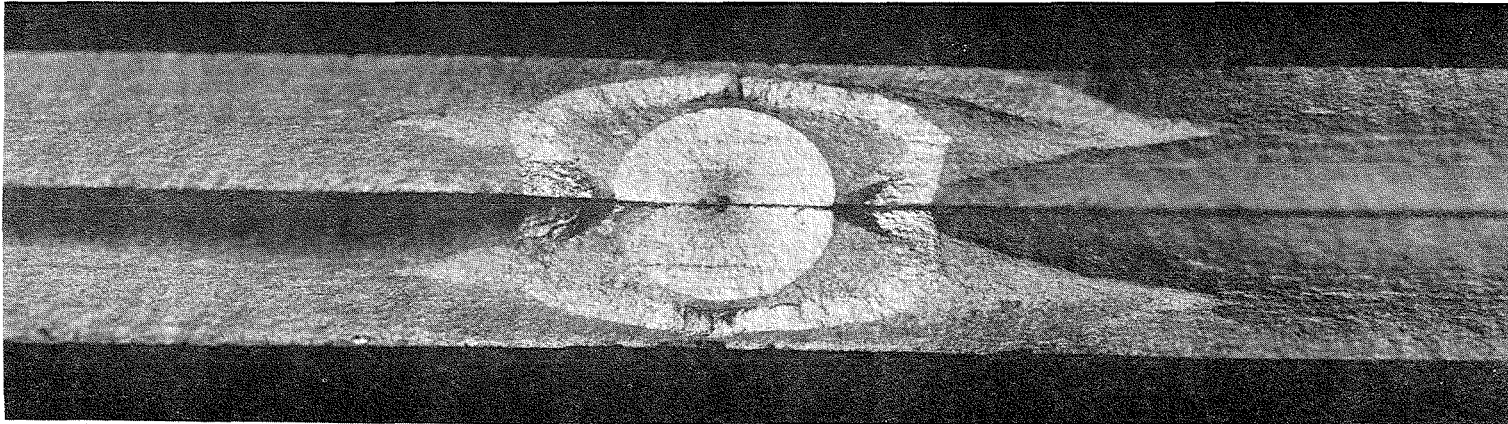
- Region 1 - Initial fatigue crack
- Region 2 - Growth during fatigue loading
- Region 3 - Final fracture at room temperature (after test)



B. Cryogenic-proof-test specimen fracture surface after testing.

- Region 1 - Initial fatigue crack
- Region 2 - Growth during cryogenic proof test
- Region 3 - Growth during fatigue loading
- Region 4 - Final fracture at room temperature (after test)

FIGURE 43. FRACTURE SURFACE APPEARANCE OF PROGRAMMED-FATIGUE-CRACK PROPAGATION SPECIMENS AFTER TESTING, 40 MIL PARENT, 3t/4 N FLAW



12X

2C858

FIGURE 44. $3t/4$ NORMAL FLAW, 60-MIL, AIR TEST SPECIMEN SHOWING FLAW GROWTH DURING THE PROOF CYCLE.

the 40-mil cryogenic proof specimen (3t/4 N flaw) shown in Figure 42b is apparent. Here again the 3t/4 N flaw in the 63-mil material exhibited a tremendous amount of growth during the proof cycles. The flaw again tunneled and greatly increased the flaw area without breaking through or fracturing. The resulting flaw did in one case propagate through the thickness during the subsequent cycling at the operating stress.

The similarity between the 63-mil air proof and 40-mil cryogenic proof specimen with 3t/4 N flaws suggests as, stated previously, that some further study of the proof load level and proof level hold time on the growth characteristics of subcritical flaws may be required.

Data Interpretation. The results of the programmed fatigue tests have yielded considerable information that is useful in considering the LEM tankage problems. The following observations can be stated:

- (1) In regard to proof tests, when flaws are greater than the critical size based upon the fracture tests, both cryogenic and air proof tests result in failure of the laboratory specimens.
- (2) When the flaws are close to the critical size, sometimes failure in proof testing occurs.
- (3) Of the two types of flaws, the elongated flaw appears more vulnerable in the proof test, largely because of the increased area of these flaws.
- (4) From the standpoint of fatigue damage, it would appear that flaws with a small $\frac{2c}{a}$ ratio (≈ 2.5) are the more dangerous type of flaw examined. Such flaws will usually survive the proof cycles and may propagate through the thickness of the sheet in less than 400 cycles at the operating stress. In these

tests it appears that any flaw ($\frac{2c}{a} = 2.5$) with a flaw depth of approximately $0.8 t$ represents a likely source of tank leakage and should be inspected out.

- (5) The 3-minute cryogenic proof test produced a large increase in size of the $3t/4$ normal flaws in the 40-mil material but did not result in fracture. This size increase resulted in propagation of the flaw through the specimen thickness during the 400 cycles of operating stress. The growth of the flaw during the cryogenic proof test indicates that further work is needed to evaluate the effect of holdtime and proof stress during the cryogenic proof cycle on fracture strength and flaw growth characteristics.
- (6) The $3t/4$ normal flaw in the 63-mil material during the air proof tests exhibited the same type of flaw growth as was observed for the 40-mil cryogenic proof specimen with the $3t/4$ normal flaw. Again this increase in flaw size occurring during the proof test did not result in fracture during the proof test, but did result in flaw breakthrough during the 400 cycles of operating stress. Thus it appears that the air proof tests may have the same effect on the 63-mil and possible thicker material that the cryogenic proof test used in this study had on the 40-mil material. For this reason further investigation into the effect of air proof stress and holdtime on the flaw growth characteristics of 63-mil and thicker gage material is recommended.
- (7) Under fatigue at a maximum operating stress of 105 ksi, breakthrough always occurred before the critical flaw size necessary for fracture at the operating stress was reached. This

indicates that leakage may occur before fracture if the tanks have survived a proof cycle.

- (8) The presence of environments such as inhibited water, demineralized water, salt-spray air, and Aerozine 50 did not result in a measurable change in the amount of flaw growth observed in the 400 cycles at the operating stress.
- (9) A given size flaw (i.e., $t/2$ normal, for example) will propagate faster as the thickness increases. However, the ratio of flaw depth growth to thickness is approximately constant for the 3 thicknesses studied. The 63-mil parent and weld material ratio do tend to be slightly higher than for the 20- or 40-mil materials.
- (10) No apparent difference in the flaw growth characteristics was observed between the parent and the weld material for any of the three thicknesses examined. Some difference was noted, however, in the flaw size which was eliminated during the proof test for the 63-mil material, the smaller size flaw being eliminated in the weld material.

Sustained Load Behavior

Because of the observation made by Naval Research Laboratories personnel a few years ago, a flurry of activity resulted regarding the possible worthiness of titanium alloys. This observation concerned the ability of certain titanium alloys to sustain a load if a specimen contained a fatigue crack and was tested in the presence of certain environments other than air. Very often the degradation of the load-bearing ability of the particular alloy was a function of time under load. Plots of gross stress (or stress intensity factor) versus time at

load have been developed for a number of environmental exposures and various alloys. These curves allow an assessment of the ability of the alloy to sustain a load in the presence of a given environment

The various tankage employed in the LM vehicle will see conditions under which it will sustain a load for long periods of time. Consequently, it was necessary to evaluate the load bearing capability of the Ti-6Al-4V alloy. The results of these studies are reported in this section. A brief description of apparatus and procedure is followed by the presentation of results and interpretation.

Apparatus. The experimental apparatus used consisted of several creep machines which were modified to accommodate the large specimen employed throughout the program.

Experimental Procedures. For each specimen, the stress employed was 105 ksi. Thus, it was not intended that a plot of gross stress versus time be obtained but rather that the specimens be loaded to 105 ksi and held for 100 hours. If no failure occurred, the specimen was removed from the machine.

The procedure consisted of loading and aligning the specimen in a machine, applying the load to yield a stress of 105 ksi, and taking a measurement of flaw length immediately after the load was applied. Crack length measurements were obtained at periodic intervals throughout a test to ascertain if flaw growth was occurring.

Experimental Results. The test results show that the t/2 flaws in the 0.040-inch thick parent and welded material did not exhibit flaw growth or failure for 100 hours at a stress of 105 ksi for the air, inhibited water, demineralized water, and Aerozine 50 tests. The specimens tested in salt-spray air did exhibit slight flaw growth, generally less than 0.002 inch. This is illustrated in Table 42, where flaw length at time under load is listed for the specimens tested in salt-spray air.

TABLE 42. SUSTAINED LOAD RESULTS FOR THE
SALT-SPRAY AIR TESTS

Specimen No. 4-34		Specimen No. 4-67		Specimen No. B 3-3		Specimen No. B 14-2	
Normal t/7-Parent		Normal t/2-Parent		Normal t/2-Welded		Normal t/2-Welded	
Time at	Length	Time at	Length	Time at	Length of	Time at	Length
Load,	of	Load	of	Load,	Crack,	Load,	of
hrs.	Crack,	hrs.	Crack,	hrs	inch	hrs.	Crack,
	inch		inch				inch
0	0.0542	0	0.0555	0	0.0585	0	0.0542
4.5	0.0545	5.1	0.0554	4.3	0.0587	4.2	0.0548
6.8	0.0542	21.9	0.0560	6.9	0.0589	6.7	0.0546
23.9	0.0550	26.5	0.0561	24.1	0.0585	24.0	0.0549
28.2	0.0551	29.1	0.0575	28.2	0.0586	28.1	0.0547
31.1	0.0550	46.1	0.0579	30.8	0.0585	30.9	0.0542
47.6	0.0564	50.5	0.0575	47.7	0.0585	47.5	0.0542
51.8	0.0564	70.3	0.0572	52.0	0.0585	51.9	0.0542
54.8	0.0562	74.3	0.0579	54.8	0.0584	54.6	0.0548
75.0	0.0564	94.0	0.0579	73.6	0.0587	73.4	0.0545
100.0	0.0566	100.0	0.0576	97.7	0.0586	47.9	0.0542
119.6	0.0566	--	--	120.0	0.0591	120.0	0.0549

TABLE 42. Cont.

Specimen No. 4-59		Specimen No 4-58	
<u>Elongated-t/2 Parent</u>		<u>Elongated t/2 Parent</u>	
Time at	Length of	Time at	Length of
load,	Crack,	load,	Crack,
hrs.	inch	hrs.	inch
0	0.0987	0	0.0940
4.7	0.0982	5.4	0.0944
7.1	0.0997	22.0	0.0941
24.1	0.0997	26.5	0.0947
28.4	0.0993	29.3	0.0950
31.3	0.0993	46.0	0.0949
47.7	0.0993	50.7	0.0955
52.1	0.0996	72.7	0.0955
55.1	0.0996	74.5	0.0951
75.4	0.0997	94.2	0.0955
100.3	0.0999	100.0	0.0958
120.0	0.0997	--	--

Interpretation. From the results of this section of the program one can state that $t/2$ flaws that may escape detection during a proof test will not cause failure from flaw growth under a sustained load of 105 ksi for up to 100 hours. Experience with flaw growth in titanium alloys exposed to various environmental conditions has indicated that failure usually occurs within the first 10 hours of loading. Consequently it appears that these results show that sustained load will not be a problem in the five environments studied. If more severe flaws can be expected after proof testing and inspection some further study is advisable.

Concluding Discussion

This comprehensive experimental program has been carried out in a relatively short period of time to provide data upon which to base a decision whether to use cryogenic proof testing of LM tankage to eliminate smaller flaws. Several kinds of studies including fracture tests, programmed fatigue tests and sustained load tests were conducted on simple laboratory coupons containing a variety of flaws. The data from the fracture tests clearly show that smaller flaws can be eliminated by a cryogenic proof test when compared with an air test. However, there is also some indication that certain moderately severe flaws, that do not cause failure, do result in slow crack growth internally (in the form of tunneling). Such growth may result in a more severe flaw for a subsequent proof cycle or during simulated operating cycles. This condition may be time dependent and was observed in cryogenic proof testing and also has been observed in air proof testing. This behavior should be examined in greater detail.

Proof testing appears to eliminate elongated flaws to a greater extent than comparable depth normal flaws. This probably results from the fact that the elongated flaw has larger area that may grow to a critical size for fracture to occur than has the normal flaw.

Also of interest is the fact that during simulated operating cycles the growth of the normal flaws (in terms of surface length) proceeds at a more rapid rate than does the growth of elongated flaws. This has led to the propagation of surface flaws to through type flaws that would cause leaks in an LM tank. As a matter of interest with the elimination of large elongated flaws by proof tests it appears quite likely that all remaining flaws, normal or elongated, can be expected to grow by the fatigue mechanism. Some of these will propagate through, and they may expect to be detected by leaks. It does not appear that any will grow to a large enough size to cause fracture before breakthrough. However, experiments to categorize the fracture strength of various length through cracks appear in order together with fatigue crack propagation under 105 ksi stress. Some through cracked samples should be included in a limited study of sustained load behavior at a stress of 105 ksi.

The results and conclusions by rights certainly apply to flat sheet specimens and are useful guides for the LM tankage. However, introduction of the cylindrical surface of the tanks provides a different stress environment than can be characterized by thin sheet specimens. One difference is in the biaxial stress field in the tankage. Another is the panel curvature, and a third the bending stresses near the flaw extremities. It is not expected that these factors will negate conclusions from the sheet tests. Instead it is thought that the added stress components will reduce critical flaw sizes below those developed herein. Consequently examination of cylindrical shaped containers has been suggested in the recommendations for further studies. These in general would be small scale models of LM tankage.

Other recommendations also have been made for what are considered useful experimental studies. All of these have been summarized in one of the opening sections of the report.

APPENDIX A

COMPUTER PROGRAMS USED IN THE ANALYSIS OF
PROGRAMMED FATIGUE CRACK PROPAGATION DATA.

PROGRAM STRESS N USED FOR NORMAL FLAWS

PROGRAM STRESS E USED FOR ELONGATED FLAWS


```

PROGRAM STRESN (INPUT,OUTPUT,PLOT,TAPE99=PLOT,TAPE60=INPUT)
C
000003 DIMENSION ARRAYS FOR PHICLC
C          TWOCR( 15,6), AREF( 15,6), PHI( 15,6)
C
000003 DIMENSION INPUT
000003 DIMENSION TWOC( 50,6), N( 50,6), SIGMAX( 6), CONST( 6)
000003 DIMENSION N2C( 6), SPECN( 6), IBLANK( 6)
000003 DIMENSION FTYPE( 3), T( 6)
000003 DIMENSION NRFF( 8), D2CDN( 15,6), KMAX( 15,6), L02C(15,6)
C
C          CALCULATED ARRAYS
C          ARRAYS FOR REG1
000003 DIMENSION W( 50), ATEMP( 5,5), YREG( 50)
000003 DIMENSION LTFMP( 15), R( 5), BSIG( 5)
000003 DIMENSION S( 5), L2CR( 15,6)
C
C          TEMPORARY ARRAYS FOR FINDING MAX AND MIN FOR PLOTS
000003 DIMENSION XTFMP( 300), YTEMP( 300)
C
C          ARRAYS FOR PLOTTING
000003 DIMENSION Y( 50), Y( 50), BCD( 10), CHAR( 6)
000003 REAL N, NREF, NREG, KMAX, L02C, L2CR
000003 INTEGER SPECN, BCD, CHAR, FTYPE
000003 EXTERNAL FUNC
000003 DATA IBLANK/ 6*2H /
000003 DATA NRFF/ 80.,100.,150.,200.,250.,300.,350.,400./
000003 DATA NR/ 8/
C
C          INPUT
C
000003 1 READ 100, FTYPE, KDFG, NSPEC, IPRINT
000017 100 FORMAT (3A10, 3I10 )
000017 IF (FOF.60) 105,108
000022 105 CALL EXIT
000023 108 DO 130 J=1,NSPEC
000025 READ 110, SPECN(J), N2C(J), T(J) , SIGMAX(J), CONST(J)
000042 110 FORMAT ( A10, I10, 3E10.0 )
000042 NUM = N2C(J)
000044 READ 120, ( ( TWOC(I,J), N(I,J) ), I=1,NUM )
000065 120 FORMAT ( 8E10.0 )
000065 130 CONTINUE
000070 IF ( IPRINT .EQ. 0 ) GO TO 220
000071 DO 170 J=1,NSPEC
000072 NP1 = N2C(J)+1
000074 DO 150 I=NP1,50
000075 N(I,J) = 0.0
000100 150 TWOC(I,J) = 0.0
000103 170 CONTINUE
000106 PRINT 180, FTYPE, ( ( IBLANK(J), SPECN(J) ), J=1,NSPEC )
000124 180 FORMAT ( 1H1, 44X,3A10, /, 6X, A2, *SPEC N *, A10,
1 A?, *SPEC N *, A10, A2, *SPEC N *, A10, A2, *SPEC N *,
2 A10, A2, *SPEC N *, A10, A2, *SPEC N *, A10 )
000124 PRINT 190, ( ( IBLANK(J), SIGMAX(J) ), J=1,NSPEC )
000141 190 FORMAT ( 6X, A?, *SIGMAX *, E10.3, A2, *SIGMAX *, E10.3, A2,
1 *SIGMAX *, F10.3, A2, *SIGMAX *, F10.3, A?, *SIGMAX *,
2 E10.3, A2, *SIGMAX *, F10.3 )
000141 PRINT 200, ( IBLANK(J), J=1,NSPEC )
000154 200 FORMAT ( 13X, 6(A?, *2C*, 7X, *N*, 8X) )

```

```

000154      DO 219 I=1,50
000156      PRINT 210, ( ( TWOC(I,J), N(I,J) ), J=1,NSPEC )
000175      210 FORMAT ( AX, 6(E12.4,F6.0,2X) )
000175      219 CONTINUE
000177      220 CALL NAMPLT

C
C          PLOT POINT PLOTS
C
C
C          SET VARIABLES FOR REG1
C
000200      NX = 1
000201      NB = KDEG+1
000203      DO 235 I=1,50
000205      235 W(I) = 1.

C
C          SET AXIS VARIABLES
C
000210      X0 = 2.0
000212      Y0 = 2.0
000213      XAX = 8.0
000214      YAX = 6.0
000216      L = 0
000217      DO 240 J=1,NSPFC
000220      CHAR(J) = J
000221      NUMR = NPC(J)
000223      DO 240 I=1,NUMR
000224      L = L+1
000226      XTEMP(L) = N(I,J)
000232      240 YTEMP(L) = TWOC(I,J)
000241      250 CALL SCALE (XTEMP,XAX,L,1)
000244      CALL SCALE (YTEMP,YAX,L,1)
000247      CALL AXIS ( X0, Y0,24HCYCLES OF PROPAGATION, N,-24.8.0,0.0,
1          XTEMP(L+1),XTEMP(L+2),0)
000264      CALL AXIS (X0 , Y0,3PHSURFACE CRACK LENGTH, 2C, INCHES, 32.6.0,90.
1          ,YTEMP(L+1),YTEMP(L+2),0)
000301      CALL SYMROL (4.0,0.5,.14,FTYPE,0.0,30)
000305      ITYPE = -1
000306      ISW = 0
000307      260 DO 310 J=1,NSPFC
000311      NUMR = NPC(J)
000313      DO 270 I=1,NUMR
000314      X(I) = N(I,J)
000320      270 Y(I) = TWOC(I,J)
000324      X(NUMR+1) = XTEMP(L+1) - X0*XTEMP(L+2)
000330      Y(NUMR+1) = YTEMP(L+1) - Y0*YTEMP(L+2)
000334      X(NUMR+2) = XTEMP(L+2)
000335      Y(NUMR+2) = YTEMP(L+2)
000337      CALL LINF (X,Y,NUMR,1,ITYPE,CHAR(J) )
000343      IF ( ISW .NE. 0 ) GO TO 310

C
000344      CALL REG1 (NX,NB,FUNC,NUMR,W,Y,X,NX ,ATEMP,LTEMP,B,YREG,SSD,
1          BSIG,S,IERR)
000364      IF ( IERR .EQ. 0 ) GO TO 280
000365      PRINT 275, IPR, I, J

```

```

000377 275 FORMAT ( * ERROR*, I5, * OCCURRED DURING REGRESSION *, 2I10 )
000377 CALL EXIT
000400 280 DO 290 I=1,NUMP
000402 290 TWOC(I,J) = YRFG(I)
000412 DO 300 I=1,NR
000413 YB = NREF(I)
000415 TWOCR(I,J) = R(1)+R(2)*YB+R(3)*YB**2+R(4)*YB**3+R(5)*YB**4
000434 300 D2CDN(I,J) = R(2)+YB*( 2.0*R(3)+3.0*R(4)*YB+4.0*R(5)*YB*YB )
000452 310 CONTINUE
000455 IF (ISW .EQ. 1 ) GO TO 340
000457 IF (ISW .EQ. 2 ) GO TO 400

C
C
C          SET UP FOR LINE-POINT PLOT
C
000461 320 ITYPE = 0
000462 ISW = 1
000463 GO TO 260
000464 340 CALL PLOT (11.0,0.0,-3)

C
C
C          PLOT LOG OF 2C VS N
C
000467 L = 0
000470 ISW = 2
000471 DO 350 J=1,NSPFC
000473 NUMR = N2C(J)
000475 DO 350 I=1,NUMR
000476 L = L+1
000500 YTEMP(L) = ALOG10( TWOC(I,J) )
000506 350 TWOC(I,J) = ALOG10( TWOC(I,J) )
000522 CALL SCALE (XTEMP,XAX,L,1)
000525 CALL SCALE (YTEMP,YAX,L,1)
000530 CALL AXIS (X0,Y0,24HCYCLES OF PROPAGATION, N,-24,R.0,0.0,
1 XTEMP(L+1),XTEMP(L+2),0)
000545 CALL AXIS ( X0, Y0,37HLOG SURFACE CRACK LENGTH, 2C, INCHES, 37,
1 6.0,90.0, YTEMP(L+1),YTEMP(L+2),0)
000562 CALL SYMBOL (4.0,0.5,.14,FTYPE,0.0,30)
000564 ITYPE = 1
000567 GO TO 260
000570 400 CALL PLOT (11.0,0.0,-3)

C
C
C          CALCULATE A REFERENCE, PHI, AND KMAX
C
000573 500 DO 510 J=1,NSPFC
000575 DO 510 I=1,NR
000576 510 AREF(I,J) = TWOCR(I,J)/CONST(J)
000612 CALL PHICLC (NR ,NSPEC,TWOCR,AREF,PHI)
000615 DO 520 J=1,NSPFC
000617 DO 520 I=1,NR
000620 520 KMAX(I,J) = SIGMAX(J)/PHI(I,J)*SQRT( 3.14159*AREF(I,J) )*.1.1
C          CALCULATE LOG 2C REF AND D2CDN
000641 DO 530 J=1,NSPFC
000643 DO 530 I=1,NR
000644 I2CR(I,J) = ALOG10( TWOCR(I,J) )
000654 IF ( D2CDN(I,J) .LE. 0.0 ) D2CDN(I,J) = .0000001
000660 530 L02C(I,J) = ALOG10( D2CDN(I,J) )

```

C
C
C

PLOT LOG 2C REF VS LOG D2CDN

```
000672      L = 0
000673      NO 540 J=1,NSPFC
000674      NO 540 I=1,NR
000675      L = L+1
000677      XTEMP(L) = L2CR(I,J)
000703 540 YTEMP(L) = LD2C(I,J)
000712      CALL SCALE (XTEMP,XAX,L,1)
000715      CALL SCALE (YTEMP,YAY,L,1)
000720      CALL AXIS ( X0, Y0,36HLOG SURFACE CRACK LENGTH, 2C, INCHES,-36.
1          8.0,0.0,XTEMP(L+1),XTEMP(L+2),0)
000735      CALL AXIS ( X0, Y0,10H          . 10.6.0.90.0,YTEMP(L+1),
1          YTEMP(L+2),0)
000752      CALL SYMROL (4.0,0.5,.14,FTYPE,0.0,30)
000756      RCD(1) = 10HLOG SURFAC
000760      RCD(2) = 10HF CRACK PR
000761      RCD(3) = 10HOPAGATION
000763      RCD(4) = 10HRATE, 0(2C
000764      RCD(5) = 10H)/DN,
000766      CALL SYMROL (.75,2.0,.14,RCD,90.0,45)
000772      RCD(1) = 10HMICRO-INCH
000774      RCD(2) = 10HES PFR CYC
000775      RCD(3) = 10HLE
000777      CALL SYMROL (1.4,3.0,.14,RCD,90.0,22)
001003      ITYPE = 1
001004 550 NO 600 J=1,NSPFC
001006      NO 560 I=1,NR
001007      X(I) = L2CR(I,J)
001013 560 Y(I) = LD2C(I,J)
001017      X(NR +1) = XTEMP(L+1)- X0*XTEMP(L+2)
001023      Y(NR +1) = YTEMP(L+1)- Y0*YTEMP(L+2)
001027      X(NR +2) = XTEMP(L+2)
001030      Y(NR +2) = YTEMP(L+2)
001032      CALL LINE (X,Y,NR ,1,ITYPE,CHAR(J) )
001036 600 CONTINUE
001041      CALL PLOT ( 11.0,0.0,-3)
001043      NO 675 J=1,NSPFC
001045      IF (XMODF(J,3) .EQ. 1 ) PRINT 660
001055 660 FORMAT ( 1H1)
001055      PRINT 670, SPECN(J), ( ( TWOCR(I,J), NREF(I) . KMAX(I,J),
1          D2CDN(I,J) ), I=1,NR )
001105 670 FORMAT ( 1H0, 25X,*SPECIMEN NUMBER *,A10,/, 33X, *2CREF*, 12X,
1          *NRFF*, 12X, *KMAX*, 10X, *D2C/DN*, /, ( 28X, E12.4, 4X,
2          E12.4, 4X, F12.4, 4X, F12.4, 4X ) )
001105 675 CONTINUE
```

C
C
C

PLOT LOG(D2CDN) VS LOG(KMAX)

```
001110      L = 0
001111      NO 710 J=1,NSPFC
001112      NO 710 I=1,NR
001113 690 KMAX(I,J) = ALOG10( KMAX(I,J) )
001122      L = L+1
```

001122

L = L+1

```

001124      XTEMP(L) = LDZC(I,J)
001130 710  YTEMP(L) = KMAX(I,J)
001137      CALL SCALE (XTFMP,XAX,L,1)
001142      CALL SCALF (YTFMP,YAX,L,1)
001145      RCD(1) = 10H
001147      CALL AXIS (X0,Y0,RCD,-10,8.0,0.0,XTEMP(L+1),XTEMP(L+2),0)
001163      CALL AXIS (X0,Y0,RCD, 10,6.0,90.0,YTFMP(L+1),YTEMP(L+2),0)
001200      CALL SYMBOL (4.0,0.5,.14,FTYPE,0.0,30)
001204      RCD(1) = 10HLOG STRESS
001206      RCD(2) = 10H INTENSITY
001207      RCD(3) = 10H FACTOR, K
001211      CALL SYMBOL (.75,3.0,.14,RCD,90.0,30)
001215      RCD(1) = 10HKS1-SQRT(I
001217      RCD(2) = 10HNCH)
001220      CALL SYMBOL (1.4,4.0,.14,RCD,90.0,14)
001224      RCD(1) = 10HLOG SURFAC
001226      RCD(2) = 10HF CRACK PR
001227      RCD(3) = 10HPROPAGATION
001231      RCD(4) = 10HRATE,D2C/
001232      RCD(5) = 10HON
001234      CALL SYMBOL (3.0,1.4,.14,RCD,0.0,42)
001240      RCD(1) = 10HMICRO-INCH
001242      RCD(2) = 10HFS PFR CYC
001243      RCD(3) = 10HLF
001245      CALL SYMBOL (4.0,.75,.14,RCD,0.0,22)
001251      DO 730 J=1,NSPEC
001253      DO 720 I=1,NR
001254      X(I) = LDZC(I,J)
001260 720  Y(I) = KMAX(I,J)
001264      X(NR +1) = XTFMP(L+1)-X0*XTFMP(L+2)
001270      Y(NR +1) = YTFMP(L+1)-Y0*YTFMP(L+2)
001274      X(NR +2) = XTFMP(L+2)
001275      Y(NR +2) = YTFMP(L+2)
001277 730  CALL LINP (X,Y,NR ,1,ITYPE,CHAR(J) )
001306      CALL PLOT (11.0,0.0,-3)
001310      GO TO 1
001311      END

```

```

PROGRAM STRESE (INPUT,OUTPUT,PLOT,TAPE99=PLOT,TAPE60=INPUT)
C
000003 DIMENSION ARRAYS FOR PHICLC
C DIMENSION TWOCR( 15,6), AREF( 15,6), PHI( 15,6)
000003 DIMENSION INPUT
000003 DIMENSION TWOC( 50,6), N( 50,6), SIGMAX( 6), A0( 6)
000003 DIMENSION N2C( 6), SPECN( 6), IBLANK( 6), TWOC0( 6)
000003 DIMENSION FTYPE( 3), T( 6)
000003 DIMENSION NPEF( 8), D2CON( 15,6), KMAX( 15,6), LD2C(15,6)
C
C CALCULATED ARRAYS
C ARRAYS FOR REG1
000003 DIMENSION W( 50), ATEMP( 5,5), YREG( 50)
000003 DIMENSION LTEMP( 15), B( 5), BSIG( 5)
000003 DIMENSION S( 5), L2CR( 15,6)
C
C TEMPORARY ARRAYS FOR FINDING MAX AND MIN FOR PLOTS
000003 DIMENSION XTEMP( 300), YTEMP( 300)
C
C ARRAYS FOR PLOTTING
000003 DIMENSION X( 50), Y( 50), BCD( 10), CHAR( 6)
000003 REAL N, NREF, NREG, KMAX, LD2C, L2CR
000003 INTEGER SPECN, BCD, CHAR, FTYPE
000003 EXTERNAL FUNC
000003 DATA IBLANK/ 6*2H /
000003 DATA NREF/ 50.,100.,150.,200.,250.,300.,350.,400./
000003 DATA NR/ 8/
C
C INPUT
C
000003 1 READ 100, FTYPE, KDEG, NSPEC, IPRINT
000017 100 FORMAT (3A10, 3I10 )
000017 IF (EOF,60) 105,108
000022 105 CALL EXIT
000023 108 DO 130 J=1,NSPEC
000025 READ 110, SPECN(J), N2C(J), T(J), SIGMAX(J), A0(J)
000042 110 FORMAT ( A10, I10, 3E10.0 )
000042 NUM = N2C(J)
000044 READ 120, ( ( TWOC(I,J), N(I,J) ), I=1,NUM )
000065 120 FORMAT ( 8E10.0 )
000065 TWOC0(J) = TWOC(1,J)
000071 130 CONTINUE
000073 IF ( IPRINT .EQ. 0 ) GO TO 220
000074 DO 170 J=1,NSPEC
000076 NP1 = N2C(J)+1
000100 DO 150 I=NP1,50
000101 N(I,J) = 0.0
000104 150 TWOC(I,J) = 0.0
000107 170 CONTINUE
000112 PRINT 180, FTYPE, ( ( IBLANK(J), SPECN(J) ), J=1,NSPEC )
000130 180 FORMAT ( 1H1, 44X,3A10, /, 6X, A2, *SPEC N *, A10,
1 A2, *SPEC N - *, -A10, -A2, *SPEC N - *, -A10, A2, *SPEC N - *,
2 A10, A2, *SPEC N *, A10, A2, *SPEC N *, A10 )
000130 PRINT 190, ( ( IBLANK(J), SIGMAX(J) ), J=1,NSPEC )
000145 190 FORMAT ( 6X, A2, *SIGMAX *, E10.3, A2, *SIGMAX *, E10.3, A2,
1 *SIGMAX *, E10.3, A2, *SIGMAX *, E10.3, A2, *SIGMAX *,
2 E10.3, A2, *SIGMAX *, E10.3 )
000145 PRINT 200, ( IBLANK(J), J=1,NSPEC )

```

```

000160 200 FORMAT (13X, 6(A2, *2C*, 7X, *N*, 8X) )
000160 DO 219 I=1,50
000162 PRINT 210, ( (TWOC(I,J), N(I,J) ), J=1,NSPEC )
000201 210 FORMAT ( 8X, 6(E12.4,F6.0,2X) )
000201 219 CONTINUE
000203 220 CALL NAMPLT
C
C PLOT POINT PLOTS
C
C SET VARIABLES FOR REG1
C
000204 NX = 1
000205 NB = KDEG+1
000207 DO 235 I=1,50
000211 235 W(I) = 1.
C
C SET AXIS VARIABLES
C
000214 X0 = 2.0
000216 Y0 = 2.0
000217 XAX = 8.0
000220 YAX = 6.0
000222 L = 0
000223 DO 240 J=1,NSPEC
000224 CHAR(J) = J
000225 NUMR = N2C(J)
000227 DO 240 I=1,NUMR
000230 L = L+1
000232 XTEMP(L) = N(I,J)
000236 240 YTEMP(L) = TWOC(I,J)
000245 250 CALL SCALE (XTEMP,XAX,L,1)
000250 CALL SCALE (YTEMP,YAX,L,1)
000253 CALL AXIS ( X0, Y0, 24HCYCLES OF PROPAGATION, N, -24, 8.0, 0.0,
1 XTEMP(L+1), XTEMP(L+2), 0 )
000270 CALL AXIS ( X0, Y0, 32HSURFACE CRACK LENGTH, 2C, INCHES, 32, 6.0, 90,
1 YTEMP(L+1), YTEMP(L+2), 0 )
000305 CALL SYMBOL (4.0, 0.5, .14, FTYPE, 0.0, 30)
000311 ITYPE = -1
000312 ISW = 0
000313 260 DO 310 J=1,NSPEC
000315 NUMR = N2C(J)
000317 DO 270 I=1,NUMR
000320 X(I) = N(I,J)
000324 270 Y(I) = TWOC(I,J)
000330 X(NUMR+1) = XTEMP(L+1) - X0*XTEMP(L+2)
000334 -Y(NUMR+1) = YTEMP(L+1) - Y0*YTEMP(L+2)
000340 X(NUMR+2) = XTEMP(L+2)
000341 -Y(NUMR+2) = -YTEMP(L+2)
000343 CALL LINE (X,Y,NUMR,1,ITYPE,CHAR(J) )
000347 IF ( ISW .NE. 0 ) GO TO 310
C
C FIND BEST FIT CURVE FOR THIS SPECIMEN
000350 CALL REG1 (NX,NB, FUNC, NUMR, W, Y, X, NX, ATEMP, LTEMP, B, YREG, SSD,
1 BSIG, S, IERR)
000370 IF ( IERR .EQ. 0 ) GO TO 280

```

```

000371 PRINT 275, IERR, I, J
000403 275 FORMAT ( * ERROR*, IS, * OCCURRED DURING REGRESSION *, 2110 )
000403 CALL EXIT
000404 280 DO 290 I=1,NUMR
000406 290 TWOC(I,J) = YREG(I)
000416 DO 300 I=1,NR
000417 YB = NREF(I)
000421 TWOCR(I,J) = B(1)+B(2)*YB+B(3)*YB**2+B(4)*YB**3+R(5)*YB**4
000440 300 D2CDN(I,J) = B(2)+YB*( 2.0*B(3)+3.0*B(4)*YB+4.0*R(5)*YB*YB )
000456 310 CONTINUE
000461 IF (ISW .EQ. 1 ) GO TO 340
000463 IF (ISW .EQ. 2 ) GO TO 400

C
C          SET UP FOR LINE-POINT PLOT
C
000465 320 ITYPE = 0
000466 ISW = 1
000467 GO TO 260
000470 340 CALL PLOT (11.0,0.0,-3)

C
C          PLOT LOG OF 2C VS N
C
000473 L = 0
000474 ISW = 2
000475 DO 350 J=1,NSPEC
000477 NUMR = N2C(J)
000501 DO 350 I=1,NUMR
000502 L = L+1
000504 YTEMP(L) = ALOG10( TWOC(I,J) )
000512 350 TWOC(I,J) = ALOG10( TWOC(I,J) )
000526 CALL SCALE (XTEMP,XAX,L,1)
000531 CALL SCALE (YTEMP,YAX,L,1)
000534 CALL AXIS (X0,Y0,24HCYCLES OF PROPAGATION,-N,-24.8,0.0,
1 XTEMP(L+1),XTEMP(L+2),0)
000551 CALL AXIS ( X0, Y0,37HLOG SURFACE CRACK LENGTH, 2C, INCHES, 37,
1 6.0,40.0, YTEMP(L+1),YTEMP(L+2),0)
000566 CALL SYMBOL (4.0,0.5,.14,FTYPE,0.0,30)
000572 ITYPE = 1
000573 GO TO 260
000574 400 CALL PLOT (11.0,0.0,-3)

C
C          CALCULATE A REFERENCE, PHI, AND KMAX
C
000577 500 DO 510 J=1,NSPEC
000601 DO 510 I=1,NR
000602 DLT2C = TWOCR(I,J)-TWOC0(J)
000606 DLT2C = DLT2C/2.
000610 510 AREF(I,J) = A0(J)+DLTA
000620 CALL PHICLC (NR ,NSPEC,TWOCR,AREF,PHI)
000624 DO 520 J=1,NSPEC
000626 DO 520 I=1,NR
000627 520 KMAX(I,J) = SIGMAX(J)/PHI(I,J)*SQRT( 3.14159*AREF(I,J) )*.1
C          CALCULATE LOG 2C REF AND D2CDN
000650 DO 530 J=1,NSPEC
000652 DO 530 I=1,NR

```



```

000653 L2CR(I,J) = ALOG10( TWOCR(I,J) )
000663 IF ( D2CDN(I,J) .LE. 0.0 ) D2CDN(I,J) = .0000001
000667 530 LD2C(I,J) = ALOG10( D2CDN(I,J) )
C
C PLOT LOG 2C REF VS LOG D2CDN
C
000701 L = 0
000702 DO 540 J=1,NSPEC
000703 DO 540 I=1,NR
000704 L = L+1
000706 XTEMP(L) = L2CR(I,J)
000712 540 YTEMP(L) = LD2C(I,J)
000721 CALL SCALE (XTEMP,XAX,L,1)
000724 CALL SCALE (YTEMP,YAX,L,1)
000727 CALL AXIS ( X0, Y0,36HLOG SURFACE CRACK LENGTH, 2C, INCHES,-36,
1 8.0,0.0,XTEMP(L+1),XTEMP(L+2),0)
000744 CALL AXIS ( X0, Y0,10H , 10,6.0,90.0,YTEMP(L+1),
1 YTEMP(L+2),0)
000761 CALL SYMBOL (4.0,0.5,.14,FTYPE,0.0,30)
000765 BCD(1) = 10HLOG SURFAC
000767 BCD(2) = 10HE CRACK PR
000770 BCD(3) = 10HOPAGATION
000772 BCD(4) = 10HRATE, D(2C
000773 BCD(5) = 10H)/DN,
000775 CALL SYMBOL (.75,2.0,.14,BCD,90.0,45)
001001 BCD(1) = 10HMICRO=INCH
001003 BCD(2) = 10HES PER CYC
001004 BCD(3) = 10HLE
001006 CALL SYMBOL (1.4,3.0,.14,BCD,90.0,22)
001012 ITYPE = 1
001013 550 DO 600 J=1,NSPEC
001015 DO 560 I=1,NR
001016 X(I) = L2CR(I,J)
001022 560 Y(I) = LD2C(I,J)
001026 X(NR +1) = XTEMP(L+1) - X0*XTEMP(L+2)
001032 Y(NR +1) = YTEMP(L+1) - Y0*YTEMP(L+2)
001036 X(NR +2) = XTEMP(L+2)
001037 Y(NR +2) = YTEMP(L+2)
001041 CALL LINE (X,Y,NR ,1,ITYPE,CHAR(J) )
001045 600 CONTINUE
001050 CALL PLOT ( 11.0,0.0,-3)
001052 DO 675 J=1,NSPEC
001054 IF (XMOD(J,3) .EQ. 1) PRINT 660
001064 660 FORMAT ( 1H1)
001064 PRINT 670, SPECN(J), ( (- TWOCR(I,J), NREF(I), AREF(I,J), KMAX(I,J)
1 D2CDN(I,J) ), I=1,NR )
001117 670 FORMAT ( 1H0, 25X,*SPECIMEN NUMBER - *,A10,/, -33X, *2CREF*, 12X,
1 *NREF*, 12X, *AREF*,12X,*KMAX*,10X,*D2C/DN*/,(28X,E12.4,4X,
2 E12.4, 4X, E12.4, 4X,-E12.4, 4X, E12.4-) )
001117 675 CONTINUE
C
C PLOT LOG(D2CDN) VS LOG(KMAX)
C
001122 L = 0
001123 DO 710 J=1,NSPEC

```

```

2 E12., 4x, E12.4, 4x, E12.4, 4x, E12.4-)
001117 675 CONTINUE
C
C PLOT LOG(D2CDN) VS LOG(KMAX)
C
001122 L = 0
001123 DO 710 J=1,NSPEC

-----

001124 DO 710 I=1,NR
001125 690 KMAX(I,J) = ALOG10( KMAX(I,J) )
001134 L = L+1
001136 XTEMP(L) = LD2C(I,J)
001142 710 YTEMP(L) = KMAX(I,J)
001151 CALL SCALE (XTEMP,XAX,L,1)
001154 CALL SCALE (YTEMP,YAX,L,1)
001157 BCU(1) = 10H
001161 CALL AXIS (X0,Y0,BCD,-10,8.0,0.0,XTEMP(L+1),XTEMP(L+2),0)
001175 CALL AXIS (X0,Y0,BCD, 10,6.0,90.0,YTEMP(L+1),YTEMP(L+2),0)
001212 CALL SYMBOL (4.0,0.5,.14,FTYPE,0.0,30)
001216 BCU(1) = 10HLOG STRESS
001220 BCU(2) = 10H INTENSITY
001221 BCU(3) = 10H FACTOR, K
001223 CALL SYMBOL (.75,3.0,.14,BCD,90.0,30)
001227 BCU(1) = 10HKSI-SQRT(I)
001231 BCU(2) = 10HNCH
001232 CALL SYMBOL (1.4,4.0,.14,BCD,90.0,14)
001236 BCU(1) = 10HLOG SUHFAC
001240 BCU(2) = 10HE CRACK PR
001241 BCU(3) = 10HOPAGATION
001243 BCU(4) = 10HRATE,U2C/
001244 BCU(5) = 10HDN
001246 CALL SYMBOL (3.0,1.4,.14,BCD,0.0,42)
001252 BCU(1) = 10HMICRO-INCH
001254 BCU(2) = 10HES PER CYC
001255 BCU(3) = 10HLE
001257 CALL SYMBOL (4.0,.75,.14,BCD,0.0,22)
001263 DO 730 J=1,NSPEC
001265 DO 720 I=1,NR
001266 X(I) = LD2C(I,J)
001272 720 Y(I) = KMAX(I,J)
001276 X(NR +1) = XTEMP(L+1)-X0*XTEMP(L+2)
001302 Y(NR +1) = YTEMP(L+1)-Y0*YTEMP(L+2)
001306 X(NR +2) = XTEMP(L+2)
001307 Y(NR +2) = YTEMP(L+2)
001311 730 CALL LINE (X,Y,NR ,1,ITYPE,CHAR(J) )
001320 CALL PLOT (11.0,0.0,-3)
001322 GO TO 1
001323 END

```

APPENDIX B

TABULATED COMPUTER INPUT AND RESULTS FOR PROGRAMMED
FATIGUE CRACK PROPAGATION DATA

SPECIMEN NUMBER	2-20	T/4		
2CREF	NREF	KMAX	D2C/DN	
0.1434E-01	0.5000E+02	0.1091E+05	0.3083E-05	
0.1450E-01	1.0000E+02	0.1097E+05	0.3250E-05	
0.1466E-01	0.1500E+03	0.1103E+05	0.3042E-05	
0.1480E-01	0.2000E+03	0.1108E+05	0.2583E-05	
0.1491E-01	0.2500E+03	0.1112E+05	0.2000E-05	
0.1500E-01	0.3000E+03	0.1116E+05	0.1417E-05	
0.1506E-01	0.3500E+03	0.1118E+05	0.9583E-06	
0.1510E-01	0.4000E+03	0.1119E+05	0.7500E-06	

SPECIMEN NUMBER	2-x	T/2		
2CREF	NREF	KMAX	D2C/DN	
0.2701E-01	0.5000E+02	0.1497E+05	0.6364E-05	
0.2727E-01	1.0000E+02	0.1504E+05	0.4211E-05	
0.2744E-01	0.1500E+03	0.1509E+05	0.2894E-05	
0.2758E-01	0.2000E+03	0.1512E+05	0.2560E-05	
0.2772E-01	0.2500E+03	0.1516E+05	0.3359E-05	
0.2793E-01	0.3000E+03	0.1522E+05	0.5436E-05	
0.2829E-01	0.3500E+03	0.1532E+05	0.8941E-05	
0.2885E-01	0.4000E+03	0.1547E+05	0.1402E-04	

SPECIMEN NUMBER	2-46	T/2		
2CREF	NREF	KMAX	D2C/DN	
0.2720E-01	0.5000E+02	0.1502E+05	0.1614E-04	
0.2786E-01	1.0000E+02	0.1520E+05	0.1043E-04	
0.2827E-01	0.1500E+03	0.1531E+05	0.6101E-05	
0.2850E-01	0.2000E+03	0.1538E+05	0.3513E-05	
0.2866E-01	0.2500E+03	0.1542E+05	0.3012E-05	
0.2884E-01	0.3000E+03	0.1547E+05	0.4946E-05	
0.2920E-01	0.3500E+03	0.1556E+05	0.9664E-05	
0.2986E-01	0.4000E+03	0.1574E+05	0.1751E-04	

SPECIMEN NUMBER	2-53 3T/4			
	ZCREF	NREF	KMAX	D2C/DN
	0.4563E-01	0.5000E+02	0.1946E+05	0.1829E-04
	0.4658E-01	1.0000E+02	0.1966E+05	0.1936E-04
	0.4754E-01	0.1500E+03	0.1986E+05	0.1913E-04
	0.4848E-01	0.2000E+03	0.2005E+05	0.1847E-04
	0.4940E-01	0.2500E+03	0.2024E+05	0.1824E-04
	0.5033E-01	0.3000E+03	0.2043E+05	0.1930E-04
	0.5136E-01	0.3500E+03	0.2064E+05	0.2251E-04
	0.5263E-01	0.4000E+03	0.2089E+05	0.2873E-04

SPECIMEN NUMBER	2-9 3T/4			
	ZCREF	NREF	KMAX	D2C/DN
	0.4521E-01	0.5000E+02	0.1937E+05	0.1789E-04
	0.4605E-01	1.0000E+02	0.1955E+05	0.1635E-04
	0.4686E-01	0.1500E+03	0.1972E+05	0.1589E-04
	0.4765E-01	0.2000E+03	0.1988E+05	0.1563E-04
	0.4841E-01	0.2500E+03	0.2004E+05	0.1469E-04
	0.4909E-01	0.3000E+03	0.2018E+05	0.1219E-04
	0.4959E-01	0.3500E+03	0.2028E+05	0.7245E-05
	0.4976E-01	0.4000E+03	0.2032E+05	1.0000E-07

SPECIMEN NUMBER	A8-5	T/4N		
ZCREF		NREF	KMAX	D2C/DN
0.1351E-01		0.5000E+02	0.1055E+05	0.5116E-05
0.1369E-01		0.1000E+03	0.1062E+05	0.2340E-05
0.1377E-01		0.1500E+03	0.1065E+05	0.1053E-05
0.1381E-01		0.2000E+03	0.1066E+05	0.8454E-06
0.1387E-01		0.2500E+03	0.1068E+05	0.1306E-05
0.1395E-01		0.3000E+03	0.1072E+05	0.2025E-05
0.1407E-01		0.3500E+03	0.1076E+05	0.2593E-05
0.1420E-01		0.4000E+03	0.1081E+05	0.2598E-05

SPECIMEN NUMBER	A7-1	T/2N		
ZCREF		NREF	KMAX	D2C/DN
0.2952E-01		0.5000E+02	0.1559E+05	0.1000E-06
0.2938E-01		0.1000E+03	0.1555E+05	0.1000E-06
0.2926E-01		0.1500E+03	0.1552E+05	0.1000E-06
0.2941E-01		0.2000E+03	0.1556E+05	0.6628E-05
0.2992E-01		0.2500E+03	0.1569E+05	0.1319E-04
0.3067E-01		0.3000E+03	0.1589E+05	0.1576E-04
0.3137E-01		0.3500E+03	0.1607E+05	0.1065E-04
0.3154E-01		0.4000E+03	0.1611E+05	0.1000E-06

SPECIMEN NUMBER	A5-1	T/2N		
ZCREF		NREF	KMAX	D2C/DN
0.2913E-01		0.5000E+02	0.1549E+05	0.1260E-04
0.2965E-01		0.1000E+03	0.1562E+05	0.8774E-05
0.3004E-01		0.1500E+03	0.1573E+05	0.6756E-05
0.3035E-01		0.2000E+03	0.1581E+05	0.5798E-05
0.3062E-01		0.2500E+03	0.1588E+05	0.5146E-05
0.3085E-01		0.3000E+03	0.1594E+05	0.4045E-05
0.3101E-01		0.3500E+03	0.1598E+05	0.1742E-05
0.3100E-01		0.4000E+03	0.1597E+05	0.1000E-06

SPECIMEN NUMBER	A2-1 3T/4N			
	2CREF	NREF	KMAX	D2C/DN
	0.4148E-01	0.5000E+02	0.1848E+05	0.9395E-05
	0.4187E-01	0.1000E+03	0.1857E+05	0.6992E-05
	0.4223E-01	0.1500E+03	0.1865E+05	0.8011E-05
	0.4270E-01	0.2000E+03	0.1875E+05	0.1097E-04
	0.4334E-01	0.2500E+03	0.1889E+05	0.1438E-04
	0.4412E-01	0.3000E+03	0.1906E+05	0.1677E-04
	0.4497E-01	0.3500E+03	0.1924E+05	0.1665E-04
	0.4572E-01	0.4000E+03	0.1940E+05	0.1253E-04

SPECIMEN NUMBER	A3-5 3T/4N			
	2CREF	NREF	KMAX	D2C/DN
	0.4087E-01	0.5000E+02	0.1834E+05	0.1153E-04
	0.4157E-01	0.1000E+03	0.1850E+05	0.1603E-04
	0.4242E-01	0.1500E+03	0.1869E+05	0.1748E-04
	0.4329E-01	0.2000E+03	0.1888E+05	0.1708E-04
	0.4412E-01	0.2500E+03	0.1906E+05	0.1600E-04
	0.4490E-01	0.3000E+03	0.1923E+05	0.1545E-04
	0.4569E-01	0.3500E+03	0.1940E+05	0.1662E-04
	0.4661E-01	0.4000E+03	0.1959E+05	0.2068E-04

SPECIMEN NUMBER	4-62	T/2		
ZCREF		NREF	KMAX	D2C/DN
0.5913E-01		0.5000E+02	0.2215E+05	0.1331E-04
0.5994E-01		1.0000E+02	0.2230E+05	0.1793E-04
0.6083E-01		0.1500E+03	0.2246E+05	0.1705E-04
0.6160E-01		0.2000E+03	0.2261E+05	0.1325E-04
0.6215E-01		0.2500E+03	0.2271E+05	0.9156E-05
0.6255E-01		0.3000E+03	0.2278E+05	0.7364E-05
0.6297E-01		0.3500E+03	0.2286E+05	0.1048E-04
0.6372E-01		0.4000E+03	0.2299E+05	0.2112E-04

SPECIMEN NUMBER	4-64	T/2		
ZCREF		NREF	KMAX	D2C/DN
0.5974E-01		0.5000E+02	0.2226E+05	0.1373E-04
0.6032E-01		1.0000E+02	0.2237E+05	0.1010E-04
0.6076E-01		0.1500E+03	0.2245E+05	0.8554E-05
0.6120E-01		0.2000E+03	0.2253E+05	0.8493E-05
0.6164E-01		0.2500E+03	0.2261E+05	0.9310E-05
0.6214E-01		0.3000E+03	0.2270E+05	0.1040E-04
0.6268E-01		0.3500E+03	0.2280E+05	0.1116E-04
0.6324E-01		0.4000E+03	0.2290E+05	0.1098E-04

SPECIMEN NUMBER	4-100	3T/4		
ZCREF		NREF	KMAX	D2C/DN
0.8240E-01		0.5000E+02	0.2615E+05	0.2904E-04
0.8393E-01		1.0000E+02	0.2639E+05	0.3306E-04
0.8563E-01		0.1500E+03	0.2665E+05	0.3225E-04
0.8716E-01		0.2000E+03	0.2689E+05	0.2896E-04
0.8852E-01		0.2500E+03	0.2710E+05	0.2558E-04
0.8976E-01		0.3000E+03	0.2729E+05	0.2446E-04
0.9104E-01		0.3500E+03	0.2748E+05	0.2798E-04
0.9267E-01		0.4000E+03	0.2773E+05	0.3850E-04

SPECIMEN NUMBER	4-115	3T/4		
ZCREF		NREF	KMAX	D2C/DN
0.8596E-01		0.5000E+02	0.2670E+05	0.4402E-04
0.8803E-01		1.0000E+02	0.2702E+05	0.3897E-04
0.8989E-01		0.1500E+03	0.2731E+05	0.3571E-04
0.9162E-01		0.2000E+03	0.2757E+05	0.3390E-04
0.9330E-01		0.2500E+03	0.2782E+05	0.3319E-04
0.9495E-01		0.3000E+03	0.2807E+05	0.3325E-04
0.9663E-01		0.3500E+03	0.2831E+05	0.3372E-04
0.9833E-01		0.4000E+03	0.2856E+05	0.3426E-04

SPECIMEN NUMBER	B12-1 T/4N			
2CREF	NREF	KMAX	D2C/DN	
0.2843E-01	0.5000E+02	0.1530E+05	0.1000E-06	
0.2843E-01	0.1000E+03	0.1530E+05	0.6004E-06	
0.2848E-01	0.1500E+03	0.1531E+05	0.1156E-05	
0.2855E-01	0.2000E+03	0.1533E+05	0.1431E-05	
0.2863E-01	0.2500E+03	0.1535E+05	0.1810E-05	
0.2873E-01	0.3000E+03	0.1538E+05	0.2681E-05	
0.2891E-01	0.3500E+03	0.1543E+05	0.4430E-05	
0.2920E-01	0.4000E+03	0.1550E+05	0.7441E-05	

SPECIMEN NUMBER	B8-2 T/4N			
2CREF	NREF	KMAX	D2C/DN	
0.2819E-01	0.5000E+02	0.1523E+05	0.6958E-05	
0.2856E-01	0.1000E+03	0.1533E+05	0.7380E-05	
0.2890E-01	0.1500E+03	0.1543E+05	0.6271E-05	
0.2917E-01	0.2000E+03	0.1550E+05	0.4463E-05	
0.2935E-01	0.2500E+03	0.1555E+05	0.2790E-05	
0.2947E-01	0.3000E+03	0.1558E+05	0.2085E-05	
0.2959E-01	0.3500E+03	0.1561E+05	0.3183E-05	
0.2983E-01	0.4000E+03	0.1567E+05	0.6915E-05	

SPECIMEN NUMBER	B23-1 T/2N			
2CREF	NREF	KMAX	D2C/DN	
0.5494E-01	0.5000E+02	0.2127E+05	0.8045E-05	
0.5542E-01	0.1000E+03	0.2136E+05	0.1053E-04	
0.5597E-01	0.1500E+03	0.2147E+05	0.1128E-04	
0.5653E-01	0.2000E+03	0.2157E+05	0.1104E-04	
0.5707E-01	0.2500E+03	0.2166E+05	0.1056E-04	
0.5760E-01	0.3000E+03	0.2178E+05	0.1059E-04	
0.5815E-01	0.3500E+03	0.2188E+05	0.1189E-04	
0.5882E-01	0.4000E+03	0.2201E+05	0.1519E-04	

SPECIMEN NUMBER	B24-4 T/2N			
2CREP	NREF	KMAX	D2C/DN	
0.5813E-01	0.5000E+02	0.2188E+05	0.1294E-04	
0.5377E-01	0.1000E+03	0.2200E+05	0.1249E-04	
0.5936E-01	0.1500E+03	0.2211E+05	0.1071E-04	
0.5985E-01	0.2000E+03	0.2220E+05	0.9295E-05	
0.6032E-01	0.2500E+03	0.2228E+05	0.9965E-05	
0.6091E-01	0.3000E+03	0.2239E+05	0.1443E-04	
0.6185E-01	0.3500E+03	0.2257E+05	0.2441E-04	
0.6347E-01	0.4000E+03	0.2286E+05	0.4160E-04	

SPECIMEN NUMBER	B22-5T3/4N			
2CREP	NREF	KMAX	D2C/DN	
0.8687E-01	0.5000E+02	0.2674E+05	0.4789E-04	
0.8975E-01	0.1000E+03	0.2718E+05	0.6517E-04	
0.9320E-01	0.1500E+03	0.2770E+05	0.7129E-04	
0.9575E-01	0.2000E+03	0.2822E+05	0.6964E-04	
0.1001E+00	0.2500E+03	0.2871E+05	0.6359E-04	
0.1031E+00	0.3000E+03	0.2913E+05	0.5656E-04	
0.1058E+00	0.3500E+03	0.2951E+05	0.5192E-04	
0.1084E+00	0.4000E+03	0.2987E+05	0.5307E-04	

SPECIMEN NUMBER	B8-3 3T/4N			
2CREP	NREF	KMAX	D2C/DN	
0.8895E-01	0.5000E+02	0.2706E+05	0.5341E-04	
0.9159E-01	0.1000E+03	0.2746E+05	0.5101E-04	
0.9397E-01	0.1500E+03	0.2781E+05	0.4397E-04	
0.9597E-01	0.2000E+03	0.2811E+05	0.3612E-04	
0.9764E-01	0.2500E+03	0.2835E+05	0.3129E-04	
0.9921E-01	0.3000E+03	0.2858E+05	0.3330E-04	
0.1011E+00	0.3500E+03	0.2886E+05	0.4598E-04	
0.1041E+00	0.4000E+03	0.2927E+05	0.7316E-04	

SPECIMEN NUMBER	4-20	T/2N		
ZCRFF		NREF	KMAX	D2C/DN
0.5805E-01		0.5000E+02	0.2194E+05	0.1211E-04
0.5877E-01		0.1000E+03	0.2208E+05	0.1624E-04
0.5962E-01		0.1500E+03	0.2224E+05	0.1736E-04
0.6047E-01		0.2000E+03	0.2240E+05	0.1636E-04
0.6123E-01		0.2500E+03	0.2254E+05	0.1414E-04
0.6183E-01		0.3000E+03	0.2266E+05	0.1159E-04
0.6240E-01		0.3500E+03	0.2275E+05	0.9613E-05
0.6286E-01		0.4000E+03	0.2284E+05	0.9106E-05

SPECIMEN NUMBER	4-17	T/2N		
ZCRFF		NREF	KMAX	D2C/DN
0.6313E-01		0.5000E+02	0.2289E+05	0.2834E-04
0.6460E-01		0.1000E+03	0.2315E+05	0.2923E-04
0.6597E-01		0.1500E+03	0.2339E+05	0.2501E-04
0.6706E-01		0.2000E+03	0.2359E+05	0.1840E-04
0.6782E-01		0.2500E+03	0.2372E+05	0.1213E-04
0.6837E-01		0.3000E+03	0.2381E+05	0.8915E-05
0.6880E-01		0.3500E+03	0.2389E+05	0.1147E-04
0.6961E-01		0.4000E+03	0.2403E+05	0.2253E-04

SPECIMEN NUMBER	4-12	3T/4N		
ZCRFF		NREF	KMAX	D2C/DN
0.1149E+00		0.5000E+02	0.3087E+05	0.1411E-03
0.1206E+00		0.1000E+03	0.3163E+05	0.9400E-04
0.1249E+00		0.1500E+03	0.3218E+05	0.7989E-04
0.1289E+00		0.2000E+03	0.3270E+05	0.8432E-04
0.1334E+00		0.2500E+03	0.3326E+05	0.9281E-04
0.1380E+00		0.3000E+03	0.3384E+05	0.9088E-04
0.1420E+00		0.3500E+03	0.3433E+05	0.6406E-04
0.1438E+00		0.4000E+03	0.3454E+05	0.1000E-06

SPECIMEN NUMBER	4-90	3T/4N		
ZCRFF		NREF	KMAX	D2C/DN
0.9923E-01		0.5000E+02	0.2869E+05	0.9329E-04
0.1032E+00		0.1000E+03	0.2926E+05	0.6801E-04
0.1063E+00		0.1500E+03	0.2969E+05	0.5648E-04
0.1090E+00		0.2000E+03	0.3007E+05	0.5419E-04
0.1118E+00		0.2500E+03	0.3045E+05	0.5664E-04
0.1147E+00		0.3000E+03	0.3084E+05	0.5932E-04
0.1176E+00		0.3500E+03	0.3124E+05	0.5773E-04
0.1203E+00		0.4000E+03	0.3159E+05	0.4735E-04

SPECIMEN NUMBER	4-87 T/4 E				
ZCREF	NREF	AREF	KMAX	U2C/UN	
0.3669E-01	0.5000E+02	0.8548E-02	0.1591E+05	0.7938E-06	
0.3071E-01	0.1000E+03	0.8554E-02	0.1591E+05	0.4970E-07	
0.3072E-01	0.1500E+03	0.8560E-02	0.1592E+05	0.5245E-06	
0.3077E-01	0.2000E+03	0.8585E-02	0.1593E+05	0.1477E-05	
0.3087E-01	0.2500E+03	0.8634E-02	0.1597E+05	0.2338E-05	
0.3099E-01	0.3000E+03	0.8696E-02	0.1601E+05	0.2502E-05	
0.3710E-01	0.3500E+03	0.8748E-02	0.1604E+05	0.1367E-05	
0.3710E-01	0.4000E+03	0.8749E-02	0.1607E+05	0.1000E-06	

SPECIMEN NUMBER	4-89 T/4 E				
ZCREF	NREF	AREF	KMAX	U2C/UN	
0.4051E-01	0.5000E+02	0.9957E-02	0.1644E+05	0.9550E-06	
0.4066E-01	0.1000E+03	0.1003E-01	0.1699E+05	0.4560E-05	
0.4096E-01	0.1500E+03	0.1018E-01	0.1708E+05	0.7404E-05	
0.4138E-01	0.2000E+03	0.1039E-01	0.1721E+05	0.8778E-05	
0.4154E-01	0.2500E+03	0.1062E-01	0.1735E+05	0.4173E-05	
0.4227E-01	0.2900E+03	0.1083E-01	0.1748E+05	0.7702E-05	
0.4259E-01	0.3500E+03	0.1099E-01	0.1757E+05	0.4977E-05	
0.4269E-01	0.4000E+03	0.1105E-01	0.1761E+05	0.1000E-06	

SPECIMEN NUMBER	4-48 T/2 F				
ZCREF	NREF	AREF	KMAX	U2C/UN	
0.1104E+00	0.5000E+02	0.2330E-01	0.2715E+05	0.2344E-04	
0.1179E+00	0.1000E+03	0.2404E-01	0.2743E+05	0.2811E-04	
0.1190E+00	0.1500E+03	0.2461E-01	0.2777E+05	0.2022E-04	
0.1199E+00	0.2000E+03	0.2508E-01	0.2791E+05	0.1814E-04	
0.1207E+00	0.2500E+03	0.2544E-01	0.2807E+05	0.1425E-04	
0.1214E+00	0.3000E+03	0.2580E-01	0.2822E+05	0.1492E-04	
0.1222E+00	0.3500E+03	0.2621E-01	0.2839E+05	0.1255E-04	
0.1233E+00	0.4000E+03	0.2675E-01	0.2861E+05	0.2550E-04	

SPECIMEN NUMBER	4-46 T/2 E				
ZCREF	NREF	AREF	KMAX	U2C/UN	
0.1185E+00	0.5000E+02	0.2304E-01	0.2715E+05	0.2210E-04	
0.1195E+00	0.1000E+03	0.2357E-01	0.2739E+05	0.2081E-04	
0.1205E+00	0.1500E+03	0.2411E-01	0.2763E+05	0.2253E-04	
0.1218E+00	0.2000E+03	0.2471E-01	0.2799E+05	0.2550E-04	
0.1232E+00	0.2500E+03	0.2538E-01	0.2817E+05	0.2819E-04	
0.1246E+00	0.3000E+03	0.2610E-01	0.2847E+05	0.2975E-04	
0.1260E+00	0.3500E+03	0.2679E-01	0.2875E+05	0.2552E-04	
0.1271E+00	0.4000E+03	0.2733E-01	0.2897E+05	0.1681E-04	

SPECIMEN NUMBER	B15-2 T/4E		AREF	KMAX	D2C/DN
2CREF	NREF				
0.3785E-01	0.5000E+02	0.9474E-02	0.1645E+05	0.4510E-05	
0.3807E-01	0.1000E+03	0.9587E-02	0.1652E+05	0.4459E-05	
0.3828E-01	0.1500E+03	0.9692E-02	0.1659E+05	0.3868E-05	
0.3846E-01	0.2000E+03	0.9779E-02	0.1664E+05	0.3096E-05	
0.3860E-01	0.2500E+03	0.9849E-02	0.1669E+05	0.2501E-05	
0.3872E-01	0.3000E+03	0.9909E-02	0.1672E+05	0.2443E-05	
0.3886E-01	0.3500E+03	0.9978E-02	0.1677E+05	0.3279E-05	
0.3907E-01	0.4000E+03	0.1008E-01	0.1683E+05	0.5370E-05	

SPECIMEN NUMBER	B18-3 T/2E		AREF	KMAX	D2C/DN
2CREF	NREF				
0.1035E+00	0.5000E+02	0.2106E-01	0.2573E+05	0.2678E-04	
0.1045E+00	0.1000E+03	0.2157E-01	0.2596E+05	0.1515E-04	
0.1052E+00	0.1500E+03	0.2188E-01	0.2610E+05	0.1019E-04	
0.1056E+00	0.2000E+03	0.2212E-01	0.2621E+05	0.1021E-04	
0.1062E+00	0.2500E+03	0.2241E-01	0.2634E+05	0.1351E-04	
0.1070E+00	0.3000E+03	0.2281E-01	0.2652E+05	0.1840E-04	
0.1081E+00	0.3500E+03	0.2333E-01	0.2674E+05	0.2320E-04	
0.1093E+00	0.4000E+03	0.2396E-01	0.2701E+05	0.2620E-04	

SPECIMEN NUMBER	B15-5 T/2E		AREF	KMAX	D2C/DN
2CREF	NREF				
0.1023E+00	0.5000E+02	0.2047E-01	0.2546E+05	0.1654E-05	
0.1024E+00	0.1000E+03	0.2049E-01	0.2547E+05	0.1352E-05	
0.1026E+00	0.1500E+03	0.2059E-01	0.2551E+05	0.7136E-05	
0.1032E+00	0.2000E+03	0.2088E-01	0.2565E+05	0.1599E-04	
0.1042E+00	0.2500E+03	0.2139E-01	0.2588E+05	0.2488E-04	
0.1056E+00	0.3000E+03	0.2210E-01	0.2620E+05	0.3079E-04	
0.1072E+00	0.3500E+03	0.2280E-01	0.2655E+05	0.3070E-04	
0.1085E+00	0.4000E+03	0.2356E-01	0.2684E+05	0.2159E-04	

SPECIMEN NUMBER	4-112 T/4E				
2CREF	NREF	AREF	KMAX	D2C/DN	
0.3985E-01	0.5000E+02	0.1012E-01	0.1694E+05	0.4513E-05	
0.4002E-01	0.1000E+03	0.1021E-01	0.1699E+05	0.2686E-05	
0.4014E-01	0.1500E+03	0.1027E-01	0.1703E+05	0.2436E-05	
0.4027E-01	0.2000E+03	0.1034E-01	0.1707E+05	0.2915E-05	
0.4043E-01	0.2500E+03	0.1041E-01	0.1711E+05	0.3276E-05	
0.4058E-01	0.3000E+03	0.1049E-01	0.1716E+05	0.2673E-05	
0.4067E-01	0.3500E+03	0.1053E-01	0.1719E+05	0.2564E-06	
0.4057E-01	0.4000E+03	0.1048E-01	0.1716E+05	0.1000E-06	

SPECIMEN NUMBER	4-42 T/2E			D2C/DN	
2CREF	NREF	AREF	KMAX		
0.1098E+00	0.5000E+02	0.1769E-01	0.2457E+05	0.4624E-04	
0.1116E+00	0.1000E+03	0.1862E-01	0.2508E+05	0.2979E-04	
0.1129E+00	0.1500E+03	0.1923E-01	0.2540E+05	0.1987E-04	
0.1137E+00	0.2000E+03	0.1967E-01	0.2562E+05	0.1584E-04	
0.1145E+00	0.2500E+03	0.2007E-01	0.2583E+05	0.1710E-04	
0.1155E+00	0.3000E+03	0.2056E-01	0.2607E+05	0.2300E-04	
0.1169E+00	0.3500E+03	0.2125E-01	0.2641E+05	0.3292E-04	
0.1189E+00	0.4000E+03	0.2223E-01	0.2687E+05	0.4624E-04	

SPECIMEN NUMBER	4-86 T/2E			D2C/DN	
2CREF	NREF	AREF	KMAX		
0.1008E+00	0.5000E+02	0.1636E-01	0.2361E+05	0.1702E-04	
0.1016E+00	0.1000E+03	0.1676E-01	0.2383E+05	0.1469E-04	
0.1023E+00	0.1500E+03	0.1709E-01	0.2402E+05	0.1176E-04	
0.1028E+00	0.2000E+03	0.1735E-01	0.2416E+05	0.9461E-05	
0.1033E+00	0.2500E+03	0.1758E-01	0.2429E+05	0.9036E-05	
0.1038E+00	0.3000E+03	0.1783E-01	0.2442E+05	0.1171E-04	
0.1045E+00	0.3500E+03	0.1820E-01	0.2462E+05	0.1873E-04	
0.1057E+00	0.4000E+03	0.1881E-01	0.2494E+05	0.3131E-04	

LINE NO.7183332802 *ERROR DATA INPUT* ILLEGAL DATA IN FIELD* FORMAT NO.110
 ERROR NUMBER 0078 DETECTED BY KRAKER AT ADDRESS 022441
 CALLED FROM INPUTC AT 012440
 CALLED FROM STRESE AT 000126

ERROR SUMMARY
 ERROR TIMES
 0078 0001

SPECIMEN NUMBER	4-62	T/2		
2CRFF		NREF	KMAX	D2C/DN
0.5913F-01		0.5000E+02	0.2215E+05	0.1331E-04
0.5994E-01		0.1000E+03	0.2230E+05	0.1793E-04
0.6083F-01		0.1500E+03	0.2246E+05	0.1705E-04
0.6160F-01		0.2000E+03	0.2261E+05	0.1325E-04
0.6215F-01		0.2500E+03	0.2271E+05	0.9150E-05
0.6255F-01		0.3000E+03	0.2278E+05	0.7364E-05
0.6297F-01		0.3500E+03	0.2286E+05	0.1048E-04
0.6372F-01		0.4000E+03	0.2299E+05	0.2112E-04

SPECIMEN NUMBER	4-64	T/2		
2CRFF		NREF	KMAX	D2C/DN
0.5974F-01		0.5000E+02	0.2226E+05	0.1373E-04
0.6032F-01		0.1000E+03	0.2237E+05	0.1010E-04
0.6078F-01		0.1500E+03	0.2245E+05	0.8554E-05
0.6120F-01		0.2000E+03	0.2253E+05	0.8493E-05
0.6164F-01		0.2500E+03	0.2261E+05	0.9310E-05
0.6214F-01		0.3000E+03	0.2270E+05	0.1040E-04
0.6268F-01		0.3500E+03	0.2280E+05	0.1116E-04
0.6324F-01		0.4000E+03	0.2290E+05	0.1098E-04

SPECIMEN NUMBER	4-24	T/2	N	
2CRFF		NREF		KMAX
0.5861F-01		0.5000E+02		0.2205E+05
0.5902F-01		0.1000E+03		0.2213E+05
0.5917F-01		0.1500E+03		0.2216E+05
0.5937F-01		0.2000E+03		0.2219E+05
0.5978F-01		0.2500E+03		0.2227E+05
0.6040F-01		0.3000E+03		0.2238E+05
0.6110F-01		0.3500E+03		0.2251E+05
0.6161F-01		0.4000E+03		0.2261E+05

SPECIMEN NUMBER	4-21	T/2	N	
2CRFF		NREF		KMAX
0.5823F-01		0.5000E+02		0.2198E+05
0.5858F-01		0.1000E+03		0.2205E+05
0.5876F-01		0.1500E+03		0.2208E+05
0.5878F-01		0.2000E+03		0.2208E+05
0.5878F-01		0.2500E+03		0.2208E+05
0.5899F-01		0.3000E+03		0.2212E+05
0.5973F-01		0.3500E+03		0.2226E+05
0.6144F-01		0.4000E+03		0.2258E+05

SPECIMEN NUMBER	B4-2 T/2N		
2CREF	NREF	KMAX	D2C/DN
0.5595E-01	0.5000E+02	0.2146E+05	0.3491E-05
0.5610E-01	0.1000E+03	0.2149E+05	0.3345E-05
0.5635E-01	0.1500E+03	0.2154E+05	0.7131E-05
0.5684E-01	0.2000E+03	0.2163E+05	0.1255E-04
0.5760E-01	0.2500E+03	0.2178E+05	0.1731E-04
0.5853E-01	0.3000E+03	0.2195E+05	0.1912E-04
0.5942E-01	0.3500E+03	0.2212E+05	0.1567E-04
0.5997E-01	0.4000E+03	0.2222E+05	0.4671E-05

SPECIMEN NUMBER	B25-2 T/2N		
2CREF	NREF	KMAX	D2C/DN
0.5787E-01	0.5000E+02	0.2183E+05	0.1702E-05
0.5851E-01	0.1000E+03	0.2195E+05	0.2189E-04
0.5988E-01	0.1500E+03	0.2220E+05	0.3120E-04
0.6152E-01	0.2000E+03	0.2250E+05	0.3368E-04
0.6320E-01	0.2500E+03	0.2281E+05	0.3335E-04
0.6487E-01	0.3000E+03	0.2311E+05	0.3426E-04
0.6671E-01	0.3500E+03	0.2344E+05	0.4044E-04
0.6907E-01	0.4000E+03	0.2385E+05	0.5593E-04

SPECIMEN NUMBER	B23-1 T/2N		
2CREF	NREF	KMAX	D2C/DN
0.5494E-01	0.5000E+02	0.2127E+05	0.8045E-05
0.5542E-01	0.1000E+03	0.2136E+05	0.1053E-04
0.5597E-01	0.1500E+03	0.2147E+05	0.1128E-04
0.5653E-01	0.2000E+03	0.2157E+05	0.1104E-04
0.5707E-01	0.2500E+03	0.2168E+05	0.1056E-04
0.5760E-01	0.3000E+03	0.2178E+05	0.1059E-04
0.5815E-01	0.3500E+03	0.2188E+05	0.1189E-04
0.5882E-01	0.4000E+03	0.2201E+05	0.1519E-04

SPECIMEN NUMBER	B24-4 T/2N		
2CREF	NREF	KMAX	D2C/DN
0.5813E-01	0.5000E+02	0.2188E+05	0.1294E-04
0.5877E-01	0.1000E+03	0.2200E+05	0.1249E-04
0.5936E-01	0.1500E+03	0.2211E+05	0.1071E-04
0.5985E-01	0.2000E+03	0.2220E+05	0.9295E-05
0.6032E-01	0.2500E+03	0.2228E+05	0.9965E-05
0.6091E-01	0.3000E+03	0.2239E+05	0.1443E-04
0.6185E-01	0.3500E+03	0.2257E+05	0.2441E-04
0.6347E-01	0.4000E+03	0.2286E+05	0.4160E-04

SPECIMEN NUMBER	4-62 T/2		
2CRFF	NREF	KMAX	D2C/DN
0.5913F-01	0.5000E+02	0.2215E+05	0.1331E-04
0.5994E-01	0.1000E+03	0.2230E+05	0.1793E-04
0.6083F-01	0.1500E+03	0.2246E+05	0.1705E-04
0.6160F-01	0.2000E+03	0.2261E+05	0.1325E-04
0.6215F-01	0.2500E+03	0.2271E+05	0.9156E-05
0.6255F-01	0.3000E+03	0.2278E+05	0.7364E-05
0.6297F-01	0.3500E+03	0.2286E+05	0.1048E-04
0.6372F-01	0.4000E+03	0.2299E+05	0.2112E-04

SPECIMEN NUMBER	4-64 T/2		
2CRFF	NREF	KMAX	D2C/DN
0.5974F-01	0.5000E+02	0.2226E+05	0.1373E-04
0.6032F-01	0.1000E+03	0.2237E+05	0.1010E-04
0.6078F-01	0.1500E+03	0.2245E+05	0.8554E-05
0.6120F-01	0.2000E+03	0.2253E+05	0.8493E-05
0.6164F-01	0.2500E+03	0.2261E+05	0.9310E-05
0.6214F-01	0.3000E+03	0.2270E+05	0.1040E-04
0.6268F-01	0.3500E+03	0.2280E+05	0.1116E-04
0.6324F-01	0.4000E+03	0.2290E+05	0.1098E-04

SPECIMEN NUMBER	4-71 T/2 N		
2CRFF	NREF	KMAX	D2C/DN
0.5418F-01	0.5000E+02	0.2120E+05	0.1000E-06
0.5416F-01	0.1000E+03	0.2120E+05	0.6316E-06
0.5427F-01	0.1500E+03	0.2122E+05	0.4134E-05
0.5459F-01	0.2000E+03	0.2128E+05	0.8633E-05
0.5514F-01	0.2500E+03	0.2139E+05	0.1374E-04
0.5590F-01	0.3000E+03	0.2154E+05	0.1707E-04
0.5682F-01	0.3500E+03	0.2171E+05	0.1924E-04
0.5778F-01	0.4000E+03	0.2189E+05	0.1885E-04

SPECIMEN NUMBER	4-78 T/2 N		
2CRFF	NREF	KMAX	D2C/DN
0.5436F-01	0.5000E+02	0.2124E+05	0.6081E-06
0.5434F-01	0.1000E+03	0.2123E+05	0.1000E-06
0.5426F-01	0.1500E+03	0.2122E+05	0.1000E-06
0.5422F-01	0.2000E+03	0.2121E+05	0.3563E-06
0.5434F-01	0.2500E+03	0.2123E+05	0.5017E-05
0.5478F-01	0.3000E+03	0.2132E+05	0.1295E-04
0.5570F-01	0.3500E+03	0.2150E+05	0.2470E-04
0.5732F-01	0.4000E+03	0.2181E+05	0.4080E-04

SPECIMEN NUMBER	B9-1 T/2N		
2CREF	NREF	KMAX	D2C/DN
0.5543E-01	0.5000E+02	0.2136E+05	0.1985E-04
0.5655E-01	0.1000E+03	0.2158E+05	0.2358E-04
0.5767E-01	0.1500E+03	0.2179E+05	0.2045E-04
0.5854E-01	0.2000E+03	0.2195E+05	0.1419E-04
0.5910E-01	0.2500E+03	0.2206E+05	0.8523E-05
0.5947E-01	0.3000E+03	0.2213E+05	0.7178E-05
0.5995E-01	0.3500E+03	0.2222E+05	0.1388E-04
0.6105E-01	0.4000E+03	0.2242E+05	0.3235E-04

SPECIMEN NUMBER	B14-1 T/2N		
2CREF	NREF	KMAX	D2C/DN
0.6252E-01	0.5000E+02	0.2269E+05	0.1210E-05
0.6222E-01	0.1000E+03	0.2263E+05	0.1000E-06
0.6177E-01	0.1500E+03	0.2255E+05	0.1000E-06
0.6175E-01	0.2000E+03	0.2255E+05	0.6266E-05
0.6243E-01	0.2500E+03	0.2267E+05	0.2068E-04
0.6375E-01	0.3000E+03	0.2291E+05	0.3063E-04
0.6531E-01	0.3500E+03	0.2319E+05	0.2962E-04
0.6642E-01	0.4000E+03	0.2338E+05	0.1116E-04

SPECIMEN NUMBER	B23-1 T/2N		
2CREF	NREF	KMAX	D2C/DN
0.5494E-01	0.5000E+02	0.2127E+05	0.8045E-05
0.5542E-01	0.1000E+03	0.2136E+05	0.1053E-04
0.5597E-01	0.1500E+03	0.2147E+05	0.1128E-04
0.5653E-01	0.2000E+03	0.2157E+05	0.1104E-04
0.5707E-01	0.2500E+03	0.2168E+05	0.1056E-04
0.5760E-01	0.3000E+03	0.2178E+05	0.1059E-04
0.5815E-01	0.3500E+03	0.2188E+05	0.1189E-04
0.5882E-01	0.4000E+03	0.2201E+05	0.1519E-04

SPECIMEN NUMBER	B24-4 T/2N		
2CREF	NREF	KMAX	D2C/DN
0.5813E-01	0.5000E+02	0.2188E+05	0.1294E-04
0.5877E-01	0.1000E+03	0.2200E+05	0.1249E-04
0.5936E-01	0.1500E+03	0.2211E+05	0.1071E-04
0.5985E-01	0.2000E+03	0.2220E+05	0.9295E-05
0.6037E-01	0.2500E+03	0.2228E+05	0.9965E-05
0.6091E-01	0.3000E+03	0.2239E+05	0.1443E-04
0.6185E-01	0.3500E+03	0.2257E+05	0.2441E-04
0.6347E-01	0.4000E+03	0.2286E+05	0.4160E-04

SPFCIMEN NIJMBER	4-62	T/2		
ZCRFF		NREF	KMAX	D2C/DN
0.5913F-01		0.5000E+02	0.2215E+05	0.1331E-04
0.5994F-01		0.1000E+03	0.2230E+05	0.1793E-04
0.6083F-01		0.1500E+03	0.2246E+05	0.1705E-04
0.6100F-01		0.2000E+03	0.2261E+05	0.1325E-04
0.6215F-01		0.2500E+03	0.2271E+05	0.9156E-05
0.6255F-01		0.3000E+03	0.2278E+05	0.7364E-05
0.6297F-01		0.3500E+03	0.2286E+05	0.1048E-04
0.6372F-01		0.4000E+03	0.2299E+05	0.2112E-04

SPFCIMEN NIJMBER	4-64	T/2		
ZCRFF		NREF	KMAX	D2C/DN
0.5974F-01		0.5000E+02	0.2226E+05	0.1373E-04
0.6032F-01		0.1000E+03	0.2237E+05	0.1010E-04
0.6078F-01		0.1500E+03	0.2245E+05	0.8554E-05
0.6120F-01		0.2000E+03	0.2253E+05	0.8493E-05
0.6164F-01		0.2500E+03	0.2261E+05	0.9310E-05
0.6214F-01		0.3000E+03	0.2270E+05	0.1040E-04
0.6268F-01		0.3500E+03	0.2280E+05	0.1116E-04
0.6324F-01		0.4000E+03	0.2290E+05	0.1098E-04

SPFCIMEN NIJMBER	4-33	T/2	N		
ZCRFF		NREF		KMAX	D2C/DN
0.5877F-01		0.5000E+02		0.2208E+05	0.2661E-04
0.6001F-01		0.1000E+03		0.2231E+05	0.2233E-04
0.6097F-01		0.1500E+03		0.2249E+05	0.1523E-04
0.6163F-01		0.2000E+03		0.2261E+05	0.1007E-04
0.6201F-01		0.2500E+03		0.2268E+05	0.5637E-05
0.6225F-01		0.3000E+03		0.2272E+05	0.4686E-05
0.6257F-01		0.3500E+03		0.2278E+05	0.8991E-05
0.6327F-01		0.4000E+03		0.2291E+05	0.2032E-04

SPECIMEN NUMBER	4-39	T/2	N		
ZCRFF		NREF		KMAX	D2C/DN
0.5780F-01		0.5000E+02		0.2190E+05	0.1595E-04
0.5913F-01		0.1000E+03		0.2215E+05	0.3342E-04
0.6086F-01		0.1500E+03		0.2247E+05	0.3348E-04
0.6231F-01		0.2000E+03		0.2274E+05	0.2374E-04
0.6319F-01		0.2500E+03		0.2290E+05	0.1184E-04
0.6359F-01		0.3000E+03		0.2297E+05	0.5396E-05
0.6395F-01		0.3500E+03		0.2303E+05	0.1205E-04
0.6514F-01		0.4000E+03		0.2325E+05	0.3941E-04

SPECIMEN NUMBER	2CREF	B22-2 T/2N NREF	KMAX	D2C/DN
0.5505E-01		0.5000E+02	0.2129E+05	0.3047E-05
0.5532E-01		0.1000E+03	0.2134E+05	0.6680E-05
0.5565E-01		0.1500E+03	0.2140E+05	0.5878E-05
0.5590E-01		0.2000E+03	0.2145E+05	0.4294E-05
0.5612E-01		0.2500E+03	0.2150E+05	0.5584E-05
0.5656E-01		0.3000E+03	0.2158E+05	0.1340E-04
0.5763E-01		0.3500E+03	0.2178E+05	0.3141E-04
0.5993E-01		0.4000E+03	0.2221E+05	0.6325E-04

SPECIMEN NUMBER	2CREF	B14-3 T/2N NREF	KMAX	D2C/DN
0.5545E-01		0.5000E+02	0.2137E+05	0.8042E-05
0.5562E-01		0.1000E+03	0.2140E+05	0.1372E-06
0.5560E-01		0.1500E+03	0.2139E+05	0.5070E-07
0.5571E-01		0.2000E+03	0.2142E+05	0.5104E-05
0.5615E-01		0.2500E+03	0.2150E+05	0.1262E-04
0.5697E-01		0.3000E+03	0.2166E+05	0.1992E-04
0.5809E-01		0.3500E+03	0.2187E+05	0.2432E-04
0.5931E-01		0.4000E+03	0.2210E+05	0.2315E-04

SPECIMEN NUMBER	2CREF	B23-1 T/2N NREF	KMAX	D2C/DN
0.5494E-01		0.5000E+02	0.2127E+05	0.8045E-05
0.5542E-01		0.1000E+03	0.2136E+05	0.1053E-04
0.5597E-01		0.1500E+03	0.2147E+05	0.1128E-04
0.5653E-01		0.2000E+03	0.2157E+05	0.1104E-04
0.5707E-01		0.2500E+03	0.2168E+05	0.1056E-04
0.5760E-01		0.3000E+03	0.2178E+05	0.1059E-04
0.5815E-01		0.3500E+03	0.2188E+05	0.1189E-04
0.5882E-01		0.4000E+03	0.2201E+05	0.1519E-04

SPECIMEN NUMBER	2CREF	B24-4 T/2N NREF	KMAX	D2C/DN
0.5813E-01		0.5000E+02	0.2188E+05	0.1294E-04
0.5877E-01		0.1000E+03	0.2200E+05	0.1249E-04
0.5936E-01		0.1500E+03	0.2211E+05	0.1071E-04
0.5985E-01		0.2000E+03	0.2220E+05	0.9295E-05
0.6032E-01		0.2500E+03	0.2228E+05	0.9965E-05
0.6091E-01		0.3000E+03	0.2239E+05	0.1443E-04
0.6185E-01		0.3500E+03	0.2257E+05	0.2441E-04
0.6347E-01		0.4000E+03	0.2286E+05	0.4160E-04

SPECIMEN NUMBER	4-55 T/2 E			
ZCREF	NREF	AREF	KMAX	U2C/UN
0.1147E+00	0.5000E+02	0.2218E-01	0.2667E+05	0.2776E-04
0.1158E+00	0.1000E+03	0.2276E-01	0.2643E+05	0.1863E-04
0.1165E+00	0.1500E+03	0.2317E-01	0.2710E+05	0.1117E-04
0.1170E+00	0.2000E+03	0.2334E-01	0.2719E+05	0.7009E-05
0.1173E+00	0.2500E+03	0.2351E-01	0.2727E+05	0.7786E-05
0.1179E+00	0.3000E+03	0.2374E-01	0.2739E+05	0.1513E-04
0.1190E+00	0.3500E+03	0.2434E-01	0.2763E+05	0.3067E-04
0.1211E+00	0.4000E+03	0.2540E-01	0.2808E+05	0.5604E-04

SPECIMEN NUMBER	4-110 T/2E			
ZCREF	NREF	AREF	KMAX	U2C/UN
0.1113E+00	0.5000E+02	0.2174E-01	0.2635E+05	0.1036E-04
0.1117E+00	0.1000E+03	0.2193E-01	0.2644E+05	0.5341E-05
0.1119E+00	0.1500E+03	0.2205E-01	0.2650E+05	0.5164E-05
0.1122E+00	0.2000E+03	0.2221E-01	0.2657E+05	0.7818E-05
0.1127E+00	0.2500E+03	0.2244E-01	0.2668E+05	0.1074E-04
0.1133E+00	0.3000E+03	0.2273E-01	0.2681E+05	0.1158E-04
0.1138E+00	0.3500E+03	0.2298E-01	0.2692E+05	0.7677E-05
0.1159E+00	0.4000E+03	0.2305E-01	0.2695E+05	0.1000E-06

SPECIMEN NUMBER	4-48 T/2 F			
ZCREF	NREF	AREF	KMAX	U2C/UN
0.1164E+00	0.5000E+02	0.2330E-01	0.2715E+05	0.3344E-04
0.1179E+00	0.1000E+03	0.2404E-01	0.2748E+05	0.2611E-04
0.1190E+00	0.1500E+03	0.2461E-01	0.2772E+05	0.2022E-04
0.1199E+00	0.2000E+03	0.2506E-01	0.2791E+05	0.1514E-04
0.1207E+00	0.2500E+03	0.2544E-01	0.2807E+05	0.1425E-04
0.1214E+00	0.3000E+03	0.2580E-01	0.2822E+05	0.1492E-04
0.1222E+00	0.3500E+03	0.2621E-01	0.2839E+05	0.1455E-04
0.1233E+00	0.4000E+03	0.2675E-01	0.2861E+05	0.2550E-04

SPECIMEN NUMBER	4-46 T/2 E			
ZCREF	NREF	AREF	KMAX	U2C/UN
0.1185E+00	0.5000E+02	0.2304E-01	0.2716E+05	0.2210E-04
0.1195E+00	0.1000E+03	0.2357E-01	0.2739E+05	0.2081E-04
0.1206E+00	0.1500E+03	0.2411E-01	0.2763E+05	0.2253E-04
0.1218E+00	0.2000E+03	0.2471E-01	0.2789E+05	0.2556E-04
0.1232E+00	0.2500E+03	0.2538E-01	0.2817E+05	0.2819E-04
0.1246E+00	0.3000E+03	0.2610E-01	0.2847E+05	0.2875E-04
0.1260E+00	0.3500E+03	0.2679E-01	0.2875E+05	0.2552E-04
0.1271E+00	0.4000E+03	0.2733E-01	0.2897E+05	0.1681E-04

SPECIMEN NUMBER	B10-4 T/2E			
2CREF	NREF	AREF	KMAX	D2C/DN
0.9901E-01	0.5000E+02	0.1991E-01	0.2508E+05	0.1000E-06
0.9914E-01	0.1000E+03	0.1997E-01	0.2511E+05	0.4029E-05
0.9933E-01	0.1500E+03	0.2007E-01	0.2515E+05	0.3293E-05
0.9945E-01	0.2000E+03	0.2013E-01	0.2518E+05	0.1657E-05
0.9955E-01	0.2500E+03	0.2018E-01	0.2520E+05	0.3060E-05
0.9988E-01	0.3000E+03	0.2034E-01	0.2528E+05	0.1144E-04
0.1009E+00	0.3500E+03	0.2084E-01	0.2551E+05	0.3075E-04
0.1032E+00	0.4000E+03	0.2200E-01	0.2604E+05	0.6492E-04

SPECIMEN NUMBER	B10-3 T/2E			
2CREF	NREF	AREF	KMAX	D2C/DN
0.1020E+00	0.5000E+02	0.2113E-01	0.2567E+05	0.3462E-04
0.1030E+00	0.1000E+03	0.2166E-01	0.2592E+05	0.1209E-04
0.1035E+00	0.1500E+03	0.2191E-01	0.2603E+05	0.1047E-04
0.1043E+00	0.2000E+03	0.2228E-01	0.2619E+05	0.2098E-04
0.1057E+00	0.2500E+03	0.2248E-01	0.2650E+05	0.3483E-04
0.1077E+00	0.3000E+03	0.2398E-01	0.2692E+05	0.4324E-04
0.1098E+00	0.3500E+03	0.2503E-01	0.2736E+05	0.3744E-04
0.1110E+00	0.4000E+03	0.2566E-01	0.2761E+05	0.8641E-05

SPECIMEN NUMBER	B18-3 T/2E			
2CREF	NREF	AREF	KMAX	D2C/DN
0.1035E+00	0.5000E+02	0.2106E-01	0.2573E+05	0.2678E-04
0.1045E+00	0.1000E+03	0.2157E-01	0.2596E+05	0.1515E-04
0.1052E+00	0.1500E+03	0.2188E-01	0.2610E+05	0.1019E-04
0.1056E+00	0.2000E+03	0.2212E-01	0.2621E+05	0.1021E-04
0.1062E+00	0.2500E+03	0.2241E-01	0.2634E+05	0.1351E-04
0.1070E+00	0.3000E+03	0.2281E-01	0.2652E+05	0.1840E-04
0.1081E+00	0.3500E+03	0.2333E-01	0.2674E+05	0.2320E-04
0.1093E+00	0.4000E+03	0.2396E-01	0.2701E+05	0.2620E-04

SPECIMEN NUMBER	B15-5 T/2E			
2CREF	NREF	AREF	KMAX	D2C/DN
0.1023E+00	0.5000E+02	0.2047E-01	0.2546E+05	0.1654E-05
0.1024E+00	0.1000E+03	0.2049E-01	0.2547E+05	0.1352E-05
0.1026E+00	0.1500E+03	0.2059E-01	0.2551E+05	0.7136E-05
0.1032E+00	0.2000E+03	0.2088E-01	0.2565E+05	0.1599E-04
0.1042E+00	0.2500E+03	0.2139E-01	0.2588E+05	0.2488E-04
0.1056E+00	0.3000E+03	0.2210E-01	0.2620E+05	0.3079E-04
0.1072E+00	0.3500E+03	0.2288E-01	0.2655E+05	0.3070E-04
0.1085E+00	0.4000E+03	0.2356E-01	0.2684E+05	0.2159E-04

SPECIMEN NUMBER	4-7	T/2 E			
ZCREF		NREF	AREF	KMAX	O2C/DN
0.1127E+00		0.5000E+02	0.2184E-01	0.2648E+05	0.4076E-05
0.1134E+00		0.1000E+03	0.2219E-01	0.2602E+05	0.2171E-04
0.1147E+00		0.1500E+03	0.2284E-01	0.2641E+05	0.2895E-04
0.1162E+00		0.2000E+03	0.2358E-01	0.2724E+05	0.2908E-04
0.1175E+00		0.2500E+03	0.2427E-01	0.2754E+05	0.2538E-04
0.1187E+00		0.3000E+03	0.2484E-01	0.2778E+05	0.2111E-04
0.1197E+00		0.3500E+03	0.2534E-01	0.2794E+05	0.1956E-04
0.1207E+00		0.4000E+03	0.2587E-01	0.2821E+05	0.2+01E-04

SPECIMEN NUMBER	4-10	T/2 E			
ZCREF		NREF	AREF	KMAX	O2C/DN
0.1178E+00		0.5000E+02	0.2415E-01	0.2750E+05	0.1872E-04
0.1184E+00		0.1000E+03	0.2480E-01	0.2778E+05	0.3130E-04
0.1205E+00		0.1500E+03	0.2562E-01	0.2812E+05	0.3219E-04
0.1220E+00		0.2000E+03	0.2637E-01	0.2843E+05	0.2772E-04
0.1233E+00		0.2500E+03	0.2701E-01	0.2878E+05	0.2425E-04
0.1246E+00		0.3000E+03	0.2764E-01	0.2893E+05	0.2811E-04
0.1264E+00		0.3500E+03	0.2853E-01	0.2928E+05	0.4585E-04
0.1295E+00		0.4000E+03	0.3009E-01	0.2966E+05	0.8321E-04

SPECIMEN NUMBER	4-48	T/2 E			
ZCREF		NREF	AREF	KMAX	O2C/DN
0.1184E+00		0.5000E+02	0.2330E-01	0.2715E+05	0.3344E-04
0.1195E+00		0.1000E+03	0.2404E-01	0.2748E+05	0.2811E-04
0.1190E+00		0.1500E+03	0.2461E-01	0.2772E+05	0.2022E-04
0.1199E+00		0.2000E+03	0.2508E-01	0.2791E+05	0.1614E-04
0.1207E+00		0.2500E+03	0.2544E-01	0.2807E+05	0.1425E-04
0.1214E+00		0.3000E+03	0.2580E-01	0.2822E+05	0.1492E-04
0.1222E+00		0.3500E+03	0.2621E-01	0.2834E+05	0.1855E-04
0.1233E+00		0.4000E+03	0.2675E-01	0.2861E+05	0.2550E-04

SPECIMEN NUMBER	4-46	T/2 E			
ZCREF		NREF	AREF	KMAX	O2C/DN
0.1185E+00		0.5000E+02	0.2304E-01	0.2716E+05	0.2210E-04
0.1195E+00		0.1000E+03	0.2357E-01	0.2739E+05	0.2081E-04
0.1206E+00		0.1500E+03	0.2411E-01	0.2763E+05	0.2253E-04
0.1218E+00		0.2000E+03	0.2471E-01	0.2784E+05	0.2556E-04
0.1232E+00		0.2500E+03	0.2538E-01	0.2817E+05	0.2819E-04
0.1246E+00		0.3000E+03	0.2610E-01	0.2847E+05	0.2875E-04
0.1260E+00		0.3500E+03	0.2679E-01	0.2875E+05	0.2552E-04
0.1271E+00		0.4000E+03	0.2733E-01	0.2897E+05	0.1681E-04

SPECIMEN NUMBER	B16-2 T/2E				
2CREF	NREF	AREF	KMAX	D2C/DN	
0.1030E+00	0.5000E+02	0.2058E-01	0.2553E+05	0.1030E-04	
0.1036E+00	0.1000E+03	0.2090E-01	0.2568E+05	0.1384E-04	
0.1043E+00	0.1500E+03	0.2123E-01	0.2583E+05	0.1238E-04	
0.1048E+00	0.2000E+03	0.2151E-01	0.2596E+05	0.9541E-05	
0.1053E+00	0.2500E+03	0.2173E-01	0.2606E+05	0.8918E-05	
0.1058E+00	0.3000E+03	0.2200E-01	0.2618E+05	0.1412E-04	
0.1068E+00	0.3500E+03	0.2251E-01	0.2641E+05	0.2876E-04	
0.1089E+00	0.4000E+03	0.2355E-01	0.2686E+05	0.5643E-04	

SPECIMEN NUMBER	B18-3 T/2E				
2CREF	NREF	AREF	KMAX	D2C/DN	
0.1035E+00	0.5000E+02	0.2106E-01	0.2573E+05	0.2678E-04	
0.1045E+00	0.1000E+03	0.2157E-01	0.2596E+05	0.1515E-04	
0.1052E+00	0.1500E+03	0.2188E-01	0.2610E+05	0.1019E-04	
0.1056E+00	0.2000E+03	0.2212E-01	0.2621E+05	0.1021E-04	
0.1062E+00	0.2500E+03	0.2241E-01	0.2634E+05	0.1351E-04	
0.1070E+00	0.3000E+03	0.2281E-01	0.2652E+05	0.1840E-04	
0.1081E+00	0.3500E+03	0.2333E-01	0.2674E+05	0.2320E-04	
0.1093E+00	0.4000E+03	0.2396E-01	0.2701E+05	0.2620E-04	

SPECIMEN NUMBER	B15-5 T/2E				
2CREF	NREF	AREF	KMAX	D2C/DN	
0.1023E+00	0.5000E+02	0.2047E-01	0.2546E+05	0.1654E-05	
0.1024E+00	0.1000E+03	0.2049E-01	0.2547E+05	0.1352E-05	
0.1026E+00	0.1500E+03	0.2059E-01	0.2551E+05	0.7136E-05	
0.1032E+00	0.2000E+03	0.2084E-01	0.2565E+05	0.1599E-04	
0.1042E+00	0.2500E+03	0.2139E-01	0.2588E+05	0.2488E-04	
0.1056E+00	0.3000E+03	0.2210E-01	0.2620E+05	0.3079E-04	
0.1072E+00	0.3500E+03	0.2288E-01	0.2655E+05	0.3070E-04	
0.1085E+00	0.4000E+03	0.2356E-01	0.2684E+05	0.2159E-04	

SPECIMEN NUMBER 4-106T/2 E		AREF	KMAX	U2C/UN
ZCREF	NREF			
0.1249E+00	0.5000E+02	0.2387E-01	0.2773E+05	0.3127E-04
0.1250E+00	0.1000E+03	0.2468E-01	0.2809E+05	0.3233E-04
0.1250E+00	0.1500E+03	0.2541E-01	0.2840E+05	0.3353E-04
0.1241E+00	0.2000E+03	0.2595E-01	0.2863E+05	0.3482E-04
0.1249E+00	0.2500E+03	0.2633E-01	0.2879E+05	0.3614E-04
0.1307E+00	0.3000E+03	0.2673E-01	0.2895E+05	0.3750E-04
0.1322E+00	0.3500E+03	0.2748E-01	0.2926E+05	0.3897E-04
0.1353E+00	0.4000E+03	0.2907E-01	0.2988E+05	0.4055E-04

SPECIMEN NUMBER 4-115 T/2 E		AREF	KMAX	U2C/UN
ZCREF	NREF			
0.1155E+00	0.5000E+02	0.2254E-01	0.2654E+05	0.2992E-04
0.1168E+00	0.1000E+03	0.2321E-01	0.2714E+05	0.3172E-04
0.1180E+00	0.1500E+03	0.2378E-01	0.2739E+05	0.3368E-04
0.1190E+00	0.2000E+03	0.2428E-01	0.2761E+05	0.3571E-04
0.1199E+00	0.2500E+03	0.2473E-01	0.2780E+05	0.3777E-04
0.1203E+00	0.3000E+03	0.2515E-01	0.2799E+05	0.3984E-04
0.1217E+00	0.3500E+03	0.2566E-01	0.2819E+05	0.4193E-04
0.1224E+00	0.4000E+03	0.2622E-01	0.2842E+05	0.4403E-04

SPECIMEN NUMBER 4-48 T/2 E		AREF	KMAX	U2C/UN
ZCREF	NREF			
0.1164E+00	0.5000E+02	0.2310E-01	0.2715E+05	0.3344E-04
0.1179E+00	0.1000E+03	0.2404E-01	0.2744E+05	0.3611E-04
0.1190E+00	0.1500E+03	0.2461E-01	0.2772E+05	0.3892E-04
0.1199E+00	0.2000E+03	0.2506E-01	0.2791E+05	0.4187E-04
0.1207E+00	0.2500E+03	0.2544E-01	0.2807E+05	0.4493E-04
0.1214E+00	0.3000E+03	0.2580E-01	0.2822E+05	0.4807E-04
0.1222E+00	0.3500E+03	0.2621E-01	0.2847E+05	0.5133E-04
0.1233E+00	0.4000E+03	0.2675E-01	0.2861E+05	0.5470E-04

SPECIMEN NUMBER 4-46 T/2 F		AREF	KMAX	U2C/UN
ZCREF	NREF			
0.1155E+00	0.5000E+02	0.2304E-01	0.2716E+05	0.2210E-04
0.1195E+00	0.1000E+03	0.2357E-01	0.2739E+05	0.2411E-04
0.1206E+00	0.1500E+03	0.2411E-01	0.2763E+05	0.2633E-04
0.1213E+00	0.2000E+03	0.2471E-01	0.2789E+05	0.2868E-04
0.1232E+00	0.2500E+03	0.2538E-01	0.2817E+05	0.3119E-04
0.1246E+00	0.3000E+03	0.2610E-01	0.2847E+05	0.3387E-04
0.1260E+00	0.3500E+03	0.2679E-01	0.2875E+05	0.3662E-04
0.1271E+00	0.4000E+03	0.2733E-01	0.2897E+05	0.3941E-04

SPECIMEN NUMBER	B23-2 T/2E		AREF	KMAX	D2C/DN
ZCREF	NREF				
0.9958E-01	0.5000E+02		0.2004E-01	0.2515E+05	0.4243E-05
0.9979E-01	0.1000E+03		0.2014E-01	0.2520E+05	0.4290E-05
0.1000E+00	0.1500E+03		0.2026E-01	0.2526E+05	0.4963E-05
0.1003E+00	0.2000E+03		0.2041E-01	0.2533E+05	0.7084E-05
0.1008E+00	0.2500E+03		0.2093E-01	0.2543E+05	0.1147E-04
0.1015E+00	0.3000E+03		0.2100E-01	0.2561E+05	0.1894E-04
0.1027E+00	0.3500E+03		0.2161E-01	0.2583E+05	0.3031E-04
0.1046E+00	0.4000E+03		0.2256E-01	0.2630E+05	0.4641E-04

SPECIMEN NUMBER	B11-2 T/2E		APEF	KMAX	D2C/DN
ZCREF	NREF				
0.1025E+00	0.5000E+02		0.2047E-01	0.2546E+05	0.7872E-05
0.1034E+00	0.1000E+03		0.2089E-01	0.2566E+05	0.2396E-04
0.1048E+00	0.1500E+03		0.2159E-01	0.2593E+05	0.3070E-04
0.1063E+00	0.2000E+03		0.2237E-01	0.2633E+05	0.3077E-04
0.1078E+00	0.2500E+03		0.2309E-01	0.2665E+05	0.2682E-04
0.1090E+00	0.3000E+03		0.2370E-01	0.2691E+05	0.2155E-04
0.1100E+00	0.3500E+03		0.2418E-01	0.2712E+05	0.1762E-04
0.1108E+00	0.4000E+03		0.2461E-01	0.2730E+05	0.1770E-04

SPECIMEN NUMBER	B18-3 T/2E		AREF	KMAX	D2C/DN
ZCREF	NREF				
0.1035E+00	0.5000E+02		0.2106E-01	0.2573E+05	0.2678E-04
0.1045E+00	0.1000E+03		0.2157E-01	0.2596E+05	0.1515E-04
0.1052E+00	0.1500E+03		0.2188E-01	0.2610E+05	0.1019E-04
0.1056E+00	0.2000E+03		0.2212E-01	0.2621E+05	0.1021E-04
0.1062E+00	0.2500E+03		0.2241E-01	0.2634E+05	0.1351E-04
0.1070E+00	0.3000E+03		0.2281E-01	0.2652E+05	0.1840E-04
0.1081E+00	0.3500E+03		0.2333E-01	0.2674E+05	0.2320E-04
0.1093E+00	0.4000E+03		0.2396E-01	0.2701E+05	0.2620E-04

SPECIMEN NUMBER	B15-5 T/2E		AREF	KMAX	D2C/DN
ZCREF	NREF				
0.1023E+00	0.5000E+02		0.2047E-01	0.2546E+05	0.1654E-05
0.1024E+00	0.1000E+03		0.2049E-01	0.2547E+05	0.1352E-05
0.1026E+00	0.1500E+03		0.2059E-01	0.2551E+05	0.7136E-05
0.1032E+00	0.2000E+03		0.2088E-01	0.2565E+05	0.1599E-04
0.1042E+00	0.2500E+03		0.2139E-01	0.2588E+05	0.2488E-04
0.1056E+00	0.3000E+03		0.2210E-01	0.2620E+05	0.3079E-04
0.1072E+00	0.3500E+03		0.2288E-01	0.2655E+05	0.3070E-04
0.1085E+00	0.4000E+03		0.2356E-01	0.2684E+05	0.2159E-04

SPECIMEN NUMBER	6-7 T/4			
	ZCRFF	NRFF	KMAX	D2C/DN
	0.3297E-01	0.5000E+02	0.1666E+05	0.1133E-04
	0.3360E-01	1.0000E+02	0.1692E+05	0.1268E-04
	0.3416E-01	0.1500E+03	0.1596E+05	0.4346E-05
	0.3450E-01	0.2000E+03	0.1704E+05	0.4169E-05
	0.3459E-01	0.2500E+03	0.1707E+05	1.0000E-07
	0.3456E-01	0.3000E+03	0.1705E+05	1.0000E-07
	0.3467E-01	0.3500E+03	0.1708E+05	0.5444E-05
	0.3531E-01	0.4000E+03	0.1724E+05	0.2176E-04

SPECIMEN NUMBER	6-9 T/2			
	ZCRFF	NRFF	KMAX	D2C/DN
	0.6945E-01	0.5000E+02	0.2418E+05	0.2996E-04
	0.7077E-01	1.0000E+02	0.2441E+05	0.2329E-04
	0.7183E-01	0.1500E+03	0.2459E+05	0.1993E-04
	0.7279E-01	0.2000E+03	0.2476E+05	0.1831E-04
	0.7374E-01	0.2500E+03	0.2432E+05	0.1415E-04
	0.7475E-01	0.3000E+03	0.2509E+05	0.2038E-04
	0.7584E-01	0.3500E+03	0.2527E+05	0.2271E-04
	0.7700E-01	0.4000E+03	0.2546E+05	0.2358E-04

SPECIMEN NUMBER	6-8 T/2			
	ZCRFF	NRFF	KMAX	D2C/DN
	0.8530E-01	0.5000E+02	0.2690E+05	0.1204E-03
	0.9035E-01	1.0000E+02	0.2758E+05	0.3459E-04
	0.9405E-01	0.1500E+03	0.2814E+05	0.5602E-04
	0.9716E-01	0.2000E+03	0.2860E+05	0.5446E-04
	0.1002E+00	0.2500E+03	0.2904E+05	0.6154E-04
	0.1034E+00	0.3000E+03	0.2950E+05	0.6532E-04
	0.1068E+00	0.3500E+03	0.2999E+05	0.7021E-04
	0.1104E+00	0.4000E+03	0.3049E+05	0.6918E-04

SPECIMEN NUMBER 6-15 3T/4			
PCRF	NRFF	KMAX	D2C/DN
0.1316E+00	0.5000E+02	0.3329E+05	0.1574E-03
0.1340E+00	1.0000E+02	0.3421E+05	0.1402E-03
0.1459E+00	0.1500E+03	0.3505E+05	0.1369E-03
0.1530E+00	0.2000E+03	0.3589E+05	0.1514E-03
0.1614E+00	0.2500E+03	0.3686E+05	0.1874E-03
0.1722E+00	0.3000E+03	0.3807E+05	0.2448E-03
0.1968E+00	0.3500E+03	0.3965E+05	0.3343E-03
0.2067E+00	0.4000E+03	0.4171E+05	0.4628E-03

SPECIMEN NUMBER 6-19 3T/4			
PCRF	NRFF	KMAX	D2C/DN
0.1326E+00	0.5000E+02	0.3341E+05	0.2632E-03
0.1425E+00	1.0000E+02	0.3464E+05	0.1459E-03
0.1485E+00	0.1500E+03	0.3536E+05	0.1041E-03
0.1537E+00	0.2000E+03	0.3597E+05	0.1079E-03
0.1597E+00	0.2500E+03	0.3666E+05	0.1315E-03
0.1667E+00	0.3000E+03	0.3747E+05	0.1479E-03
0.1739E+00	0.3500E+03	0.3826E+05	0.1301E-03
0.1787E+00	0.4000E+03	0.3879E+05	0.5120E-04

SPECIMEN NUMBER	C6-4	T/4N		
2CREF		NREF	KMAX	D2C/DN
0.3188E-01		0.5000E+02	0.1632E+05	0.2953E-05
0.3204E-01		0.1000E+03	0.1636E+05	0.3851E-05
0.3231E-01		0.1500E+03	0.1643E+05	0.7244E-05
0.3278E-01		0.2000E+03	0.1655E+05	0.1163E-04
0.3347E-01		0.2500E+03	0.1672E+05	0.1552E-04
0.3430E-01		0.3000E+03	0.1693E+05	0.1740E-04
0.3515E-01		0.3500E+03	0.1713E+05	0.1578E-04
0.3540E-01		0.4000E+03	0.1729E+05	0.9149E-05

SPECIMEN NUMBER	C5-2	T/4 N		
2CREF		NREF	KMAX	D2C/DN
0.3313E-01		0.5000E+02	0.1663E+05	0.9994E-05
0.3382E-01		0.1000E+03	0.1681E+05	0.1606E-04
0.3459E-01		0.1500E+03	0.1700E+05	0.1383E-04
0.3514E-01		0.2000E+03	0.1713E+05	0.7817E-05
0.3539E-01		0.2500E+03	0.1719E+05	0.2540E-05
0.3548E-01		0.3000E+03	0.1722E+05	0.2511E-05
0.3580E-01		0.3500E+03	0.1729E+05	0.1225E-04
0.3694E-01		0.4000E+03	0.1757E+05	0.3626E-04

SPECIMEN NUMBER	C1-5	T/2N		
2CREF		NREF	KMAX	D2C/DN
0.6757E-01		0.5000E+02	0.2376E+05	0.2741E-04
0.6886E-01		0.1000E+03	0.2398E+05	0.2409E-04
0.6997E-01		0.1500E+03	0.2418E+05	0.2047E-04
0.7092E-01		0.2000E+03	0.2434E+05	0.1763E-04
0.7177E-01		0.2500E+03	0.2448E+05	0.1664E-04
0.7263E-01		0.3000E+03	0.2463E+05	0.1858E-04
0.7369E-01		0.3500E+03	0.2481E+05	0.2453E-04
0.7517E-01		0.4000E+03	0.2506E+05	0.3556E-04

SPECIMEN NUMBER	C5-1	T/2N		
2CREF		NREF	KMAX	D2C/DN
0.6805E-01		0.5000E+02	0.2384E+05	0.2127E-04
0.6950E-01		0.1000E+03	0.2409E+05	0.3352E-04
0.7118E-01		0.1500E+03	0.2438E+05	0.3190E-04
0.7257E-01		0.2000E+03	0.2462E+05	0.2350E-04
0.7353E-01		0.2500E+03	0.2478E+05	0.1545E-04
0.7424E-01		0.3000E+03	0.2490E+05	0.1485E-04
0.7526E-01		0.3500E+03	0.2507E+05	0.2883E-04
0.7749E-01		0.4000E+03	0.2544E+05	0.6448E-04

SPECIMEN NUMBER	0-40 T/4 E				
ZCHEF	NREF	AREF	KMAX	U2C/UN	
0.5251E-01	0.5000E+02	0.1625E-01	0.2061E+05	0.4452E-05	
0.5300E-01	0.1000E+03	0.1650E-01	0.2071E+05	0.4406E-05	
0.5343E-01	0.1500E+03	0.1871E-01	0.2021E+05	0.7037E-05	
0.5376E-01	0.2000E+03	0.1884E-01	0.2088E+05	0.5514E-05	
0.5400E-01	0.2500E+03	0.1900E-01	0.2093E+05	0.4245E-05	
0.5422E-01	0.3000E+03	0.1911E-01	0.2098E+05	0.4341E-05	
0.5451E-01	0.3500E+03	0.1925E-01	0.2104E+05	0.7825E-05	
0.5504E-01	0.4000E+03	0.1952E-01	0.2115E+05	0.1416E-04	

SPECIMEN NUMBER	0-31 T/4 E				
ZCHEF	NREF	AREF	KMAX	U2C/UN	
0.5385E-01	0.5000E+02	0.1942E-01	0.2047E+05	0.2189E-04	
0.5384E-01	0.1000E+03	0.1942E-01	0.2096E+05	0.1000E-05	
0.5266E-01	0.1500E+03	0.1883E-01	0.2071E+05	0.1000E-06	
0.5151E-01	0.2000E+03	0.1825E-01	0.2046E+05	0.1000E-06	
0.5110E-01	0.2500E+03	0.1805E-01	0.2037E+05	0.1321E-05	
0.5103E-01	0.3000E+03	0.1831E-01	0.2049E+05	0.1819E-04	
0.5262E-01	0.3500E+03	0.1891E-01	0.2075E+05	0.2594E-04	
0.5389E-01	0.4000E+03	0.1944E-01	0.2047E+05	0.1244E-04	

SPECIMEN NUMBER	0-42 T/2 E				
ZCHEF	NREF	AREF	KMAX	U2C/UN	
0.1270E+00	0.5000E+02	0.3304E-01	0.3041E+05	0.2130E-04	
0.1297E+00	0.1000E+03	0.3445E-01	0.3037E+05	0.5517E-04	
0.1325E+00	0.1500E+03	0.3583E-01	0.3132E+05	0.5348E-04	
0.1350E+00	0.2000E+03	0.3711E-01	0.3173E+05	0.4425E-04	
0.1375E+00	0.2500E+03	0.3833E-01	0.3211E+05	0.4455E-04	
0.1402E+00	0.3000E+03	0.3962E-01	0.3252E+05	0.6045E-04	
0.1438E+00	0.3500E+03	0.4150E-01	0.3307E+05	0.4512E-04	
0.1493E+00	0.4000E+03	0.4427E-01	0.3362E+05	0.1243E-03	

DISTRIBUTION LIST FOR FINAL REPORT NASA CR-65811

CONTRACT NAS 9-6969

DETERMINATION OF FLAW GROWTH CHARACTERISTICS OF
Ti-6Al-4V SHEET IN THE SOLUTION-TREATED AND AGED CONDITION

Battelle Memorial Institute
Columbus Laboratories

Copies

National Aeronautics and Space Administration
Manned Spacecraft Center
Houston, Texas 77058

Attention: Contracting Officer, BG 721 1
Glenn Ecord, ES4 50

National Aeronautics and Space Administration
Washington, D. C. 20546

Attention: Code RV-2 1

Scientific and Technical Information Facility
Post Office Box 5700
Bethesda, Maryland 20014

Attention: NASA Representative 1
Code CRT

National Aeronautics and Space Administration
Ames Research Center
Moffett Field, California 94035

Attention: Library 1

National Aeronautics and Space Administration
Lewis Research Center
2100 Brookpark Road
Cleveland, Ohio 44135

Attention: G. T. Smith, MS 49-1 1
Library 1
W. F. Brown, MS 105-1 1
J. L. Shannon, MS 105-1 1

Wright-Patterson Air Force Base, Ohio 45433

Attention: AFML(MAAE) 1

Copies

Wright-Patterson Air Force Base, Ohio 45433

Attention: AFML(MAAM) 1

SSBDD
Space Systems Division
Los Angeles, AFS
Los Angeles, California 90045

Attention: Maj. R. H. Falke 1

National Aeronautics and Space Administration
Langley Research Center
Langley Station
Hampton, Virginia 23365

Attention: Library 1

E. E. Mathauser 1

National Aeronautics and Space Administration
George C. Marshall Space Flight Center
Huntsville, Alabama

Attention: Library 1

J. Kingsbury 1

National Aeronautics and Space Administration
John F. Kennedy Space Center
Cocoa Beach, Florida

Attention: Library 1

R. Ketterer (KC-42-MSOB Bldg.) 1

H. Lambreth (MSOB Bldg.) 1

G. T. Carter (RE-3, Headquarters Bldg.) 1

Bureau of Naval Weapons
Department of the Navy
Washington, D. C. 20360

Attention: DLI-3 1

Bureau of Naval Weapons
Department of the Navy
Washington, D. C. 20360

Attention: RMMP-2 1

Bureau of Naval Weapons
Department of the Navy
Washington, D. C. 20360

Attention: RMMP-4 1

Copies

Bureau of Naval Weapons
Department of the Navy
Washington, D. C. 20360

Attention: RRRE-6 1

Aerospace Corporation
Post Office Box 95085
Los Angeles, California 90045

Attention: Library-Documents 1

E. G. Kendall 1

R. F. Johnson 1

K. T. Kamber 1

Aerojet-General Corporation
Post Office Box 1947
Sacramento, California 95809

Attention: Technical Library 2484-2015A 1

C. E. Hartbower 1

Douglas Aircraft Company, Inc.
Santa Monica Division
3000 Ocean Park Boulevard
Santa Monica, California 90405

Attention: Mr. J. L. Waisman 1

G. V. Bennett, Missiles and Space Systems Division 1

B. V. Whiteson, Missiles and Space Systems Division 1

E. I. duPont deNemours and Company
Eastern Laboratory
Gibbstown, New Jersey 08027

Attention: Mrs. Alice R. Steward 1

General Dynamics/Astronautics
Post Office Box 1128
San Diego, California 92112

Attention: Library and Information Services (128-00) 1

General Dynamics/Ft. Worth
Ft. Worth, Texas

Attention: F. C. Nordquist 1

Copies

A1Research Manufacturing Company
 9851 Sepulveda Boulevard
 Los Angeles 45, California

Attention: C. M. Campbell 1

National Aeronautics and Space Administration
 NASA/Headquarters
 Washington, D. C. 20546

Attention: George Deutsch 1

Wright-Patterson Air Force Base, Ohio 45433

Attention: Howard Zoeller, AFML 1

Capt. N. Tupper, AFML 1

RPMCH/
 Edwards, California 93523

Attention: William Payne 1

RPRPT/
 Edwards, California 93523

Attention: John Branigan 1

North American Aviation, Inc.
 Space and Information Systems Division
 12214 Lakewood Boulevard
 Downey, California 90242

Attention: Technical Information Center
 D/096-722 (AJ01) 1

L. J. Korb 1

R. Nicholas 1

Rocketdyne
 6633 Canoga Avenue
 Canoga Park, California 91304

Attention: Library, Department 596-306 1

W. T. Chandler 1

Martin-Marietta Corporation
 Denver Division G 0438
 Denver, Colorado 80201

Attention: F. R. Schwartzberg 1

R. D. Masteller 1

Copies

General Dynamics/Convair
San Diego, California

Attention: W. E. Witzel, Materials Research Group 2
J. Cristian, M. S. 572-10 1

Grumman Aircraft Engineering Corp.
Bethpage, Long Island, New York 11714

Attention: R. Hilderman 3
S. Renton 1

National Aeronautics and Space Administration
John F. Kennedy Space Center
Cocoa Beach, Florida 32931

Attention: N. Koenig (MSOB, Rm 1400) 2

National Aeronautics and Space Administration
Manned Spaceflight Center
Houston, Texas 77058

Attention: Library 5

The Boeing Company
Seattle, Washington 98124

Attention: C. F. Tiffany 1



End of Document